LIMITS TO WINTER WHEAT (*Triticum aestivum* L.) PRODUCTIVITY AND RESOURCE-USE EFFICIENCY IN THE SOUTHERN GREAT PLAINS

By

ROMULO PISA LOLLATO

Master of Science in Plant and Soil Sciences
Oklahoma State University
Stillwater, Oklahoma
2012

Bachelor of Science in Agronomy
Universidade Estadual de Londrina
Londrina, Paraná, Brazil
2009

Submitted to the Faculty of the
Graduate College of the
Oklahoma State University
in partial fulfillment of
the requirements for
the Degree of
DOCTOR OF PHILOSOPHY
July, 2015

LIMITS TO WINTER WHEAT (*Triticum aestivum* L.)

PRODUCTIVITY AND RESOURCE-USE EFFICIENCY

IN THE SOUTHERN GREAT PLAINS

Dissertation Approved:

Dr. Jeffrey T. Edwards

Dissertation Adviser

Dr. Tyson E. Ochsner

Dr. Daryl B. Arnall

Dr. Carla Goad

ACKNOWLEDGEMENTS

I would like to aknowledge all the advising, knowledge sharing, freedom to pursue research, as well as friendship, provided by my major advisor Dr. Jeff Edwards throughout the five years I worked under his advisory for both my M.S. and Ph.D. programs. I am also grateful to the Oklahoma Agricultural Experiment Stations (OAES) and the Oklahoma Cooperative Extension Services for providing financial support for my graduate assistantship at Oklahoma State University through Dr. Jeff Edwards' aplied research and extension program. I am also grateful to my committee members Drs. Daryl Arnall and Carla Goad, for providing advising not only within their specific areas of research but also on several matters during many different steps of the research. I am especially grateful to Dr. Tyson Ochsner, also committee member, not only for the advising on professional and life matters, but also for making the Soil Physics Laboratory structure at OSU available for me to pursue this research.

I am grateful to the Small Grains personnel and interns at Oklahoma State University who helped me with field and laboratory work, including Robert Calhoun, Matt Knori, Victor Bodnar, Mason Jones, Jose Leme, and Jose Pinto. I would like to aknowledge the OAES staff, including Erich Wehrenberg, Chet Venard, Michael Pettijohn, Josh Massey, and Richard Austin, whose support with field activities was crucial for the completion of this research. I am also grateful to Luciano Cegobias Jr., who was always willing to help regardless of date and time.

I thank Andres Patrignani, co-author on Chapter III of this dissertation, for the many discussions, challenges, and helpful input throughout the course of my PhD. I am also grateful to Dr. Jason Warren for the freedom to use field equipment within his program as needed for completion of this research.

I would also like to aknowledge service climatologist Mary Knapp (Kansas State University) for sharing long-term weather data necessary for the analyses performed on Chapter V of this dissertation, and Dr. Justin Van Wart (University of Nebraska) for providing suggestions on dealing with missing weather data. I also thank Mr. David Kleinsorge for the soil water measurements performed during 2009 and 2010 at the long-term crop rotation experiment at Lahoma and used in Chapter III of this dissertation.

This research would not be completed hadn't I had the support from my family and friends. Thus, I would like to thank the Brazilian community of Stillwater, including but not limited to Alexandre and Mariela Barreiro, Rolf Prade, Beatriz Soleira, Samuel Zoca, Thatiani Kievitsbosch, Guilherme and Camila Torres, among many others who at some point in time made this journey more enjoyable. I would like to thank, especially, Jim and Connie Stiegler, who I consider my family in the US for all the love and friendship. I also extend a very special thanks to my father, Marco Antonio Lollato, my mother, Lina Maria Pisa Lollato, my sister and her husband, Marcela Pisa Lollato Kikumoto and Rodrigo Kikumoto, and my nephew, Rafael Lollato Kikumoto, who provided love and support at a distance, which were essential to keep me moving forward throughout such a challenging road. I am extremely grateful to Giovana Cruppe, for baring the challenges by my side and for being the best companionship I could have asked for. Finally, I thank God for providing me strength during difficult times and joy throughout the journey.

Name: ROMULO PISA LOLLATO

Date of Degree: JULY, 2015

Title of Study: LIMITS TO WINTER WHEAT (*Triticum aestivum* L.) PRODUCTIVITY AND RESOURCE-USE EFFICIENCY IN THE SOUTHERN GREAT PLAINS

Major Field: CROP SCIENCE

Abstract: Wheat yields have been stagnant at ~2 Mg ha^{-1} for 30-yr in the southern Great Plains and evidences suggest yields are below the potential (Y_w). Our objectives were to quantify the wheat Y_w and determine its meteorological drivers, and to assess how acidic soils restrict yields of wheat varieties. A field study evaluated forage and grain yields of four wheat varieties grown in a 4.1-7.6 soil pH gradient during six site-years across Oklahoma. Minimum soil pH for maximum forage yield ranged from 5.5 to 6 and for maximum grain yield ranged from 4.8 to 5.8. Tolerant varieties improve wheat yields in acidic soils. Secondly, 29 site-years were sampled for plant available water at wheat sowing (PAW_s) to test mechanistic soil-water balance models and develop empirical models to predict PAW_s. Mechanistic models initiated during early summer-fallow using lognormally-distributed starting PAW or empirical models were able to predict PAW_s with ±30% accuracy. Third, wheat was grown under non-limiting conditions during 11 site-years across Oklahoma to determine Y_w. Greatest irrigated Y_w was 7.7 Mg ha^{-1} and rainfed Y_w ranged from 3 to 7.1 Mg ha^{-1}. Intensive management led to radiation-use efficiency (RUE) of 1.9 g MJ^{-1} and water-use efficiency (WUE) of 12.6 kg ha^{-1} mm^{-1}. A crop simulation model was calibrated using this dataset and used to predict Y_w at 37 locations for 28-yr across Texas, Kansas, and Oklahoma and assess meteorological variables dictating Y_w. Mean Y_w increased from 3.5 Mg ha^{-1} to 7 Mg ha^{-1} west to east (>103°W to 98.5°W) and plateaued east of 98.5°W. Interannual Y_w variability was greater in the west (30% < CV < 50%) and decreased towards east (CV < 20%). Precipitation and PAW_s explained 81.7% of Y_w variation in the west and solar radiation 86.9% in the east. Water-productivity (24.2 to 10.2 kg ha^{-1} mm^{-1}) and transpiration-efficiency (25.8 to 22.5 kg ha^{-1} mm^{-1}) decreased, and RUE (0.43 to 1.15 g MJ^{-1}) increased, from west to east. While variety selection can improve acidic soils' productivity, great interannual Y_w variability likely renders producers reluctant when investing in the wheat crop and possibly contributes to the regional yield stagnation.

TABLE OF CONTENTS

Chapter Page

Chapter Page

Chapter Page

LIST OF TABLES

Table Page

Table Page

Table Page

Table Page

LIST OF FIGURES

Figure Page

Figure Page

Figure Page

Figure Page

Figure Page

CHAPTER I

INTRODUCTION, RESEARCH JUSTIFICATION, AND OBJECTIVES

1.1. INTRODUCTION

Wheat (*Triticum aestivum* L.), rice (*Oryza sativa* L.), and maize (*Zea Mays* L.) combined account for approximately 89% of global cereal production, and are major sources of human calories either directly consumed as staple food or indirectly as livestock fed with grain (Fig. 1.1). More than 215 million hectares of wheat were planted in 2013, with worldwide production greater than 715 million metric tons (FAOSTAT, 2014). The United States is the third major producer of wheat, accounting for approximately 58 million metric tons of wheat produced from a planted area of around 20 million hectares (FAOSTAT, 2014). While China and India usually have a greater total annual wheat production (Fig. 1.2A); the U.S. establishes its worldwide importance in the international wheat supply chain as the greatest wheat exporter (Fig. 1.2B), with more than 8 million metric tons annually exported which accounts for roughly 15% of its annual wheat production (FAOSTAT, 2014).

The majority of the wheat grown in the U.S. is winter wheat, and a great portion of its production comes from the Great Plains. In 2013, for instance, more than 41 million metric tons of winter wheat was produced in the U.S. from a planted area of approximately 17.5 million hectares (USDA-NASS, 2014). From this total, 16.4 million metric tons were harvested from an area of 10.7 million hectares

in the states that comprise the Great Plains: Colorado, Kansas, Nebraska, Oklahoma, South Dakota, Texas, and Wyoming (USDA-NASS, 2014). In this context, the southern Great Plains of the U.S., namely the states of Kansas, Oklahoma, and Texas, account for roughly 30% of the U.S. wheat production, with total annual production of hard red winter wheat around 13 million metric tons in a planted area of over 8.7 million hectares (USDA-NASS, 2014).

Despite the importance of the southern Great Plains to the U.S. wheat production, recent analysis of historical wheat yields in the region indicates that state level wheat yields in Kansas, Oklahoma, and Texas, have not surpassed 3 Mg ha^{-1} in the last 30-yr period and have been in a near stagnant state at ~2 Mg ha^{-1} since 1980 (Fig. 1.3, Patrignani et al., 2014). Similar yield plateaus are true for other wheat producing regions of the world, such as India, the Netherlands, United Kingdom, France, Germany, and Denmark (Grassini et al., 2013). A possible explanation for yield plateaus is that average farm yields are approaching the environmental-limited potential yield of that crop, and there is only a small exploitable gap remaining to increase yields (Lobell et al., 2009). This likely holds true for high-yielding systems such as wheat grown in Europe (Grassini et al., 2013). However, wheat yields in the southern Great Plains are remarkably low for cereal production in developed countries and are likely far below the environmental potential yield (Licker et al., 2010; Patrignani et al., 2014).

Recent efforts to elucidate the reasons behind the yield stagnation observed in the southern Great Plains indicate that neither a small remaining exploitable yield gap, nor inadequate total rainfall amount in the growing season or genetic yield potential of the current wheat cultivars, can be considered causes of the large wheat yield gap in the region (Patrignani et al., 2014). Instead, the observed yield plateau is more likely resultant from several other agronomic attributes of the system. Possible management practices behind the low yields may be the lack of crop rotation. Winter wheat yields have been shown to increase 10% or more when rotated with winter canola (Bushong et al., 2012); still, the main cropping system in the region is continuous monocrop winter wheat and many

producers are reluctant to adopt crop rotations (Patrignani et al., 2014). Dual-purpose wheat production, where wheat is grown for both forage and grain, also contributes to a certain extent of the yield stagnation as it accounts for ~50% of the area planted to wheat in Oklahoma (True et al., 2001) and leads to an average 14% decrease in grain yields due to sub-optimal planting date and biomass removal by cattle (Edwards et al., 2011). Another key factor that may be holding wheat yields at low levels in the southern Great Plains is poor soil quality. Conventional tillage practices coupled with high erodibility of most soils in the wheat producing region can decrease soil quality and impose severe limitations to increases in grain yield (Patrignani et al., 2014).

Limitations imposed by soil physical constraints are not the only problem in the southern Great Plains. Although acidity was not an inherent problem in most soils in the region, intensive monocropping wheat production and continuous use of nitrogen fertilizer resulted in increased acidification in many of the most fertile soils in the region. More than 35% of the fields in the central wheat growing region of Oklahoma had soil pH < 5.5 in a 1996 review of soil test results (Zhang et al., 1998), and there is no indication that pH levels have improved since the survey was conducted (Schroder et al., 2011). The low pH levels in continuous monocrop wheat systems likely result from heavy use of ammonium based fertilizers, which lead to topsoil acidification due to the net positive balance of hydrogen ions in the soil during the oxidation of ammonium to nitrate (Schroder et al., 2011). Soil acidification is further worsened by removal of basic cations during harvest of forage (e.g. grazing) and grain. A direct consequence of decreased soil pH is an exponential increase in aluminum (Al) solubility in the soil solution, as small decreases in soil pH can lead to large increases in Al solubility (Kariuki et al., 2007; Lollato et al., 2013). Increased Al solubility can result in Al toxicity to the crop, which is one of the major causes of crop failure in acidic soils in Oklahoma (Schroder et al., 2011). Liming is the recommended practice for alleviation of acidic soils (Zhang and Raun, 2006); still, the costs of lime application (Sloan et al., 1995) in addition to its uncertain net return (Liu et al., 2004; Lollato et al., 2013) may render producers reluctant when applying lime. Under these

circumstances, wheat varietal selection may be a viable avenue to overcome problems associated with acidic soils and maintain enterprise profitability (Johnson et al., 1997).

Furthermore, wheat producers in the southern Great Plains may not seek the highest attainable wheat yield, but actually seek to maximize profitability or minimize risks associated with year-to-year yield variability (Grassini et al., 2013; Patrignani et al., 2014). Wheat yields in the central region of Oklahoma are highly variable, with 5-yr running average coefficient of variation (CV) close to 25% (Fig. 1.4, Patrignani et al., 2014). This problem is particularly important in several regions of world where climate is uncertain and can vary substantially from one year to another (Connor et al., 2011). Limitations imposed by weather, such as inadequate rainfall distribution or high temperatures during critical phases of crop development, have been suggested as contributing to the year-to-year variability in wheat yields in the southern Great Plains (Barkley et al., 2014; Patrignani et al., 2014). Nonetheless, the extent to which weather limits winter wheat yield and contributes to yield variability in the region has not been quantified. Assessments of the influence of weather variables in cereal yields under non-limiting conditions can be performed using historical weather data to run validated crop simulation models, coupled with regression analysis of model's output against mean values of meteorological variables for the growing season (e.g. solar radiation, temperature, rainfall, and evaporative demand; e.g. Grassini et al., 2009). The advantages of using crop simulation models is that not only models can provide a very robust estimation of environmental potential yield for a certain crop at a given region, but simulations can be performed over several years and account for the year-to-year yield variability (Van Ittersum et al., 2013).

One drawback of using crop models is the time-consuming testing against reliable empirical data required before model analysis can be extrapolated to other environments and situations (Boote et al., 1996). Ideally, a robust testing of crop model performance includes detailed and consistent data covering several aspects of the soil-plant-atmosphere (Archontoulis et al., 2014; Lü et al., 2009). However, the scarcity of complete datasets encompassing below and aboveground crop dynamics

results in model evaluations restricted to limited datasets (Hunt and Boote, 1998) and can lead to the comparison of only few simulated variables to measured results, neglecting other critical components throughout the crop cycle (Sinclair and Seligman, 2000). Limited datasets are an especially important issue when simulating a crop's yield potential, given that these yield levels are achieved when crops are grown under non-limiting conditions (Fischer, 2007). Datasets where yield-limiting factors were effectively controlled and the crop actually reached the environmental potential yield are rare.

Environmental potential yield is the yield of a crop limited only by incident solar radiation, air temperature, and photoperiod (Fischer, 2007); conditions achieved when the crop is grown in the absence of limitations imposed by water and management (Evans and Fischer, 1999). In rainfed agricultural systems, environmental potential yield can be decreased due to lack of appropriate water supply and therefore it is crucial to account for the amount of water limitation in these environments (Connor et al., 2011). Determination of the potential yield of a crop in a given region is fundamental to elucidate the regional food production capacity (e.g. Lu and Fan, 2013), as well as to characterize the yield gap between actual- and potential- yields (Van Ittersum et al., 2013). Existing methods for determination of environmental potential yield are (i) well managed field experiments; (ii) yield contests among farmers; (iii) maximum farmer yields based on surveys; and (iv) validated crop simulation models (Lobell et al., 2009; Van Ittersum et al., 2013). Among the existing methods, validated mechanistic crop simulation models with plausible physiological and agronomic assumptions can provide the most robust and cost-effective estimations of environmental potential yield over several years (Cassman, 1999; Van Ittersum et al., 2013). Wheat potential yield has been assessed using crop simulation models across several of the most significant wheat producing regions of the globe (Table 1.1), including the Yaqui Valley in Mexico (Bell and Fischer, 1994; Lobell and Ortiz-Monasterio, 2006); throughout India (Aggarwal and Kalra, 1994); and across the wheat producing regions of Australia (Hochman et al., 2009; Peake et al., 2014) and China (Liang et al.,

2011; Lu and Fan, 2013). Still, a crop simulation study of the yield potential of winter wheat has not been performed in the southern Great Plains.

A very important component responsible for realization of yield potential of crops in rainfed systems, which also is crucial information when running crop simulation models, is plant available water at sowing (PAW_s). In rainfed cropping systems, PAW_s can account for a significant fraction of the total water available for crop transpiration throughout a crop's life cycle (Connor et al., 2011). Wheat yields have a positive linear relation to PAW_s; therefore, reduced PAW_s can result in decreased wheat yields (Lyon et al., 2007; Nielsen et al., 1999; Nielsen and Vigil, 2005; Nielsen et al., 2002; Norwood, 2000). Yield reductions from 39.7 kg ha^{-1} up to 141.2 kg ha^{-1} for every depleted centimeter of PAW at sowing have been reported across the Great Plains (Nielsen et al., 1999; Nielsen and Vigil, 2005; Nielsen et al., 2002; Norwood, 2000). A simulation analysis using long-term weather data in central Oklahoma indicated that wheat yields increase with increased PAW_s in dry growing seasons but are not as responsive when the growing season has abundant precipitation (Zhang, 2003). In addition to the importance of PAW at sowing for winter wheat grain yield, simulation of yield potential assuming a fully recharged soil profile can lead to erroneous conclusions about the system's yield and water-use efficiency (WUE; Grassini et al., 2009). Thus, a robust methodology to predict PAW_s can be a valuable tool for farmers and crop consultants to minimize agronomic risks based on long-term weather data (Virmani et al., 1982) as well as to researchers, improving the accuracy of crop simulation model predictions and estimations of the system's WUE.

Water-use efficiency is the efficiency with which a crop transforms water evaporated or transpired into biomass or grain yield (Tanner and Sinclair, 1983). For a given crop, grown under specific management conditions, WUE can be calculated as the slope of the relationship between aboveground biomass and cumulative crop evapotranspiration (ET_c; Fig. 1.5A) or as the ratio of grain yield over cumulative ET_c. Similarly, radiation-use efficiency (RUE) is the efficiency with which a crop transforms incident solar radiation into crop biomass (Sinclair and Muchow, 1999) and can be

calculated as the slope of the relationship between aboveground biomass and intercepted solar radiation (Fig. 1.5B). Within the context of this dissertation, WUE was calculated as the ratio of grain yield over total cumulative seasonal evapotranspiration and RUE was calculated as the slope of the relationship between aboveground biomass and cumulative intercepted solar radiation.

Resource-use efficiency can also be evaluated at a regional level rather than within a given experiment. Within the context of this dissertation, regional patterns of water productivity (WP) was evaluated using boundary function analysis of the most efficient points relating the 95th percentile grain yield to total water supply (PAW_s plus growing season precipitation). When evaluating regional patterns of transpiration efficiency (TE), the slope of the boundary function between grain yield and seasonal ET_c was used (French and Schultz, 1984). In this approach, the *x*-axis has either total water supply (PAW_s + growing season precipitation) or seasonal ET_c, and the *y*-axis has grain yield information (Fig. 1.6). The *x*-axis is divided into bins and a linear regression model is built between the average bin value and the 95th percentile yields (i.e. the values that most efficiently used the available resource). An additional feature of this approach is that the *x*-intercept is an indication of the amount of water lost during the growing season (French and Schultz, 1984). Quantifying the maximum attainable yield per unit of available resource is essential to create benchmarks for producers to target for and identify other yield reducing factors within their management (Passioura, 2006).

1.2. RESEARCH JUSTIFICATION

Detailed research justification for this research is given in the following chapters of this dissertation (Chapters II, III, IV, and V). Concisely, the southern Great Plains of the United States (32 – 40°N; 96 – 103°W) is among the most important wheat producing regions in the world, planting over 8 million hectares to winter wheat per year in the states of Kansas, Oklahoma, and Texas (USDA-NASS, 2014). This region is characterized by low yields (~2 Mg ha^{-1}), great year-to-year

variability, and accentuated yield variability and stagnation (Patrignani et al., 2014). Understanding the reasons behind yield variability and stagnation in this region is an important step to overcome yield limiting barriers and assure food security for an increasing global population.

Poor soil quality, great year-to-year weather variability, and minimal investment by the farmers, are suggested as contributors to wheat yield stagnation in the southern Great Plains (Connor et al., 2011; Patrignani et al., 2014). Understanding the effects of soil low pH on commercial wheat cultivars and linking variability of weather to wheat potential yield are important steps in understanding the causes of yield stagnation in Oklahoma and in the southern Great Plains. In order to perform the aforementioned analyses, this dissertation encompassed different studies, including: (i) testing different wheat varieties across a soil pH gradient to determine whether variety selection is a cost-effective alternative to overcome acidic soil problems; (ii) elucidating and characterizing environmental potential yield of winter wheat given non-limiting management conditions; (iii) calibration and validation of crop simulation models to represent the environmental potential yield; (iv) means to predict PAW_s, an important component of dryland winter wheat water budget in the growing season; and finally (v) long-term weather data to perform simulations of wheat maximum attainable yields. Results derived from this research may allow for strategic planning and resource allocation to help overcome the observed yield stagnation and enhance local and global food security (Cassman et al., 2003).

1.3. RESEARCH OBJECTIVES

The main objective of this research is to evaluate the extent to which acidic soils and meteorological variables influence winter wheat grain yields in the southern Great Plains as steps to elucidate the causes of yield stagnation in the region. To assess the extent which acidic soils contributes to yield stagnation; this dissertation begins evaluating the effects of a pH and Al concentration gradient on commercial winter wheat cultivars forage and grain yields (Chapter 2). This

dissertation then tests both mechanistic and empirical approaches to predict PAW_s in continuous wheat systems of the southern Great Plains, a critical component of the total water supply for dryland winter wheat that can culminate in more accurate simulations of wheat yields (Chapter 3). After that, the study determines winter wheat potential yield at field level in several site-years across Oklahoma by providing the crop with non-limiting management conditions, while concomitantly creating a broad dataset of winter wheat growth, development, yield, and resource use efficiency (Chapter 4). This dataset is then used to evaluate the performance of a dynamic crop simulation model with robust agronomic assumptions when simulating winter wheat growth, development, and yield, under non-limiting conditions (Chapter 5). Finally, still in Chapter 5, this dissertation presents a long-term simulation assessment of winter wheat potential yield across several locations in the southern Great Plains, which aims to identify the most sensitive meteorological factors accounting for variation in wheat potential grain yield. The main findings were summarized on Chapter 6, together with questions that arose from this research and future steps in the assessment of regional winter wheat cropping systems.

1.4. REFERENCES

Aggarwal, P.K. and N. Kalra. 1994. Analyzing the limitations set by climatic factors, genotype, and water and nitrogen availability on productivity of wheat. 2. Climatically potential yields and management strategies. Field Crops Res. 38: 93-103.

Aggarwal, P.K., N. Kalra, A.K. Singh and S.K. Sinha. 1994. Analyzing the limitations set by climatic factors, genotype, and water and nitrogen availability on productivity of wheat. 1. The model description, parametrization and validation. Field Crops Res. 38: 73-91.

Archontoulis, S.V., F.E. Miguez and K.J. Moore. 2014. Evaluating APSIM maize, soil water, soil nitrogen, manure, and soil temperature modules in the Midwestern United States. Agron. J. 106: 1025-1040.

Asseng, S., B.A. Keating, I.R.P. Fillery, P.J. Gregory, J.W. Bowden, N.C. Turner, et al. 1998. Performance of the APSIM-Wheat model in Western Australia. Field Crops Res. 57: 163-179.

Barkley, A., J. Tack, L.L. Nalley, J. Bergtold, R. Bowden and A. Fritz. 2014. Weather, disease, and wheat breeding effects on Kansas wheat varietal yields, 1985 to 2011. Agron. J. 106: 227-235.

Bell, M.A. and R.A. Fischer. 1994. Using yield prediction models to assess yield gains - a case-study for wheat. Field Crops Res. 36: 161-166.

Boote, K.J., J.W. Jones and N.B. Pickering. 1996. Potential uses and limitations of crop models. Agron. J. 88: 704-716.

Bushong, J.A., A.P. Griffith, T.F. Peeper and F.M. Epplin. 2012. Continuous winter wheat versus a winter canola-winter wheat rotation. Agron. J. 104: 324-330.

Cassman, K.G. 1999. Ecological intensification of cereal production systems: Yield potential, soil quality, and precision agriculture. Proceedings of the National Academy of Sciences 96: 5952-5959.

Cassman, K.G., A. Dobermann, D.T. Walters and H. Yang. 2003. Meeting cereal demand while protecting natural resources and improving environmental quality. Annual Review of Environment and Resources 28: 315-358.

Connor, D.J., R.S. Loomis and K.G. Cassman. 2011. Crop ecology: Productivity and management in agricultural systems. Cambridge Univ. Press, Cambridge, UK.

Edwards, J.T., B.F. Carver, G.W. Horn, and M.E. Payton. 2011. Impact of dual-purpose management on wheat grain yield. Crop Sci. 51: 2181-2185.

Evans, L.T. and R.A. Fischer. 1999. Yield potential: Its definition, measurement, and significance. Crop Sci. 39: 1544-1551.

FAOSTAT. 2014. Food and Agriculture Organization of the United Nations. Available at: http://faostat.fao.org/ (acessed 05 august 2014).

Fischer, R.A. 2007. Understanding the physiological basis of yield potential in wheat. J. Agric. Sci. 145: 99-113.

French, R.J. and J.E. Schultz. 1984. Water-use efficiency of wheat in a Mediterranean-type environment.1. The relation between yield, water-use and climate. Aust. J. Agric. Res. 35: 743-764.

Grassini, P., K.M. Eskridge and K.G. Cassman. 2013. Distinguishing between yield advances and yield plateaus in historical crop production trends. Nature Communications 4.

Grassini, P., H.S. Yang and K.G. Cassman. 2009. Limits to maize productivity in Western Corn-Belt: A simulation analysis for fully irrigated and rainfed conditions. Agric. For. Meteorol. 149: 1254-1265.

Hochman, Z., D. Holzworth and J.R. Hunt. 2009. Potential to improve on-farm wheat yield and WUE in australia. Crop & Pasture Science 60: 708-716.

Hunt, L. and K. Boote. 1998. Data for model operation, calibration, and evaluation: understanding options for agricultural production. Springer. p. 9-39.

Johnson, J.P., B.F. Carver, and V.C. Baligar. 1997. Productivity in Great Plains acid soils of wheat genotypes selected for aluminium tolerance. Plant Soil 188: 101-106.

Kariuki, S.K., H. Zhang, J.L. Schroder, J. Edwards, M. Payton, B.F. Carver, et al. 2007. Hard red winter wheat cultivar responses to a pH and aluminum concentration gradient. Agron. J. 99: 88-98.

Liang, W.L., C. Peter, G.Y. Wang, R.H. Lu, H.Z. Lu and A.P. Xia. 2011. Quantifying the yield gap in wheat-maize cropping systems of the Hebei Plain, China. Field Crops Res. 124: 180-185.

Licker, R., M. Johnston, J.A. Foley, C. Barford, C.J. Kucharik, C. Monfreda, et al. 2010. Mind the gap: How do climate and agricultural management explain the 'yield gap' of croplands around the world? Global Ecol. Biogeogr. 19: 769-782.

Lobell, D.B., M.B. Burke, C. Tebaldi, M.D. Mastrandrea, W.P. Falcon and R.L. Naylor. 2008. Prioritizing climate change adaptation needs for food security in 2030. Science 319: 607-610.

Lobell, D.B., K.G. Cassman and C.B. Field. 2009. Crop yield gaps: Their importance, magnitudes, and causes. Annual Review of Environment and Resources 34: 179-204.

Lobell, D.B. and J.I. Ortiz-Monasterio. 2006. Evaluating strategies for improved water use in spring wheat with CERES. Agric. Water Manage. 84: 249-258.

Lollato, R.P., J.T. Edwards and H.L. Zhang. 2013. Effect of alternative soil acidity amelioration strategies on soil pH distribution and wheat agronomic response. Soil Sci. Soc. Am. J. 77: 1831-1841.

Lu, C.H. and L. Fan. 2013. Winter wheat yield potentials and yield gaps in the North China Plain. Field Crops Res. 143: 98-105.

Lü, H., W. Liang, G. Wang, D.J. Connor and G.M. Rimmington. 2009. A simulation model assisted study on water and nitrogen dynamics and their effects on crop performance in the wheat-maize system: (ii) model calibration, evaluation and simulated experimentation. Frontiers of Agriculture in China 3: 109-121.

Lyon, D.J., D.C. Nielsen, D.G. Felter and P.A. Burgener. 2007. Choice of summer fallow replacement crops impacts subsequent winter wheat. Agron. J. 99: 578-584.

Muchow, R.C. and T.R. Sinclair. 1994. Nitrogen response of leaf photosynthesis and canopy radiation-use efficiency in field-grown maize and sorghum. Crop Sci. 34: 721-727.

Nielsen, D.C., R.L. Anderson, R.A. Bowman, R.M. Aiken, M.F. Vigil and J.G. Benjamin. 1999. Winter wheat and prose millet yield reduction due to sunflower in rotation. J. Prod. Agric. 12: 193-197.

Nielsen, D.C. and M.F. Vigil. 2005. Legume green fallow effect on soil water content at wheat planting and wheat yield. Agron. J. 97: 684-689.

Nielsen, D.C., M.F. Vigil, R.L. Anderson, R.A. Bowman, J.G. Benjamin and A.D. Halvorson. 2002. Cropping system influence on planting water content and yield of winter wheat. Agron. J. 94: 962-967.

Norwood, C.A. 2000. Dryland winter wheat as affected by previous crops. Agron. J. 92: 121-127.

Passioura, J. 2006. Increasing crop productivity when water is scarce - from breeding to field management. Agric. Water Manage. 80: 176-196.

Patrignani, A., R.P. Lollato, T.E. Ochsner, C.B. Godsey and J. Edwards. 2014. Yield gap and production gap of rainfed winter wheat in the southern Great Plains. Agron. J. 106: 1329 - 1339.

Peake, A.S., N.I. Huth, P.S. Carberry, S.R. Raine and R.J. Smith. 2014. Quantifying potential yield and lodging-related yield gaps for irrigated spring wheat in sub-tropical Australia. Field Crops Res. 158: 1-14.

Sadras, V.O. and J.F. Angus. 2006. Benchmarking water-use efficiency of rainfed wheat in dry environments. Aust. J. Agric. Res. 57: 847-856.

Schroder, J.L., H.L. Zhang, K. Girma, W.R. Raun, C.J. Penn and M.E. Payton. 2011. Soil acidification from long-term use of nitrogen fertilizers on winter wheat. Soil Sci. Soc. Am. J. 75: 957-964.

Sinclair, T.R., and R.C. Muchow. 1999. Radiation use efficiency. Adv. Agron. 65: 215-265.

Sinclair, T.R. and N. Seligman. 2000. Criteria for publishing papers on crop modeling. Field Crops Res. 68: 165-172.

Sloan, J.J., N.T. Basta, and R.L. Westerman. 1995. Aluminum transformations and solution equilibria induced by banded phosphorus-fertilizer in acid soil. Soil Sci. Soc. Am. J. 59: 357-364.

Tanner, C.B. and T.R. Sinclair. 1983. Efficient water use in crop production: Research or re-search? In: H. M. Taylor, W. R. Jordan and T. R. Sinclair, Eds., Limitations to efficient water use in crop production. ASA-CSSA-SSSA, Madison, WI. p. 1-27.

True, R.R., F.M. Epplin, E.G. Krenzer, and G.W. Horn. 2001. A survey of wheat production and wheat forage use practices in Oklahoma. B-815. Okla. Coop. Ext. Serv., Stillwater, OK.

USDA-NASS. 2014. United States Department of Agriculture. National Agricultural Statistics Service. Available at: http://www.nass.usda.gov/Statistics_by_State/Oklahoma/Publications/County_Estimates/index.asp (data retrieved July 2014).

Van Ittersum, M.K., K.G. Cassman, P. Grassini, J. Wolf, P. Tittonell and Z. Hochman. 2013. Yield gap analysis with local to global relevance-a review. Field Crops Res. 143: 4-17.

Virmani, S., M. Sivakumar and S. Reddy. 1982. Rainfall probability estimates for selected locations of semi-arid India. Research bulletin no. 1.

Zhang, H.L., G. Johnson, G. Krenzer and R. Gribble. 1998. Soil testing for an economically and environmentally sound wheat production. Commun. Soil Sci. Plant Anal. 29: 1707-1717.

Zhang, H., and W.R. Raun. 2006. Oklahoma soil fertility handbook, Dept. of Plant and Soil Sci., Oklah. St. Univ., Stillwater, OK.

Table 1.1. Compilation of regional assessments of winter wheat yield potential using crop simulation models for different regions of the world.

Country	Region	Crop simulation model	Years	Locations	Management	Yield potential	Reference
			———	n ———		Mg ha^{-1}	
Mexico	Yaqui Valley	CERES Wheat Photothermal quotient (PQT)	22	1	Irrigated	6.9 - 7.3 6.3	Bell and Fischer, 1994
Mexico	Yaqui Valley	CERES Wheat	23	1	Irrigated†	5.5 - 8.1	Lobell and Ortiz-Monasterio, 2006
Argentina	Pampas	CERES Wheat	30	15	Rainfed	5.0 - 7.3	Menendez and Satorre, 2007
India	Entire country	WTGROWS	20	138	Rainfed	2.6 - 8.3	Aggarwal and Kalra, 1994
Australia	Victoria, South Australia, New South Wales, Western Australia, and Queensland	APSIM	4	334	Rainfed	2.6	Hochman et al., 2009
Australia	Queensland and New South Wales	APSIM	111	3	Irrigated	8.0 - 9.0	Peake et al., 2014
Russia	Entire country	SWAT	15	28	Rainfed Irrigated	2.7 - 4.6 4.6 - 5.6	Schierhorn et al., 2014
Spain	Ebro Valley	CERES Wheat	17	1	Rainfed	3.5 - 8.1	Abeledo et al., 2008
China	Hebei Plain	-‡	1	365	Rainfed	10.7 - 12.6	Wei-li et al., 2011
China	Entire country	EPIC	47	43	Rainfed	6.6 - 9.1	Lu and Fan, 2013

† - Several irrigation treatments were evaluated. Values in this table represent the maximum number of irrigation events in the growing season.

‡ - Crop simulation model used to assess regional yield potential does not have a name.

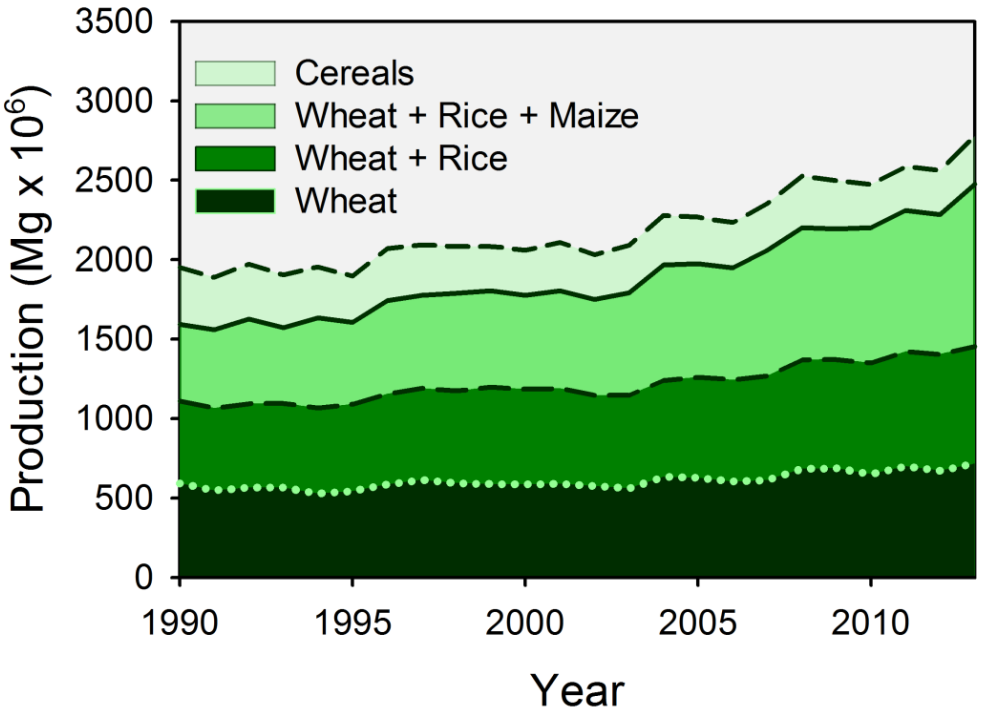

Figure 1.1. Total world production of wheat, rice, maize, and cereals. Data spans the time period between 1990 and 2013. Data retrieved from FAOSTAT (2014).

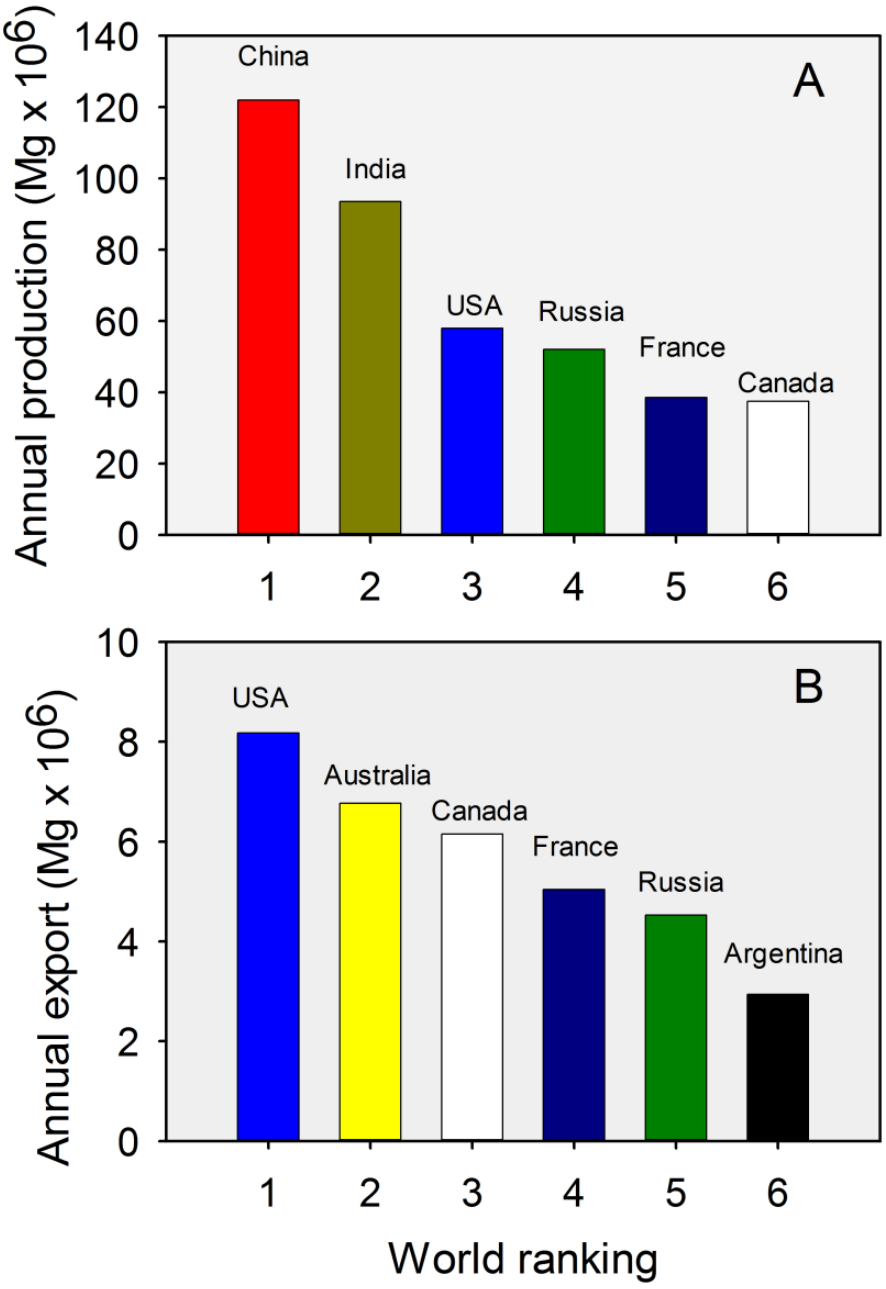

Figure 1.2. World ranking of (A) wheat annual production by country and (B) wheat annual export by country. Data retrieved from FAOSTAT (2014).

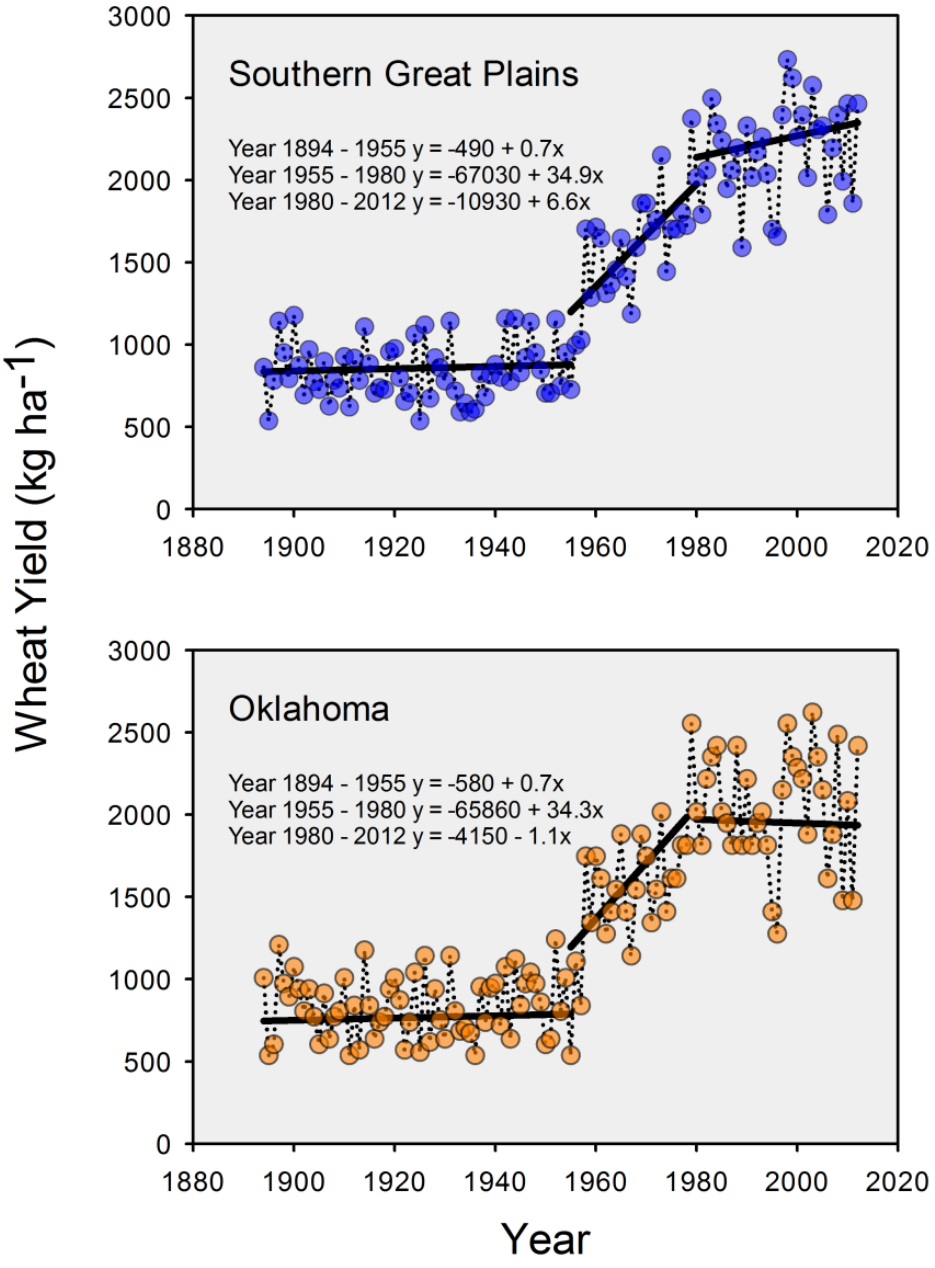

Figure 1.3. Timeline showing the evolution of winter wheat grain yield in the (A) southern Great Plains (SGP), and (B) Oklahoma. Data spans the period from 1894 to 2012. Trend lines were calculated for the period of 1894 to 1955, 1955 to 1980, and 1980 to 2012. Data were obtained from the USDA National Agricultural Statistics Service. Figure adapted from Patrignani et al., 2014.

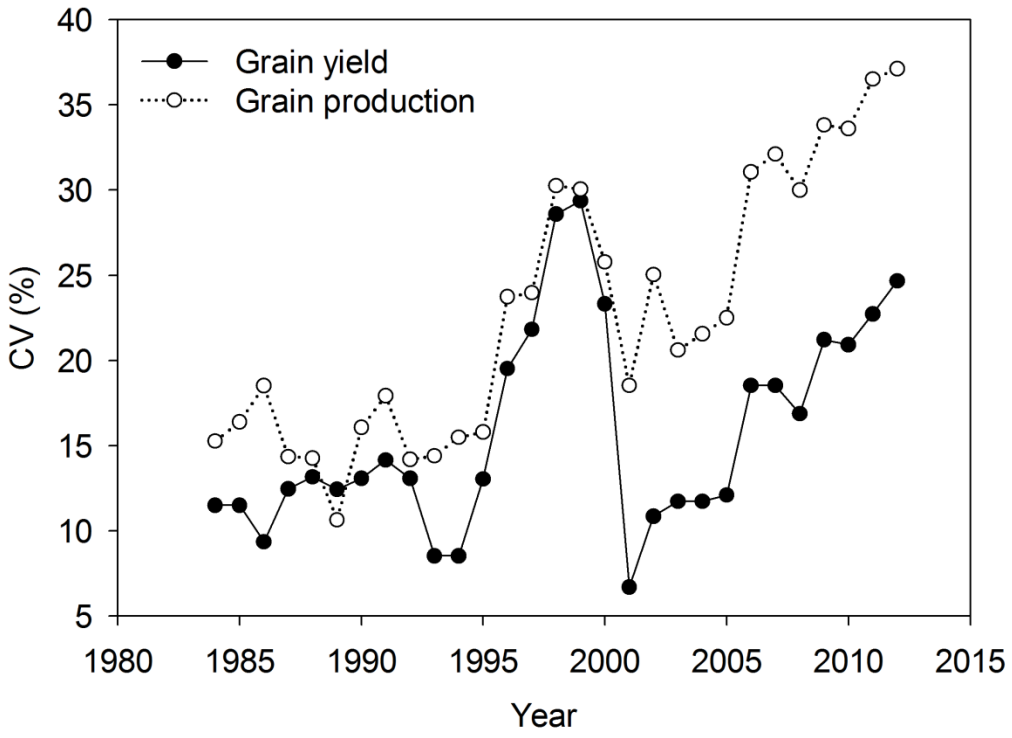

Figure 1.4. Time series of the 5-yr coefficient of variation (CV) of Oklahoma hard red winter wheat yield and production. Data are plotted as the CV for the preceding 5 yr. Adapted from Patrignani et al., 2014.

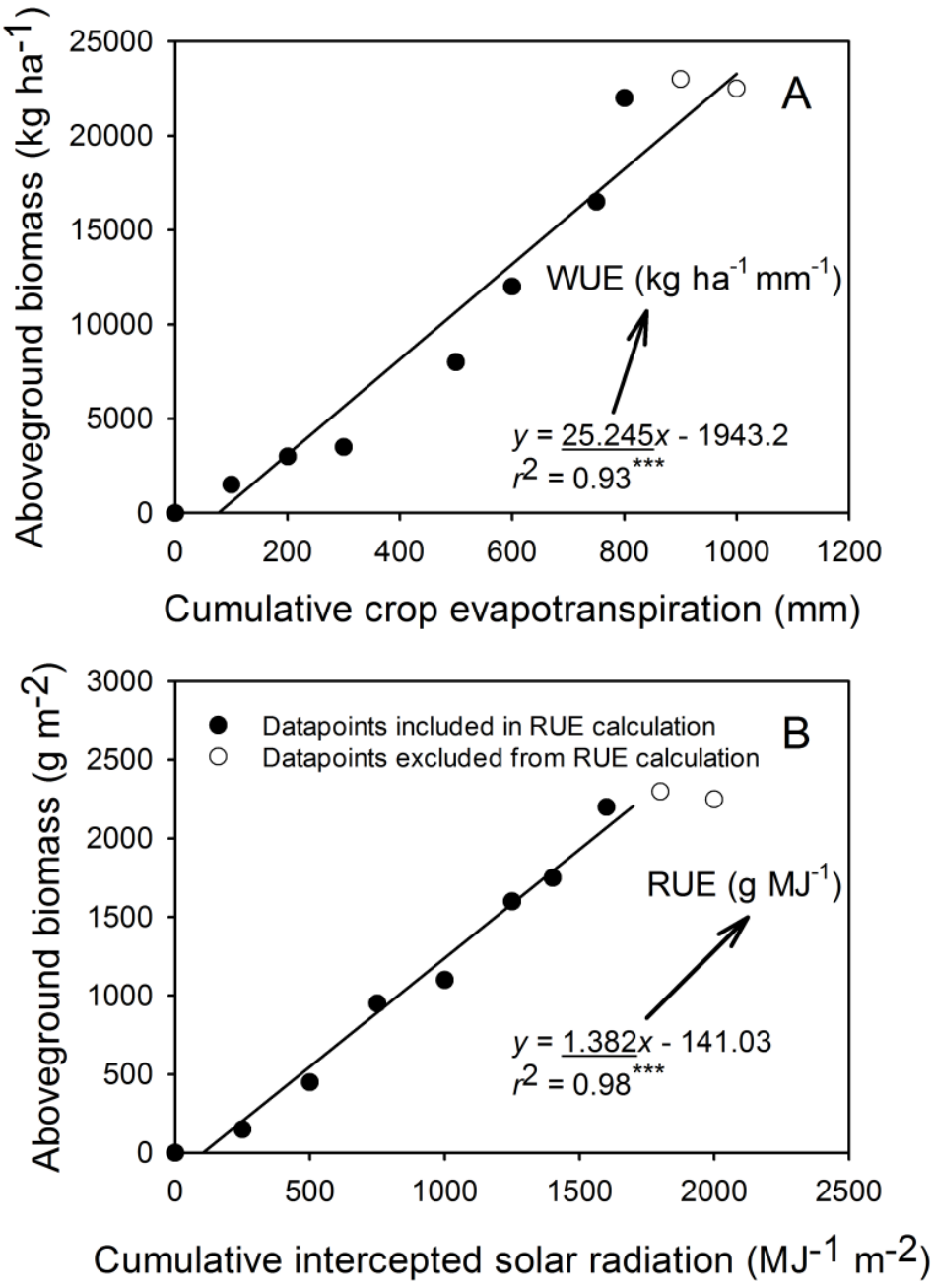

Fig. 1.5. Relationship between aboveground biomass and (A) cumulative crop evapotranspiration and derivation of water-use efficiency (WUE), and (B) cumulative intercepted solar radiation and derivation of radiation-use efficiency (RUE). Points towards physiological maturity typically result in lower estimates of WUE or RUE and are not included in the analyses (Muchow and Sinclair, 1994). Panels (A) and (B) were built with random data and do not represent actual experiments.

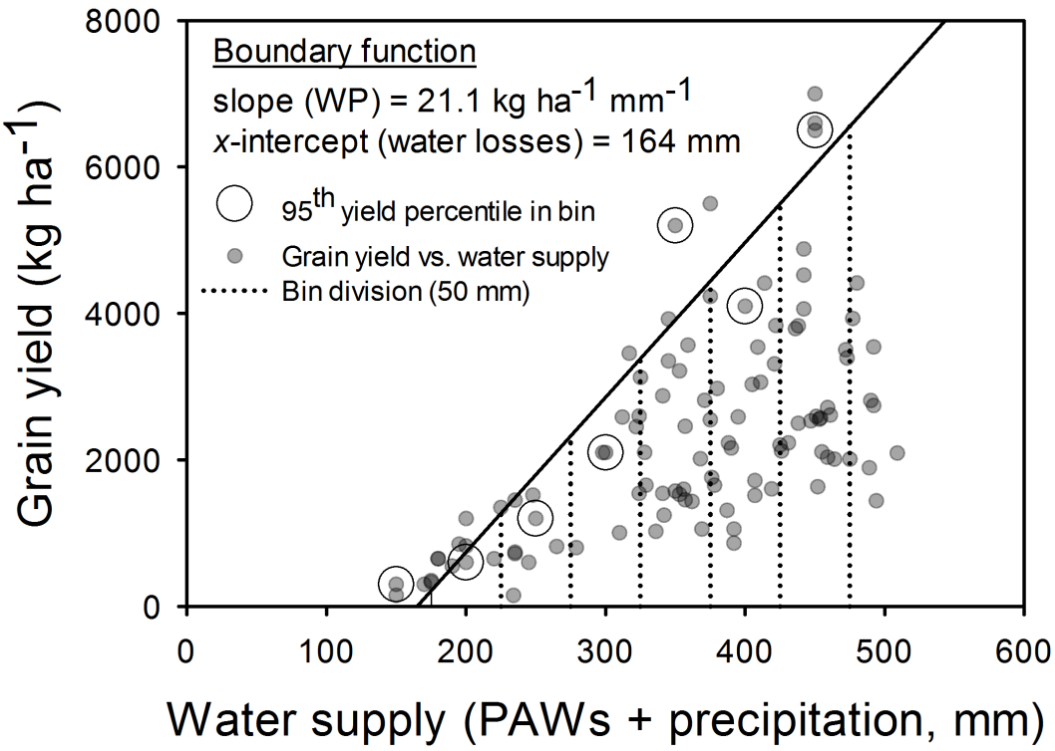

Figure 1.6. Methodology to evaluate water productivity (WP) in regional assessments as the slope of the relationship between grain yield and seasonal water supply [plant available water at sowing (PAW_s) plus precipitation] suggested by French and Schultz (1984). Water losses are assessed as the *x*-intercept of the linear regression. Bin division are 95th grain yield percentile within each bin used for the linear fit are shown. Figure built with random data and does not represent actual experiments.

CHAPTER II

EFFECTS OF A pH AND ALUMINUM CONCENTRATION GRADIENT ON DUAL-PURPOSE AND GRAIN ONLY HARD RED WINTER WHEAT PRODUCTIVITY

ABSTRACT

Soil acidification has become a major yield limiting factor for winter wheat (*Triticum aestivum* L.) in the southern Great Plains, where wheat is grown for forage and grain (dual purpose) or grain only. Variety selection may be a cost-effective measure to overcome low soil pH constraints. Our objective was to evaluate different wheat varieties' susceptibility to a soil pH and aluminum (Al) concentration gradient under both dual-purpose and grain-only management. A split-plot arrangement of a randomized complete block design with three replications was conducted for three growing seasons (2012-13 to 2014-15) at Stillwater (dual-purpose site) and Chickasha (grain only site), OK. Main plots were six target levels of soil pH ranging from 4 to 7 and subplots were the wheat varieties 2174, Duster, Ruby Lee, and TAM 203. Measurements included percent wheat emergence, percent canopy closure, normalized difference vegetative index (NDVI) and its coefficient of variation (CV), fall forage yield, grain yield, grain volume weight, and grain protein concentration. Soil pH < 4.5 decreased wheat emergence at Stillwater for all varieties, and soil pH < 5.2 at Chickasha for the sensitive varieties, respectively. Aluminum saturation (Al_{sat}) linearly decreased wheat emergence at five out of six site-years. Soil

pH < 4.5 delayed the increased in percent canopy cover, decreased maximum percent canopy cover from >80% to < 40% when compared to plots where pH > 7, and decreased plant population homogeneity (NDVI CV > 17%). Maximum forage yields were achieved at soil pH of 5.5, 5.9, 5.9, and 6 and maximum relative grain yields were achieved at soil pH of 4.8, 4.8, 5.8, and 5.5 for 2174, Duster, Ruby Lee, and TAM 203. Increased Al_{sat} linearly decreased forage (~89 to 96 kg ha^{-1} Al_{sat}^{-1}) and relative grain yields (0 to 1.5% Al_{sat}^{-1}). Wheat forage yield is more sensitive to decreased pH than grain yield, and variety selection can be used as a cost-effective tool to overcome acidic soil conditions.

Key words: soil pH, extractable aluminum, aluminum saturation, acidic soils, wheat, dual purpose, forage, variety selection.

Abbreviations: Al_{KCl}: potassium-chloride extractable aluminum; Al_{sat}: aluminum saturation, ECEC: effective cation exchange capacity, ET_o: reference evapotranspiration; NDVI: normalized difference vegetative index; CV: coefficient of variation.

2.1. INTRODUCTION

Hard red winter wheat is a crucial component of farm income in the southern Great Plains, with a planted area of over eight million hectares per year among the states of Texas, Oklahoma, and Kansas (USDA-NASS, 2014). In Oklahoma, winter wheat is planted in approximately 2.4 million hectares every year, representing as much as 75% of total planted cropland in the state and around 20% of the total winter wheat planted in the Great Plains (USDA-NASS, 2014). Wheat is managed as a forage and grain crop (dual purpose) in approximately half of the area planted to winter wheat in Oklahoma (True et al., 2001), which offers a more stable source of income by diversifying and producing both stocker cattle (*Bos Taurus* L.) and grain (Redmon et al., 1996).

Although acidity was not an inherent problem in many Oklahoma soils, intensive monocropping wheat production and continuous use of nitrogen fertilizer resulted in increased soil acidification in many Oklahoma fields. More than 35% of the fields in the central wheat growing region of Oklahoma had a soil pH < 5.5 in a 1996 review of soil test results (Zhang et al., 1998), and there is no indication that pH levels have improved since the survey was conducted (Schroder et al., 2011). The observed low pH levels in continuous monocropping wheat systems likely results from heavy use of ammonium based fertilizers, which leads to topsoil acidification due to the net positive balance of hydrogen ions in the soil during the oxidation of ammonium to nitrate (Schroder et al., 2011). Soil acidification is further worsened by removal of basic cations during harvest of forage (e.g. grazing) and grain.

A direct consequence of decreased soil pH is an exponential increase in aluminum (Al) solubility in the soil solution. Potassium chloride-extracted aluminum (Al_{KCl}) and aluminum saturation (Al_{sat}) have an inverse exponential relationship with soil pH, and small decreases in soil pH can lead to increases of great magnitude in Al_{KCl} and Al_{sat} at soil pH levels < 5 (Kariuki et

al., 2007; Lollato et al., 2013). Increased Al solubility can result in Al toxicity to the crop, which is one of the major causes of crop failure in extreme acidic soils in Oklahoma (Schroder et al., 2011). Wheat responses to Al toxicity include decreased root growth, resulting in a reduced capacity of the root system to explore soil for moisture and nutrients (Tang et al., 2003). This further results in reduced aboveground biomass and forage production (Kaitibie et al., 2002; Kariuki et al., 2007), and, consequently, reduced grain yield (Kariuki et al., 2007; Valle et al., 2009). If the soil has acceptable levels of base cations, the presence of Al_{KCl} per se may not induce Al toxicity symptoms in the crop (Johnson et al., 1997). Hence, a more consistent indicator of Al toxicity potential is the Al_{sat}, a measure of Al concentration expressed as a percentage of total exchangeable base cations (i.e. Ca, Mg, K, and Na) of the soil (Sumner and Miller, 1996). Due to differences in soil chemical properties and texture in the Great Plains, fields with similar soil pH can result in vastly different Al_{sat} (Johnson et al., 1997), affecting wheat grain yield in different ways (Kariuki et al., 2007; Schroder et al., 2011).

Dual-purpose wheat production is more affected by soil acidity than grain only wheat. A summary of 20 years of grazing research in Oklahoma indicated that grazing per se often offers yield penalty to winter wheat grain yields (Edwards et al., 2011). In addition, Kariuki et al. (2007) showed that soil acidity has greater impact on wheat forage production than on wheat yields, with pH thresholds for critical forage production greater (i.e. mean 6.3) than for grain yield (i.e. mean 5.8). The greater decrease in wheat forage production by low pH soils in addition to the decreased yield due to grazing indicate a more detrimental effect of acidic soils on dual-purpose wheat production, which represents roughly 50% of total wheat production in Oklahoma.

Broadcast incorporated agricultural lime is the most frequently recommended method for managing low pH and high Al_{KCl} and Al_{sat} soils, and its effectiveness is well documented (Kaitibie et al., 2002; Liu et al., 2004; Tang et al., 2003). In wheat production systems of Oklahoma, agricultural lime is the suggested management practice for soil acidity amelioration

(Zhang and Raun, 2006). However, its application does not always result in increased wheat grain yields (Liu et al., 2004; Lollato et al., 2013). Additionally, economics of liming due to large amounts of product required or transportation costs (Sloan et al., 1995) and increased soilborne disease pressure (Christensen et al., 1987) sometimes makes producers reluctant when applying lime to overcome low soil pH.

An alternative to agricultural lime when cultivating wheat in low pH soils is adoption of Al-tolerant cultivars (Johnson et al., 1997). Wheat sensitivity to soil pH and Al are cultivar specific (Kariuki et al., 2007; Valle et al., 2009), and cultivars with increased tolerance to Al show greater nutrient uptake than non-tolerant cultivars (Lidon and Barreiro, 2002) due to inhibition of root growth in the latter (Kochian, 1995). Tolerance to soluble Al has been associated with exudation of organic acid (e.g. citrate and malate) by the roots, which increases nutrient solubility and can complex Al and hinder its impacts on the crop (Yang et al., 2004). Still, even cultivars with increased tolerance to Al may be impacted by high Al levels. For instance, Kariuki et al. (2007) showed that while Al sensitive cultivars had a rate of decrease in grain yield of 30.7 to 38.7 kg ha^{-1} per unit increase in Al_{sat}, the rate of decrease in grain yield per unit Al_{sat} declined to 10.8 to 14.3 kg ha^{-1} in Al tolerant cultivars. While Al_{sat} above 30% led to complete crop failure in Al sensitive cultivars, the yield reduction in Al tolerant cultivars associated with increased Al_{sat} ranged from 12 to 52%. In the same study, Kariuki et al. (2007) found that some cultivars respond linearly to augment in soil pH and others present a linear-plateau response, with the threshold varying with cultivar. While most of the cultivars studied by Kariuki et al. (2007) tended to show an yield plateau at pH levels of 5.5 or higher and to be strongly affected by soil pH levels lower than that, recent studies in Oklahoma indicate other modern wheat varieties may be more tolerant to low soil pH, with no increase in grain yield as affected by an increase in soil pH from 4.9 to 5.9 (Lollato et al., 2013).

Testing wheat cultivars in extreme pH values such as a pH of 4.2 versus a limed control (Carver et al., 2003) is one approach often adopted to rank cultivars in their response to soil pH. However, this approach limits the possibility of optimizing pH for individual cultivars by restricting the range of pH needed to obtain a response threshold (Kariuki et al., 2007). Another methodology to quantify cultivar responses to soil pH and Al concentration is to measure root development of plants grown in nutrient solution with various concentration of Al (Bolt, 1996). Still, results obtained from nutrient-solution cultures may differ from field conditions and there are insufficient quantitative data to extrapolation results from one environment to the other (Kariuki et al., 2007). To overcome this barrier, creating a soil pH gradient from approximately 4.0 to 7.0 with the aid of amendments and testing modern wheat cultivars over this pH range is a valuable option that allows determination of critical pH and Al concentration thresholds below which farmers should adopt alternative acidity amelioration practices. This approach has been adopted for several crops such as grain sorghum (Butchee et al., 2012), sunflower (Sutradhar et al., 2014), and for wheat in Chile (Valle et al., 2009), and for older cultivars of wheat in the southern Great Plains (Kariuki et al., 2007). However, it has not been performed for modern cultivars with widespread use in the state.

Given the importance of wheat to the Oklahoma agricultural economy, evaluating the agronomic behavior and developing new thresholds of responses of modern wheat varieties' forage production and grain yield to soil pH and Al concentration is warranted to guide wheat producers in choosing appropriate cultivars suitable for their conditions. Thus, the objective of this study was to quantitatively assess the effects of a pH and Al-concentration gradient on growth, development, and forage and grain yields of commercial wheat varieties differing in Al sensitivity under dual-purpose and grain only management.

2.2. MATERIAL AND METHODS

2.2.1. Sites, treatments, and experimental design

Two field experiments were initiated in the 2012-13 winter wheat growing season and conducted over three years on a Dale silt loam (Fine-silty, mixed, superactive, thermic Pachic Haplustolls) at the Oklahoma State University (OSU) South Central Agricultural Research Station in Chickasha, OK (35.05° N, 97.91° W, and elevation 333 m), and on a Easpur loam (Fine-loamy, mixed, superactive, thermic Fluventic Haplustolls) at the OSU Agronomy Research Station in Stillwater, OK (36.13° N, 97.10° W, and elevation 270 m). A six by four treatment structure was arranged in split plot design with three replications and main plots arranged as randomized complete block design. Main plots were 7.6-m long by 7.6-m wide separated by a 1.5-m alley, and subplots were 6.1-m long by 1.2-m wide, with 17-cm row spacing. Main plots were target soil pH, which ranged from 4.0 to 7.0 (i.e. 4.0, 4.5, 5.0, 5.5, 6.0, and 7.0), and sub-plots were wheat cultivar, completely randomized within main plots.

The four cultivars evaluated in this study were Ruby Lee, Duster, TAM 203, and 2174, which are four commonly grown hard red winter wheat varieties in the southern Great Plains. Duster and Ruby Lee together accounted for 19.1% of the wheat grown in Oklahoma during the 2014-15 growing season (USDA-NASS, 2015), and still the threshold pH below which these varieties show yield losses have not been established. Previous work evaluating these varieties' tolerances to soil pH < 4.7 indicate high susceptibility of TAM 203 (Edwards et al., 2012), moderate susceptibility of Ruby Lee (Edwards, 2013), a relative tolerance of 2174 (Kariuki et al., 2007), and a high tolerance to low soil pH by Duster (Edwards et al., 2012). Experiments were placed within 1500 m from an environmental monitoring station from the Oklahoma Mesonet network (McPherson et al., 2007), which provided daily weather data used to calculate daily reference evapotranspiration (ET_o) according to the FAO-56 procedure (Allen et al., 1998).

Hydrated lime ($Ca(OH)_2$) and aluminum sulfate ($Al_2(SO_4)_3$) were applied to each main plot to obtain target soil pH (Butchee et al., 2012; Sutradhar et al., 2014). The amount of material needed to reach a given target soil pH was determined with a laboratory experiment conducted in 2012 to develop a response curve to the soil of each location, as described by Butchee et al. (2012). In this approach, composite soil samples were collected from both experimental sites to characterize initial soil pH using a combination pH electrode in a 1:1 soil/deionized water suspension (Thomas, 1996). Subsamples weighing 500 g were taken from each composite sample and mixed with five incremental rates of $Al_2(SO_4)_3$ and $Ca(OH)_2$. The samples were then wetted and, after two, three, and four weeks, soil pH of each subsample was measured. The resultant relationship between pH values and $Ca(OH)_2$ and $Al_2(SO_4)_3$ was studied to produce response curves for each study location from which the amount of $Ca(OH)_2$ and $Al_2(SO_4)_3$ needed to achieve a target soil pH was determined. Hydrated lime was applied to raise or $Al_2(SO_4)_3$ was used to lower actual pH to the target pH according to initial soil pH values. Treatments were applied few months before planting and plots were cultivated to incorporate the amendment products down to approximately 20 cm depth, which represents the typical surface acidic layer depth in Oklahoma (Schroder et al., 2011). Initial soil fertility and amount of amendment needed to change soil pH by a unit for both locations are shown in Table 2.1.

2.2.2. Wheat management

Wheat managed for dual-purpose production is generally planted 1 mo earlier in the season at planting densities 1.5 to 2 times greater as compared to grain only, allowing for greater biomass production and extended grazing period (Edwards et al., 2011). Thus, wheat was sown 18 Sept. 2012, 19 Sept. 2013, and 17 Sept. 2014 at Stillwater, which served as dual-purpose experimental site; and 18 Oct. 2012, 22 Oct. 2013, and 21 Oct. 2014 at Chickasha, the grain only experimental site. Conventional tillage methods were adopted so that less than ~10% of previous crop residue remained at soil surface at time of planting, and both sites were sown with a Hege

small-plot conventional drill (Wintersteiger, Salt Lake City, UT). Planting density was 4.2 million seeds ha^{-1} (approximately 134 kg seed ha^{-1}) at the dual-purpose site, and 2.1 million seeds per ha^{-1} (approximately 67 kg seed ha^{-1}) at the grain only site.

Nitrogen management occurred according to Oklahoma State University extension recommendations for a 3000 kg ha^{-1} wheat forage crop followed by a 4000 kg ha^{-1} grain crop. Thus, soil samples (0 – 46 cm) were taken approximately 1 month before planting each year and preplant N in form of urea (46-0-0) was applied to ensure that 100 kg ha^{-1} N was available for wheat fall forage growth. Simulated grazing occurred at Stillwater using a rotary-blade, self-propelled mower with bagging attachment (Hustler manufacturing, Hesston, KS) following the procedure adopted by Butchee and Edwards, 2013. Plots were mowed at approximately 9 cm height in 04 Dec. 2013 and 11 Dec. 2014 (approximately 8-9 weeks after emergence). Topdress N (46-0-0) was applied just before jointing to ensure that 120 kg ha^{-1} was available for wheat grain production. Weeds and insects were controlled using commercially available pesticides as needed. Plots were treated with 0.09 kg ha^{-1} of propiconazole (1-[[2-(2,4-dichlorophenyl)-4-propyl-1,3-dioxolan-2-yl]methyl]-1,2,4-triazole) and 0.10 kg ha^{-1} of azoxystrobin (Methyl (2E)-2-(2-{[6-(2-cyanophenoxy) pyrimidin-4-yl]oxy phenyl)-3-methoxyacrylate) at approximately Feekes GS 10.1 (Large, 1954), after flag leaf was fully emerged, to decrease yield losses associated with foliar diseases. Plots were harvested for grain on 21 June 2013, 14 June 2014, and 6 June 2015 at Stillwater, and 13 June 2013, 13 June 2014, and 5 June 2015 at Chickasha, with a Hege 140 self-propelled small-plot combine (Wintersteiger). Grain moisture content was measured at harvest and yields were corrected for a 130 g kg^{-1} water basis.

2.2.3. Soil pH and exchangeable cation assessment

A composite soil sample consisting of approximately 15 soil cores 0 – 15 cm depth was taken from the trial areas before the establishment of the study for the evaluation of initial

conditions (Table 2.1), and $Ca(OH)_2$ and $Al_2(SO_4)_3$ were applied to main plots prior to the first year of the study according to results from this analysis. To determine soil pH achieved after amendment application, composite samples were collected from each main plot June 2013, June 2014, and June 2015 same day wheat was harvested. A total of 108 composite soil samples were collected from the study sites over the 3-yr period. Samples were oven-dried at 65°C for 24 h and ground to pass a 2-mm sieve.

A combination pH electrode was used to measure soil pH in a 1:1 soil/deionized water suspension (Thomas, 1996). The analysis of the exchangeable cations Ca, Mg, and K, was done using Mehlich-3 procedure. Levels of exchangeable Al_{KCl} were determined using the Bertsch and Bloom (1996) method, by mixing 5g of soil with 25 ml of 1M KCl. Aluminum, K, Mg, and Ca in the extracts were analyzed by inductively coupled plasma-atomic emission spectroscopy (Soltanpour et al., 1996). The equation suggested by Sumner and Miller (1996) was used to determine the soil's effective cation exchange capacity (ECEC):

$$ECEC\ (cmol_c\ kg^{-1}) = [K] + [Ca] + [Mg] + [Al_{KCl}] \quad [1]$$

with the exception that Sumner and Miller (1996) suggested including Na in the calculation, which was not assessed in this experiment since it is insignificant in Oklahoma acid soils. Aluminum saturation (Al_{sat}) was calculated as:

$$\%\ Al_{sat} = (Al_{KCl} / ECEC) \times 100 \quad [2]$$

2.2.4. Vegetative development evaluations

Final plant stand was evaluated approximately 2-3 weeks after emergence by counting the number of wheat plants present in four linear meters per subplot. Percent emergence was than estimated as the quotient of emerged plants by the number of seeds planted per linear meter based on average weight of 100 seeds determined prior to planting. Wheat forage production prior to

winter dormancy was measured at the dual-purpose site Stillwater prior to mowing by hand-clipping two linear meters from each subplot. Clippings occurred 13 Dec. 2012, 3 Dec. 2013, and 11 Dec. 2014. The two samples collected from each subplot were combined and ovendried at 50°C until constant weight was achieved. A method similar to the one described by Purcell (2000) was used to measure percent canopy closure. In this method digital photographs are taken in different stages of development, with the camera lens pointing down and encompassing approximately 1 m^2 of the front part of each individual plot. Digital photographs were analyzed using a macro program for Sigma Scan Pro (v. 5.0, systat software, Point Richmond, CA) (Karcher and Richardson, 2005). The software has selectable options defining hue and saturation values. According to Purcell (2000), setting hue and saturation values selectively include the green pixels in the digital image. For this study hue was set for the range of 30 to 150, and saturation was set for the range of 0 to115. The output of the program is percent canopy coverage, defined as the number pixels within the selected range divided by the total number of pixels per image (Purcell, 2000). Normalized-difference vegetative index (NDVI) was measured using GreenSeekerTM sensor (model 505, NTech Industries, Ukiah, CA) at the same time as digital pictures were taken and the by-plot coefficient of variation (CV) obtained from the NDVI readings was analyzed, as it can be used as an indicator of plant population and homogeneity (Arnall et al., 2006). Percent canopy cover assessment and NDVI readings were performed at intervals of approximately two weeks from emergence until heading. Grain protein concentration (g kg^{-1}) was measured with near-infrared reflectance spectroscopy using a Perten DA 7200 and was reported on a 130 g kg^{-1} water basis (Perten Instruments Inc., Springfield, Illinois).

2.2.5. Data analysis

Data were analyzed by location, as Stillwater had dual-purpose and Chickasha had grain only management. Data within variety was subjected to Levene's homogeneity of variances test for each dependent variable to determine whether to combine years within location. Due to

differences in weather during the three growing seasons, most dependent variables had heterogeneous variance across years and year was treated as a fixed effect. The exceptions were forage yield and relative forage and grain yields, which had homogeneity of variances across years and were analyzed treating year as random effect.

Percent wheat emergence and wheat grain yield were modeled as a linear-plateau function of soil pH according to Eq. [3]:

$$Y = \beta_0 + \beta_1 X + \text{error; if } X < \gamma$$

$$Y = \gamma + \text{error; if } X > \gamma \quad [3]$$

where Y is the response (percent wheat emergence or grain yield), X is soil pH, and γ is the level of soil pH in which an increase in soil pH did not result in increased percent emergence or grain yield. The above linear-plateau model has been successfully used to predict wheat response to soil pH (Kariuki et al., 2007). Linear-plateau models were built using PROC NLIN in SAS Version 9.3 (SAS Institute, Cary, NC).

Dynamics of canopy development were modeled by variety, soil pH, location, and year, as a sigmoidal function of days after sowing (DAS) using the non-linear regression model:

$$Y = \frac{a}{1 + e^{-\left(\frac{t - t_0}{b}\right)}} \quad [4]$$

where a is the asymptotic maximum percent canopy cover, t is time (DAS), t_0 is the inflection point at which the rate in percent canopy cover increase is maximized (DAS), and b is a parameter determining the shape of the curve. Sigmoid functions are suggested when evaluating crop growth as function of time (Archontoulis and Miguez, 2015).

Forage yield and relative grain and forage yields across years were modeled as exponential function of soil pH using the non-linear regression model:

$$Y = \beta_0 + \alpha(1 - e^{-\beta_1 x}) \quad [5]$$

where β_1 represents the responsiveness of Y to an increase in soil pH (x). Relative forage and grain yields were determined by location, year, and variety, by expressing the yield of each plot relative to the average yield of the same variety among the three highest pH plots. The exponential model was then used to evaluate soil pH threshold in which forage yield or relative grain yield reached 95% of asymptotic maximum and to estimate the x-intercept, which indicates the pH below which yield is zero. This exponential model has been successfully used in experiments assessing crop responses characterized by decreasing marginal return to increased input level, such as N fertilizer (Cerrato and Blackmer, 1990), increased plant population (Edwards and Purcell, 2005), or increasing percent canopy cover (Butchee and Edwards, 2013). Analyses based on Eq. [4] and [5] were performed using SigmaPlot 11 (Systat Software, San Jose, CA).

Wheat responses to Al_{sat} are typically linear and negative (Kariuki et al., 2007). Thus, percent emergence, forage yield, grain volume weight, and grain protein concentration, were analyzed treating Al_{sat} as a covariate. Variety was treated as a nominal variable whereas Al_{sat} was a continuous variable in the same model. Linear models to describe the relationship between the dependent and independent variables were tested. Covariance analysis combines regression and analysis of variance (Cochran, 1957) and is favored to multiple comparison procedures or means separation when a continuous series of treatments is adopted (Petersen, 1977). Based on the shape of the response of each variety's grain yield to Al_{sat} at each site-year, grain yield was modeled as a plateau-linear (opposite of Eq. 3) or a linear function of soil Al_{sat}. Threshold Al_{sat} above which an increase in Al_{sat} led to linear decrease in grain yields were established by determining the inflexion point of the plateau-linear model. Relative grain yield was modeled as a linear function of Al_{sat}. Analyses of covariance and plateau-linear models were performed in SAS Version 9.3 using PROC GLM and PROC NLIN.

2.3. RESULTS AND DISCUSSION

2.3.1. Amendment effects on soil pH

Hydrated lime or $Al_2(SO_4)_3$ applied to the Easpur loam in Stillwater resulted in actual soil pH similar to target soil pH, with 49 out of 54 measured soil pH within ±0.4 from the target pH across the three studied growing seasons (Fig. 2.1). As a result, a wide pH gradient (i.e. 4.1 to 7.4) was created at Stillwater for the analysis of wheat growth and yield under dual-purpose management. Actual soil pH values were further apart from the targeted pH in the Dale silt loam at Chickasha, especially in the 2012-13 growing season when final soil pH gradient only ranged from 5.4 to 6.3 (Fig. 2.1). Further application of amendments improved the relationship between actual and target pH for a total of 29 out of 36 measured pH samples within ±0.4 from the target pH across the growing seasons 2013-14 and 2014-15. As a result, wheat sensitivity to soil pH was evaluated in a soil pH gradient range from 4.4 to 7.6 under grain-only management across the last two growing seasons at Chickasha. Application of $Ca(OH)_2$ or $Al_2(SO_4)_3$ to create a soil pH gradient has been used successfully to evaluate sorghum (Butchee et al., 2012) and sunflower (Sutradhar et al., 2014) response to soil acidity and estimate threshold pH beyond which further increase in soil pH did not result in increased grain yields.

2.3.2. Soil pH, extractable aluminum, and aluminum saturation

Extractable Al_{KCl} ranged from 0.02 to 137.2 mg kg^{-1} in Stillwater, and from 0 to 63.58 mg kg^{-1} in Chickasha (Fig. 2.2A), and Al_{sat} ranged from <0.01 to 22.5% in Stillwater and from 0 to 7.8% in Chickasha (Fig. 2.2B), across the three studied growing seasons. Inverse exponential relationships explained the availability of Al_{KCl} or the percent Al_{sat} as function of soil pH at both locations ($r^2 > 0.85$, $p < 0.001$). As a consequence, slight changes in soil pH at pH levels < 5 resulted in dramatic increases in both Al_{KCl} and Al_{sat} (Fig. 2.2). For instance, a decrease in soil pH from 5 to 4.5 increased Al_{KCl} from 21.53 to 59.1 mg kg^{-1} while a decrease in soil pH of same

magnitude from 6.5 to 6 only increased Al_{KCl} from 1.04 to 2.86 mg kg^{-1} in the Easpur loam in Stillwater (Fig. 2.2A). The Dale silt loam in Chickasha had less Al_{KCl} at a given soil pH but the shape of the response to soil pH was similar, as Al_{KCl} increased from 9.18 to 45.24 mg kg^{-1} when soil pH decreased from 5 to 4.5, and from 0.08 to 0.38 mg kg^{-1} when soil pH decreased from 6.5 to 6. Percent Al_{sat} resulted in the same response pattern than did Al_{KCl} (Fig. 2.2B). The exponential nature of the relationship between Al_{KCl} or Al_{sat} and soil pH have been previously suggested (Kariuki et al., 2007; Lollato et al., 2013) and is function of the greater availability of hydrogen ions (H^+) at low pH soils, which react with three hydroxide (OH^-) from water molecules surrounding the Al atom and originate the toxic Al^{3+} (Bohn et al., 2001).

Extractable Al levels are soil specific and different soils can result in vastly different Al_{KCl} levels (Johnson et al., 1997). The Easpur loam in Stillwater resulted in greater Al_{KCl} and Al_{sat} than the Dale silt loam at Chickasha at a given soil pH, and our results differ considerably than those for other acid soils in the literature. For instance, a soil pH of 4.7 in our study resulted in Al_{KCl} of 39.5 mg kg^{-1} in Stillwater and 6.8 mg kg^{-1} in Chickasha, whereas the same pH level resulted in Al_{KCl} of 126.6 mg kg^{-1} in a Konawa fine loamy soil in Perkins, OK (Kariuki et al., 2007), and Al_{KCl} of 56, 35.3, and 29.2 mg kg^{-1} in a Teller sandy loam, a Taloka silt loam, and a Grant silt loam studied in three locations across Oklahoma (Sutradhar et al., 2014). Still, Al_{KCl} does not take into account the base cation concentration of each particular soil and therefore may not be a good indicator of Al toxicity (Johnson et al., 1997). Percent Al_{sat}, which is a ratio of extractable Al over base cations and thus a better indicator of soil acidity potential of the system as shown in Eq. [2], was also soil specific. At a soil pH of 4.7, Al_{sat} was 23.9% at Stillwater and only 3.3% at Chickasha, serving as an indication of the strong base concentration in the Dale silt loam in Chickasha. At the same soil pH level of 4.7, previous studies in other regions demonstrated soil Al_{sat} ranging from 17.4 to 47.7% (Kariuki et al., 2007; Sutradhar et al., 2014). Thus, our study not only encompasses the Al_{sat} levels on the published literature but expand it to

soils less prone to acidity, with lower Al_{sat} values, which may be more representative of the wheat growing region of Oklahoma.

2.3.3. Weather conditions

Growing season 2012-13 was characterized by a dry start at both Stillwater and Chickasha, with cumulative precipitation during September through December of 65 mm at Stillwater, and during October through December of 58 mm at Chickasha (Table 2.2). Cumulative ET_o during the same period was 369 mm at Stillwater and 238 mm at Chickasha. Despite the dry start, weather during the spring was favorable to wheat grain yields with total precipitation from March to May, when most of wheat grain yield determination occurs (Lollato and Edwards, 2015), of 321 and 371 mm at Stillwater and Chickasha, respectively (Table 2.2). These totals were similar to the ET_o during the same period (i.e. 329 and 355 mm) and allowed for average wheat yields of 4157 kg ha^{-1} at Stillwater and 4264 kg ha^{-1} at Chickasha. The opposite weather pattern occurred during 2013-14, when a more moist fall was followed by an extremely dry spring (Table 2.2). September through December precipitation at Stillwater summed 148 mm and October through December precipitation at Chickasha summed 111 mm, with corresponding ET_o of 325 and 202 mm, respectively. Meanwhile, March through May precipitation was only 68 mm at Stillwater for an ET_o of 441 mm, and 140 mm at Chickasha for an ET_o of 457 mm. The moist start allowed for lush vegetative development in the fall 2013, which was followed by a severe water deficit and leveled wheat yields at an average of 1978 kg ha^{-1} at Stillwater and 1615 kg ha^{-1} at Chickasha. The 2014-15 growing season, on the other hand, had plenty of moisture during both fall and spring (Table 2.2), and yields averaged 3325 kg ha^{-1} at Stilwater and 3444 kg ha^{-1} at Chickasha. The differences in grain yield levels among studied growing seasons did not allow for combination of years when analyzing absolute wheat yields and year was treated as a fixed effect.

2.3.4. Wheat emergence and canopy dynamics as affected by soil acidity

The linear-plateau model in Eq. [3] explained percent wheat emergence as affected by soil pH well (Table 2.3). Percent wheat emergence was decreased by low soil pH during the three studied growing seasons at Stillwater and during the 2013-14 and 2014-15 growing seasons at Chickasha for the more sensitive varieties TAM 203 and Ruby Lee (Table 2.3). Threshold soil pH for maximum wheat emergence (γ) ranged from 4.5 to 5.9 depending on growing season and wheat variety. On average, early-planted Duster in dual-purpose management achieved maximum percent emergence at soil pH of 4.8 and above, whereas γ for the varieties 2174, Ruby Lee, and TAM 203, also under dual-purpose management at Stillwater were 5.1, 4.9, and 5.2, respectively. Wheat emergence was not affected by low soil pH for the varieties Duster and 2174 when planted for grain only, at Chickasha, across all studied growing seasons (Table 2.3). The varieties Ruby Lee and TAM 203 were more sensitive to low soil pH and percent emergence at Chickasha was decreased by soil pH < 4.5 in 2013-14 for the variety TAM 203, and by soil pH < 5.2 or 5.9 in 2014-15 for the varieties TAM 203 and Ruby Lee, respectively (Table 2.3).

Analysis of covariance between wheat emergence and soil Al_{sat} indicated that wheat variety was a significant factor affecting percent wheat emergence in the six studied site-years, and Al_{sat} affected wheat emergence in all site-years except Chickasha during 2012-13 (Table 2.4). The soil pH achieved at Chickasha on 2012-13 following amendment application were far from pH the goal (Fig. 2.1), resulting in a soil pH gradient range restricted to the range 5.4 to 6.3, and Al_{sat} consistently below 1%, which may explain the lack of response to both soil pH (Table 2.3) and Al_{sat} in that site-year (Table 2.4). Increased Al_{sat} decreased wheat emergence linearly in as much as 7.3% per unit increase in Al_{sat}, and the effects of Al_{sat} on wheat emergence were also more apparent at Stillwater, where Al_{sat} reached values of 22.5%, than at Chickasha, where Al_{sat} was consistently < 7.8% (Table 2.5). Wheat emergence was decreased from 1.12 to 4.61% Al_{sat}^{-1} for the variety TAM 203, from 1.09 to 7.28 % Al_{sat}^{-1} for Ruby Lee, from 0.73 to 6.07 % Al_{sat}^{-1} for

Duster, and from 0 to 5.7 % Al_{sat}^{-1} for 2174 (Table 2.4). Similarly to soil pH, the variety Ruby Lee tended to be more sensitive to Al_{sat} and had a steeper decline in percent emergence as function of increased Al_{sat} in most of the studied site-years (Table 2.5).

Although the effects of Al on wheat germination have been studied under controlled conditions (De Lima and Copeland, 1990; Jamal et al., 2006), most of the research conducted under field conditions do not report decreased wheat emergence due to low soil pH or high Al concentration. De Lima and Copeland (1990) reported that high concentrations of Al were necessary to inhibit the growth of the emerging roots and shoots of germinating seedlings, in opposition to the more Al sensitive established seedlings. Similarly, Jamal et al. (2006) reported that seed germination was not affected by Al concentration up to 160 g kg^{-1} applied to the seed, but root, shoot, and seedling length were. Results from the aforementioned researches support the strong acidity necessary to reduce wheat emergence measured in our study, where wheat emergence decreased at Stillwater where soil pH reached values as low as 4.1 (Al_{sat} < 22.5%), and was not as apparent in Chickasha where soil pH was consistently above 4.4 (Al_{sat} < 7.8%). Also, previous researches suggest that the decreased emergence was actually due to an effect of soil acidity on the emerging roots and shoot of the seedling rather than decreased seed germination (De Lima and Copeland, 1990; Jamal et al., 2006), although we did not evaluate seed germination in this study.

The sigmoidal model in Eq. [4] explained dynamics of canopy cover development as affected by soil pH within site-year, variety, and pH range, very well (Figure 2.3). Analysis of the parameters derived from the sigmoidal model indicate that low soil pH reduced the asymptotic maximum percent canopy cover (a) from 85.3 to 42.7% for Duster and from 89.2 to 28.9% for Ruby Lee comparing soil pH levels > 7 to soil pH in the 4 to 4.5 range (Fig. 2.3). Additionally, low soil pH delayed the achievement of maximum rate of canopy cover development (t_0). For example, in Stillwater 2012-13, t_0 in the variety Duster increased from 25.6 DAS at soil pH > 7.0,

to 53.2 DAS in the pH range from 4 – 4.5 (Fig. 2.3A), whereas for Ruby Lee t_0 increased from 25.9 to 55.4 DAS (Fig. 2.3B). Similar patterns of canopy cover as affected by soil pH occurred for all varieties in all site-years (Tables 2. 6 and 2.7). The only exception was Chickasha during the 2014-15 growing season, when model failed to converge for most varieties at the majority of the soil pH levels (Table 2.7). The reason for lack of convergence in Chickasha is probably insufficient measurements towards the end of the growing season (last measurement taken at DAS 164) combined to a late achievement of maximum rate of canopy development (t_0 ~130 DAS), which resulted in measurements taken only during the first portion of the S shape typical from sigmoid type models (Archontoulis and Miguez, 2015).

Decreased percent canopy cover reduces wheat radiation interception, decreasing aboveground biomass production and grain yield (Sinclair and Muchow, 1999). A minimum wheat percent canopy cover of 53% prior to winter dormancy, or 62% at grazing termination, is needed to achieve maximum yields in dual-purpose wheat systems in the southern Great Plains (Butchee and Edwards, 2013). In most cases, a minimum soil pH of 4.5 was needed for percent canopy coverage to reach these critical thresholds for achievements of maximum grain yields as soil pH < 4.5 did not allow for maximum canopy cover of > ~60% (Tables 2.6 and 2.7). An additional feature apparent from Fig. 2.3 and Tables 2.6 and 2.7 is the greater variation about the fitted line in low soil pH as compared to high soil pH (i.e. lower r^2 at low pH values), which indicates greater stand and canopy development variability, or less population uniformity, throughout the growing seasons led by increased soil acidity.

Plant population uniformity at jointing, assessed as the CV of NDVI readings, ranged from 1 to 55% and decreased exponentially with an increase in soil pH (Fig. 2.4). A critical NDVI CV for winter wheat is considered 17%, value that corresponds to a stand of approximately 100 plants m^{-2} (Arnall et al., 2006). Additionally, values of NDVI CV beyond 17% decrease the crop's ability to recover from early season stresses such as N (Arnall et al., 2006; Morris et al.,

2006). Across all years and locations, a minimum soil pH of 4.5 led to NDVI CV of 17% and increases in soil pH decreased NDVI CV for a minimum soil pH of 4.9 to a NDVI CV of 10% (Fig. 2.4). Greater plant population uniformity or lesser NDVI CV occurred with increases in soil pH, and pH above 6 showed little improvement in plant homogeneity (Fig. 2.4). Jointing is a critical stage for wheat N fertilization in the southern Great Plains, and the application of mid-season N is essential for improving wheat yields (Krenzer, 2000). Increased wheat population homogeneity increases wheat responsiveness to mid-season N application (Morris et al., 2006). Our results indicate that pH values below 4.5 to 4.9 may not only be limiting wheat growth, but are also reducing wheat plant population homogeneity and consequently wheat responsiveness to N. Increased wheat heterogeneity due to decreased soil pH has been previously reported (Lollato et al., 2013), but, to our knowledge, this is the first assessment of critical pH thresholds levels for greater wheat uniformity.

2.3.5. Critical soil pH and Al concentration for wheat forage yield

The exponential rise to maximum model explained the relationship between forage yield and soil pH across years very well (Fig. 2.5). The variation about Eq. [5] in Fig. 2.5 indicates that there was some year variation in forage yield response to low soil pH, possibly explained by differences in weather pattern and precipitation distribution prior to forage sampling. According to the fitted equations, 95% of the asymptotic forage biomass would be achieved at pH of 5.5 for the variety 2174, at pH of 5.9 for both Duster and Ruby Lee, and at pH of 6 for TAM 203. The lower pH threshold for maximum forage yields by the 2174 variety indicates a good tolerance to acid soil conditions. Additionally, the β_1 parameter was greater for the variety 2174 (2.15 ± 0.49), indicating a steep increase in forage production at pH values ranging from 4 to the 5.5 threshold for asymptotic yield. Interestingly, the fitted equations for Duster and Ruby Lee resulted in same β_1 (1.64 ± 0.42 and 1.69 ± 0.37, respectively), indicating similar increase in forage production from pH of about 4 to the 5.9 pH threshold. The most sensitive wheat variety to low soil pH was

TAM 203, with β_1 of 1.57 ± 0.45. Finally, the pH below which there was no forage yield, assessed as the *x*-intercept in Fig. 2.5, was 4.1 for the four studied wheat varieties, indicating that in extremely acidic soils with soil pH of 4.1 or below, cultivar selection is not an option to overcome low soil pH problems and other amendment strategies should be adopted. Similarly, Johnson et al. (1997) reported no measurable early-season forage production by wheat varieties sensitive to acidic soils when cultivated in sites with soil pH of 4.5 and Al_{sat} > 30%.

Wheat forage yield decreased linearly with an increase in soil Al_{sat}. For each 1% increase in Al_{sat}, what forage yield decreased 92 ± 12.5 kg ha^{-1} for the variety 2174 (r^2 = 0.51, p < 0.001), 93.0 ± 12.8 kg ha^{-1} for Duster (r^2 = 0.51, p < 0.001), 96.4 ± 11.2 kg ha^{-1} for Ruby Lee (r^2 = 0.59, p < 0.001), and 89.2 ± 12.3 kg ha^{-1} for TAM 203 (r^2 = 0.50, p < 0.001). A linear and negative association between wheat forage yields and Al_{sat} has been previously reported (Kariuki et al., 2007), and occurs because Al^{3+} enters the root tip and restrains root development (Zhou et al., 2007), resulting in reduced root growth unable to explore deeper portions of the soil profile for water and nutrients, consequently decreasing wheat forage yield.

2.3.6. Critical soil pH and Al concentration for wheat grain yield and quality

The linear-plateau model in Eq. [3] explained each variety's grain yield sensitivity to soil pH well in 2012-13 and 2014-15 at Stillwater, and the yield of the most sensitive varieties to soil pH in Chickasha during 2013-14 and 2014-15 (Table 2.8). Soil pH did not affect grain yields in Stillwater during the 2013-14 growing season when a severe spring drought drastically reduced and leveled wheat yields; or at Chickasha (2012-13) when soil amendments were not sufficient to create a pH gradient and soil pH only ranged from 5.4 to 6.3. Threshold pH (γ) for wheat grain yield plateau ranged from 4.3 to 5 in the Easpur loam at Stillwater, and from 5.1 to 5.2 in the Dale silt loam at Chickasha for the more sensitive varieties Ruby Lee and TAM 203 (Table 2.8). Although the variety TAM 203 had previously been suggested as very susceptible to low soil pH

(Edwards et al., 2012), a minimum pH threshold below which grain yields decrease had not been yet studied for TAM 203, Duster, or Ruby Lee.

In most cases when wheat yield was significantly modeled as linear-plateau function of soil pH, wheat yield reduction was accentuated in the lowest pH plots (soil pH < 4.5) and was not as apparent in the remaining plots in which soil pH ranged from 4.5 to 7.5 (Fig. 2.6A). As a result, the linear-plateau models of wheat yield as function of soil pH had steep slopes in the linear portion, and γ at low pH values. The lack of wheat yield response to soil pH > 4.5 in our study agrees with literature evaluating acidity amelioration strategies in which liming acid soils not always result in increased wheat yields at pH levels > 4.7 (Barbieri et al., 2015; Liu et al., 2004; Lollato et al., 2013). The extremely low soil pH needed to induce grain yield reductions in our study partially explains the lack of response the more tolerant varieties Duster and 2174 at Chickasha (Table 2.8), location in which soil pH were consistently > 4.4 and Al_{sat} < 7.8%.

Figure 2.6A illustrates the difference in sensitivity to soil pH of the varieties Duster and TAM 203 at Stillwater during the 2014-15 growing season. In this site-year the variety Duster resulted in γ of 4.5 as compared to 4.9 for TAM 203, indicating a greater tolerance to low soil pH of the former. Examination of mean grain yields for each variety within soil pH levels indicated a yield advantage of Duster at soil pH < 4.5. This yield advantage ranged from 17 to 65% when compared to Ruby Lee, 14 to 117% when compared to TAM 203, and 24 to 58% when compared to 2174. Duster has been shown to be superior to other wheat varieties in low soil pH conditions (Edwards et al., 2012) and the reason for the better low soil pH tolerance by Duster is the root-tip staining pattern (Heyne and Niblett, 1978) and a functional allele of the Al-induced malate transporter gene (Zhou et al., 2007), which results in increased tolerance to low soil pH and extractable Al. At soil pH of 7 or above, Ruby Lee had a yield advantage ranging from 4 to 46% over Duster, 4 to 20% over TAM 203, and 4 to 39% over 2174. The cultivar Ruby Lee has great

yield potential and is very responsive to management (Edwards, 2013), characteristic that may partially explain its higher yields in less acidic soils.

The linear plateau model indicated that threshold pH varies from year to year for the same variety, according to growing season weather (Table 2.8). Still, analysis of relative yields using the exponential rise to maximum model in Eq. [5] resulted in more consistent parameters as data were analyzed across years (Fig. 2.7). Asymptotic relative grain yield predicted by the non-linear regression was 0.97 for the variety 2174, 0.99 for Duster and Ruby Lee, and 1.01 for TAM 203. Considering that 95% of the asymptotic yield could be achieved, maximum attainable relative yield was 0.92 for 2174, 0.94 for Duster and Ruby Lee, and 0.96 for TAM 203. These relative yields were achieved at soil pH of 4.8, 4.8, 5.8, and 5.5, respectively, confirming results from individual years and indicating that 2174 and Duster have greater tolerance to acid soil conditions relative to Ruby Lee and TAM 203.

The threshold pH values obtained in our study are greater than those reported by Kariuki et al. (2007) which ranged from 5.3 to 6.6 for different wheat varieties. Specifically, the 5.5 threshold pH for 2174 in our study is less than the 5.9 threshold pH suggested for the same variety by Kariuki et al. (2007). The differences obtained in our study versus Kariuki et al. (2007) for the same variety (i.e. 2174) may be attributed to soil chemical characteristics. Kariuki et al. (2007) tested wheat tolerance to acidic soils in a Konawa fine loamy soil, with Al_{sat} values as great as 70%, indicating a greater toxicity potential (Johnson et al., 1997) and explaining the higher threshold pH found in their study. Site-specific symptoms of soil acidity on wheat yield of the same variety tested at locations where soil differed in chemical properties were also reported by Johnson et al. (1997). Additionally, all pH thresholds in our study were between 4.8 and 5.8, whereas the threshold pH range previously reported for other wheat varieties was 5.3 to 6.6 (Kariuki et al., 2007). These differences may be attributed not only to differences in soil chemistry but to the modern wheat varieties, such as Duster, released from a breeding program

characterized by efforts to increase Al tolerance in wheat varieties (Johnson et al., 1997; Tang et al., 2002; Zhou et al., 2007). While segregation of varietal effects from soil properties effects is not possible for most varieties when comparing our dataset to Kariuki et al. (2007), we provide empirical evidence for variety-specific wheat yield unaffected by soil pH > 4.8 to 5.8 at soils with ECEC ranging between 6.3 and 14.8 $cmol_c\ kg^{-1}$.

Wheat grain yield was modeled as a plateau-linear function of soil Al_{sat} at Stillwater during the 2012-13 and 2014-15 growing seasons, and at Chickasha for the more sensitive varieties during 2013-14 and 2014-15 growing seasons (Table 2.9). The linear decrease in grain yield as function of Al_{sat} previously reported (Kariuki et al., 2007; Schroder et al., 2011; Valle et al., 2009) occurred for the varieties Ruby Lee and TAM 203 at Stillwater 2014-15 and at Chickasha 2013-14 and 2014-15 (Table 2.9). In all other cases, grain yields plateaued at low Al_{sat} levels until a minimum threshold Al_{sat} was reached beyond which an increase in Al_{sat} reduced grain yields. In Stillwater, threshold Al_{sat} averaged 11.7% for the variety 2174, 9.6% for Duster, 8.7% for Ruby Lee, and 7.1% for TAM 203 (Table 2.9). Higher threshold Al_{sat} indicates that the variety can endure greater levels of Al toxicity without the associated grain yield penalty. In Stillwater 2012-13, when growing season precipitation during spring was plentiful, the yield of the variety 2174 plateaued up to Al_{sat} values of 17%, whereas Ruby Lee plateaued up to Al_{sat} of 15% (Fig. 2.6B), exemplifying the strong environmental effect on wheat sensitivity to acidic soils. These results align well with published literature in which Al_{sat} levels below ~12% did not significantly decrease wheat yields (Johnson et al., 1997; Lollato et al., 2013). Careful evaluation of a comprehensive study of wheat yield as affected by Al_{sat} (Schroder et al., 2011) provides evidence that Al_{sat} levels below ~13% may often result in grain yields above 80% of the control yield (non-acidic soil).

Relative wheat yield as affected by Al_{sat} evaluated across years resulted in a variety-specific Al sensitivity (Fig. 2.8). Duster proved to be more tolerant to Al_{sat} and the linear

regression between relative grain yield and Al_{sat} was non-significant at Chickasha or Stillwater, with only 15 out of 108 relative grain yield values below 0.8 reference yields (average yields of the three highest pH plots). The variety 2174 was more susceptible to Al_{sat} than Duster, with relative grain yields showing significant relationship at with Al_{sat} at both locations, decreasing at 1.1 ± 0.3% Al_{sat}^{-1} at Stillwater ($r^2 = 0.15$, $p < 0.01$) and decreasing at 3.3 ± 1.1% at Chickasha ($r^2 = 0.14$, $p < 0.01$). A total of 20 out of 108 measured relative grain yields for 2174 were below 0.8 from reference yield (Fig. 2.8). The variety Ruby Lee showed greater sensitivity to Al_{sat}, and relative yields decreased 1.2 ± 0.4% Al_{sat}^{-1} at Stillwater ($r^2 = 0.18$, $p < 0.001$), and 5.7 ± 1.6% Al_{sat}^{-1} at Chickasha ($r^2 = 0.2$, $p < 0.0001$). For Ruby Lee, a total of 27 out of 108 relative yields were below 0.8 from the reference yield. The variety TAM 203 was also susceptible to Al_{sat}, as relative yields decreased 1.5 ± 0.4% Al_{sat}^{-1} at Stillwater, and 6.3 ± 1.3% Al_{sat}^{-1} at Chickasha, and there were a total of 21 out of 108 values below 0.8 the reference yield. These results expand previously published literature evaluating wheat yields as affected by Al_{sat} (Johnson et al., 1997; Kariuki et al., 2007; Lollato et al., 2013; Schroder et al., 2011) by showing that tolerant varieties, such as Duster can be adopted in environments with relatively high Al_{sat} levels without the associated yield penalty measured in susceptible varieties such as Ruby Lee or TAM 203. As Al toxicity is the major cause for limited productivity in low pH soils (Schroder et al., 2011), our results suggest that variety selection can be an effective method to improve wheat productivity on acid soils.

Analysis of covariance for wheat grain volume weight and grain protein concentration as function of variety and Al_{sat} indicated that, in most years, grain quality parameters were affected by wheat variety but not by Al_{sat} (Table 2.4). Grain volume weight was unaffected by Al_{sat} in all studied site-years, and grain protein concentration increased with increased Al_{sat} in Chickasha 2013-14 but was otherwise unaffected. While Ruby Lee consistently resulted in greater or similar grain volume weight when compared to the other studied wheat varieties across four out of six

site-years, TAM 203 resulted in greater or similar grain protein concentration across all site-years (Table 2.10).

Our results demonstrate that wheat forage yield is more sensitive to acidic soil conditions than grain yield, as evidenced by greater threshold pH for forage yields to plateau (i.e. 5.5 to 6.0) as compared to grain yields (i.e. 4.8 to 5.8). The greater sensibility of forage yields as compared to grain yields agrees well with previous literature studying acid soil effects on wheat production (Johnson et al., 1997; Kaitibie et al., 2002; Kariuki et al., 2007; Lollato et al., 2013) and may be due to forage yield formation occurring prior to full root development, whereas grain yield is formed after a more extensive rooting system is achieved (Kariuki et al., 2007). Many Oklahoma soils are only acidic on the upper 0 – 15 cm soil layer (Schroder et al., 2011), which would allow for a more developed rooting system later in the growing season to uptake water and nutrients from deeper portions of the soil profile and buffer grain yield formation to a certain extent. Additionally, the decreased population uniformity in acid soils evidenced by greater NDVI CV is function of less plants m^{-2} (Arnall et al., 2006), which directly affects forage yield. Grain yield may still be buffered when population uniformity is low if the weather during spring, when grain yield determination occurs (Lollato and Edwards, 2015), is favorable and tiller survival is improved. This can potentially translate into more spikes m^{-2}, buffering grain yields.

Current recommendations for optimal soil pH for wheat production is 5.5 to 7.5, values below which acidity amelioration techniques are recommended (Zhang and Raun, 2006). Our results indicate that wheat varieties tolerant to low soil pH, such as Duster, can be grown in soils with pH as low as 4.8 without major reductions in grain yield when the enterprise focuses on grain only wheat production and soil ECEC allows for low Al_{sat} at a given pH level. For a dual-purpose wheat and cattle enterprise, the minimum threshold pH of 5.5 is valid in the abovementioned soil types to safeguard maximum forage production. In either case, we

demonstrated that wheat variety selection is a cost-effective measure to improve wheat productivity in acidic soils.

2.4. CONCLUSION

Wheat sensitivity to soil pH studied over a gradient of soil pH 4.1 to 7.6 indicate that wheat forage and grain yields increased with an increase in soil pH and a consequent decrease in soil Al_{sat}, and were variety- and site-year- specific. Wheat grain yield is less sensitive to low soil pH than wheat forage yield, as pH of 4.8 to 5.8 and above, depending on variety, resulted in similar grain yields at all locations whereas a pH of 5.5 to 6 or above was needed for similar forage yields across years. All varieties had lesser pH thresholds for grain yields (4.8 to 5.8) as compared to the one determined for forage yields (5.5 to 6.0). Our results indicate that dual-purpose wheat systems may have a greater penalty than grain only systems when soil becomes acidic. Forage and grain yields were reduced at acidic soils by lesser percent emergence and greater stand variability in acid plots, as well as by a delayed canopy development and decreased maximum percent canopy coverage. A minimum pH of 4.5 was needed for wheat to obtain relative plant population homogeneity (NDVI CV = 17%), and better stand establishement was achieved at soil pH > 4.9. We also demonstrated that soil acidity not only decreases maximum percent canopy cover, but also delays its achievement, which culminates in less intercepted solar radiation in the growing season. To our knowledge, this is the first assessment of critical pH levels to obtain minimum wheat plant population homogeneity and how pH levels affect wheat canopy development and closure. Our results indicate that wheat variety selection can be an effective method to improve wheat productivity on acid soils.

2.5. REFERENCES

Allen, R.G., L.S. Pereira, D. Raes, and M. Smith. 1998. Crop evapotranspiration: Guidelines for computing crop water requirements. Irrigation and Drainage Paper No. 56, FAO, Rome, Italy.

Archontoulis, S.V., and F.E. Miguez. 2015. Nonlinear regression models and applications in agricultural research. Agron. J. 107: 786-798.

Arnall, D.B., W.R. Raun, J.B. Solie, M.L. Stone, G.V. Johnson, K. Girma, et al. 2006. Relationship between coefficient of variation measured by spectral reflectance and plant density at early growth stages in winter wheat. J. Plant Nutr. 29: 1983-1997.

Barbieri, P.A., H.E. Echeverría, H.R.S. Rozas, and J.P. Martínez. 2015. Soybean and wheat response to lime in no-till argentinean mollisols. Soil and Tillage Research 152: 29-38.

Bertsch, P.M., and P.R. Bloom. 1996. Aluminium. In: D. Sparks, A. Page, P. Helmke, R. Loeppert, P. Soltanpour, M. Tabatabai, C. Johnston and M. Sumner, Eds., Methods of soil analysis. Part 3-chemical methods. p. 517-550.

Bohn, H.L., B.L. McNeal, and G.A. Connor. 2001. Soil chemistry. 3rd ed. John Wiley & Sons, New York, NY.

Bolt, V. 1996. Tolerance of wheat cultivars to soil acidity. Farmnote 2/96. Western Australia Dep. of Agric., South Perth, WA, Australia.

Butchee, J.D., and J.T. Edwards. 2013. Dual-purpose wheat grain yield as affected by growth habit and simulated grazing intensity. Crop Sci. 53: 1686-1692.

Butchee, K., D.B. Arnall, A. Sutradhar, C. Godsey, H. Zhang, and C. Penn. 2012. Determining critical soil pH for grain sorghum production. International Journal of Agronomy 2012.

Carver, B.F., E.L. Smith, E.G. Krenzer, R.M. Hunger, D.R. Porter, A.R. Klatt, et al. 2003. Registration of 'OK101' wheat. Crop Sci. 43: 2298-2299.

Cerrato, M.E., and A.M. Blackmer. 1990. Comparison of models for describing corn yield response to nitrogen-fertilizer. Agron. J. 82: 138-143.

Christensen, N.W., R.L. Powelson, and M. Brett. 1987. Epidemiology of wheat take-all as influenced by soil-ph and temporal changes in inorganic soil n. Plant Soil 98: 221-230.

Cochran, W.G. 1957. Analysis of covariance: Its nature and uses. Biometrics 13: 261-281.

De Lima, M.L., and L. Copeland. 1990. The effect of aluminum on the germination of wheat seeds. J. Plant Nutr. 13: 1489-1497.

Edwards, J.T. 2013. Ruby lee - endurance parentage, top-end yield potential, and hessian fly resistance. Okla. St. Univ. Coop. and Ext. Serv. L-414.

Edwards, J.T., B.F. Carver, G.W. Horn, and M.E. Payton. 2011. Impact of dual-purpose management on wheat grain yield. Crop Sci. 51: 2181-2185.

Edwards, J.T., R.M. Hunger, E.L. Smith, G.W. Horn, M.S. Chen, L. Yan, et al. 2012. 'Duster' wheat: A durable, dual-purpose cultivar adapted to the southern great plains of the USA. Journal of Plant Registrations 6: 37-48.

Edwards, J.T., and L.C. Purcell. 2005. Soybean yield and biomass responses to increasing plant population among diverse maturity groups: I. Agronomic characteristics. Crop Sci. 45: 1770-1777.

Heyne, E., and C. Niblett. 1978. Registration of ‘Newton’ wheat. Crop Sci. 18: 696.

Jamal, S.N., M.Z. Iqbal, and M. Athar. 2006. Phytotoxic effect of aluminum and chromium on the germination and early growth of wheat (*Triticum aestivum* L.) varieties Anmol and Kiran. International Journal of Environmental Science & Technology 3: 411-416.

Johnson, J.P., B.F. Carver, and V.C. Baligar. 1997. Productivity in Great Plains acid soils of wheat genotypes selected for aluminium tolerance. Plant Soil 188: 101-106.

Kaitibie, S., F.M. Epplin, E.G. Krenzer, and H.L. Zhang. 2002. Economics of lime and phosphorus application for dual-purpose winter wheat production in low-pH soils. Agron. J. 94: 1139-1145.

Karcher, D.E., and M.D. Richardson. 2005. Batch analysis of digital images to evaluate turfgrass characteristics. Crop Sci. 45: 1536-1539.

Kariuki, S.K., H. Zhang, J.L. Schroder, J. Edwards, M. Payton, B.F. Carver, et al. 2007. Hard red winter wheat cultivar responses to a pH and aluminum concentration gradient. Agron. J. 99: 88-98.

Kochian, L.V. 1995. Cellular mechanisms of aluminum toxicity and resistance in plants. Annu. Rev. Plant Biol. 46: 237-260.

Krenzer, E.G. 2000. Production management. In: T. A. Royer and E. G. Krenzer, Eds., Wheat management in Oklahoma. E-831. Oklahoma State Univ. Coop. Ext. Serv., Stillwater, OK. p. 11-18.

Large, E.C. 1954. Growth stages in cereals illustration of the feekes scale. Plant Pathol. 3: 128-129.

Lidon, F.C., and M. Barreiro. 2002. An overview into aluminum toxicity in maize. Bulg. J. Plant Physiol 28: 96-112.

Liu, D.L., K.R. Helyar, M.K. Conyers, R. Fisher, and G.J. Poile. 2004. Response of wheat, triticale and barley to lime application in semi-arid soils. Field Crops Res. 90: 287-301.

Lollato, R.P., and J.T. Edwards. 2015. Maximum attainable wheat yield and resource use efficiency in the southern Great Plains. Crop Sci. accepted for publication.

Lollato, R.P., J.T. Edwards, and H.L. Zhang. 2013. Effect of alternative soil acidity amelioration strategies on soil pH distribution and wheat agronomic response. Soil Sci. Soc. Am. J. 77: 1831-1841.

McPherson, R.A., C.A. Fiebrich, K.C. Crawford, R.L. Elliott, J.R. Kilby, D.L. Grimsley, et al. 2007. Statewide monitoring of the mesoscale environment: A technical update on the Oklahoma mesonet. J. Atmos. Ocean. Technol. 24: 301-321.

Morris, K.B., K. Martin, K. Freeman, R. Teal, K. Girma, D. Arnall, et al. 2006. Mid-season recovery from nitrogen stress in winter wheat. J. Plant Nutr. 29: 727-745.

Petersen, R. 1977. Use and misuse of multiple comparison procedures. Agron. J. 69: 205-208.

Purcell, L.C. 2000. Soybean canopy coverage and light interception measurements using digital imagery. Crop Sci. 40: 834-837.

Redmon, L.A., E.G. Krenzer, D.J. Bernardo, and G.W. Horn. 1996. Effect of wheat morphological stage at grazing termination on economic return. Agron. J. 88: 94-97.

Schroder, J.L., H.L. Zhang, K. Girma, W.R. Raun, C.J. Penn, and M.E. Payton. 2011. Soil acidification from long-term use of nitrogen fertilizers on winter wheat. Soil Sci. Soc. Am. J. 75: 957-964.

Sinclair, T.R., and R.C. Muchow. 1999. Radiation use efficiency. Adv. Agron. 65: 215-265.

Sloan, J.J., N.T. Basta, and R.L. Westerman. 1995. Aluminum transformations and solution equilibria induced by banded phosphorus-fertilizer in acid soil. Soil Sci. Soc. Am. J. 59: 357-364.

Soltanpour, P.N., G.W. Johnson, S.M. Workman, J.B. Jones, and R.O. Miller. 1996. Inductively coupled plasma emission spectrometry and inductively coupled plasma-mass spectrometry. In: D. L. Sparks, A. L. Page, P. A. Helmke and R. H. Loeppert, Eds., Methods of soil analysis part 3—chemical methods. Soil Science Society of America, American Society of Agronomy. p. 91-139.

Sumner, M.E., and W.P. Miller. 1996. Cation exchange capacity and exchange coefficients. In: D. Sparks, A. Page, P. Helmke and R. Loeppert, Eds., Methods of soil analysis part 3—chemical methods. SSSA Book Ser., Madison, W.I. p. 1201-1253.

Sutradhar, A., R.P. Lollato, K. Butchee, and D.B. Arnall. 2014. Determining critical soil pH for sunflower production. International Journal of Agronomy 2014.

Tang, C., Z. Rengel, E. Diatloff, and C. Gazey. 2003. Responses of wheat and barley to liming on a sandy soil with subsoil acidity. Field Crops Res. 80: 235-244.

Tang, Y., D. Garvin, L. Kochian, M. Sorrells, and B. Carver. 2002. Physiological genetics of aluminum tolerance in the wheat cultivar Atlas 66. Crop Sci. 42: 1541-1546.

Thomas, G. 1996. Soil pH and soil acidity. In: D. Sparks, A. Page, P. Helmke, R. Loeppert, P. Soltanpour, M. Tabatabai, C. Johnston and M. Sumner, Eds., Methods of soil analysis. Part 3-chemical methods. p. 475-490.

True, R.R., F.M. Epplin, E.G. Krenzer, and G.W. Horn. 2001. A survey of wheat production and wheat forage use practices in Oklahoma. B-815. Okla. Coop. Ext. Serv., Stillwater, OK.

USDA-NASS. 2014. United States Department of Agriculture. National Agricultural Statistics Service. Available at: http://www.nass.usda.gov/Statistics_by_State/Oklahoma/Publications/County_Estimates/index.asp (data retrieved July 2014).

USDA-NASS. 2015. United States Department of Agriculture. National Agricultural Statistics Service. Available at: http://www.nass.usda.gov/Statistics_by_State/Oklahoma/Publications/Oklahoma_Crop_Reports/2015/ok_wheat_variety_2015.pdf. Verified 06-Jun-2015.

Valle, S.R., J. Carrasco, D. Pinochet, and D.F. Calderini. 2009. Grain yield, above-ground and root biomass of Al-tolerant and Al-sensitive wheat cultivars under different soil aluminum concentrations at field conditions. Plant Soil 318: 299-310.

Yang, Z.-M., H. Yang, J. Wang, and Y.-S. Wang. 2004. Aluminum regulation of citrate metabolism for al-induced citrate efflux in the roots of *Cassia tora*. Plant Sci. 166: 1589-1594.

Zhang, H., and W.R. Raun. 2006. Oklahoma soil fertility handbook, Dept. of Plant and Soil Sci., Oklah. St. Univ., Stillwater, OK.

Zhang, H.L., G. Johnson, G. Krenzer, and R. Gribble. 1998. Soil testing for an economically and environmentally sound wheat production. Commun. Soil Sci. Plant Anal. 29: 1707-1717.

Zhou, L.L., G.H. Bai, H.X. Ma, and B.F. Carver. 2007. Quantitative trait loci for aluminum resistance in wheat. Mol. Breed. 19: 153-161.

Table 2.1. Initial soil pH, extractable aluminum (Al_{KCl}), calcium (Ca), magnesium (Mg), potassium (K), effective cation exchange capacity (ECEC), and aluminum saturation (Al_{sat}) for the 0-15 and 15-45 cm soil layers at Chickasha and Stillwater, Oklahoma. Amount of hydrated lime ($Ca(OH)_2$) and aluminum sulfate ($Al_2(SO_4)_3$) required to change soil pH by a unit are also shown.

Location	Depth	Initial soil pH	Al_{KCl}	Ca	Mg	K	ECEC	Al_{sat}	$Ca(OH)_2$	$Al_2(SO_4)_3$
	cm				$cmol_c\ kg^{-1}$			%		ton pH^{-1}
Chickasha	0 - 15	6.2	0	7.6	4.1	0.5	12.2	0	2.4	1.56
	15 - 45	7	0	9.1	5.3	0.4	14.8	0		
Stillwater	0 - 15	5.2	<0.01	4.3	1.8	0.3	6.3	0.1	1.29	0.82
	15 - 45	5.9	0	5.2	1.8	0.2	7.2	0		

Table 2.2. Monthly cumulative precipitation (Precip.) and reference evapotranspiration (ET_o) for the growing seasons 2012-13, 2013-14, and 2014-15 at Stillwater and Chickasha, OK.

		2012-2013		2013-14		2014-15	
Location	Month	Precip.	ET_o†	Precip.	ET_o	Precip.	ET_o
		mm					
Stillwater	Sep.	28	138	43	141	106	129
	Oct.	15	101	48	86	55	96
	Nov.	11	74	41	61	53	59
	Dec.	11	56	16	37	14	31
	Jan.	25	51	2	61	26	49
	Feb.	79	55	10	56	13	51
	Mar.	28	95	31	110	35	87
	Apr.	135	109	21	151	99	116
	May	158	125	16	180	234	111
	June	100	185	160	168	81	117
Growing season total		590	989	388	1051	716	846
Chickasha	Oct.	14	101	67	98	57	112
	Nov	22	78	37	65	126	68
	Dec	22	59	7	39	19	45
	Jan	38	47	1	50	36	53
	Feb	73	58	9	60	3	58
	Mar	27	101	36	116	53	89
	Apr	268	108	64	151	73	117
	May	76	146	40	190	430	106
	Jun	112	190	150	190	125	80
Growing season total		652	888	411	959	922	728

† - Reference evapotranspiration, calculated according to the FAO 56 procedure (Allen et al., 1998).

Table 2.3. Intercept (β_0), slope (β_1), threshold pH beyond which increases in soil pH did not result in increased response (γ), plateau following γ, and regression significance for the linear-plateau model in Eq. [3] describing percent wheat emergence as function of soil pH for the varieties 2174, Duster, Ruby Lee, and TAM 203 at Stillwater and Chickasha during the 2012-13, 2013-14, and 2014-15 growing seasons.

Location	Growing season	Variety	β_0	β_1	γ	Plateau	r^2
Stillwater	2012-13	2174	-171.5	49.2	5.70	108.8	0.66***
		Duster	-235.0	61.0	4.96	67.2	0.67***
		Ruby Lee	-1047.1	257.5	4.50	111.5	0.61***
		TAM 203	-247.1	66.5	5.20	98.6	0.72***
	2013-14	2174	-937.5	225.6	4.50	77.1	0.48**
		Duster	-269.4	73.7	4.67	75.2	0.47**
		Ruby Lee	-80.7	29.0	5.34	74.0	0.49**
		TAM 203	-3.5	16.4	5.46	85.9	0.36*
	2014-15	2174	-319.1	75.0	4.99	55.1	0.84***
		Duster	-389.1	90.5	4.91	55.7	0.84***
		Ruby Lee	-504.6	117.3	4.89	69.1	0.90***
		TAM 203	-264.9	62.0	4.90	38.9	0.66***
Chickasha	2012-13	2174	-19.2	20.0	5.50	90.8	0 ns
		Duster	-11.3	20.0	5.07	90.1	0 ns
		Ruby Lee	-19.6	25.0	5.00	105.4	0 ns
		TAM 203	-21.9	25.0	4.75	96.9	0 ns
	2013-14	2174	51.4	6.7	5.44	87.9	0.14 ns
		Duster	8.9	13.7	4.86	75.6	0.16 ns
		Ruby Lee	49.6	6.1	5.70	84.3	0.16 ns
		TAM 203	-1203.7	284.2	4.49	73.7	0.45*
	2014-15	2174	-9.9	20.0	4.49	80.0	0 ns
		Duster	-18.4	20.0	4.89	79.5	0.02 ns
		Ruby Lee	2.7	15.7	5.90	95.5	0.31 *
		TAM 203	-214.7	56.9	5.16	78.9	0.58 **

*, **, and *** - significant at $p < 0.05$, 0.01, and 0.001, respectively.
ns, non-significant.

Table 2.4. Analysis of covariance results for percent emergence, forage yield, grain volume weight, and grain protein concentration as function of wheat variety, soil aluminum saturation (Al_{sat}) and their interaction, for the growing seasons 2012-13, 2013-14, and 2014-15 at Stillwater and Chickasha, OK.

	Stillwater			Chickasha		
Source	2012-13	2013-14	2014-15	2012-13	2013-14	2014-15
	Percent emergence					
Variety	***	**	***	***	***	**
Al_{sat}	***	***	***	ns	**	***
Variety x Al_{sat}	*	ns	*	ns	ns	*
	Grain volume weight					
Variety	***	***	ns	***	***	ns
Al_{sat}	ns	ns	ns	ns	ns	ns
Variety x Al_{sat}	ns	ns	ns	ns	ns	ns
	Grain protein concentration					
Variety	***	***	*	***	***	***
Al_{sat}	ns	ns	ns	ns	***	ns
Variety x Al_{sat}	ns	ns	ns	ns	ns	*

*, **, and *** - significant at $p < 0.05$, 0.01, and 0.001, respectively.

ns, non-significant.

† - Forage yield was not measured in Chickasha, site characterized by grain-only wheat management.

Table 2.5. Coefficients and standard errors (SE) for covariate analysis using the model $Y = \beta_0 + \beta_1 x$ describing percent wheat emergence of the wheat varieties 2174, Duster, Ruby Lee, and TAM 203 as function of soil aluminum saturation (Al_{sat}) during the growing seasons 2012-13, 2013-14, and 2014-15 at Stillwater and Chickasha, OK.

Location	Growing season	Variety	β_0	SE	β_1	SE
Stillwater	2012-13	2174	103.1	± 11.6	-3.93	± 0.93
		Duster	68.0	± 11.6	-2.33	± 0.93
		Ruby Lee	136.3	± 11.6	-5.15	± 0.93
		TAM 203	98.4	± 8.2	-3.50	± 0.66
	2013-14	2174	79.2	± 4.8	-1.18	± 0.53
		Duster	77.6	± 4.8	-1.34	± 0.53
		Ruby Lee	72.7	± 4.8	-1.61	± 0.53
		TAM 203	85.2	± 3.4	-1.12	± 0.38
	2014-15	2174	57.4	± 3.2	-5.70	± 1.22
		Duster	58.7	± 4.6	-6.07	± 1.22
		Ruby Lee	72.4	± 4.6	-7.28	± 1.22
		TAM 203	40.5	± 3.2	-3.87	± 0.86
Chickasha	2012-13	2174	93.2	± 5.5	-†	-
		Duster	84.2	± 5.5	-	-
		Ruby Lee	107.3	± 5.5	-	-
		TAM 203	97.1	± 3.9	-	-
	2013-14	2174	87.8	± 3.1	-1.43	± 1.15
		Duster	75.5	± 3.1	-0.73	± 1.15
		Ruby Lee	83.6	± 3.1	-1.09	± 1.15
		TAM 203	74.2	± 2.2	-1.29	± 0.81
	2014-15	2174	79.9	± 3.8	0.06	± 1.91
		Duster	81.9	± 3.8	-2.44	± 1.91
		Ruby Lee	93.1	± 3.8	-4.25	± 1.91
		TAM 203	79.7	± 2.7	-4.61	± 1.35

† - Aluminum saturation was not a significant factor affecting wheat emergence at Chickasha during the 2012-13 growing season.

Table 2.6. Coefficient estimates and significance level for the equation $Y = a/\{1+e[-(t-t0)/b]\}$ describing percent wheat canopy cover development as function of soil pH for the wheat varieties 2174, Duster, Ruby Lee, and TAM203, under dual-purpose management grown in an Easpur loam at Stillwater, OK, during the growing seasons 2012-13, 2013-14, and 2014-15.

		Soil pH range																	
		4 .0 - 4.5			4.5 - 5.0			5.0 - 5.5			5.5 - 6.0			6.0 - 7.0			> 7		
Growing season	Variety	*a*	t_0	r^2	*a*	t_0	r^2	*a*	t_0	r^2	*a*	t_0	r^2	*a*	t_0	r^2	*a*	t_0	r^2
2012-13		%	d		%	d		%	d		%	d		%	d		%	d	
	2174	34.6	98.4	0.41**	61.4	35.5	0.50***	70.6	27.6	0.64***	82.4	25.5	0.86***	-†	-	-	86.6	25.5	0.92***
	Duster	42.7	53.2	0.79***	64.1	42.2	0.56***	74.6	29.6	0.70***	83.2	26.1	0.82***	-	-	-	85.3	25.6	0.85***
	Ruby Lee	28.9	55.4	0.44**	67.5	39.1	0.53***	72.4	28.7	0.61***	87.6	25.1	0.87***	-	-	-	89.2	25.9	0.90***
	TAM 203	62.8	116.4	0.77***	69.3	60.2	0.51***	68.4	27.2	0.49**	85.8	23.9	0.82***	-	-	-	87.4	25.8	0.86***
2013-14																			
	2174	-	-	-	69.8	38.2	0.50***	91.5	36.2	0.93***	92.6	36.1	0.94***	88.9	36.3	0.89***	90.1	36.2	0.91***
	Duster	-	-	-	74.1	39.8	0.67**	91.1	36.5	0.94***	92.5	36.2	0.92***	89.1	36.3	0.87***	90.5	36.1	0.91***
	Ruby Lee	-	-	-	70.7	43.7	0.55***	93.5	38.2	0.96***	93.7	36.3	0.94***	92.2	36.1	0.94***	91.9	39.5	0.96***
	TAM 203	-	-	-	72.1	36.8	0.67***	91.6	36.2	0.94***	93.3	36.3	0.96***	91.9	36	0.93***	89.4	37.5	0.92***
2014-15																			
	2174	na‡	na	na	na	na	na	71.6	28.4	0.56***	79.7	27.9	0.79***	82.1	27.8	0.78***	80.7	27.6	0.64***
	Duster	16.2	133.5	0.68***	na	na	na	69.3	29.1	0.67***	77.9	27.9	0.66***	75.2	27.9	0.55**	79.3	27.9	0.57***
	Ruby Lee	na	na	na	na	na	na	75.7	38.1	0.70***	84.6	28.2	0.84***	85.1	28.1	0.88***	89.1	28.2	0.96***
	TAM 203	20.8	128.4	0.70***	na	na	na	61.6	35.8	0.34***	84.9	27.9	0.88***	83.3	27.6	0.79***	86.2	28.4	0.96***

*, **, and *** - significant at $p < 0.05$, 0.01, and 0.001, respectively.

† - Soil pH range not achieved with amendment application and therefore inexistent at that site-year.

‡ - na, not applicable. Data failed to converge for a after the maximum number of iterations had been exceeded or the confidence interval for *a* included zero and was not significant.

Table 2.7. Coefficient estimates and significance level for the equation $Y = a/\{1+e[-(t-t0)/b]\}$ describing percent wheat canopy cover development as function of soil pH wheat varieties 2174, Duster, Ruby Lee, and TAM203, under grain-only management grown in an Dale silt loam at Chickasha, OK, during the growing seasons 2012-13, 2013-14. Model did not converge or was not significant during the 2014-15 growing season and therefore data is not shown.

		Soil pH range														
Growing		4.5 - 5.0			5.0 - 5.5			5.5 - 6.0			6.0 - 7.0			> 7		
season	Variety	a	t_0	r^2	a	t_0	r^2	a	t_0	r^2	a	t_0	r^2	a	t_0	r^2
2012-13		%	d		%	d		%	d		%	d		%	d	
	2174	-†	-	-	-	-	-	87.3	42.1	0.88***	86.4	43.9	0.89***	-	-	-
	Duster	-	-	-	-	-	-	89.9	38.1	0.92***	90.3	38.5	0.93***	-	-	-
	Ruby Lee	-	-	-	-	-	-	85.4	42.4	0.87***	88.8	41.7	0.91***	-	-	-
	TAM 203	-	-	-	-	-	-	88.9	38.5	0.92***	90.7	37.5	0.94***	-	-	-
2013-14																
	2174	66.8	173.6	0.90***	85.2	152.9	0.92***	70.7	153.4	0.71***	92.5	150.2	0.96***	96.2	149.6	0.90***
	Duster	49.3	166.6	0.82***	86.3	155.6	0.96***	75.3	152.7	0.84***	88.4	151.8	0.94***	108.2	151.1	0.91***
	Ruby Lee	26.9	169.4	0.71***	80.1	161.4	0.96***	74.5	164.1	0.76***	88.1	155.24	0.97***	95.3	154.7	0.94***
	TAM 203	26.6	72.5	0.68***	90.3	156.5	0.98***	76.9	154.4	0.81***	76.9	152.9	0.97***	107.9	154.6	0.92***

*, **, and *** - significant at $p < 0.05$, 0.01, and 0.001, respectively.

† - Soil pH range not achieved with amendment application and therefore inexistent at that site-year.

Table 2.8. Intercept (β_0), slope (β_1), threshold pH beyond which increases in soil pH did not result in increased response (γ), plateau following γ, and regression significance for the linear-plateau model in Eq. [3] describing wheat grain yield as function of soil pH for the varieties 2174, Duster, Ruby Lee, and TAM 203 at Stillwater and Chickasha during the 2012-13, 2013-14, and 2014-15 growing seasons.

Location	Growing season	Variety	β_0	β_1	γ	Plateau	r^2
Stillwater	2012-13	2174	-31615.6	8375.5	4.33	4629.0	0.64***
		Duster	-7296.3	2592.7	4.47	4287.9	0.67***
		Ruby Lee	-20647.9	5753.6	4.44	4888.0	0.64***
		TAM 203	-8152.4	2713.3	4.53	4144.9	0.72***
	2013-14	2174	-3100.8	1076.1	4.50	1740.7	0.04 ns
		Duster	-2025.8	952.3	4.50	2255.1	0.02 ns
		Ruby Lee	496.1	318.7	5.38	2210.8	0.14 ns
		TAM 203	459.0	280.9	5.59	2027.7	0.14 ns
	2014-15	2174	-8668.6	2395.1	5.01	3335.1	0.53*
		Duster	-44455.9	10622.6	4.50	3394.6	0.72***
		Ruby Lee	-59545.8	14151.8	4.52	4433.9	0.86***
		TAM 203	-21753.4	5221.0	4.88	3739.8	0.87***
Chickasha	2012-13	2174	-626.3	840.9	6.10	4503.0	0.18 ns
		Duster	-2561.0	1248.8	5.94	4861.2	0.15 ns
		Ruby Lee	390.0	728.7	6.10	4835.4	0.16 ns
		TAM 203	17.7	750.0	5.00	3767.7	0 ns
	2013-14	2174	-1047.1	586.5	5.20	2002.7	0.23 ns
		Duster	-829.0	519.3	5.20	1871.4	0.14 ns
		Ruby Lee	-1216.9	496.8	5.58	1556.5	0.27 ns
		TAM 203	26.2	253.6	-†	-	0.35 *
	2014-15	2174	-6933.0	1986.3	5.12	3242.0	0.27 ns
		Duster	-3635.5	1447.0	5.10	3743.9	0.14 ns
		Ruby Lee	-17864.7	4154.4	5.18	3661.2	0.59**
		TAM 203	-21935.0	5054.2	5.13	3989.4	0.81***

*, **, and *** - significant at $p < 0.05$, 0.01, and 0.001, respectively.

ns, non-significant.

† - Plateau not reached within the range in pH values studied. Coefficients refer to the linear portion of the model.

Table 2.9. Intercept (β_0), slope (β_1), threshold pH beyond which increases in soil Al_{sat} resulted in decreased response (γ), plateau preceding γ, and regression significance for the plateau-linear or linear model describing wheat grain yield as function of soil Al_{sat} for the varieties 2174, Duster, Ruby Lee, and TAM 203 at Stillwater and Chickasha during the 2012-13, 2013-14, and 2014-15 growing seasons.

Location	Growing season	Variety	β_0	β_1	γ	Plateau	r^2
Stillwater	2012-13	2174	13482.7	-503.05	17.6	4629.0	0.68***
		Duster	6562.8	-151.12	15.1	4287.9	0.70***
		Ruby Lee	9774.2	-319.92	15.3	4878.5	0.69***
		TAM 203	5304.5	-106.95	10.6	4170.4	0.76***
	2013-14	2174	1810.8	-8.80	11.9	1705.6	0 ns
		Duster	2388.9	-12.17	10.7	2258.5	0.01 ns
		Ruby Lee	2817.2	-61.06	10.7	2163.1	0.21 ns
		TAM 203	2461.8	-48.41	10.7	1943.3	0.38 ns
	2014-15	2174	6442.7	-575.23	5.5	3284.3	0.77***
		Duster	4358.4	-310.23	3.2	3372.6	0.57***
		Ruby Lee	4592.8	-284.26	-†	-	0.62***
		TAM 203	3916.4	-332.24	-	-	0.81***
Chickasha	2012-13	2174	na‡	na	na	na	0 ns
		Duster	na	na	na	na	0 ns
		Ruby Lee	na	na	na	na	0 ns
		TAM 203	na	na	na	na	0 ns
	2013-14	2174	2117.0	-87.98	1.6	1972.2	0.15 ns
		Duster	1902.0	-66.29	1.2	1821.3	0.08 ns
		Ruby Lee	1466.7	-75.42	-0.5	1504.9	0.15 ns
		TAM 203	1588.3	-90.55	-	-	0.22*
	2014-15	2174	3252.6	-113.33	0.0	3252.6	0.13 ns
		Duster	3744.3	-56.05	0.0	3744.3	0.03 ns
		Ruby Lee	3664.5	-315.62	-	-	0.4**
		TAM 203	4084.0	-360.61	-	-	0.61***

*, **, and *** - significant at $p < 0.05$, 0.01, and 0.001, respectively.
ns, non-significant.
† - Linear model explained the relationship between wheat yield and aluminum saturation.
‡ - na, not applicable. Model failed to converge due to small range in aluminum saturation values in 2012-13 at Chickasha, OK.

Table 2.10. Grain volume weight and grain protein concentration of the wheat varieties 2174, Duster, Ruby Lee, and TAM 203, following the 2012-13, 2013-14, and 2014-15 growing seasons at Stillwater and Chickasha, OK.

Growing season	Variety	Grain volume weight		Grain protein concentration	
		Stillwater	Chickasha	Stillwater	Chickasha
		kg m^{-3}		g kg^{-1}	
2012-13	2174.00	67.9 b	75.0 a	148 b	160 b
	Duster	69.7 a	72.5 b	137 c	150 c
	Ruby Lee	70.2 a	74.9 a	144 b	157 bc
	TAM 203	65.9 c	69.9 c	154 a	169 a
2013-14	2174.00	70.8 a	69.5 a	191 a	170 ab
	Duster	66.6 b	69.8 a	171 c	164 b
	Ruby Lee	68.9 a	69.7 a	183 b	175 a
	TAM 203	64.7 b	66.9 b	186 ab	174 a
2014-15	2174.00	70	67.1	138 a	139 a
	Duster	68.7	69.7	133 ab	133 b
	Ruby Lee	68.8	69.5	125 b	133 b
	TAM 203	69.8	70.1	137 a	139 a

† - Values followed by the same letter within site-year are not statistically different at $\alpha = 0.05$.

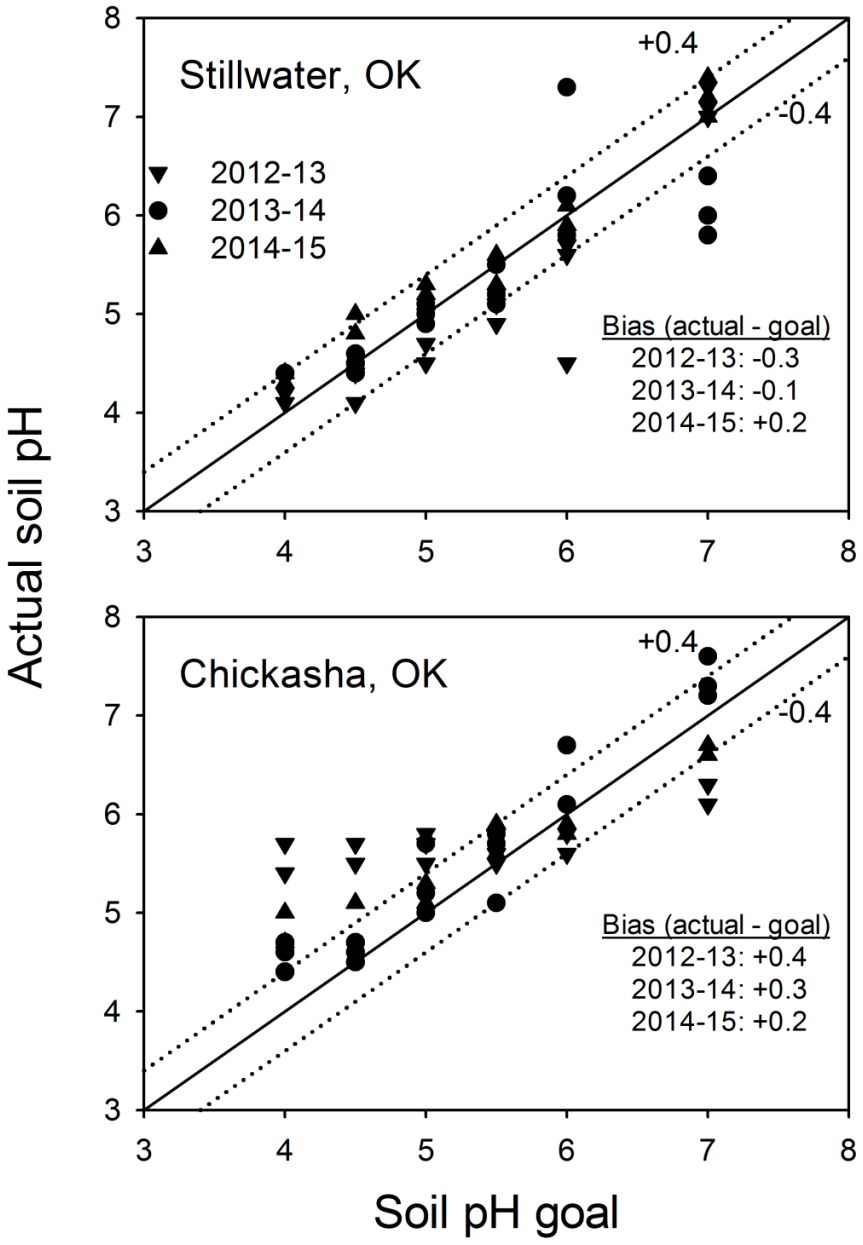

Figure 2.1. Actual soil pH following wheat harvest versus soil pH goal for the growing seasons 2012-13, 2013-14, and 2014-15 at Stillwater and Chickasha, OK. Solid line is 1:1 line, dashed lines are ±0.4 deviation from 1:1.

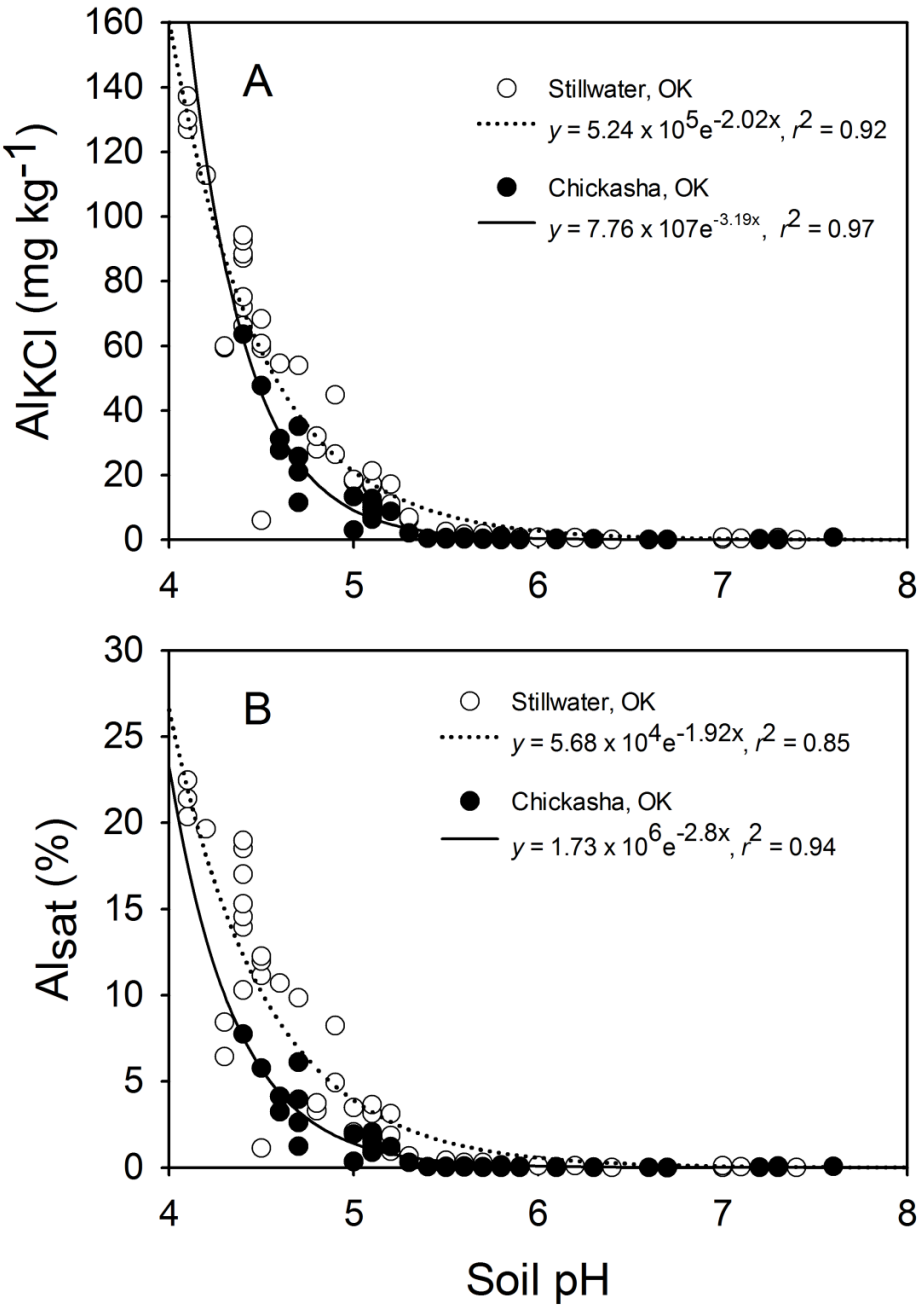

Figure 2.2. Potassium chloride extractable aluminum (Al_{KCl}) and aluminum saturation (Al_{sat}) as affected by soil pH in a Easpur loam at Stillwater, OK, and in a Dale silt loam at Chickasha, OK, during the growing seasons 2012-13, 2013-14, and 2014-15.

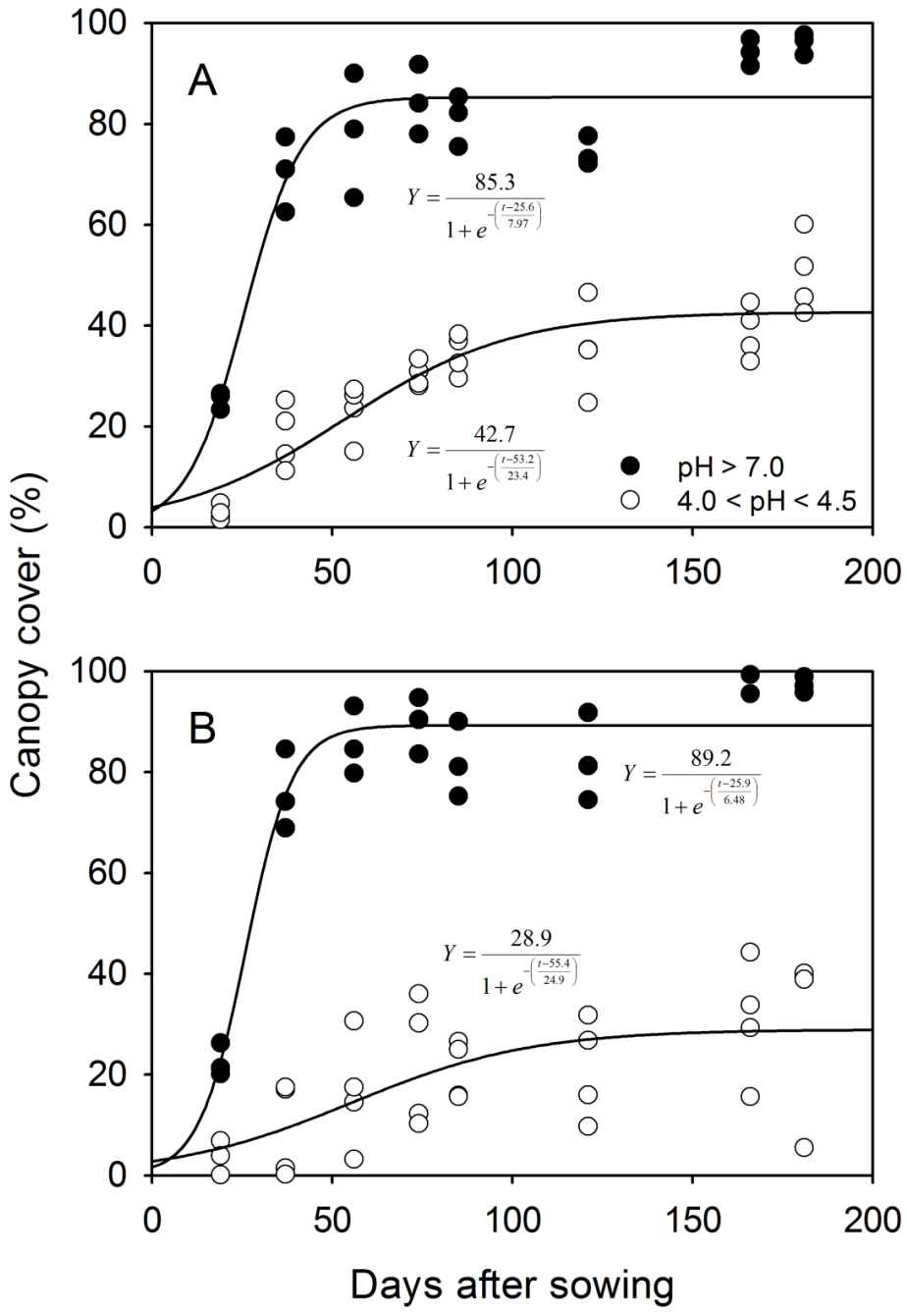

Figure 2.3. Dynamics of canopy cover development during the growing season as function of days after sowing for (A) the wheat variety Duster and (B) Ruby Lee grown in soil pH > 7 versus soil pH in the 4.0 to 4.5 range at Stillwater, OK, during the 2012-13 growing season.

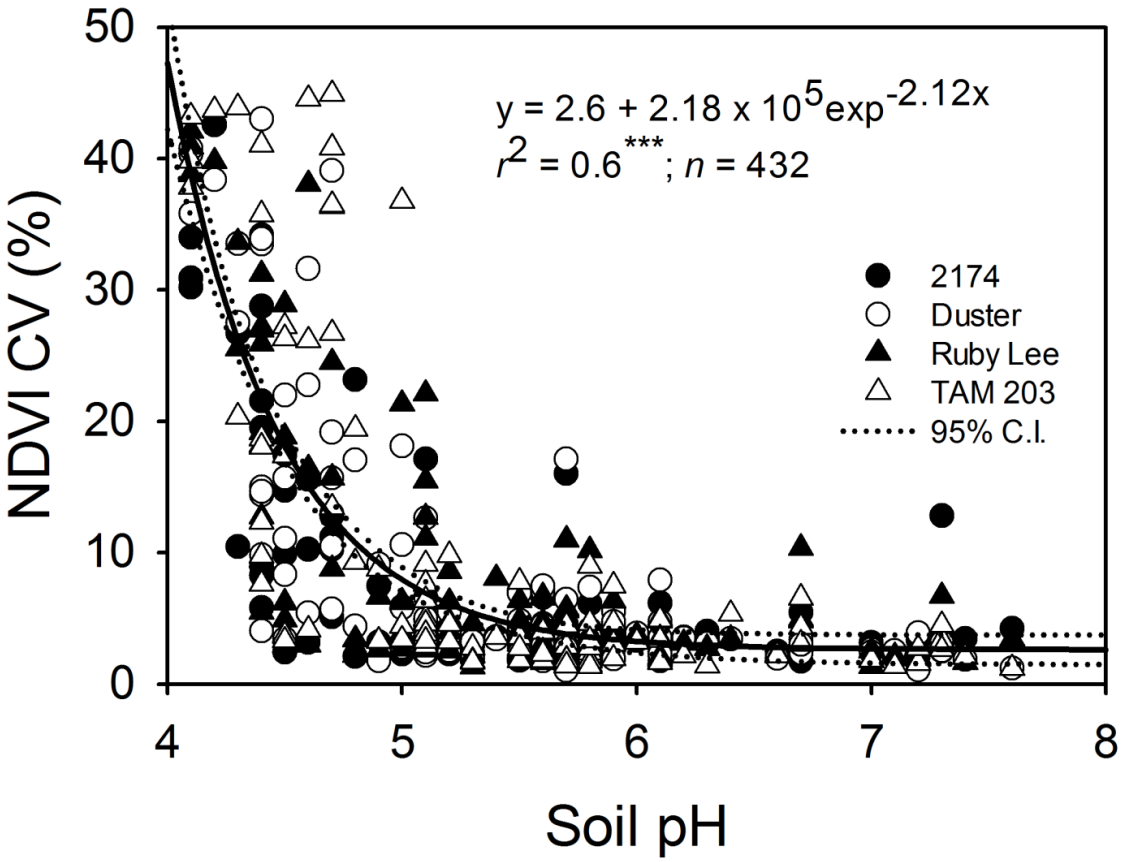

Figure 2.4. Coefficient of variation of normalized difference vegetative index (NDVI CV) measured at winter wheat jointing as affected by soil pH for the varieties 2174, Duster, Ruby Lee, and TAM 203 at Stillwater and Chickasha, OK, during the growing seasons 2012-13, 2013-14, and 2014-15.

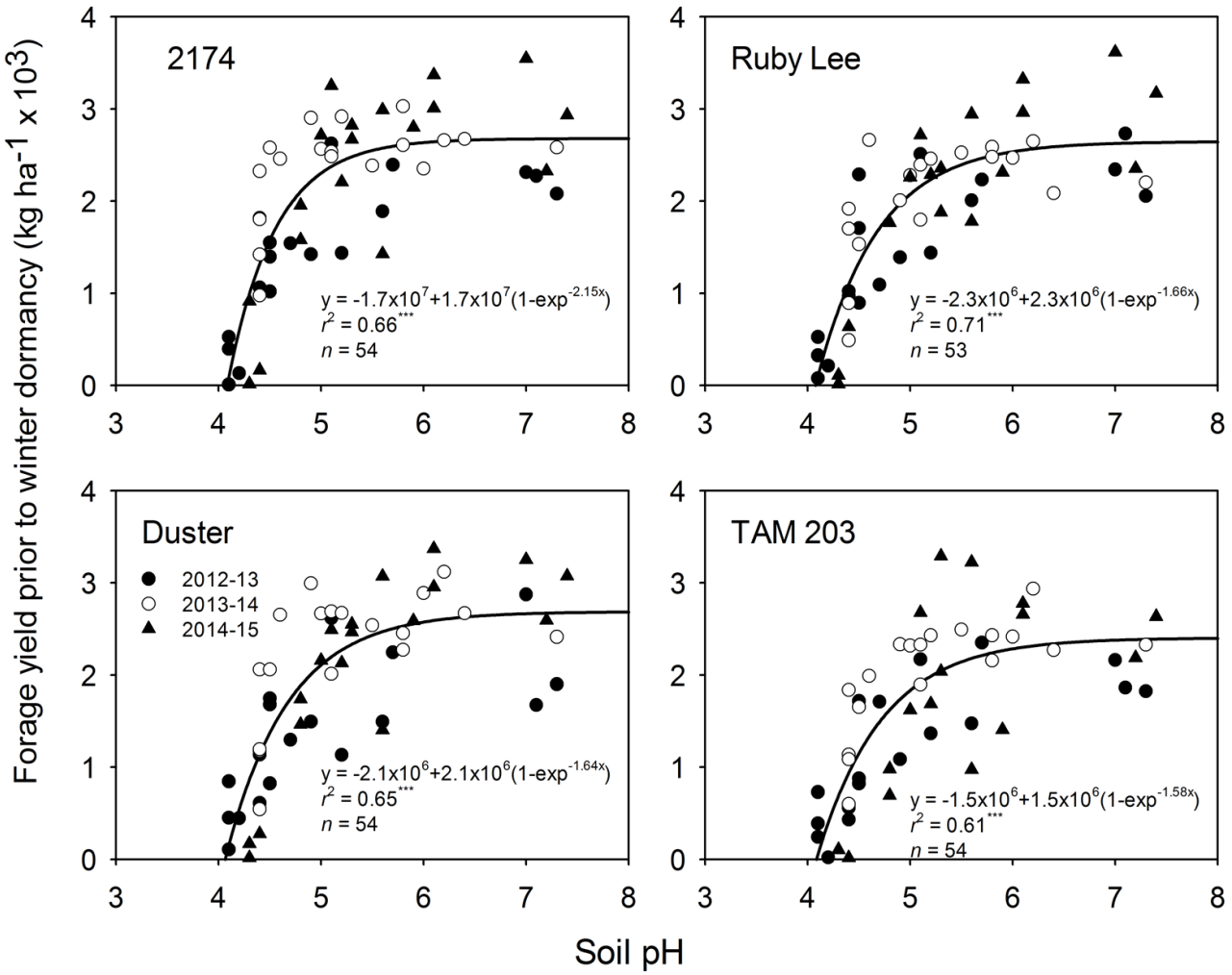
2174
y = -1.7x10^7+1.7x10^7(1-exp^-2.15x)
r^2 = 0.66***
n = 54
Ruby Lee
y = -2.3x10^6+2.3x10^6(1-exp^-1.66x)
r^2 = 0.71***
n = 53
Duster
2012-13
2013-14
2014-15
y = -2.1x10^6+2.1x10^6(1-exp^-1.64x)
r^2 = 0.65***
n = 54
TAM 203
y = -1.5x10^6+1.5x10^6(1-exp^-1.58x)
r^2 = 0.61***
n = 54
Forage yield prior to winter dormancy (kg ha-1 x 10^3)
Soil pH

Figure 2.5. Forage yield prior to winter dormancy of wheat varieties 2174, Ruby Lee, Duster, and TAM 203, as affected by soil pH at Stillwater, OK, during the 2012-13, 2013-14, and 2014-15 growing seasons.

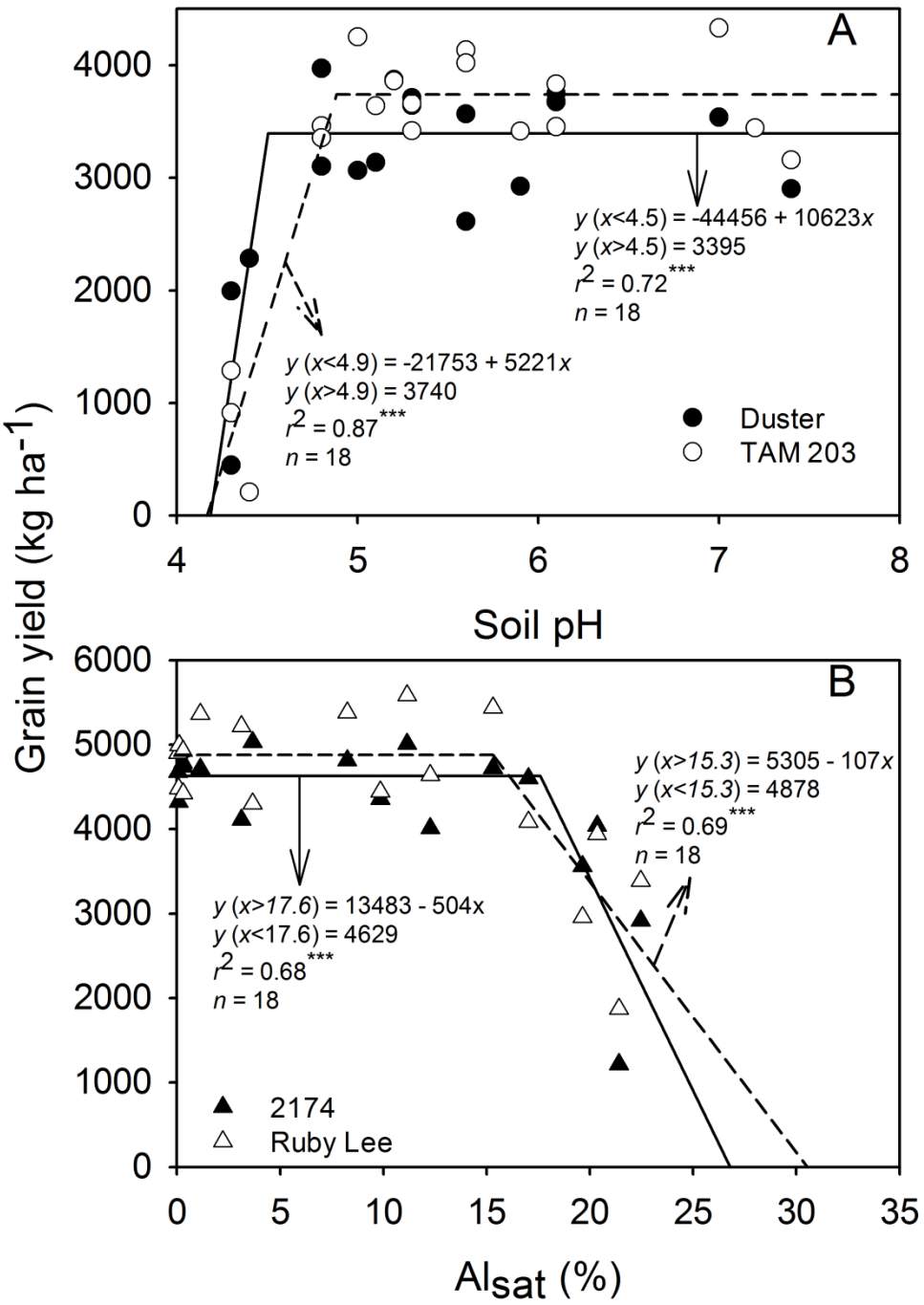

Figure 2.6. Grain yield of the wheat varieties (A) Duster and TAM 203 as affected by soil pH during the 2014-15 growing season in Stillwater, OK; and (B) 2174 and Ruby Lee as affected by soil aluminum saturation (Al_{sat}) during the 2012-13 growing season in Stillwater, OK.

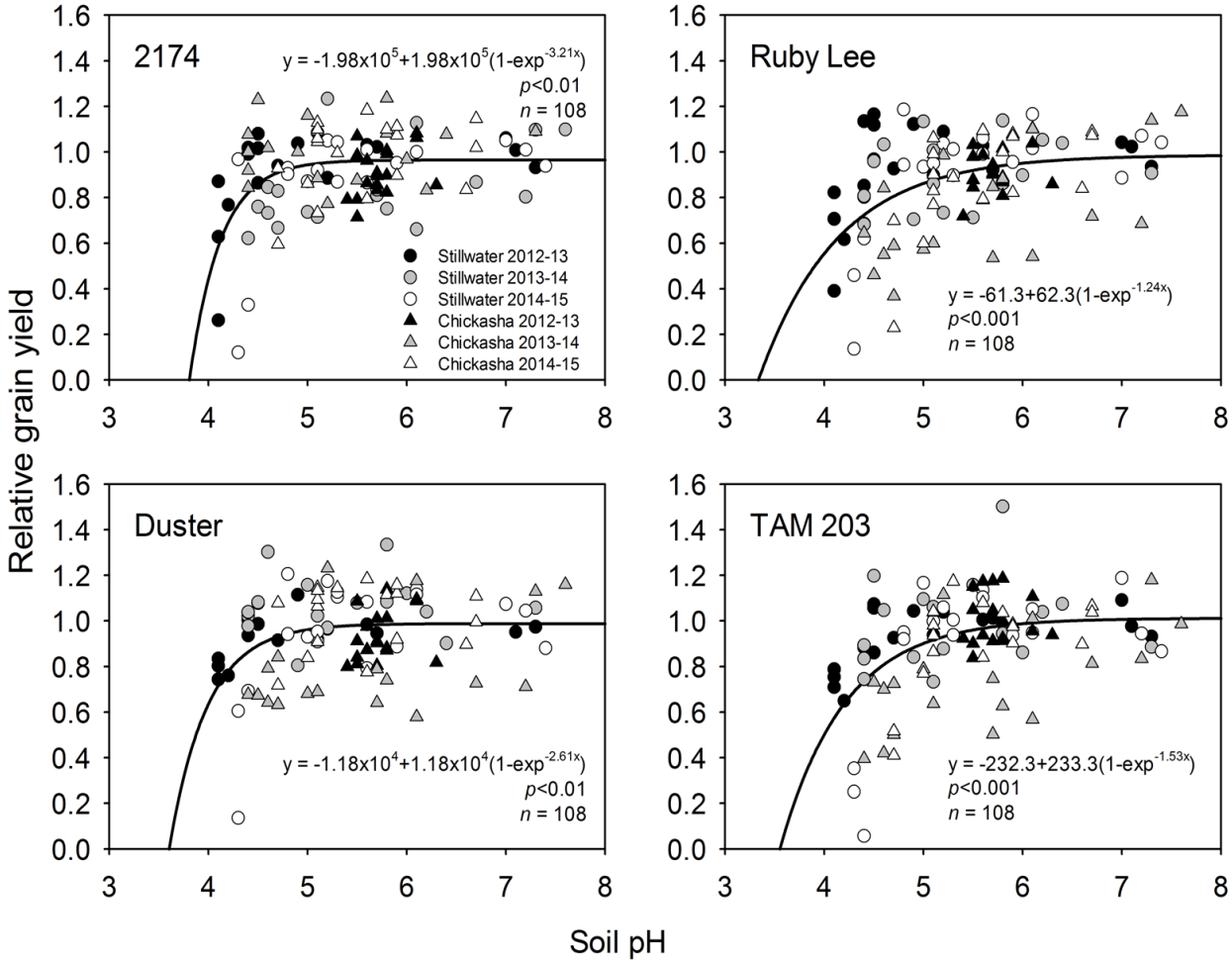
2174
y = -1.98x10^5+1.98x10^5(1-exp^-3.21x)
p<0.01
n = 108
Stillwater 2012-13
Stillwater 2013-14
Stillwater 2014-15
Chickasha 2012-13
Chickasha 2013-14
Chickasha 2014-15
Ruby Lee
y = -61.3+62.3(1-exp^-1.24x)
p<0.001
n = 108
Duster
y = -1.18x10^4+1.18x10^4(1-exp^-2.61x)
p<0.01
n = 108
TAM 203
y = -232.3+233.3(1-exp^-1.53x)
p<0.001
n = 108
Relative grain yield
Soil pH

Figure 2.7. Relative grain yield of the wheat varieties 2174, Ruby Lee, Duster, and TAM 203, as affected by soil pH during the 2012-13, 2013-14, and 2014-15 growing seasons at Stillwater and Chickasha, OK.

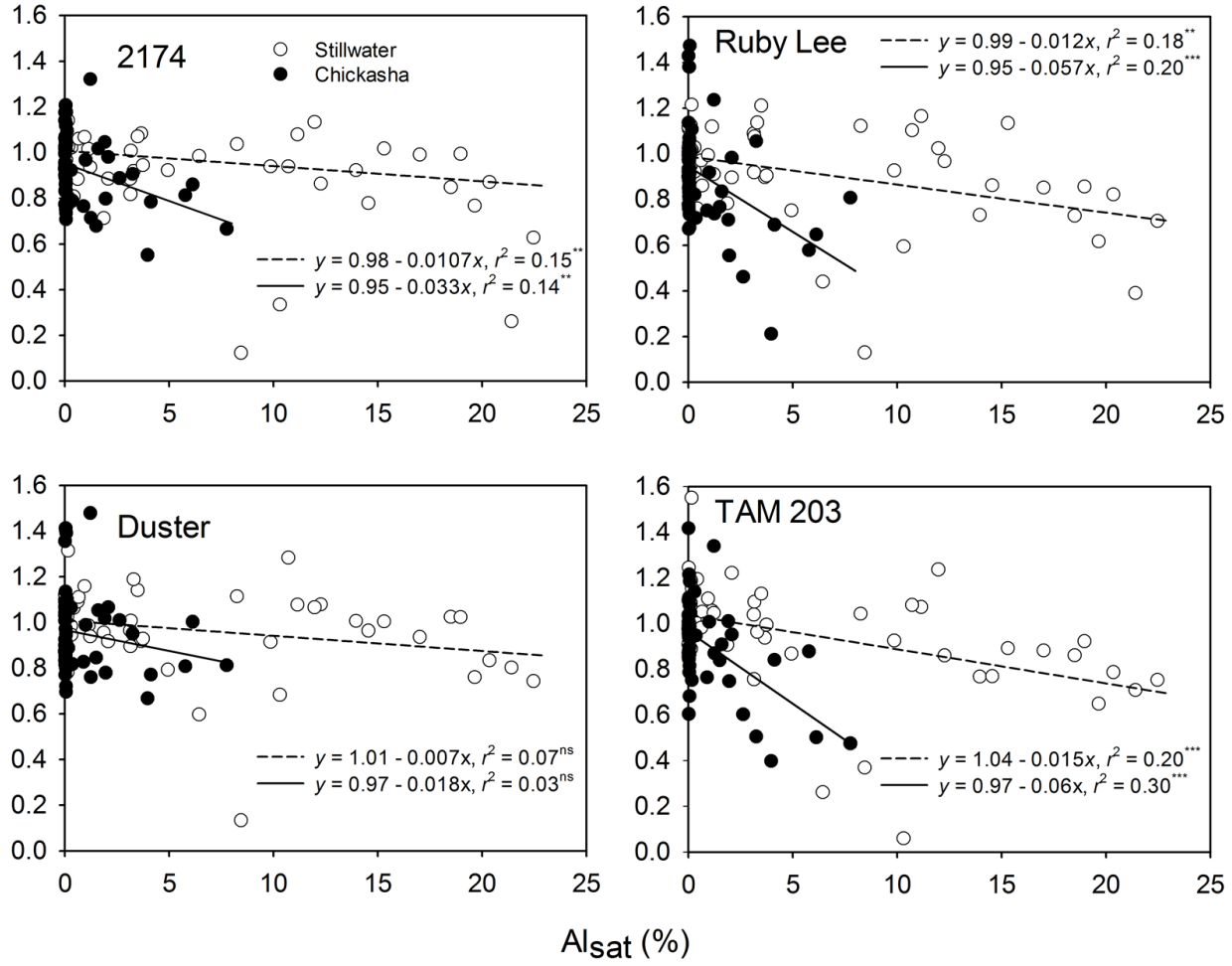

Figure 2.8. Relative grain yield of the wheat varieties 2174, Ruby Lee, Duster, and TAM 203, as affected by percent aluminum saturation (Al_{sat}) during the 2012-13, 2013-14, and 2014-15 growing seasons at Stillwater and Chickasha, OK.

CHAPTER III

PREDICTION OF PLANT AVAILABLE WATER AT SOWING FOR WINTER WHEAT IN THE SOUTHERN GREAT PLAINS

ABSTRACT

Plant available water at sowing (PAW_s) can impact wheat stand establishment, early crop development, and yield. Consequently, PAW_s is an essential input in crop simulation models and its estimation can improve agronomic decisions. Our objective was to predict PAW_s in continuous winter wheat (*Triticum aestivum* L.) by modeling the soil moisture dynamics of the preceding 4-mo summer fallow. The mechanistic soil water balance models dual crop coefficient (dual K_c) and Simple Simulation Modeling (SSM), were calibrated, validated, and tested using soil moisture datasets collected from 2009 to 2013 in Oklahoma totaling 29 site-years. Additionally, PAW_s was predicted using empirical non-linear models based on cumulative fallow precipitation and the soil's plant available water capacity (PAWC). Both the dual K_c and SSM models resulted in normalized root mean squared error ($RMSE_n$) below 12% (20 mm) for the calibration and validation datasets. Modeled PAW_s for the prediction dataset was within ±30% of field observations in 67% of the site-years for both dual K_c and SSM models, with $RMSE_n$ of 27 and 32%, respectively. An exponential and a logarithmic model of PAW_s using cumulative fallow precipitation and PAWC both resulted in $RMSE_n$ = 23 and 29% in the calibration and validation

datasets, respectively. The dual K_c model was slightly superior to empirical models based on non-linear regression analysis, and was superior to the SSM model. Initializing the dual K_c at the start of the preceding fallow or using empirical relationships allow for acceptable predictions of PAW_s, eliminating the need for subjective PAW_s values.

Keywords: prediction, plant available water at sowing, winter wheat, mechanistic simulation, soil water balance models, empirical models, dual crop coefficient, simple simulation modeling.

Abbreviations: D: drainage; *d*: Willmott's index of agreement; Dual K_c: dual crop coefficient; E: evaporation from bare soil; ET_o: evapotranspiration; I: irrigation; K_{cb}: crop basal coefficient; $K_{c\ min}$: crop minimum coefficient; P: precipitation; PAW: plant available water; PAWC: plant available water capacity; PAW_i: initial plant available water in the summer fallow; PAW_s: plant available water at sowing; RMSE: root mean square error; $RMSE_n$: normalized root mean square error; RO: runoff; Rs: incident solar radiation; SSM: simple simulation modeling; T: crop transpiration; T_{max}: maximum daily temperature; T_{min}: minimum daily temperature; Ze: depth of soil layer subjected to soil evaporation; θ_{DUL}: volumetric soil water content at the drained upper limit; θ_{LL}: volumetric soil water content at the lower limit; θ_S: volumetric soil water content at saturation; θ_v: volumetric soil water content.

3.1. INTRODUCTION

Hard red winter wheat is the dominant crop in the southern Great Plains with a planted area of approximately 8 million hectares per year in Kansas, Oklahoma, and Texas (USDA-NASS, 2014). In this region, the long-term (30-yr) annual precipitation ranges from ~400 mm in the west to more than 1100 mm in the east. The precipitation regime during the wheat growing season (October through June) follows the same geospatial gradient as the annual precipitation, ranging from 200 mm to more than 500 mm. For the same period, the cumulative reference evapotranspiration (ET_o) ranges from 700 to 900 mm (Musick and Porter, 1990), substantially exceeding growing season rainfall. The resulting atmospheric water deficit creates a challenging environment for rainfed winter wheat systems (Norwood, 2000), in which plant available water at sowing (PAW_s) can account for a significant fraction of the total crop water requirement during the growing season (Stone and Schlegel, 2006).

Adequate PAW_s can improve wheat germination, emergence, stand establishment, and winter hardiness, resulting in greater wheat yield potential (Paulsen, 1987). As a result, PAW_s is an important factor in determining both grain only and dual-purpose wheat systems productivity in the southern Great Plains. In dual-purpose wheat systems, wheat is grazed early in the growing season and is later harvested for grain, and an increase in PAW_s from 40 to 60% PAW (~36 mm) can increase wheat forage production in as much as 28% (~826 kg ha^{-1}) (Garbrecht et al., 2010). Additionally, a simulation analysis using long-term weather data in central Oklahoma indicated that wheat yields increase with increased PAW_s in dry growing seasons but are not as responsive when the growing season has abundant precipitation (Zhang, 2003). The simulations by Zhang (2003) were performed in a region where the 28-yr growing season precipitation average was ~485 mm, suggesting that PAW_s may be a stronger limiting factor to wheat grain yields in the western portion of the Great Plains, region characterized by lower growing season precipitation. Indeed, Lyon et al. (2007), Norwood (2000), and Stone and Schlegel (2006) found reduced wheat

yields associated with reduced PAW_s in Colorado and western Kansas, highlighting the positive linear relationship between PAW_s and rainfed wheat yields in wheat-fallow systems in the Great Plains.

Knowledge of PAW_s can help identifying favorable planting dates and lead to better management decisions such as appropriate plant population, timing of nutrient application, irrigation scheduling (Grassini et al., 2010), and grazing intensity (Garbrecht et al., 2010). Furthermore, PAW_s is often a required input in crop simulation models to describe the initial soil moisture conditions (Sinclair et al., 2007). Generally, an arbitrary value of PAW_s is assumed when running a soil water balance (Garbrecht et al., 2010; Zhang, 2003). However, choosing arbitrary values can result in erroneous predictions when using crop models, especially in water-limited regions like the southern Great Plains. Therefore, a reliable methodology to predict PAW_s not only has the potential to improve on-farm management decisions, but also to increase the reliability of regional assessments based on crop simulation models by reducing uncertainties in the initial conditions.

Existing approaches to predict PAW_s typically rely on regression techniques that use observed weather information during the preceding fallow period. Grassini et al. (2010) developed a linear-plateau regression model based on the remaining plant available water (PAW) from the previous crop, cumulative precipitation during the fallow period, and the soil's plant available water capacity (PAWC) to estimate PAW_s for maize in the western Corn Belt. A similar approach including more explanatory variables was developed by Nielsen and Vigil (2010) to estimate precipitation storage efficiency of wheat-fallow systems (14-mo fallow) in the central Great Plains based on linear regression including tillage practices, rainfall and snowfall, vapor pressure deficit, wind speed, and average solar radiation. However, the 14-mo fallow periods in wheat-fallow systems in the central Great Plains (Colorado) greatly differs from the 4-mo summer fallow periods in continuous wheat in the southern Great Plains, as the latter is

characterized by shorter duration, higher evaporative demand, and lower water storage (Mathews and Army, 1960). Thus, extrapolation of the empirical relationships developed for other regions is not a prudent approach to predict PAW_s in continuous wheat systems of the southern Great Plains.

A plausible alternative to the aforementioned empirical models to predict PAW_s is by simulating the soil water dynamics of the preceding fallow period using a soil water balance model with daily time steps. Although this approach does not eliminate the need to set the initial soil moisture conditions of the water balance, prior research studies have shown that soil water balance models initialized at different soil moisture contents tend to converge toward a single soil moisture value (Capehart and Carlson, 1994). This convergence seems to rely on the total rainfall during the simulated period, the depth of the soil profile, and the length of the simulated period (Capehart and Carlson, 1994). An initially wet soil profile may experience greater water losses than initially dry soil profiles when subjected to the same environmental conditions and, conversely, dry soil profiles may experience greater water storage due to greater infiltration and decreased losses (Capehart and Carlson, 1994). This phenomenon has been successfully used to predict initial soil water content for regional-scale meteorological and hydrological models in northeastern U.S with the period required for model convergence ranging from few weeks to several months (Capehart and Carlson, 1994; Grunmann, 2005; Smith et al., 1994). Given the notable difference in meteorological characteristics and precipitation totals, results obtained for the northeastern part of the U.S. may not be applicable in the southern Great Plains. Therefore, there is a need to examine the effectiveness of soil water balance models to predict PAW_s in continuous wheat systems in the southern Great Plains.

We hypothesize that PAW_s can be effectively predicted by initializing a soil water balance model at the beginning of the preceding summer fallow period using arbitrary initial plant available water (PAW_i) value within the PAWC interval. The objective of this study was to

identify effective methods to predict PAW_s in continuous winter wheat (i) by simulating the soil water dynamics of the preceding summer fallow period, and (ii) by using empirical non-linear models to predict PAW_s using observed weather during the summer fallow period.

3.2. MATERIAL AND METHODS

3.2.1. Site description

The study was conducted at 10 sites across Oklahoma, USA (34.5°N-36.8°N; 97°W-99.3°W), spanning a geographic range that encompasses the majority of Oklahoma's wheat cropland (Fig. 3.1). Wheat fields in the region typically have mild slopes (1-6%), and common soil textures are silt loam (e.g. Kirkland and Pond Creek soil series) and silty clay loam (e.g. Hollister and Tillman soil series). Summer fallow periods typically occur during the months of June, July, August, and September, and are characterized by evaporative demands exceeding cumulative rainfall. Long-term averages (1994 – 2013) of selected weather variables for the fallow period for the studied sites are shown in Table 3.1.

3.2.2. Mechanistic soil water balance approach

3.2.2.1. Calibration, validation, and prediction datasets

To calibrate the soil water balance models we used a dataset composed of soil moisture values recorded at two locations: i) the Oklahoma State University Agronomy Research Station in Stillwater, OK (36.12°N, 97.09°W), and ii) the Oklahoma State University North Central Research Station at Lahoma, OK (36.38°N, 98.11°W). The part of the calibration set recorded in Stillwater contained soil moisture values measured approximately two times per week during the summer fallow period of 2013 (July – October) in a conventional till continuous wheat experiment on a Norge loam (fine-silty, mixed, active, thermic Udic Paleustolls) soil. The part of the calibration set recorded at Lahoma consisted of soil moisture measurements during the

summer fallow of 2009 in continuous conventional till winter wheat on a Grant silt loam (fine-silty, mixed, superactive, thermic Udic Argiustoll) soil. Models were validated with data collected from the same soil at Lahoma during the summer fallow periods of 2010, 2011, and 2012 (Patrignani et al., 2012). A separate prediction set that consisted of wheat PAW_s of four summer fallow periods (2009-2012) for the no-till treatment at Lahoma (Patrignani et al., 2012) and 20 site-years obtained during the summer fallows of 2012 and 2013 (Fig. 3.1) was used to assess the predictive power of the models. The selected fields for the 2012 and 2013 summer fallows were part of the Oklahoma State University Small Grains Variety Performance Tests and are representative of a wide variety of agricultural soils and typical planting dates for the cultivated wheat producing region of the southern Great Plains (Edwards et al., 2013; Edwards et al., 2014).

The calibration and validation datasets consisted of soil moisture measured to a depth of 1.2 m using a neutron moisture meter (CPN, Model 503 DR). Galvanized metal tubes of 3.8 cm i.d. were installed in four replications to facilitate the access of neutron probe into the soil. Readings were taken at 0.1, 0.3, 0.5, 0.7, 0.9, and 1.1 m below ground with the neutron probe device placed on a depth control stand (Evett et al., 2003). Two extra access tubes were installed in each field to calibrate the neutron probe readings against volumetric water content (θ_v, $m^3\ m^{-3}$) under dry and wet soil conditions. During both the dry and the wet calibrations of the neutron probe, a total of four 1.2-m depth 4.02-cm diameter soil cores were taken adjacent to the access tube using a Giddings hydraulic probe (#25-TS Model HDGSRTS, Soil Exploration Equipment, Windsor, CO) and each core was divided into 0.2 m intervals. Soil samples were weighed and oven dried at 105°C for 72 hours for determination of soil water content by the thermo-gravimetric method. Bulk density was determined for each sample using the core method. Volumetric soil water content of each sample was calculated using the gravimetric water content and the bulk density, and the relationship between neutron counts and volumetric water content

was determined using linear regression. Separate regression equations were generated for the top layer and the rest of the profile.

Soil porosity was estimated based on the soil bulk density and an assumed particle density of 2.65 Mg m^{-3} (Danielson et al., 1986). Particle size analysis was performed using the hydrometer method (Gavlak et al., 2003). Soil water content at the lower limit (θ_{LL}, m^3 m^{-3}) was assumed to be the soil water retention at -1500 kPa, measured using the pressure plate method (Klute, 1986; Richards and Weaver, 1943). Volumetric soil water content at the drained upper limit (θ_{DUL}, m^3 m^{-3}) for the calibration and validation datasets were measured in field conditions by collecting soil samples after thoroughly wetting the soil profile and allowing water to drain (Ratliff et al., 1983). Efforts to wet the soil profile included adding approximately 170 mm of water at biweekly intervals to a portion of the field isolated with a soil barricade and covered with a plastic sheet to decrease evaporative losses (Ratliff et al., 1983). After two to three months of periodically wetting the soil profile (cumulative water added >1000 mm), soil samples were collected 48 to 72 h after no water was present on the soil surface from the last application. The PAWC of the soil was calculated for each layer as the difference between θ_{DUL} and θ_{LL} multiplied by the soil layer thickness (Ritchie, 1981). Plant available water (PAW) was calculated as the difference between the measured soil water content and the θ_{LL}. Average soil physical properties for each site are given in Table 3.2.

Percent residue cover at the beginning of the fallow for the calibration and validation datasets was estimated from four downward-facing images that covered 1 m^2 of ground near each individual neutron probe access tube. Digital images were analyzed using SamplePoint software (Booth et al., 2006) using a total of 100 pixels automatically selected for each image and manually classified as residue or soil.

At each location within the prediction dataset, four soil cores (0 to 1.2 m depth) were collected using the Giddings probe from the plots planted to the winter wheat variety Iba in the Small Grains Variety Performance Tests the same day wheat was planted. Cores were divided into 0.2-m intervals, weighed, and oven dried. Soil moisture was calculated by the thermo-gravimetric method and soil texture, bulk density, θ_S, and θ_{LL}, were determined following the methodology previously described. To estimate θ_{DUL} in the prediction dataset, we used the relationships described by Saxton and Rawls (2006). Percent residue cover in the prediction dataset was not measured, so an arbitrary but reasonable value was assigned based on tillage practices adopted in each site (CTIC, 2002). A fraction residue cover of 0.85 and 0.2 were adopted for no-till and conventional-till, respectively, and drainage factor, curve number (CN), and soil albedo values were assigned to each soil based on the particle size distribution analysis (Table 3.2).

Daily weather data used in the calibration, validation, and prediction simulations were obtained from the nearest Oklahoma Mesonet station, an automated environmental network of 120 stations across the state of Oklahoma (McPherson et al., 2007). Monitoring stations were located within 800 m from the experimental plots in the calibration and validation datasets, and within 1500 m from fields in the prediction dataset.

3.2.2.2. Description of the soil water balance models

The FAO 56 dual crop coefficient model (Allen et al., 1998) and the water budget described within the Simple Simulation Modeling model (Soltani and Sinclair, 2012) were used to simulate the soil moisture dynamics of summer fallow periods, from which we obtained PAW_s. The soil-water balance in both models is represented by:

$$PAW_t = PAW_{t-1} + P_t + I_t - D_t - RO_t - E_t - T_t \quad [1]$$

where PAW_t represents plant available water in the root zone at time t, PAW_{t-1} is the PAW in the previous time step, P_t is precipitation, I_t is irrigation, D_t is deep drainage, RO_t is surface runoff, E_t is soil evaporation, and T_t is plant transpiration. Both models compute the soil water balance using a two-layer soil profile at daily time steps. The use of a two-layer soil profile is a common technique to improve estimations of surface evaporative losses while maintaining model parsimony. The subroutines of each model were implemented using Matlab R2014a (The Mathworks Inc., 2014).

3.2.2.2.1. Dual crop coefficient – dual K_c

The dual K_c model is a soil water balance that estimates crop evapotranspiration based on the evapotranspiration of a well-watered reference crop (ET_o) according to the Penman-Monteith equation and a set of empirical crop coefficients that change with the development of the crop (Allen et al., 1998). Weather variables needed to calculate daily ET_o are wind speed (m s^{-1}), maximum and minimum temperatures (T_{max} and T_{min}, °C), maximum and minimum relative humidity (or alternatively vapor pressure deficit), incident solar radiation (Rs, MJ m^{-2} d^{-1}), and site elevation (m). Missing relative humidity, Rs, and wind speed values were calculated using T_{max} and T_{min} (Allen et al., 1998). Soil inputs are θ_{LL} and θ_{DUL}, depth of soil for which simulations will occur (1.2 m), depth of surface soil layer subjected to soil E (Ze), initial soil water content (PAW_i), and fraction of surface covered by residue. The dual K_c method also requires as input the empirical crop basal coefficient (K_{cb}), crop minimum coefficient ($K_{c\,min}$), and depletion coefficient for water stress. Soil E is simulated using a two stage model similar to that suggested by Ritchie (1972), and reduction of soil E in Stage II is assumed to be proportional to the cumulative E (Allen et al., 2005). The dual K_c model allows the soil surface to dry to values lower than the θ_{LL}. Drainage is simulated by assuming that soil water exceeding θ_{DUL} is lost from the root zone the same day as the wetting event, and surface runoff is estimated following the USDA CN procedure (Hawkins et al., 1985).

3.2.2.2.2. Simple Simulation Modeling - SSM

The SSM model calculates E and T independently and does not require calculation of daily ET_o. Soil E is calculated using a simplified Penman equation taking into account the slope of saturated vapor pressure curve as a function of air temperature. Transpiration was not simulated in our study due to the lack of actively growing vegetation during the summer fallow. Weather data needed to run SSM are daily values for T_{max}, T_{min}, Rs, and precipitation (mm) and soil input consists of PAWC, volumetric water content at saturation (θ_S, $m^3\ m^{-3}$), Ze, CN, drainage factor, soil albedo, percent residue cover, and PAW_i. In the SSM model, reduction of soil E is a function of the square root of time since wetting (Amir and Sinclair, 1991; Ritchie, 1972), and the lowest possible soil moisture content is equal to the θ_{LL}. Daily drainage is simulated as the product of excess of water ($\theta_v > \theta_{DUL}$) and a drainage factor that depends on the soil texture. Surface runoff is estimated using a simplified CN procedure (Williams, 1991) that takes into account actual soil water content in the top layer (Ritchie, 1998) and surface residue (Chapman et al., 1993). Drainage factor, CN, and soil albedo values were assigned to each soil based on the particle size distribution (Table 3.2). The original SSM model considers an increasing soil layer thickness determined by root growth simulation. Since our simulations were performed for fallow period, a fixed soil profile of 1.2 m was considered and the T subroutine was not implemented.

3.2.2.3. Calibration and validation of soil water balance models

Models were calibrated using a soil moisture dataset collected during the summer fallow of 2013 at Stillwater and during the summer fallow of 2009 at Lahoma, and model validation used soil moisture data from the conventional till summer fallows of 2010, 2011, and 2012 recorded at Lahoma (Patrignani et al., 2012). Simulations were performed for the summer fallow periods, which started one day after the harvest date of the preceding wheat crop and ended at

wheat planting. The soil moisture recorded at wheat harvest was used as input in simulations as the initial plant available water at the beginning of the summer fallow (PAW_i).

The depth of the surface layer in which evaporative losses are assumed to happen (Ze) is a parameter common to both dual K_c and SSM models. In fact, it is the only parameter to be calibrated in the SSM model when simulating soil water dynamics during fallow periods. The Ze parameter for the SSM model was calibrated by running simulations for the fallows of Stillwater 2013 and Lahoma 2009 using Ze values ranging from 5 to 60 cm depth (Fig. 3.2a). The optimum value of Ze was determined as that with lowest difference between measured and simulated PAW. In the dual K_c model, evapotranspiration is estimated by an empirical basal crop coefficient (i.e. K_{cb}). Allen et al. (1998) suggests that this parameter should be set equal to zero when simulating soil water balance during fallow periods, assumption that forces the model to simulate soil E only from the top layer (i.e. Ze). However, our data provided empirical evidence to suggest a slow decrease in soil water content at deeper layers during long periods without rainfall. To account for these evaporative losses, we tested setting the empirical coefficient K_{cb} to values ranging from 0 to 0.1 across the range of tentative Ze (Fig. 3.2b).

3.2.2.4. Evaluation of model robustness

The comparison between predicted and measured PAW to 1.2 m depth was performed using absolute and normalized root mean square error (RMSE and $RMSE_n$, respectively), and the index of agreement of Willmott (1982). Linear regression was used test the predictive power of each model.

The $RMSE_n$ is calculated according to Loague and Green (1991) and gives a percent measure of the relative difference between predicted and measured data:

$$RMSE_n = \sqrt{\sum_{i=1}^{n} \frac{(P_i - M_i)^2}{n}} x \frac{100}{\overline{M}} \quad [2]$$

where P_i is the predicted value, M_i is the measured value, n is the number of observations, and $\overline{M}$ is the mean of the measured variable. Thresholds for $RMSE_n$ when evaluating model performance were suggested by Jamieson et al. (1991), where $RMSE_n < 10\%$ is considered excellent, 10 - 20% is considered good, 20% - 30% is considered fair, and >30% is considered poor.

The index of agreement (d) proposed by Willmott (1982) is a descriptive measurement that has values ranging from 0 to 1:

$$d = 1 - \left[\frac{\sum_{i=1}^{n} (P_i - M_i)^2}{\sum_{i=1}^{n} \left(\left| P_i - \overline{M} \right| + \left| M_i - \overline{M} \right| \right)^2} \right] \quad [3]$$

where n is the number of observations, Pi is the predicted value, M_i is the measured observation, and $\overline{M}$ is the mean of the measured variable. High values of d indicate good agreement between predicted and measured variables.

3.2.2.5. Prediction of PAW_s using the mechanistic approach

After the soil water balance models were calibrated and validated, we simulated PAW_s for the 24 site-years across Oklahoma in the prediction dataset. Data regarding PAW left by the previous wheat crop at the beginning of the fallow for these fields was not available (unknown PAW_i); therefore, we tested whether initializing the soil water balance models at different PAW_i values would result in convergence of simulated PAW dynamics during the summer fallow period as well as a reliable prediction of wheat PAW_s in this dataset. Soil moisture dynamics during the summer fallow periods were initialized 1000 times using randomly generated PAW_i

drawn from a log-normal distribution within the range delimited by θ_{LL} to θ_{DUL} (i.e. PAWC). The log-normal distribution was chosen because it represents the actual distribution of 58 sampled PAW_i values available for this study (data not shown). Log-normal distribution was built using the mean and standard deviation of PAW_i /PAWC of the 58 samples, which was 0.33 and 0.22, respectively. The lognormal equivalent of the mean and standard deviation of the 58 samples were -1.65 and 1.05, respectively. For all cases, simulations started on June 15th, a representative date for wheat harvest in the region, and ended same day wheat was planted and PAW_s measured, which happened during October at all site-years. Simulations for a site-year with different PAW_i were considered to converge when all simulated PAW_s resulted in a single PAW_s value regardless of PAW_i. The mean and standard deviation of the 1000 simulated PAW_s were compared to mean and standard deviation of measured PAW_s when evaluating model performance.

3.2.3. Empirical model to predict wheat PAW_s

Empirical models were developed using the same five site-years used for calibration and validation of the mechanistic model (Table 3.3), in addition to 37 site-years of PAW_s data reported in the literature for continuous wheat following summer fallow in the southern Great Plains. The latter included PAW_s data reported for seven site-years and three tillage practices in El Reno, OK (Dao, 1993); two tillage practices and three site-years in Lahoma, OK (Heer and Krenzer, 1989); and ten site-years in Bushland, TX (Jones and Popham, 1997). Tillage practices were not discriminated when creating the empirical models. The empirical models were then validated using the same 24 site-years used for prediction with the mechanistic approach (Table 3.3), which allowed for comparison between mechanistic and empirical model performance against the same dataset of PAW_s.

Cumulative precipitation during the summer fallow was used as independent variable to predict PAW_s (dependent variable) at a given site-year, both variables normalized by the soil's

PAWC as efforts to avoid the confounding effects of different soil types in the analysis. Visual evaluation of the resulting graph between PAW_s /PAWC and precipitation/PAWC indicated that the relationship between both variables would either be exponential rise to an asymptotic maximum or logarithmic, due to the rapid increase in PAW_s at low cumulative precipitation levels, followed by slower rates of increase with increased cumulative precipitation. Both exponential rise to maximum and logarithmic models were created using SigmaPlot 11 (Systat Software, Point Richmond, CA), and residuals were tested for normality using the Shapiro-Wilk test (Shapiro and Wilk, 1965), for autocorrelation using the Durbin-Watson test (Durbin and Watson, 1950), and for constant variance using *P* values.

3.3. RESULTS AND DISCUSSION

3.3.1. Measured PAW_s in the calibration, validation, and prediction datasets

Plant available water at sowing measured to a depth of 1.2 m ranged from 133 mm in Stillwater (2013) to 161 mm in Lahoma (2009) in the calibration dataset, and from 117 to 143 mm in Lahoma 2010-2012 in the validation dataset (Table 3.3). Among the 24 site-years in the prediction dataset, measured PAW_s ranged from 18 mm in the westernmost site Altus to 174 mm at Chickasha (Table 3.3). Interestingly, both extreme values within the prediction dataset were recorded after the summer fallow of 2013. Wheat PAW_s was lower than 0.4 PAWC in 25% of the evaluated site-years, 33% resulted in PAW_s between 0.4 and 0.6 PAWC, 29% had PAW_s between 0.6 and 0.8 PAWC, and only 13% resulted in wheat PAW_s between 0.8 and 1.0 PAWC. These results indicate that the assumption of a fully recharged soil profile at the beginning of the growing season is typically not justified when modeling continuous wheat systems in the southern Great Plains.

3.3.2. Mechanistic approach

3.3.2.1. Calibration of dual K_c and SSM models

Simulated PAW_s was within 7% of measured PAW_s by both dual K_c and SSM models for the two locations in the calibration set (Fig. 3.3). Measured PAW_s following the summer fallow at Stillwater in 2013 was 133 mm and the simulated values were 127 mm for the dual K_c model and 144 mm for the SSM model. At Lahoma in 2009, measured PAW_s was 161 mm and the simulated PAW_s was 164 mm for both dual K_c and SSM models. Also, both models were able to capture the observed soil moisture dynamics (peaks and valleys) throughout the simulated period for the summer fallows at Stillwater 2013 and Lahoma 2009 (Fig. 3.3a and 3.3b). The dual K_c model tended to dry the profile faster than the SSM model after rainfall events. We hypothesize two possible reasons behind this observation. First, the faster drying of the soil profile by the dual K_c may be a result of draining all the excess water in the profile in a single day (Allen et al., 1998), while the SSM model typically requires up to five days to drain the soil profile depending drainage factor (Soltani and Sinclair, 2012). Another possible explanation for higher water depletion by the dual K_c is that this model allows the top layer of the soil profile to have soil moisture content below the θ_{LL} due to evaporative losses. These differences between models resulted in greater underestimation of PAW by the dual K_c model (mean residual of -8.71 mm) than by the SSM model (mean residual of 0.29 mm) in the calibration set. Both the SSM and the dual K_c models showed good predictive power for PAW, with r^2 values of 0.91 and 0.93 for the linear regression of simulated versus measured PAW, and a total of 83% and 90% of simulated PAW values were within 20% of measured PAW values (Fig. 3.3c). Overall, both models accurately predicted wheat PAW_s and effectively simulated PAW dynamics during the summer fallow periods for the calibration set.

The Ze that minimized the $RMSE_n$ for the SSM model for the calibration set of Stillwater 2013 and Lahoma 2009 was 25 cm, which resulted in $RMSE_n$ of 6.9% for Stillwater in 2013 and 7.8% for Lahoma in 2009 (Fig. 3.2a). The magnitude of the estimated Ze parameter was consistent with empirical data from Stillwater in 2013 which demonstrated water losses below the 0.2 m depth during a period of 38 days without measurable rainfall (Table 3.4). Results from this analysis indicate that the upper 0.2 m lost 38.2 mm in a period of 38 consecutive days without rainfall, which is equivalent to a loss of 1.03 mm d^{-1} mainly due to E. In the layer from 0.2 m to 1.2 m, water losses totals 15.28 mm during the same period, with greater losses in the 0.2 to 0.4 m and 0.4 to 0.6 m layers (i.e. 6.41 and 3.14 mm, respectively). In order to account for the losses below the top 0.2 m of the soil profile in the dual K_c model, we first assumed that the change in soil water storage was due to evaporative losses, and then we estimated the K_{cb} from measured data as the ratio of the change in storage to the cumulative ET_o during the period (233 mm). The procedure to simultaneously calibrate both the Ze and K_{cb} for the dual K_c model is illustrated in Fig. 3.2b. The combination that minimized average $RMSE_n$ for the 2009 summer fallow at Lahoma ($RMSE_n$ = 14.4%) and 2013 summer fallow at Stillwater ($RMSE_n$ = 9%) for the dual K_c model was a Ze of 20 cm and a K_{cb} of 0.01.

3.3.2.2. Validation of dual K_c and SSM models

Models were validated using data from the Lahoma crop rotation experiment for the summer fallows of 2010, 2011, and 2012 for wheat under conventional till (Table 3.3). The dual K_c simulated PAW remarkably well with 96% of the simulated PAW values within ±20% of measured values throughout the three fallow periods (Fig. 3.4). Statistics of model validation were RMSE = 13.5 mm, $RMSE_n$ = 8.8%, and d = 0.78, which is excellent. Still, mean residual between simulated and observed PAW was -7.52 mm, indicating a negative bias for PAW by the dual K_c model. For the dual K_c model, linear regression between simulated measured PAW resulted in an r^2 of 0.53 with intercept statistically equal to zero and slope equal to one (data not

shown). The dual K_c was very robust in predicting PAW_s, as predicted values were within 2 to 6% of observed wheat PAW_s for the three studied fallow periods.

The SSM simulated PAW reasonably well with 76% of simulated values falling within ±20% of measured PAW values (Fig. 3.4). Statistics for model fit were RMSE = 19.2 mm, $RMSE_n$ = 11.9%, and d = 0.62. The SSM model tended to overestimate PAW as compared to observed values, with a mean residual of 12.3 mm. Similarly to the dual K_c model, linear regression between measured PAW and PAW simulated by the SSM model and also resulted in an r^2 of 0.53, with intercept statistically equal to zero and slope equal to one (data not shown). The wheat PAW_s values predicted by the SSM model were within 14 to 28% of observed PAW_s for the three studied fallow periods, indicating weaker predictive power relative to the dual K_c model.

The validation of the dual K_c model resulted in excellent ($RMSE_n$ = 8.8%) and the SSM model in good ($RMSE_n$ = 11.85%) simulations of PAW during summer fallow periods in continuous wheat systems in the southern Great Plains. The SSM model with Ze = 25 cm and the dual K_c model with Ze = 20 cm and K_{cb} = 0.01 can be used with confidence to simulate PAW dynamics during summer fallow periods and to predict wheat PAW_s in continuous wheat systems in the southern Great Plains.

3.3.2.3. Convergence of simulated PAW

The 1000 simulations of PAW dynamics using log-normally distributed PAW_i values for each of the 24 site-years revealed two major patterns. The first pattern is characterized by the convergence of the soil moisture dynamics as shown in Fig. 3.5a. The PAW dynamics from simulations with different PAW_i converged at some point during the summer fallow. As a result of convergence, the 1000 simulated PAW_s had the same or similar values with minimal standard deviation (data not shown). Convergence occurred for both dual K_c and SSM models in 2009,

2010, 2011, and 2013 at Lahoma, and at Alva, Apache, Cherokee, Perkins, and Chickasha following the 2013 summer fallow period (9 out of 24 site-years). Convergence of simulated PAW occurred when fallow periods had above-average precipitation totals (386 mm vs. 320 mm 16-yr mean) and average cumulative ET_o of 737 mm, which is close to the 16-yr mean (742 mm). Above-average precipitation during the ~125-d summer fallow forced the simulations starting at different PAW_i to converge due to higher simulated water losses when assumed PAW_i was high (greater surface runoff, soil E, and deep drainage due to an already wet soil condition), as opposed to minimal simulated water losses and greater water infiltration when assumed PAW_i was low (Capehart and Carlson, 1994).

The second observed pattern, which was consistent for both models, consisted in the absence of soil moisture convergence (Fig. 3.5b). In this case, the distribution of the 1000 simulated PAW_s values was similar to the distribution of PAW_i (i.e. log-normal) following summer fallows with less than 200 mm cumulative precipitation. When cumulative precipitation during the summer fallow was between ~200 and 350 mm, distribution of PAWs shifted towards a normal one (data not shown). Standard deviation of the 1000 simulated PAW_s decreased with increased cumulative fallow precipitation, as an indication of the influence of fallow precipitation total on model convergence ($p < 0.001$). Simulated PAW did not converge in 15 out of the 24 summer fallow periods, namely all sites during the 2012 fallow periods and for Altus, Alva, and Marshall during the 2013 fallow period. Fallow periods when convergence did not occur were characterized by lower precipitation totals (average 199 mm) and higher than normal atmospheric evaporative demand (average ET_o: 807 mm). Simulations that started with values of PAW_i closer to θ_{LL} resulted in low wheat PAW_s, while values of PAW_i closer to θ_{DUL} resulted in fully recharged soil profiles. The dependence of PAW_s on PAW_i for approximately two thirds of the studied cases means that simulations of fallow PAW dynamics starting on June 15 and using a random PAW_i will not always result in accurate estimation of wheat PAW_s in continuous wheat

systems in the southern Great Plains. Similarly, Grunmann (2005) found that convergence of simulations starting at contrasting soil moisture contents (saturated versus dry soil) took as long as five years to occur in Illinois, depending on environmental conditions. Although starting simulations earlier than 15 June may result in model convergence in a greater number of years, the objective of this study was to predict PAW_s in continuous wheat systems only considering simulations during the preceding summer fallow period in order to avoid simulating prior wheat growing seasons, which would require additional model parameters.

3.3.2.4. Predicted PAW_s and associated uncertainty

The mean of the 1000 simulated PAW_s was within ± 30% from measured PAW_s in 67% of the site-years for both models (Fig. 3.6). The dual K_c model resulted in average residual between measured and mean simulated PAW_s of 1 mm, RMSE = 29 mm, and $RMSE_n$ = 27% (Fig. 3.6a). In contrast, the SSM model overestimated PAW_s with average residual of 26 mm, RMSE = 34 mm, and $RMSE_n$ = 32% (Fig. 3.6b). Standard deviation around the mean for PAW_s simulated by the dual K_c model overlapped with measured PAW_s standard deviation in 15 out of 24 site-years, and in 13 out of 24 site-years for the SSM model. Errors in simulated PAW_s were function of variability and uncertainty in PAW_i, and standard deviation around the simulated mean decreased with increased fallow precipitation total for both models ($p < 0.001$), leading to convergence of simulated PAW. Errors associated with measured PAW_s were related to sub-field scale variability in soil properties, and tended to decrease with increased fallow precipitation total ($p = 0.09$).

The dual K_c model resulted in more accurate prediction of PAW_s than the SSM model. The dual K_c model has been proven to be more accurate in simulating components of the soil water balance when compared to other models (Paredes et al., 2015). However, it is important to notice that the original SSM model was developed as a subroutine in a crop simulation model and

not solely a soil water balance model (Soltani and Sinclair, 2012). In fact, the soil water balance only accompanies the crop model, which is the most complex portion of the SSM model. In this manuscript, we modified the original SSM model to simulate fallow periods and to not account for T, which is an important component of the soil water budget (Soltani and Sinclair, 2012). Removing the T component may be the cause of some of the discrepancies between simulated and measured PAW, as the SSM model resulted in accurate simulations of PAW under a developing wheat crop for a wide range of environments (Lollato et al., *in preparation*).

These results indicate that stochastic simulations drawing PAW_i from a lognormal distribution with mean in the dry range of the PAWC interval using the dual K_c model will provide fair (± 30%) predictions of PAW_s and its associated uncertainty for continuous wheat systems. Accounting for the uncertainty in PAW_s in subsequent simulations of wheat growth and development can improve the accuracy of the final simulated yields, leading to probabilistic distributions rather than deterministic predictions, which should be the nature of forecasts (Garbrecht et al., 2010). Low PAW_i, as indicated by a distribution of measured PAW_i with a mean in the dry range of PAWC, is a consequence of the great water demand of the previous wheat crop late in the spring during reproductive stages (Lollato and Edwards, 2015). If no significant rain occurs after wheat approaches physiological maturity late in the spring, the soil profile is not replenished and the summer fallow starts with reduced PAW_i (Patrignani et al., 2012). Simulated wheat PAW_s was overestimated by both the dual K_c and SSM models at the western sites, Altus and Alva, following the 2013 summer fallow period. Western Oklahoma, including Altus and Alva, went through a severe drought during the years of 2012 and 2013, which resulted in extremely low PAW_s for the wheat crop sown in October 2012 and 2013 (Edwards et al., 2013; Edwards et al., 2014). Neither model was capable of reproducing the low PAW_s caused by the severe drought, and overestimation of wheat PAW_s at these locations was probably an effect of the long-term water deficit accumulation.

3.3.3. Empirical non-linear models for prediction of PAW_s

Logarithmic and exponential rise to maximum models were created using cumulative precipitation during the fallow period as independent variable to predict PAW_s, both variables normalized by PAWC. Both models performed similarly in the calibration (Fig. 3.7a, $RMSE_n$ = 23%) and validation datasets (Fig. 3.7b, $RMSE_n$ = 29%). Performance of the empirical models in the validation dataset was inferior to the dual K_c model ($RMSE_n$ = 27%), but superior to the modified SSM model ($RMSE_n$ = 32%). While the diminishing rate of increase in PAW_s with increasing cumulative precipitation was well represented by both empirical models (Fig. 3.7), models differed in simulated PAW_s at low cumulative fallow precipitation totals (precipitation/PAWC < 0.65 PAWC). The exponential rise to maximum model resulted in higher predicted PAW_s than the logarithmic model when the summer fallow preceding wheat planting was characterized by low cumulative precipitation (Fig. 3.7).

The diminishing rate of increase in PAW_s with increased fallow precipitation may be function of a wetter soil profile in summer fallows with greater precipitation totals, which would increase water losses through runoff, E, and deep drainage. Both models were congruent in indicating that PAW_s may approach the soil's PAWC when fallow precipitation exceeds approximately 3 times the soil's PAWC, but will rarely reach full profile at sowing. This is in agreement with our data, in which only 13% of the site years had PAW_s greater than 0.8 PAWC. An additional interesting feature in the logarithmic model in Fig. 3.7 is the positive *x*-intercept, which indicates inevitable water losses during the summer fallow period. The value of the *x*-intercept suggests that approximately 43 ± 6% of the soil's PAWC is unavoidably lost during the fallow period. Figure 3.7 also indicates that wheat PAW_s is highly variable, with high variation around either fitted line. This variation is likely caused by differences in precipitation distribution during the fallow period or differences in tillage practices, which are not accounted for in this model.

The simple empirical approach can be easily implemented to predict PAW_s using as input data the cumulative precipitation during the fallow period and PAWC, which can be retrieved for dominant soil series from soil databases as the Web Soil Survey (USDA-NRCS, 2014). The inherent weakness of the empirical approach is its failure to account for fallow periods with similar precipitation totals but different precipitation distribution. In contrast, soil water balance models account for year-to-year and site-specific variation in precipitation distribution and evaporative demand. For instance, the summer fallow of 2012 in Chickasha had total precipitation of 225 mm and McLoud had 213 mm in the same fallow period (Table 3.3). Despite the similar precipitation totals, the 31-d period preceding wheat sowing had a total of 119 mm precipitation in Chickasha (53% of total precipitation), while only 69 mm were recorded in the same period at McLoud (32% of total precipitation), meaning that most of the precipitation fell in the beginning of the fallow period in McLoud and was subjected to water losses (i.e. E and deep drainage) for a greater period of time. As a result of differences in precipitation distribution, measured PAW_s differed greatly between the two sites (i.e. 152 mm in Chickasha vs. 84 mm in McLoud). The empirical models of wheat PAW_s based on cumulative precipitation and PAWC resulted in prediction of similar PAW_s values following both fallow periods (i.e. 105 mm in Chickasha by both models, and 121 or 126 mm in McLoud by the exponential and logarithmic models, respectively), whereas prediction of PAW_s using the soil water balance method was sensitive to rainfall distribution and PAW_s was predicted within 30% of measured values for both cases (predicted PAW_s: 101 mm in McLoud, 140 mm in Chickasha).

Since PAW_s in continuous wheat systems of the southern Great Plains can be estimated with fair accuracy (± 30%) using mechanistic and empirical non-linear models, modeling studies can be used to improve fall forage production estimates (Garbrecht et al., 2010), identify favorable winter wheat planting dates (Stone and Schlegel, 2006), and better estimate plant population, timing of nutrient application, and irrigation scheduling (Grassini et al., 2010).

Additionally, the methods that we tested in this manuscript can be used to increase the reliability of regional assessments based on crop simulation models by reducing the uncertainty in the initial conditions.

3.4. CONCLUSION

In this manuscript we explored objective approaches to estimate PAW_s for winter wheat in the southern Great Plains. Mechanistic soil water balance models and non-linear empirical regression models (i.e. logarithmic or exponential rise to maximum) were used to predict PAW_s using observed weather conditions during the preceding summer fallow period. For the mechanistic models, the ~125-d summer fallow period was insufficient to force convergence of simulated PAW in 15 out of 24 fallow periods. However, stochastic simulations drawing PAW_i from log-normal distribution predicted wheat PAW_s within ±30% of measured values in in 16 out of 24 cases, implying that scenario analysis can be used to predict PAW_s regardless of model convergence. Simulation of the soil moisture dynamics during the fallow period using multiple PAW_i values enables the opportunity to quantify the uncertainty associated with PAW_s estimation, information that can be incorporated in subsequent simulations during the growing season. The logarithmic or exponential regression models developed to predict wheat PAW_s based on cumulative precipitation during the summer fallow period and the soil's PAWC may be a suitable alternative against arbitrary choices to predict wheat PAW_s for continuous wheat systems in the southern Great Plains, although this approach should be used with caution because it does not account for precipitation distribution during the fallow or tillage practices. Plant available water at sowing was < 0.8 PAWC in 87% of the studied site-years, indicating that the assumption of a full profile at the beginning of the growing season typically should not be adopted in continuous winter wheat systems in the southern Great Plains. Initializing a mechanistic soil water balance model at the beginning the summer fallow period can eliminate the need for arbitrary choices of initial soil moisture at wheat sowing when using crop simulation

models, and may provide a basis for determining optimal planting dates for winter wheat based on scenario analysis.

3.5. REFERENCES

Allen, R.G., L.S. Pereira, D. Raes and M. Smith. 1998. Crop evapotranspiration: Guidelines for computing crop water requirements. Irrigation and Drainage Paper No. 56, FAO, Rome, Italy.

Allen, R.G., L.S. Pereira, M. Smith, D. Raes and J.L. Wright. 2005. FAO-56 dual crop coefficient method for estimating evaporation from soil and application extensions. J. Irrig. Drain. Eng. ASCE 131: 2-13.

Amir, J. and T.R. Sinclair. 1991. A model of water limitation on spring wheat growth and yield. Field Crops Res. 28: 59-69.

Booth, D.T., S.E. Cox and R.D. Berryman. 2006. Point sampling digital imagery with 'samplepoint'. Environ. Monit. Assess. 123: 97-108.

Capehart, W.J. and T.N. Carlson. 1994. Estimating near-surface soil-moisture availability using a meteorologically driven soil-water profile model. J. Hydrol. 160: 1-20.

Chapman, S.C., G.L. Hammer and H. Meinke. 1993. A sunflower simulation-model.1. Model development. Agron. J. 85: 725-735.

CTIC. 2002. Conservation Technology Information Center. Data retrieved on November 2014. Available at: http://www.conservationinformation.org/resourcedisplay/322/.

Danielson, R., P. Sutherland and A. Klute. 1986. Porosity. Methods of soil analysis. Part 1. Physical and mineralogical methods: 443-461.

Dao, T.H. 1993. Tillage and winter-wheat residue management effects on water infiltration and storage. Soil Sci. Soc. Am. J. 57: 1586-1595.

Durbin, J. and G.S. Watson. 1950. Testing for serial correlation in least squares regression. Biometrika 37: 409-428.

Edwards, J.T., R.D. Kochenower, R.E. Austin, M.W. Knori, R.P. Lollato, G. Cruppe, et al. 2013. Oklahoma small grains variety performance tests 2012-2013. Okla. St. Univ. Coop. Ext. Serv. Cur. Rep. CR-214, Oklahoma State University, Stillwater.

Edwards, J.T., R.D. Kochenower, S.R. Calhoun, M.W. Knori, R.P. Lollato, G. Cruppe, et al. 2014. Oklahoma small grains variety performance tests 2013-2014. Okla. St. Univ. Coop. Ext. Serv. Cur. Rep. CR-2141. Stillwater, OK.

Evett, S.R., J.A. Tolk and T.A. Howell. 2003. A depth control stand for improved accuracy with the neutron probe. Vadose Zone Journal 2: 642-649.

Garbrecht, J.D., X.C. Zhang, J.M. Schneider and J.L. Steiner. 2010. Utility of seasonal climate forecasts in management of winter-wheat grazing. Appl. Eng. Agric. 26: 855-866.

Gavlak, R., D. Horneck, R.O. Miller and J. Kotuby-Amacher. 2003. Soil, plant and water reference methods for the western region. 2nd ed. Rep. WREP-125, Wetlands Reserve Enhancement Program. Fort Collins, CO. 199 pp.

Grassini, P., J.S. You, K.G. Hubbard and K.G. Cassman. 2010. Soil water recharge in a semi-arid temperate climate of the central US Great Plains. Agric. Water Manage. 97: 1063-1069.

Grunmann, P.J. 2005. Variational data assimilation of soil moisture information. Ph.D. Diss. Univ. Maryland, College Park.

Hawkins, R.H., A.T. Hjelmfelt and A.W. Zevenbergen. 1985. Runoff probability, storm depth, and curve numbers. J. Irrig. Drain. Eng. ASCE 111: 330-340.

Heer, W.F. and E.G. Krenzer. 1989. Soil-water availability for spring growth of winter-wheat (*Triticum aestivum* L.) as influenced by early growth and tillage. Soil & Tillage Research 14: 185-196.

Jamieson, P.D., J.R. Porter and D.R. Wilson. 1991. A test of the computer-simulation model ArchWheat1 on wheat crops grown in New-Zealand. Field Crops Res. 27: 337-350.

Jones, O.R. and T.W. Popham. 1997. Cropping and tillage systems for dryland grain production in the southern High Plains. Agron. J. 89: 222-232.

Klute, A. 1986. Methods of soil analysis. Part 1. Physical and mineralogical methods. Am. Soc. Agron., Inc., Madison, WI.

Loague, K. and R.E. Green. 1991. Statistical and graphical methods for evaluating solute transport models: Overview and application. J. Cont. Hydol. 7: 51-73.

Lollato, R.P. and J.T. Edwards. 2015. Maximum attainable wheat yield and resource-use efficiency in the southern Great Plains. Crop. Sci. *Accepted*.

Lyon, D.J., D.C. Nielsen, D.G. Felter and P.A. Burgener. 2007. Choice of summer fallow replacement crops impacts subsequent winter wheat. Agron. J. 99: 578-584.

Mathews, O.R. and T.J. Army. 1960. Moisture storage on fallowed wheatland in the Great Plains. Soil Sci. Soc. Am. J. 24: 414-418.

McPherson, R.A., C.A. Fiebrich, K.C. Crawford, R.L. Elliott, J.R. Kilby, D.L. Grimsley, et al. 2007. Statewide monitoring of the mesoscale environment: A technical update on the Oklahoma Mesonet. J. Atmos. Ocean. Technol. 24: 301-321.

Musick, J.T. and K.B. Porter. 1990. Wheat. In: B. A. Stewart and D. R. Nielsen, Eds., Irrigation of agricultural crops. Agron. Monogr. 30. ASA, CSSA, and SSSA., Madison, WI. p. 597-638.

Nielsen, D.C. and M.F. Vigil. 2010. Precipitation storage efficiency during fallow in wheat-fallow systems. Agron. J. 102: 537-543.

Norwood, C.A. 2000. Dryland winter wheat as affected by previous crops. Agron. J. 92: 121-127.

Paredes, P., Z. Wei, Y. Liu, D. Xu, Y. Xin, B. Zhang, et al. 2015. Performance assessment of the FAO Aquacrop model for soil water, soil evaporatino, biomass and yield of soybeans in North China Plain. Agric. Water Manage. 152: 57-71.

Patrignani, A., C.B. Godsey, T.E. Ochsner and J.T. Edwards. 2012. Soil water dynamics of conventional and no-till wheat in the southern Great Plains. Soil Sci. Soc. Am. J. 76: 1768-1775.

Paulsen, G.M. 1987. Wheat stand establishment. In: E. G. Heyne, Ed. Wheat and wheat improvement. 2nd ed. Agron. Monog. 13. ASA, CSSA, and SSSA, Madison, WI.

Ratliff, L.F., J.T. Ritchie and D.K. Cassel. 1983. Field-measured limits of soil-water availability as related to laboratory-measured properties. Soil Sci. Soc. Am. J. 47: 770-775.

Richards, L.A. and L.R. Weaver. 1943. Fifteen-atmosphere percentage as related to the permanent wilting percentage. Soil Science 56: 331-339.

Ritchie, J.T. 1972. Model for predicting evaporation from a row crop with incomplete cover. Water Resour. Res. 8: 1204-&.

Ritchie, J.T. 1981. Soil-water availability. Plant Soil 58: 327-338.

Ritchie, J.T. 1998. Soil water balance and plant water stress. In: G. Y. Tsuji, G. Hoogenboom and P. K. Thornton, Eds., Understanding options for agricultural production. Kluwer Academic Publishers, Dordrecht, the Netherlands. p. 41-54.

Saxton, K.E. and W.J. Rawls. 2006. Soil water characteristic estimates by texture and organic matter for hydrologic solutions. Soil Sci. Soc. Am. J. 70: 1569-1578.

Shapiro, S.S. and M.B. Wilk. 1965. An analysis of variance test for normality (complete samples). Biometrika 52: 591-&.

Sinclair, T.R., L.R. Salado-Navarro, G. Salas and L.C. Purcell. 2007. Soybean yields and soil water status in Argentina: Simulation analysis. Agric. Syst. 94: 471-477.

Smith, C.B., M.N. Lakhtakia, W.J. Capehart and T.N. Carlson. 1994. Initialization of soil-water content in regional-scale atmospheric prediction models. Bull. Am. Meteor. Soc. 75: 585-593.

Soltani, A. and T.R. Sinclair. 2012. Modeling physiology of crop development, growth and yield. CAB International, Cambridge, MA.

Stone, L.R. and A.J. Schlegel. 2006. Yield-water supply relationships of grain sorghum and winter wheat. Agron. J. 98: 1359-1366.

USDA-NASS. 2014. United States Department of Agriculture. National Agricultural Statistics Service. Available at: http://www.nass.usda.gov/Statistics_by_State/Oklahoma/Publications/County_Estimates/index.asp (data retrieved July 2014).

USDA-NRCS. 2014. Web Soil Survey. Soil Survey Staff. USDA-NRCS, Lincoln, NE. Available at: http://websoilsurvey.sc.egov.usda.gov/App/HomePage.htm (accessed 26 June 2014).

Williams, J.R. 1991. Runoff and soil erosion. In: R. J. Hanks and J. T. Ritchie, Eds., Modeling plant and soil systems. Agronomy Monograph No. 31, Am. Soc. Agron., Crop Sci. Soc. Am., Soil Sci. Soc. Am., Madison, WI. p. 439-456.

Willmott, C.J. 1982. Some comments on the evaluation of model performance. Bull. Am. Meteor. Soc. 63: 1309-1313.

Zhang, X.C. 2003. Assessing seasonal climatic impact on water resources and crop production using Cligen and WEPP models. Trans. ASAE 46: 685-693.

Table 3.1. Elevation, average daily maximum (T_{max}) and minimum (T_{min}) air temperatures for the period 1 June to 30 September, solar radiation at the soil surface (R_S), average cumulative reference evapotranspiration (ET_o), precipitation (Precip.), and atmospheric water deficit (AWD, ET_o – Precip.) for the ten study sites across Oklahoma. Values are the average of 16 consecutive summer fallow periods from 1998 to 2013.

Site	Elev.	T_{max}	T_{min}	R_s	ET_o †	Precip.	AWD‡
	m	°C		MJ m^{-2} d^{-1}	mm	mm	
Altus	426	34.1	20.2	23.1	787	268	519
Alva	411	33.3	19.0	22.6	783	297	487
Apache	394	32.6	19.7	22.8	766	304	462
Cherokee	360	33.4	19.5	22.7	777	343	434
Chickasha	333	33.4	19.5	22.4	710	318	393
Lahoma	380	33.0	19.0	22.6	770	354	416
Marshall	321	33.0	19.6	22.2	723	309	414
McLoud	333	32.4	20.3	22.3	719	268	451
Perkins	273	32.7	20.0	22.0	716	369	347
Stillwater	300	32.5	19.7	22.0	665	375	290

† ET_o calculated using the FAO-56 modified form of the Penman-Monteith equation (Allen et al., 1998)
‡ Fallow atmospheric water deficit, calculated as the long-term average cumulative rainfall subtracted from the long-term average cumulative ET_o.

Table 3.2. Soil texture, percent sand and clay, volumetric soil water content at saturation (θ_S), at drained upper limit (θ_{DUL}), and at lower limit (θ_{LL}), bulk density (ρ_b), plant available water capacity (PAWC), runoff curve number (CN), drainage factor (Dr. F.), albedo (Alb.), and fraction residue cover (Residue) for the sites used for model calibration, validation, and prediction throughout central-western Oklahoma. Soil physical properties represent the average of the top 1.2 m of the soil profile.

Site	Soil texture	Sand	Clay	θ_S	θ_{DUL}	θ_{LL}	ρ_b	PAWC	CN	Dr. F.	Alb.	Residue
		—— % ——		——	$m^3\ m^{-3}$	——	$Mg\ m^{-3}$	mm				
Calibration and validation sites												
Stillwater	Silt Loam	27	32	0.39	0.31	0.18	1.61	153	94	0.2	0.11	0.37
Lahoma conv. Till	Silt Loam	35	24	0.41	0.28	0.15	1.56	156	80	0.2	0.12	0.30
Prediction sites												
Alva	Silt Loam	25	28	0.43	0.32	0.13	1.51	224	90	0.2	0.12	0.20
Altus	Clay Loam	17	44	0.43	0.39	0.22	1.51	254	94	0.1	0.11	0.20
Apache I†	Silty Clay Loam	12	38	0.41	0.37	0.24	1.51	163	90	0.1	0.12	0.85
Apache II†	Silty Clay Loam	16	28	0.44	0.34	0.17	1.47	201	86	0.2	0.12	0.85
Cherokee	Silt Loam	36	21	0.43	0.28	0.14	1.51	173	86	0.3	0.12	0.85
Chickasha	Silt Loam	23	17	0.46	0.27	0.07	1.43	234	86	0.4	0.12	0.20
Lahoma no-till	Silt Loam	35	24	0.43	0.28	0.14	1.51	179	86	0.2	0.12	0.85
Marshall	Silty Clay Loam	11	43	0.40	0.39	0.22	1.59	202	94	0.1	0.11	0.20
McLoud	Loam	39	14	0.47	0.24	0.07	1.40	211	86	0.4	0.12	0.20
Perkins I‡	Sandy Loam	57	16	0.40	0.26	0.10	1.59	197	77	0.5	0.13	0.20
Perkins II‡	Sandy Loam	61	16	0.41	0.24	0.09	1.56	173	77	0.5	0.13	0.20
Stillwater	Silt Loam	27	32	0.39	0.31	0.18	1.61	153	94	0.2	0.11	0.37

† The variety trial was located at different fields in Apache in the years of 2012 and 2013. Apache I show data from 2012, and Apache II show data for 2013.

‡ Two different fields were sampled at Perkins following both summer fallow periods of 2012 and 2013 for a total of four site-years.

Table 3.3. Cumulative precipitation (P) and reference evapotranspiration (ET_o) during the fallow period preceding wheat sowing, sowing date, mean plant available water at wheat sowing (PAW_s) and standard deviation (SD) measured at the 29 site-years included in this study. Fallow is defined as the period from 15 June through the specified sowing date. Dataset in which each site-year was included is shown.

			Fallow			PAW_s	
Site	Year	Dataset†	P	Et_o	Sowing	Mean	SD
			mm			mm	
Alva	2012	p	122	879	16-Oct	38	± 33
Alva	2013	p	388	705	3-Oct	95	± 33
Altus	2012	p	149	837	8-Oct	86	± 8
Altus	2013	p	168	885	16-Oct	18	± 10
Apache I	2012	p	154	809	9-Oct	101	± 38
Apache II	2013	p	345	752	23-Oct	171	± 8
Cherokee	2012	p	112	784	3-Oct	72	± 20
Cherokee	2013	p	343	738	3-Oct	143	± 34
Chickasha	2012	p	225	791	18-Oct	152	± 10
Chickasha	2013	p	434	704	23-Oct	174	± 16
Lahoma	2012	p	127	800	5-Oct	98	± 10
Lahoma	2013	p	434	704	11-Oct	172	± 10
Lahoma no-till	2009	p	368	604	24-Oct	152	± 3
Lahoma no-till	2010	p	474	851	25-Oct	149	± 6
Lahoma no-till	2011	p	226	978	18-Oct	113	± 24
Lahoma no-till	2012	p	146	887	9-Oct	86	± 39
Lahoma conv. Till	2009	c	368	604	24-Oct	161	± 11
Lahoma conv. Till	2010	v	474	851	25-Oct	143	± 6
Lahoma conv. Till	2011	v	226	978	18-Oct	138	± 14
Lahoma conv. Till	2012	v	146	887	9-Oct	117	-
Marshall	2012	p	199	816	25-Oct	79	± 33
Marshall	2013	p	430	684	23-Oct	103	± 35
McLoud	2012	p	213	731	10-Oct	84	± 16
Perkins I	2012	p	191	783	16-Oct	103	± 23
Perkins I	2013	p	421	655	11-Oct	144	± 13
Perkins II	2012	p	191	783	16-Oct	73	± 10
Perkins II	2013	p	421	655	11-Oct	129	± 6
Stillwater	2012	p	144	757	19-Oct	84	± 30
Stillwater	2013	c	270	452	12-Oct	133	± 31

† Dataset indicates in which dataset the site-year was included, c - calibration dataset, v - validation dataset, p - prediction dataset.

Table 3.4. Change in the soil water storage of different layers of the soil profile during a 38-day period without measurable precipitation (August 17th to September 24th, 2013) at Stillwater, OK. Crop basal coefficient (K_{cb}) and statistics of linear regression analyses between plant available water and days after precipitation for each soil layer are also shown.

			Linear regression	
Soil layer	Water depletion†	K_{cb}‡	r^2	Slope
m	mm			mm d^{-1}
0 - 0.2	38.19	0.16	0.93**	-1.03
0.2 – 0.4	6.41	0.03	0.91**	-0.16
0.4 – 0.6	3.14	0.01	0.90 **	-0.08
0.6 – 0.8	2.73	0.01	0.98***	-0.07
0.8 – 1.0	1.91	0.01	0.48 ns	-0.04
1.0 – 1.2	1.09	0.005	0.59 ns	-0.03

*, **, and *** - significant at $p < 0.05$, 0.01, and 0.001, respectively.
ns - non-significant
† Calculated as the difference between plant available water at August 27th and at September 24th.
‡ Calculated as the ratio of total water loss cumulative reference evapotranspiration during the period (233 mm; ET_o calculated using the FAO-56 modified form of the Penman-Monteith equation; Allen et al., 1998)

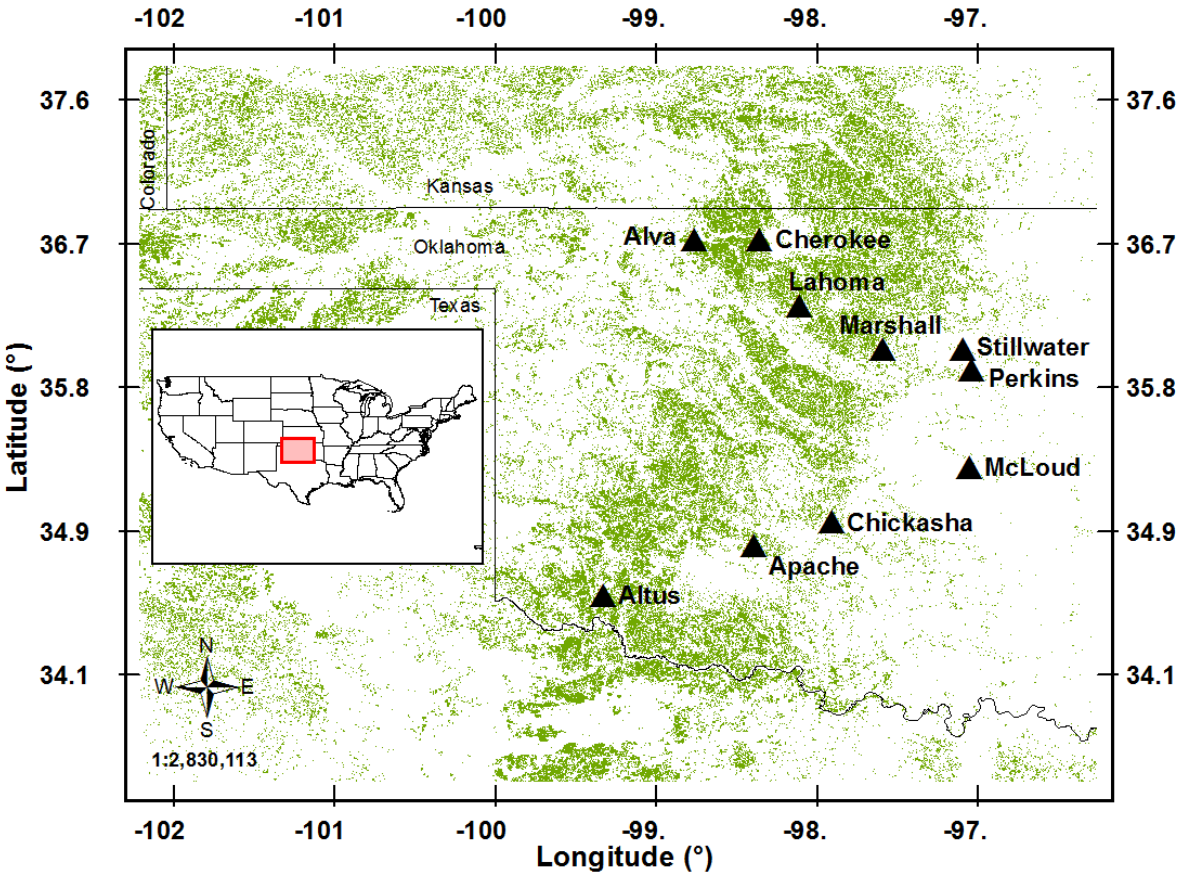

Figure 3.1. Map of the state of Oklahoma showing the primary wheat production area (green area) concentrated in the central-western portion of the state. Black triangles represent study locations.

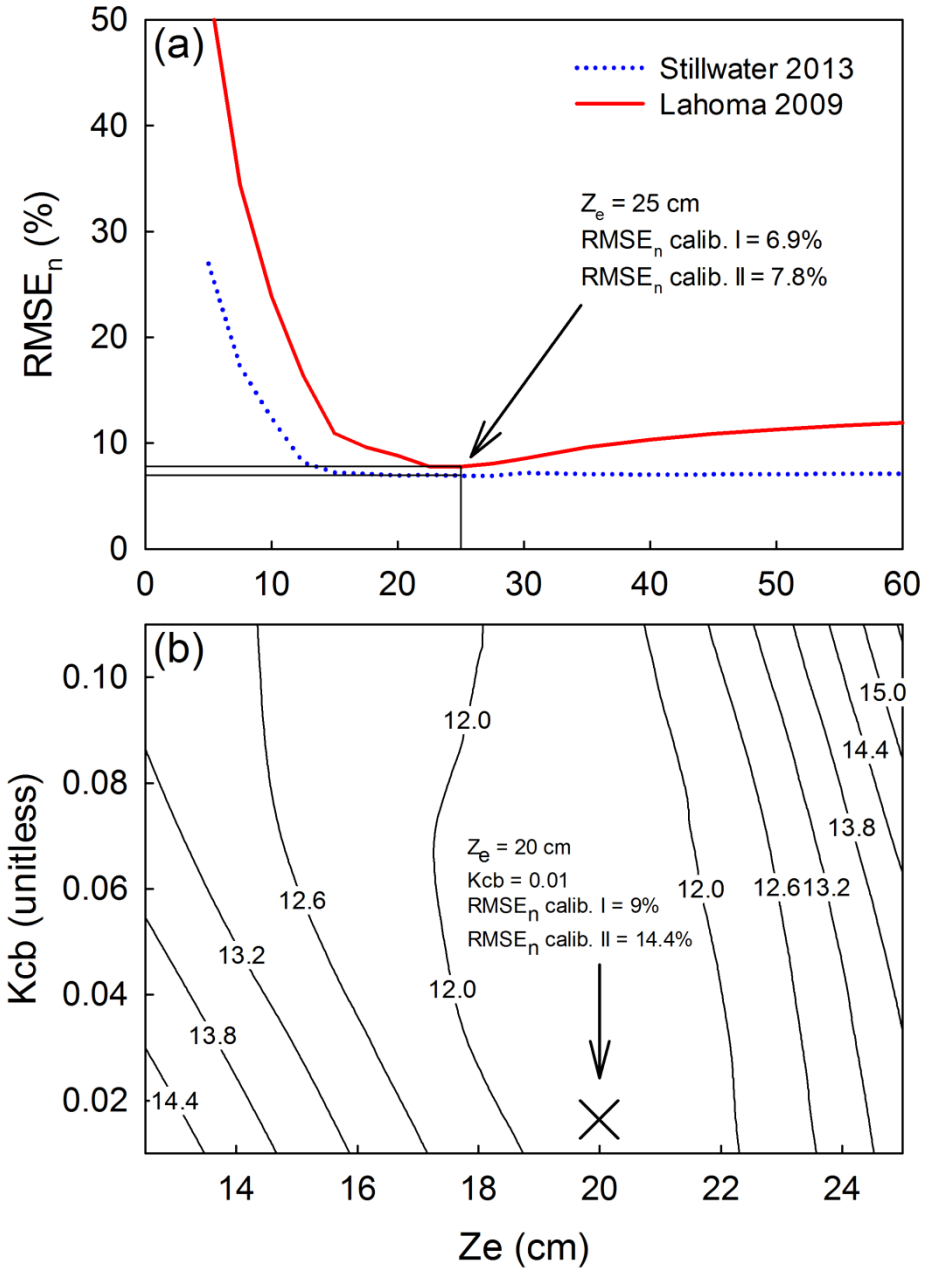

Figure 3.2. Calibration of (a) soil surface layer depth subjected to water evaporation (Ze) for the SSM model for Stillwater in 2013 (Calibration site I) and for Lahoma in 2009 (Calibration site II); and (b) simultaneous calibration of Ze and crop basal coefficient (K_{cb}) for the dual K_c, where contour lines are average normalized root mean square error ($RMSE_n$) of the two calibration sites. Lowest average $RMSE_n$ is indicated by the cross.

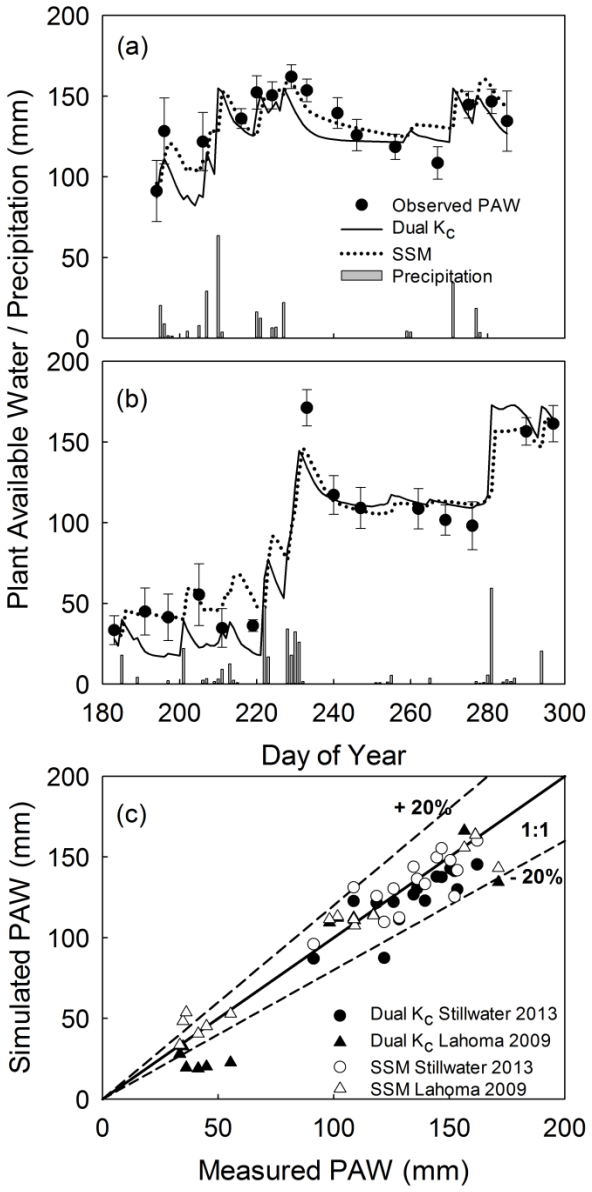

Figure 3.3. Measured and simulated plant available water (PAW) dynamics (1.2 m depth) for both dual K_c and SSM models for calibration summer fallows of (a) Stillwater in 2013 and (b) Lahoma in 2009. Daily precipitation and standard error of the mean (bars) are also shown. (c) Observed vs. simulated PAW values as compared to the 1:1 ratio (solid line) and ±20% deviation from 1:1 line (dotted line).

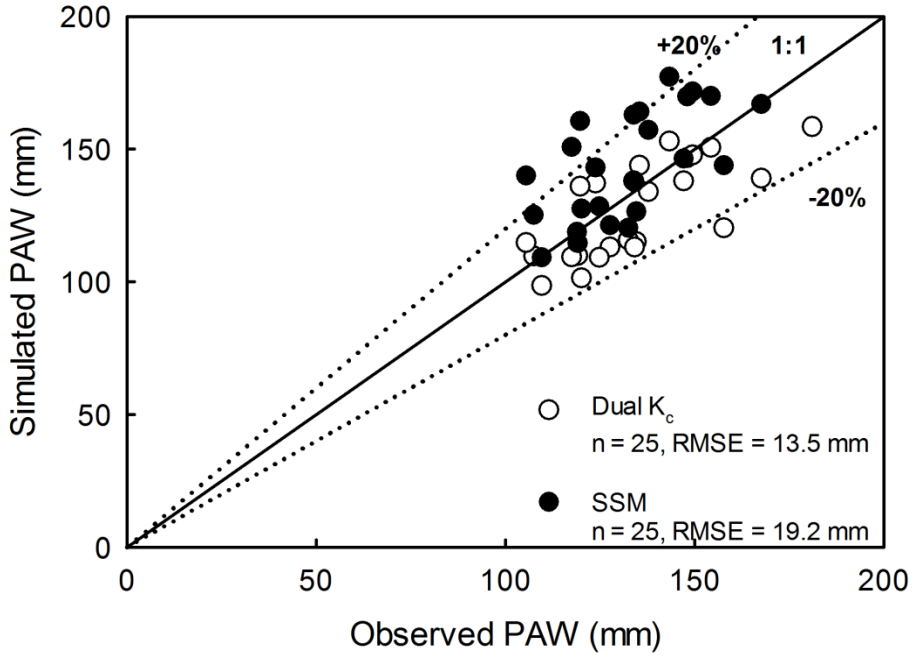

Figure 3.4. Observed vs. simulated PAW by the dual K_c and SSM models for the three validation fallow periods of 2010, 2011, and 2012 at Lahoma, OK. Diagonal solid line: 1:1; dotted lines: ±20% deviation from 1:1 line. Reported root mean square error (RMSE) is the average of the three fallow periods for each model.

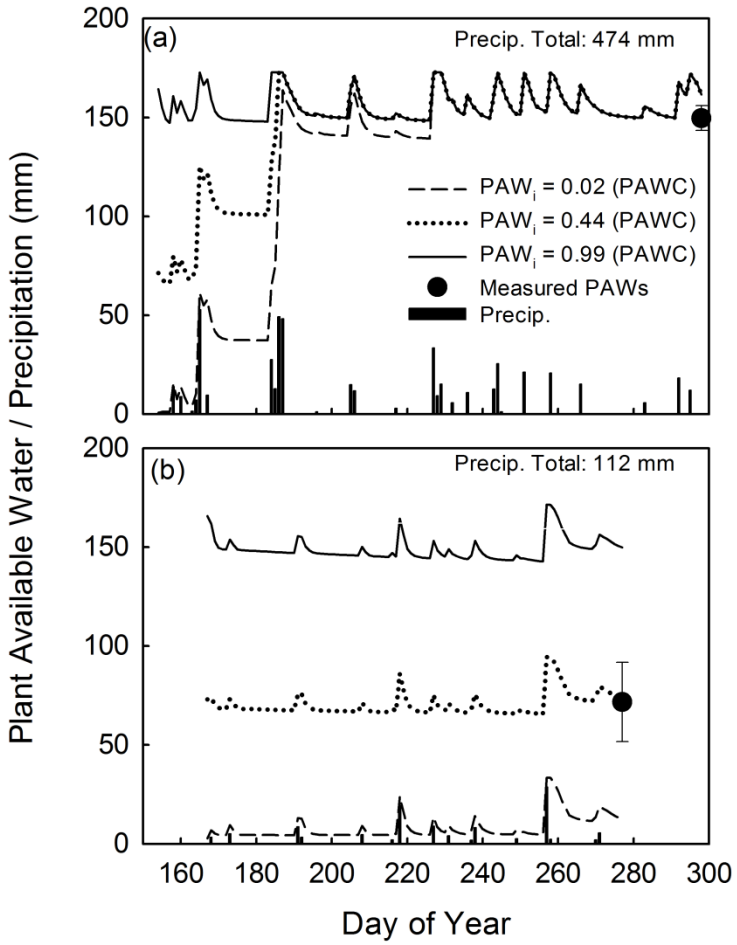

Figure 3.5. Two major patterns of PAW dynamics resulting from different plant available water contents at the beginning of the summer fallow period (PAW_i) simulated by the dual K_c model. (a) Simulated PAW converged to similar values regardless of PAW_i at Lahoma during the 2010 summer fallow and (b) simulated PAW did not converge at Cherokee in the summer fallow of 2012.

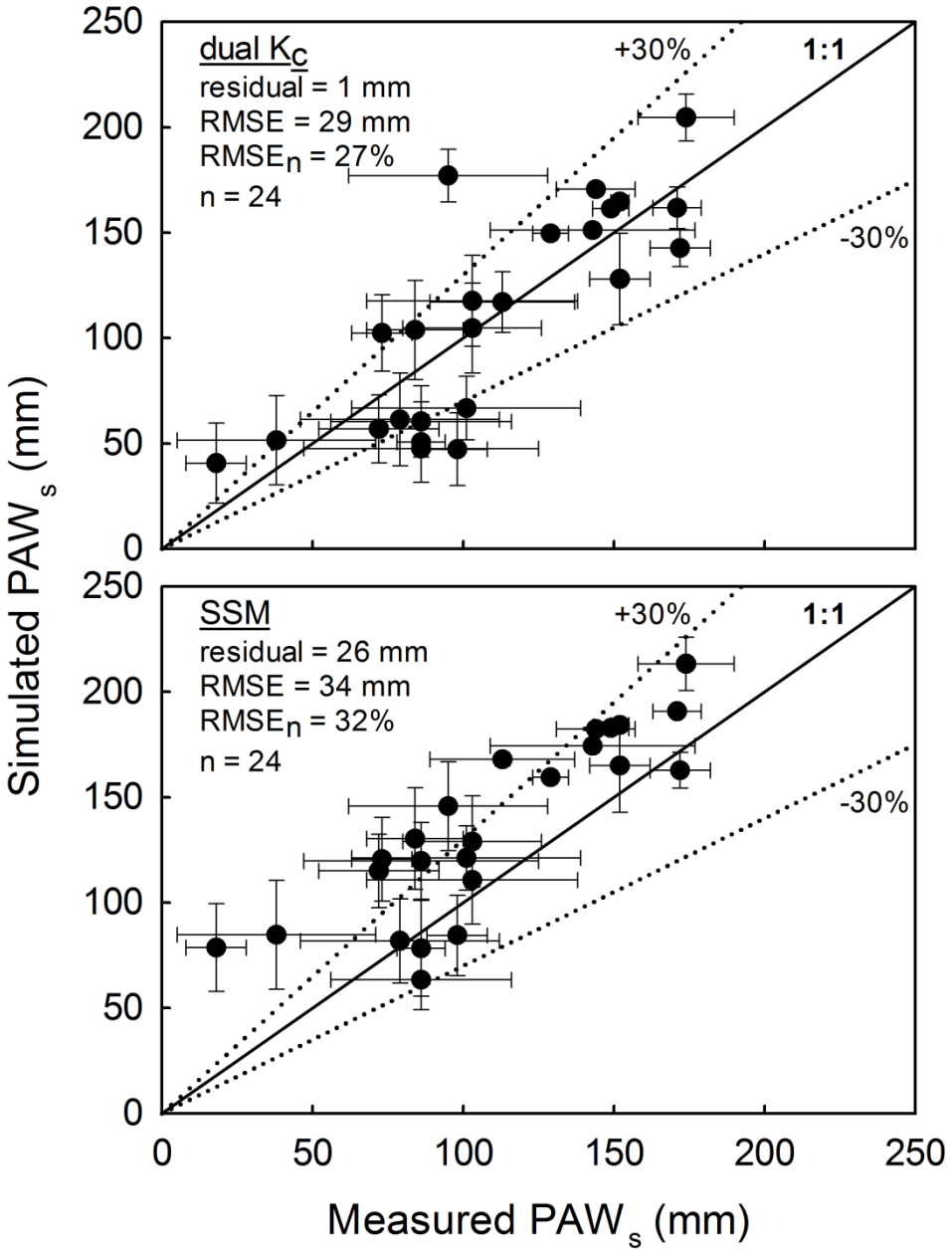

Figure 3.6. Measured versus simulated PAW_s for 24 site-years across Oklahoma for the dual K_c (upper panel) and SSM (lower panel) models. Simulated PAW_s are mean and standard deviation of 1000 simulations performed for each site-year (vertical error bars), whereas measured PAW_s are mean and standard deviation of four replications (horizontal error bars).

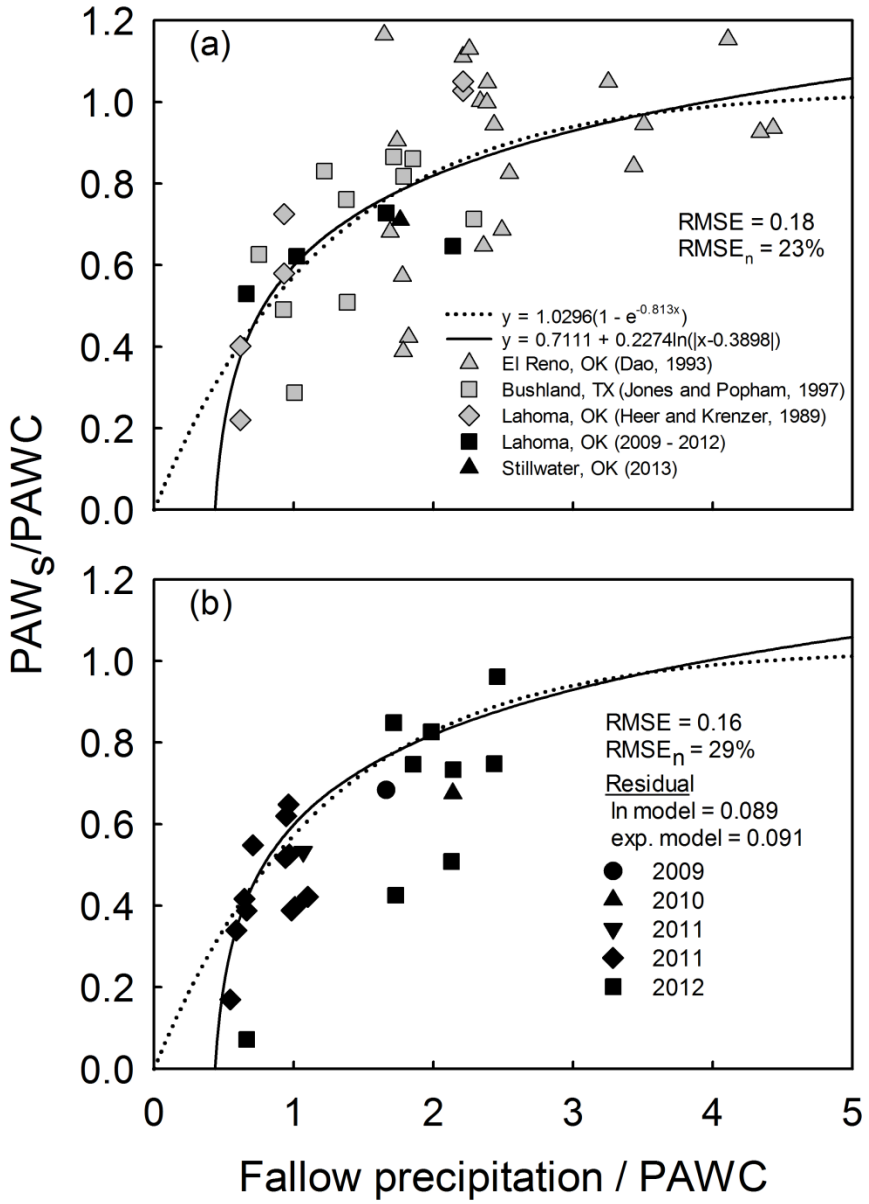

Figure 3.7. Logarithmic and exponential rise to maximum models of plant available water at sowing normalized by the soil's plant available water capacity (PAW_s /PAWC) as a function of cumulative fallow precipitation (Precip.) normalized by PAWC (a) for five locations in the current study and literature used for model development; and (b) for 24 site-years used for model validation with data collected in the current study. Statistics of model performance were the same for both models in both the calibration and validation datasets.

CHAPTER IV

MAXIMUM ATTAINABLE WHEAT YIELD AND RESOURCE USE-EFFICIENCY IN THE SOUTHERN GREAT PLAINS

ABSTRACT

Maximum reported grain yields for hard red winter wheat (*Triticum aestivum* L.) in the southern Great Plains range from 6 to 8 Mg ha^{-1} and are significantly lower than yields achieved in other regions of the world. The lack of empirical data for wheat under non-limiting conditions in this region, however, suggests that maximum reported grain yields for the region might not represent maximum attainable yields. Our objective was to perform the agronomic characterization of wheat grown under non-limiting conditions across the southern Great Plains. Four dryland and two irrigated fields were sown to 'Iba' winter wheat in the 2012-13 growing season and repeated during 2013-14 in central Oklahoma. Fields were intensively managed for fertility for maximum yield and freedom from weeds, insects, and disease. Aboveground dry matter at maturity ranged from 9.95 to 20.5 Mg ha^{-1} but harvest index (HI) did not surpass 0.41 and grain yields ranged from 3.06 to 7.68 Mg ha^{-1}. The highest yield was achieved under irrigated conditions in 2013-14, but one dryland site produced 7.11 Mg ha^{-1} grain in 2012-13. Maximum radiation use-efficiency (RUE) ranged from 0.8 to 1.9 g MJ^{-1} and water use-efficiency (WUE) from 7.8 to 12.6 kg ha^{-1} mm^{-1}. The wheat characteristics measured in this study were near or above maximum values

reported in the literature for the region, and our data provide empirical evidence to support maximum attainable wheat yields of 7.68 Mg ha^{-1} when wheat is grown under non-limiting conditions in the southern Great Plains.

Keywords: yield potential, maximum attainable yields, yield gap; winter wheat; water-use efficiency, radiation-use efficiency, evapotranspiration.

Abbreviations: AWHC: available water holding capacity; DAP: diammonium phosphate; ET_c: crop evapotranspiration; ET_o: reference evapotranspiration; HI: harvest index; I_c: rainfall interception by the crop canopy; K_c: crop coefficient; PAW: plant available water; PQ: photothermal quotient; Rs: incident solar radiation; RUE: radiation-use efficiency; T_{max}: maximum daily temperature; T_{min}: minimum daily temperature; WUE: water-use efficiency; θ_{DUL}: volumetric soil water content at the drained upper limit; θ_{LL}: volumetric soil water content at the lower limit; θ_S: volumetric soil water content at saturation; θ_v: volumetric soil water content.

4.1. INTRODUCTION

Yield potential is the yield of a cultivar grown in an environment to which it is adapted, in the absence of water, nutrient, disease, and weed limitations (Evans and Fischer, 1999). Maximum attainable yield is the maximum yield that can be reached by a crop in a certain environment; thus, it is the yield potential decreased by climatic factors such as below-optimal incident solar radiation, air temperature, photoperiod, and atmospheric CO_2 concentration during the growing season (Evans and Fischer, 1999). In rainfed agricultural systems, such as the majority of the winter wheat grown in the southern Great Plains (i.e. Kansas, Oklahoma, and Texas), maximum attainable yield can be decreased due to lack of adequate water supply. Thus, the amount of water limitation needs to be taken into account in such environments when estimating maximum attainable yield (Connor et al., 2011).

A theoretical value for potential yield, given non-limiting water conditions, can be derived as the product of total amount of radiation intercepted during the growing season and RUE, multiplied by HI (Hay and Porter, 2006). Assuming a total radiation intercepted during the growing season of 1600 MJ m^{-2}, a RUE of 1.4 g MJ^{-1}, and a HI of 0.5, a physiological estimate of the potential yield of wheat is around 12.9 Mg ha^{-1} on a 135 g kg^{-1} water basis (Sinclair, 2013). The achievement of 11.4 Mg ha^{-1} under experimental conditions in the United Kingdom (Fischer and Edmeades, 2010; Shearman et al., 2005) and 15.5 Mg ha^{-1} in New Zealand (Armour et al., 2004) provided empirical data to support the achievability of these theoretical yields. However, maximum reported winter wheat grain yields in the southern Great Plains remain well below the theoretical potential both at plot and farm level.

The southern Great Plains of the United States accounts for ~30% of the U.S. wheat production. The states of Kansas, Oklahoma, and Texas combined produce a total of ~14 million metric tonnes of hard red winter wheat per year in an area of over 8 million hectares (USDA-

NASS, 2014). Still, state level wheat yields are lower than other regions of the world, lying around 2.3 Mg ha^{-1} (Patrignani et al., 2014), and maximum reported yields have not surpassed 8 Mg ha^{-1}. Wheat yield contests have been performed in Kansas since 2010, and contest winners' yields ranged from 5.69 Mg ha^{-1} in 2012 to 7.05 Mg ha^{-1} in 2011 (http://kswheat.com/producers/yield-contest; verified 31 March 2015). The greatest wheat yields reported in small grains variety performance tests across the southern Great Plains are 7.46 Mg ha^{-1} in 2012 in Kansas, 6.59 Mg ha^{-1} in 2007 in Oklahoma, and 6.38 Mg ha^{-1} in 2009 in Texas (Patrignani et al., 2014). A long-term (1971 to date) soil fertility experiment conducted in Lahoma, OK, provides empirical data for yields close to 6.0 Mg ha^{-1} (Raun et al., 2011). Moreover, an ~8 Mg ha^{-1} was reported in Bushland, TX (Musick et al., 1994), but still accounts only for approximately 64% of the theoretical physiological potential wheat yield.

The low maximum reported yields in the southern Great Plains indicate that either these studies do not represent winter wheat yields grown under non-limiting conditions, or that limiting factors other than radiation govern maximum attainable wheat yields in this region. It is difficult to conclude whether the aforementioned yields are close to the environmental potential of the region because it is unclear if all biotic and abiotic stresses were properly avoided in the course of the growing seasons. Additionally, despite the importance of a complete documentation on crop growth and development, most of these studies only report final grain yield.

In areas dominated by rainfed agriculture and prone to stress, such as the majority of the wheat grown in the southern Great Plains, total water supply and distribution are likely the main limiting factors to crop yields (Hay and Porter, 2006). When water is the primary limiting factor to crop production, crop biomass accumulation is linearly related to cumulative transpiration (Ludlow and Muchow, 1990). Using a similar approach to the radiation-limited potential yield, water-limited crop yields will depend on the total transpired water in the growing season, WUE, and HI (Hay and Porter, 2006). A recent assessment of historical data in Oklahoma using the

WUE approach concluded that the water-limited yield potential of winter wheat in the region is 6.7 Mg ha^{-1} (Patrignani et al., 2014). While this yield is congruent with maximum yields recorded at plot and farm levels in the region, the lack of field-measured data reporting wheat growth, development, and yield, under non-limiting conditions renders unclear whether higher yield levels could possibly be achieved with intensive management practices. A complete assessment of agronomic attributes of winter wheat grown under non-limiting conditions has not yet been conducted in the region.

A crop grown under non-limiting conditions may use the available natural resources, such as water or solar radiation, more efficiently than a crop grown under below-optimal management. Radiation use-efficiency and WUE represent the efficiency with which a crop transforms incident solar radiation (Sinclair and Muchow, 1999) or water evaporated and transpired (Tanner and Sinclair, 1983) into biomass. Quantifying the maximum attainable yield per unit of available resource is essential to create benchmarks for producers and to identify other yield reducing factors within their management (Passioura, 2006). The suggested maximum RUE for wheat is 1.4 g MJ^{-1} based on intercepted solar radiation (Sinclair and Muchow, 1999), and maximum WUE is 22.3 kg ha^{-1} mm^{-1} (Sadras and Angus, 2006). These values may be adjusted using data collected for wheat grown under non-limiting conditions.

We hypothesize that maximum attainable wheat yields in the southern Great Plains are comparable to other regions in the world (i.e. greater than 10 Mg ha^{-1}) and that this yield level is attainable when adopting best management practices. Given the limited empirical data collected from wheat grown under non-limiting conditions in this region, the objectives of this research were (i) to characterize wheat growth (i.e. biomass accumulation, canopy cover, leaf area index development, soil water dynamics), development, and yield under non-limiting conditions; (ii) to elucidate physiological and environmental determinants of record-breaking wheat yields in this region; and (iii) to determine radiation- and water- use-efficiencies in this system.

4.2. MATERIAL AND METHODS

4.2.1. Field experiments

Four dryland and two irrigated field trials to estimate maximum yield of winter wheat were established across central-western Oklahoma in the growing season of 2012-2013, and five of these sites were repeated in 2013-2014. Irrigated fields were located in Stillwater (36.12°N, 97.09°W, alt. 300 m) on a Norge Loam (fine-silty, mixed, active, thermic Udic Paleustoll) and in Perkins (35.99°N, 97.04°W, alt. 273 m) on a Teller Fine Sandy Loam (fine-loamy, mixed, active, thermic Udic Argiustoll), and dryland fields were located in the same soil in Stillwater, in Perkins on a Teller Loam (fine-loamy, mixed, active, thermic Udic Argiustoll), in Lahoma (36.39°N, 98.11°W, alt. 380 m) on a Grant Silt Loam (Fine-silty, mixed, superactive, thermic Udic Argiustoll), and in Chickasha (35.05°N, 97.91°W, alt. 333 m) on a Dale Silt Loam (fine-silty, mixed, superactive, thermic Pachic Haplustoll). The experiment was not repeated in the dryland site at Lahoma during the 2013-2014 growing season. All field trials were located in an experiment station of the Oklahoma Agricultural Experiment Station network and within ~500 m of a weather station from the Oklahoma Mesonet network, which provided daily weather data for rainfall (mm d^{-1}), incident solar radiation (R_s, MJ m^{-2} d^{-1}), minimum and maximum temperatures (T_{min} and T_{max}; °C), wind speed (m s^{-1}), and relative humidity (%).

At each location, an area of approximately 1000 m^2 was sown to ‘Iba’ winter wheat and intensively managed to avoid stresses from weeds, insects, diseases, and also water stress in the irrigated fields. Areas with relatively homogenous soils were selected, and management was performed across the whole field to mimic large-scale production. Four random blocks were established in these intensive management fields, where data regarding typical soil characteristics, soil water dynamics, and crop growth and development were collected. This

methodology is often adopted to evaluate crop yields under non-limiting conditions (Peake et al., 2014; Yang et al., 2004).

4.2.2. Crop management

Adoption of no-till production practices has been shown to decrease (Decker et al., 2009) or have no effect (Patrignani et al., 2012) on grain yield in continuous wheat systems in Oklahoma, and the majority of wheat in the region is still produced using conventional tillage. Thus, conventional tillage techniques were used and soils were worked to approximately 20 cm deep during the 2012 and 2013 summer fallows. Tillage operations during fallow periods to incorporate pre-plant fertilizer and control weeds were performed using a solid shank chisel followed by offset disking, ensuring < 10% residue at planting. Urea (46-0-0) or urea and diammonium phosphate (DAP, 18-46-0) were broadcast and incorporated prior to planting according to soil needs, and 56 kg DAP ha^{-1} was placed in furrow at planting. An S-Tine field cultivator with a rolling basket harrow was used on all fields to work the ground to approximately 8-cm deep for seedbed preparation at time of planting. The winter wheat variety Iba was sown using a Hege small-plot, conventional drill (Wintersteiger, Salt Lake City, UT), with 17-cm row spacing. Seeding density was 67 kg ha^{-1} (approximately 2.1 million seeds ha^{-1}), and planting occurred during the month of October (Table 4.2). The variety Iba has high yield potential, broad area of adaptation in the southern Great Plains, and a broad spectrum of disease resistance (Edwards, 2013).

Nitrogen fertilization was performed to ensure N would not be a limiting factor to crop growth or yield, with total N available in the growing season (i.e. pre-plant N fertilizer, N at sowing, and topdress N fertilizer) greater than 240 kg N ha^{-1}. Fall nitrogen fertilization ensured at least 100 kg N ha^{-1} was available for early plant development during the fall and phosphorus fertilization ensured 100% sufficiency levels (Table 4.1). Amounts were adjusted by site-year to

reflect soil test results, but N fertilization generally consisted of 46 to 69 kg N ha^{-1} pre-planting, 9 kg N ha^{-1} in furrow at sowing, 25 kg N ha^{-1} topdressed at Feekes GS 2 (mid-fall), 50 kg N ha^{-1} at Feekes GS 4 (early spring) and 100 kg N ha^{-1} at Feekes GS 5 (mid spring) in the form of urea. Applications of N fertilizer were made under favorable weather conditions to reduce volatilization losses. Fields were kept weed[1], insect[2], and disease[3] free. Plots were harvested with a Hege 140 self-propelled small plot combine (Wintersteiger, Salt Lake City, UT), and harvest dates are provided in Table 4.2. Grain moisture content was measured at time of harvest and final grain yield was reported on a 135 g kg^{-1} water basis.

Overhead sprinkler irrigation at Perkins and Stillwater was scheduled based on an atmospheric water balance that employs meteorological, soil, and crop data for a daily estimation of soil water depletion in the effective rooting zone. The FAO Penman-Monteith method (Allen et al., 1998) was used to estimate daily reference evapotranspiration (ET_o) using weather data retrieved from a nearby weather station from the Mesonet network. Crop coefficient values (K_c) for winter wheat were derived from the FAO Irrigation and Drainage Paper no. 56 (Allen et al., 1998) and adjusted by field observations of crop phenological stages and ranged from 0.4 in the beginning of the growing season to 1.25 mid-season, based on canopy development (Allen et al., 1998). A 15-d running sum of crop evapotranspiration (ET_c) was subtracted from a 15-d running sum of rainfall, and irrigation was applied to replenish soil profile to field capacity when the 15-d water deficit achieved ~50% of available soil water holding capacity (AWHC). Cumulative

[1] Weeds were controlled late fall and, if needed, early spring, with 0.47 kg ha^{-1} MCPA ((4-Chloro-2-methylphenoxy) acetic acid) and 0.25 kg ha^{-1} pyroxsulam (N-(5,7-dimethoxy[1,2.4]triazolo[1,5-a] pyrimidin-2-yl)-2-methoxy-4-(trifluoromethyl)-3-pyridinesulfonamide).

[2] Insects were controlled during the fall and early spring with 0.25 kg ha^{-1} lamba-cyhalothrin ([1a(S*),3a(Z)]-cyano(3-phenoxyphenyl)methyl-3-(2-chloro-3,3,3-trifluoro-1-propenyl)-2,2-Dimethylcyclopropanecarboxylate).

[3] Foliar diseases were controlled with 0.08 kg ha^{-1} propiconazole (1-[[2-(2,4-dichlorophenyl)-4-propyl-1,3-dioxolan-2-yl]methyl]-1,2,4-triazole) at flag leaf emergence, followed by 0.09 kg ha^{-1} propiconazole and 0.10 kg ha^{-1} azoxystrobin (Methyl (2E)-2-(2-{[6-(2-cyanophenoxy) pyrimidin-4-yl]oxy phenyl)-3-methoxyacrylate) when approximately 50% of heads were emerged.

irrigation applied in Stillwater was 168 mm during the 2012-13 growing season and 376 mm during the 2013-14 growing season; and cumulative irrigation applied in Perkins was 73 and 279 mm during the 2012-13 and 2013-14 growing seasons, respectively.

4.2.3. Soil physical properties and water dynamics measurements

Soil water content to a 120-cm depth was measured at planting and at intervals of approximately 2-3 weeks throughout the growing season using a neutron moisture meter (CPN, Model 503 DR). Galvanized metal tubes of 3.8 cm i.d. were installed in the four replications to facilitate the access of neutron probe into the soil, and readings were taken at 10, 30, 50, 70, 90, and 110 cm below ground with the neutron probe device placed on a depth control stand (Evett et al., 2003). Two extra access tubes were installed in each field to calibrate the neutron probe readings against volumetric water content (θ_v, m^3 m^{-3}) under dry and wet soil conditions. During both the dry and the wet calibrations of the neutron probe, a total of four 120-cm depth 4.02-cm diameter soil cores were taken adjacent to the access tube using a Giddings hydraulic probe (#25-TS Model HDGSRTS, Soil Exploration Equipment, Windsor, CO) and each core was divided into 20-cm intervals. Soil water content was determined by the thermo-gravimetric method and bulk density was determined by the core method, and both were used to calculate θ_v. The relationship between neutron counts and θ_v was determined using linear regression for either the top 20-cm layer or the rest of the profile. Volumetric soil water content at lower limit (θ_{LL}) was considered the soil water retention at -1500 kPa measured by the pressure plate method (Ratliff et al., 1983) and volumetric soil water content at the drained upper limit (θ_{DUL}) was measured by collecting soil samples after thoroughly wetting the soil profile and allowing water to drain (Ratliff et al., 1983). The soil's AWHC was calculated for each layer as the difference between θ_{DUL} and θ_{LL} multiplied by the soil layer thickness (Allen et al., 1998). Plant available water (PAW) was calculated as the difference between θ_v and θ_{LL}. Soil porosity was estimated based on the soil bulk density and an assumed particle density of 2.65 Mg m^{-3} (Danielson et al., 1986) and

assumed to be equal to the volumetric soil water content at saturation (θ_S). Particle size analysis was performed using the hydrometer method. Soil physical properties for the studied sites are shown in Table 4.1.

4.2.4. Plant growth, development, and yield measurements

Plots were approximately 7.5-m wide by 13-m in length, centered on the galvanized tubes placed in the four randomized blocks across the field used for neutron probe access into the soil. In-season plant measurements and grain yield were collected from opposite sides of tubes. Final grain yield was determined from three subsamples per plot, each subsample accounting for a harvested area 13-m long and 1.5-m wide, encompassing roughly 20 m^2 and resulting in 12 representative grain yield samples per site-year. An area 1.5 m by 13 m surrounding the tubes, as well as the area harvested for grain yield, was spared from destructive measurements not to interfere in the natural crop soil water balance or grain production.

Plant measurements included dates of major phenological events, percent canopy cover, LAI, and aboveground biomass. Digital photographs were taken with the camera lens pointing down and encompassing approximately 1 m^2 of the crop area to estimate percent canopy closure using a macro program for Sigma Scan Pro (v. 5.0, Systat Software, Point Richmond, CA) as described by Karcher and Richardson (2005). The software has selectable options defining hue and saturation values, which in this study were set for 30–150 and 0–115, respectively. Percent canopy coverage was estimated as the number of pixels within the selected range divided by the total number of pixels per image (Purcell, 2000). Leaf area index (LAI) was destructively estimated by clipping one linear meter of aboveground matter and screening the recently collected green leaves through an optical leaf area meter (LI-COR, model LI-3100, Lincoln Nebraska, USA). Samples were then dried to a constant weight at 50 °C for estimation of aboveground biomass. Plant measurements occurred at intervals of approximately 2-3 weeks

from emergence until harvest and were accompanied by soil water content measurements. At physiological maturity (growth stage Feekes 11.4), a 0.25 m^2 sample was collected for estimation of final aboveground biomass, harvest index (HI), kernel m^{-2}, and individual kernel weight. Grain protein concentration (g kg^{-1}) was measured with near-infrared reflectance spectroscopy using a Perten DA 7200 and was reported on a 135 g kg^{-1} water basis (Perten Instruments Inc., Springfield, Illinois).

4.2.5. Radiation- and Water Use-Efficiencies

Interception of R_s by the crop canopy was calculated using an exponential radiation-interception equation based on LAI and extinction coefficient (Sinclair, 2006). Leaf area index was measured approximately every two weeks and daily increase in LAI within the ~14-d interval between measurements was calculated using linear regression interpolation (Van Roekel and Purcell, 2014). A constant extinction coefficient of 0.65 was used throughout the growing seasons (Soltani and Sinclair, 2012). Daily fractional interception derived from LAI was multiplied by R_s to calculate daily intercepted R_s, and cumulative intercepted R_s was obtained by successively summing daily intercepted R_s over the period from emergence to maturity. Seasonal RUE was calculated as the ratio of final aboveground biomass to total cumulative intercepted R_s. Maximum RUE was calculated as the slope of linear regression between cumulative aboveground biomass and cumulative intercepted R_s using a stepwise regression procedure as described in Muchow and Sinclair (1994). Only samples collected following winter dormancy were included in the maximum RUE analysis.

Water use efficiency (WUE) was calculated as the ratio of grain yield to cumulative ET_c during the growing season, the latter being derived from a soil water balance from neutron probe data. In the soil water balance adopted, neutron probe data taken approximately every two weeks was used to calculate ET_c during the time interval between measurements as the change in profile

soil water storage to 120-cm depth plus precipitation and irrigation, minus losses via canopy interception (I_c) .Cumulative ET_c in the growing season was then calculated using Eq. 1:

$$ET_C = \sum_{i=1}^{n} \left(-\Delta TSW + precipitation + irrigation - I_c \right)_i \quad [1]$$

where ΔTSW is the change in total soil water (mm) in the 120-cm soil profile during the i^{th} time interval between soil water measurements, precipitation and irrigation are cumulative values measured during the i^{th} time interval, and I_c is cumulative crop canopy interception during the i^{th} time interval. Daily I_c was estimated as a function of crop canopy interception based on LAI, following the model used in the CropSyst Crop Production Model (Campbell. and Diaz, 1988). In Oklahoma, losses associated with I_c are especially important given that more than 70% of daily rainfall totals in the wheat growing region are less than 10 mm (Patrignani et al., 2014). Deep drainage and runoff were considered negligible. Considering deep drainage negligible was supported by neutron probe data, which provided evidence for little drainage below 120-cm in the studied period (data not shown). Considering runoff negligible is a reasonable assumption given that the experimental field areas had 0-2% slope and average annual runoff during the study period for the study-sites, calculated using the online version of Water Erosion Prediction Project (WEPP) (Frankenberger et al., 2011), ranged from 1 to 3% of annual precipitation.

4.2.6. Statistical approach

All the measured (i.e. percent canopy cover, biomass, leaf area index, grain yield, percent protein concentration, and PAW) and calculated (i.e. ET_c and water- and radiation use-efficiencies) variables were analyzed using a generalized linear mixed model procedure using PROC GLIMMIX in SAS v. 9.3 (SAS Institute, Cary, NC) to determine the least square means and standard errors for each variable in each year. Least square means were separated using a

Tukey test and $\alpha = 0.05$. Physiological and environmental determinants of wheat yields were evaluated using linear regression analysis.

4.3. RESULTS AND DISCUSSION

4.3.1. Weather conditions

Great variability in weather conditions occurred among the eleven studied site-years. The 2012-13 growing season had greater than average precipitation totals, particularly during spring when precipitation ranged from 253 mm in Lahoma to 432 mm in Chickasha, exceeding the long-term spring mean by 33 to 191 mm. Precipitation totals during the spring allowed for greater and less variable yields under dryland conditions during the 2012-13 growing season as compared to the 2013-14 growing season, which had exceptionally dry winter and spring seasons (Table 4.3). Spring precipitation in 2013-14 ranged from 195 mm in Stillwater to 247 mm in Chickasha and occurred mostly when the crop was close to or past physiological maturity, resulting in lower and more variable wheat yields compared to the prior year. Still, favorable R_s and temperature during the 2013-14 growing season led to greater yields in the irrigated experiments as compared to the previous growing season. Winter and spring daily R_s were greater than the long-term average across the eleven site-years, but the greatest positive deviation was observed in the 2013-14 growing season (Table 4.3). During the wheat reproductive stages in the spring 2012-13, R_s ranged from 18.9 to 20.4 MJ m^{-2} d^{-1}; whereas R_s during the same period in 2013-14 ranged from 21 to 21.6 MJ m^{-2} d^{-1} (2.3 to 2.6 MJ m^{-2} d^{-1} above the long term mean). Fall T_{max} and T_{min} were below the long-term mean for all site years, and the differences were more pronounced during the 2013-14 season (Table 4.3).

4.3.2. Maximum attainable wheat yields

Winter wheat grain yield across the irrigated and dryland sites ranged from 5.53 Mg ha^{-1} to 7.11 Mg ha^{-1} in the 2012-13 growing season and from 3.06 Mg ha^{-1} to 7.68 Mg ha^{-1} in the

2013-14 growing season (Table 4.4). The yields achieved in our study were supported by aboveground dry matter at physiological maturity (Feekes GS 11.4) ranging from 14.0 Mg ha^{-1} to 19.6 Mg ha^{-1} in 2012-13, and from 9.9 to 20.5 Mg ha^{-1} in 2013-14; and by HI ranging from 0.31 to 0.40 in 2012-13, and from 0.29 to 0.41 in 2013-14 (Table 4.4). Number of spikes m^{-2} ranged from 740 to 1272 in 2012-13, and from 757 to 1051 in 2013-14; while kernels m^{-2} ranged from 15,100 to 21,800 in 2012-13, and from 12,100 to 21,700 in 2013-14. Individual kernel weight ranged from 24.9 to 31.6 mg and 25.7 to 37.8 mg in the 2012-13 and 2013-14 growing seasons, respectively. Grain protein concentration ranged from 112 to 144 g kg^{-1} during the 2012-13 growing season, and from 116 to 155 g kg^{-1} during the 2013-14 growing season. Lower protein concentration was measured in the irrigated treatments when compared to dryland both years.

The narrower range in grain yields in 2012-13 as compared to 2013-14 can be attributed to greater growing season cumulative precipitation (average among sites: 522 mm in 2012-13 vs. 326 mm in 2013-14). The greatest dryland yield (i.e. 7.11 Mg ha^{-1}) was produced at Chickasha during the 2012-13 growing season, with total precipitation during the growing season of 587 mm (195 mm above the long-term average, Table 4.3). Additional weather characteristics leading to 7.11 Mg ha^{-1} grain yield in Chickasha under dryland management were low average spring T_{max} and T_{min} (averaged 21.9 and 8.3 °C respectively, both 0.7 °C below the mean), and above average R_s (20 MJ m^{-2} d^{-1}, Table 4.3). Wheat yield in Perkins under irrigated conditions (6.67 Mg ha^{-1}) was statistically the same as that achieved in Chickasha during 2012-13 and as the yield achieved in Stillwater under dryland conditions (6.5 Mg ha^{-1}). The irrigated wheat crop in Stillwater 2012-13 had great yield potential, with 1272 spikes m^{-2} (Table 4.4); however, severe lodging occurred at the beginning of grain filling (Feekes GS 10.54) and drastically reduced grain yields (5.92 Mg ha^{-1}). Dryland wheat yield at Perkins in 2012-13 (5.78 Mg ha^{-1}) was significantly less than irrigated, and was reduced by water deficit stress between full anthesis (Feekes GS 10.53) and physiological maturity, when soil PAW was consistently below 30% (data not shown). Although

there was no statistical difference in kernels m^{-2} between the irrigated and dryland treatments in Perkins 2012-13, individual kernel weight was greater in the irrigated treatment (35.6 vs 27.6 mg). The lowest yield in the 2012-13 growing season occurred under dryland conditions in Lahoma (5.53 Mg ha^{-1}), the site with the smallest total growing season rainfall (374 mm, Table 4.3). That yield is still close to the greatest yield reported from a long-term soil fertility experiment at Lahoma of 6 Mg ha^{-1} (Raun et al., 2011).

Less spring precipitation during the 2013-14 season resulted in a wider grain yield range, with significant differences between irrigated and non-irrigated trials (Table 4.4). The highest yield was obtained in Stillwater under irrigated conditions (i.e. 7.68 Mg ha^{-1}), and was not significantly different from the 7.42 Mg ha^{-1} irrigated yield achieved at Perkins. The high irrigated yields were supported by over 1000 spikes m^{-2} and 21,000 kernels m^{-2}, and individual kernel weight above 37 mg (Table 4.4). Wheat yields under dryland conditions did not differ statistically among Perkins, Stillwater, and Chickasha, and ranged from 3.06 to 3.45 Mg ha^{-1}. Similarly, dryland trials resulted in significantly fewer spikes m^{-2} (<900) and kernels m^{-2} (<16,000), with lower individual kernel weight (<30 mg).

The yields reported in this study are the maximum reported wheat yields for Oklahoma, and similar to the maximum yield reported for the southern Great Plains. The maximum reported yield in Oklahoma to date was 6.59 Mg ha^{-1} at Balko in 2007 as part of the Oklahoma State University (OSU) Small Grains Variety Performance Tests (Edwards et al., 2007), whereas Musick et al. (1994) reported ~8 Mg ha^{-1} for irrigated wheat in Bushland, TX. While our study provides empirical evidence for winter wheat grain yields of 7.68 Mg ha^{-1} when grown under non-limiting conditions in the southern Great Plains, the yields reported here are well below the 12.9 Mg ha^{-1} theoretical potential (Sinclair, 2013) and below yields obtained in other regions of the world such as 11.4 Mg ha^{-1} in the United Kingdom (Fischer and Edmeades, 2010; Shearman et al., 2005) and 15.5 Mg ha^{-1} in New Zealand (Armour et al., 2004). Weather characteristics

inherent to the southern Great Plains, including higher average temperatures and lower R_s during the reproductive phase as compared to other regions, and uneven precipitation distribution, may be among the main limiting factors to the achievement of yields close to the theoretical potential in this region.

Armour et al. (2004) reported an average wheat yield of 15.5 Mg ha^{-1} and individual kernel weight of 53.3 mg in New Zealand following a growing season when mean daily temperature and R_s during the 40-d period comprising anthesis – physiological maturity were 16.5°C and 26.2 MJ m^{-2} d^{-1}. In our experiments, the highest yield (7.68 Mg ha^{-1}) had an average kernel weight of 37 g and was achieved with mean temperature during the 39-d period encompassing anthesis – physiological maturity of 21.8°C and mean R_s of 22.8 MJ m^{-2} d^{-1}. Respiratory losses are dependent on temperature, and an increase in mean daily temperature of 10°C doubles the rate of crop maintenance respiration (Hay and Porter, 2006). Following the same stoichiometry, the 5.3°C greater temperatures in our study likely led to respiration rates at least 50% greater when compared to Armour et al. (2004), decreasing net photosynthesis available for grain fill (Hay and Porter, 2006). Likewise, R_s is converted into biomass and later into grain yield through a HI component. Adopting the maximum RUE and HI among all our site years of 1.9 g MJ^{-1} and 0.41 respectively, the additional 3.4 MJ m^{-2} d^{-1} R_s in New Zealand would have allowed for an additional 1.06 Mg ha^{-1} grain yield in our experiment. Finally, higher temperatures during grain filling can greatly reduce individual wheat kernel weight (Fischer, 2007), which explains individual kernel weight 44% greater in New Zealand when compared to the highest yielding location in our experiments.

An important factor possibly limiting maximum attainable wheat grain yields in the southern Great Plains is the high protein concentration of hard red winter wheat, relative to soft classes of wheat. Grain protein concentration at a 135 g kg^{-1} water basis was consistently above 116 g kg^{-1} in the irrigated treatments following both growing seasons, whereas the dryland

treatments resulted in over 125 g kg^{-1} grain protein concentration following the high-yielding 2012-13 growing season and over 145 g kg^{-1} following the low-yielding 2013-14 growing season. The negative linear association between wheat grain yield and grain protein concentration in our results (Fig. 4.1A) confirms the previously reported tradeoff between both variables (Barraclough et al., 2010). This tradeoff has been attributed to the dilution of the available nitrogen supply into more kernels m^{-2} (Fig. 4.1B) for comparisons within the same species (Acreche and Slafer, 2009b); and to a possible competition between carbon and nitrogen for energy when evaluating a range of species with varying seed composition (Munier-Jolain and Salon, 2005). The latter might be a possible explanation for the lower maximum attainable yields in the southern Great Plains when compared to wheat grown in other regions of the world. The yields exceeding 15 Mg ha^{-1} reported by Armour et al. (2004) were obtained from feed wheat cultivars, whereas wheat grown in high yielding regions of Western Europe can be classed as soft red winter wheat (Curtis et al., 2002). Both wheat types typically have lower protein concentration as compared to hard red winter wheat (Curtis et al., 2002; Snape et al., 1993), resulting in lesser energy cost per unit seed produced (Munier-Jolain and Salon, 2005).

The yields we report are still well above the state average wheat yields, which lies around 2.3 Mg ha^{-1} averaged for TX, OK, and KS (Patrignani et al., 2014). The large gap between maximum attainable wheat yields and state average yields indicates that there is room for improvement in current crop management practices and statewide wheat production. One unique feature of the region is that approximately half of the wheat grown in Oklahoma is managed as a forage and grain crop in a dual-purpose system (True et al., 2001). The yield penalty of the dual-purpose system on winter wheat compared to grain only averages 14% and is associated with both earlier-than-optimal sowing date and forage grazing (Edwards et al., 2011). The predominance of this system in the central portion of the southern Great Plains certainly contributes to the large yield gap in the region. Additionally, producers may be reluctant to adopt

intensive management practices due to the unpredictable weather typical in the southern Great Plains. Evaluation of the weather patterns that regulate wheat yields in this region as well as the long-term maximum attainable yields dictated by the observed weather is warranted.

4.3.3. Characterization of winter wheat growth and development under non-limiting conditions

Two major patterns of dryland crop development occurred between growing seasons 2012-13 and 2013-14, exemplified in Fig. 4.2 using data collected from Chickasha. Similar results were measured at Stillwater and Perkins when comparing the two consecutive growing seasons and are not shown. Leaf area index (Fig. 4.2A), percent canopy cover (Fig. 4.2B), and aboveground biomass (Fig. 4.2C) had an early, lush start during 2012-13 growing season due to greater fall temperatures (20.6 °C vs. 14.1°C) despite similar PAW during the vegetative phase across both growing seasons (Fig. 4.2D). The precipitation in 2012-13 was sufficient to sustain PAW in the top 120-cm soil depth above 0.3 to 0.4 AWHC over the majority of the growing season, a range below which crop growth is decreased due to water stress (Amir and Sinclair, 1991). Cooler spring temperatures and greater PAW favored delayed leaf senescence (Fig. 4.2A) and resulted in a longer grain-filling period (40 vs. 30 days, Fig. 4.2C) which, coupled to aboveground biomass >15 Mg ha^{-1} and LAI > 7 following anthesis, ensured little to no source limitation for grain set and filling for an yield of 7.11 Mg ha^{-1}. Contrarily, the wheat crop experienced accentuated water stress during spring (reproductive stages) during the 2013-14 growing season (Fig. 4.2D). Aboveground biomass (10.5 Mg ha^{-1}) and LAI (5.6) and at anthesis were significantly less than those measured in the 2012-13 growing season, which contributed to the lower grain yields due to increased source limitation in addition to low precipitation. Soil PAW was consistently below 30% during the reproductive stages (Fig. 4.2D), resulting in water deficit stress during grain fill. This, coupled to warmer temperatures, accelerated leaf senescence (Fig. 4.2A) and did not allow for increase in aboveground biomass following anthesis, and

shortened the duration of grain fill (Fig. 4.2C). The lack of increase in aboveground biomass after anthesis in 2013-14 (Fig. 4.2C) indicates that most of the grain yield was formed from redistribution of pre-existing resources. Thus, the reduced grain yield in 2013-14 dryland crop (3.06 to 3.45 Mg ha^{-1}) when compared to the previous season (5.78 to 7.11 Mg ha^{-1}) was resultant from photosynthesis-reducing water deficit stress, which decreased both source supply for photosynthesis (LAI) and sink demand (kernels m^{-2}) (Frederick and Bauer, 2000).

A complete soil-plant characterization of wheat in the highest-yielding environment (Stillwater irrigated 2013-14) is shown in Fig. 4.3, along with wheat grown in the same location and year without supplemental irrigation. The cooler start to the 2013-14 season led to lower early-season LAI (Fig. 4.3A), canopy cover (Fig. 4.3B), and aboveground biomass (Fig. 4.3C), as compared to the previous growing season (data not shown). This indicates that the early lush vegetative growth measured in Chickasha during 2012-13 (Fig. 4.2A) is not mandatory to achieve high yields. The weather during the spring, when grain formation occurs, appears to be more crucial than the fall weather, provided the wheat stand is adequate. Both irrigated and dryland wheat had very similar biomass until DAS 174 (Fig. 4.3C), when PAW levels were above 0.3 AWHC (45 mm). After DAS 174, PAW fell below 30% (Fig. 4.3D) and biomass production was reduced in the dryland trial. Our data supports the threshold of 0.3 AWHC for wheat biomass production sensitivity to drought suggested by Amir and Sinclair (1991) as biomass production fell considerably when PAW reached this threshold (Fig. 4.3). Anthesis LAI of 6.8 and aboveground biomass of 12.8 Mg ha^{-1} in addition to 376 mm supplemental irrigation during the spring provided the wheat crop little to no source limitation, leading to 7.68 Mg ha^{-1} wheat yield. Aboveground biomass increased from 12.8 Mg ha^{-1} at anthesis to 20.5 Mg ha^{-1} at harvest, providing evidence for post-anthesis photosynthesis contributing to grain yields. In contrast, the dryland wheat had insignificant increase in aboveground biomass following anthesis and showed a sharp decrease in LAI and percent canopy cover due to late season water deficit stress.

4.3.4. Physiological and environmental determinants of wheat grain yield

The concept of coarse and fine regulators of wheat yield (i.e. kernels per m^{-2} as coarse regulator and individual kernel weight as fine regulator) was proposed by Slafer et al. (2014). Pooled across the whole dataset, number of kernels per m^{-2} explained a similar proportion of the variation in wheat grain yield ($r^2 = 0.42$, $p < 0.001$) as that explained by individual kernel weight ($r^2 = 0.43$, $p < 0.001$). Kernel number is a coarse regulator of wheat grain yield because wheat yield grown under non-limiting conditions is often sink-limited during grain filling (Reynolds et al., 2005). Thus, increasing kernels m^{-2} increases wheat sink strength, leading to greater yields (Fischer, 2007). Individual kernel weight was also an important determinant of grain yield in our study, most likely as result of measured kernel weight being well below the genetic potential due to heat and water stresses experienced during the grain filling period, typical in the southern Great Plains.

In the next few paragraphs we extrapolated the analysis of Slafer et al. (2014) from plant components to weather variables to understand how the observed weather during the growing season dictated record breaking yields in the southern Great Plains. The contrasting weather between the 2012-13 and the 2013-14 growing seasons allowed for assessment of coarse and fine regulators of wheat yield by comparing dryland and irrigated crop development, respectively. Coarse regulators of grain yield were determined studying weather variables that led to yields ranging from about 3.06 Mg ha^{-1} (dryland experiments 2013-14) to 7.11 Mg ha^{-1} (dryland experiments 2012-13). Fine regulators of wheat yield were assessed examining weather variables that led to yields ranging from 6.67 Mg ha^{-1} during the 2012-13 growing season to 7.68 Mg ha^{-1} in the irrigated trials during 2013-14.

Precipitation was the greatest driver for dryland wheat yields throughout the studied site-years. Across all dryland experiments, precipitation was positively and linearly associated with grain yields ($r^2 = 0.77$, $p < 0.01$), and variation in precipitation amount led to yields ranging from 3.06 Mg ha^{-1} to over 7.11 Mg ha^{-1}. Precipitation is therefore considered a coarse regulator of wheat yield under dryland management. Photothermal quotient (PQ, ratio of R_s over average temperature, Nix (1976)) during the 31-d period preceding anthesis was also positive and linearly associated with dryland wheat yields ($r^2 = 0.71$, $p < 0.05$), and there was no collinearity between precipitation and PQ ($r^2 = 0.16$, $p > 0.2$). The 31-d period immediately prior to anthesis is characterized by great partitioning of assimilates to spike formation (Slafer et al., 1990) as well as formation of the flag and penultimate leaves, the two most important leaves responsible for photosynthate production during wheat grain fill (Frederick and Bauer, 2000). Thus, the weather during this period influences kernels m^{-2}, and consequently grain yields (Fischer, 2007; Frederick and Bauer, 2000). Neither R_s nor T_{max}, T_{min}, or T_{ave} during the grain filling period, were linearly related to dryland grain yields ($r^2 < 0.24$, $p > 0.17$).

Fine regulators of grain yield were assessed using data from the highest-yielding dryland environment (Chickasha 2012-13) and the irrigated experiments during both 2012-13 and 2103-14 growing seasons. The Stillwater irrigated treatment during the 2012-13 growing season was not included in the analyses due to severe lodging. Total precipitation plus supplemental irrigation were not linearly associated with grain yields ($r^2 = 0.01$, $p = 0.89$), so the confounding factor water deficit stress was removed from this analysis. In the absence of water deficit stress, both average R_s and T_{max} during the anthesis - physiological maturity period were positive and linearly associated with grain yield ($r^2 > 0.89$, $p < 0.05$). However, the collinearity between T_{max} and R_s ($r^2 = 0.78$, $p < 0.001$) hinders our ability to separate the individual effects of each on wheat yield within our dataset. Increased temperatures during the reproductive stages of wheat often have negative effect on kernel weight and grain yield (Calderini et al., 1999a; Calderini et al.,

1999b; Fischer, 2007; Wiegand and Cuellar, 1981). On the other hand, increased R_s during the same period can result in increased kernel weight (Wardlaw, 1994), as 70 to 90% of the kernel weight comes from photosynthates produced during grain fill (Frederick and Bauer, 2000). Thus, despite the unclear separation between T_{max} and R_s in our analysis, coupling our data with a wealth of literature on the subject allows us to identify R_s during the anthesis – physiological maturity interval as a fine regulator of wheat yields in the absence of water limitation.

4.3.5. Radiation-use efficiency and water use-efficiency

Maximum RUE measured during the spring ranged from 1.4 to 1.8 g MJ^{-1} during the 2012-13 growing season and from 0.8 to 1.9 g MJ^{-1} during the 2013-14 growing season (Table 4.4). The highest RUE (1.7 and 1.9 g MJ^{-1}) were measured in the irrigated experiments in 2013-14. Drought stress significantly reduced RUE, which ranged from 0.8 to 1.1 g MJ^{-1} in the dryland experiments in 2013-14 Seasonal RUE was lower than maximum RUE mostly due to the long period winter wheat is subjected to cold stress during fall and winter, and due to a decrease in RUE towards physiological maturity. As a result, seasonal RUE ranged from 0.7 to 1.1 g MJ^{-1} in 2012-13 and from 0.6 to 1.1 g MJ^{-1} in 2013-14. Lower seasonal RUE for wheat when compared to the jointing – anthesis phase has been previously reported (Acreche et al., 2009). The maximum RUE measured in our experiments across both growing seasons were in the upper range of maximum RUE values reported in the literature, which ranged from 0.7 to 1.8 g MJ^{-1}, with an average of 1.3 g MJ^{-1} (Supplemental Table S1). The RUE values reported in Supplemental Table S1 were selected as the greatest RUE reported among several treatments and site-years for 36 independent manuscripts and converted to incident R_s basis as described in Sinclair and Muchow (1999). The greatest reported wheat RUE to date was 1.8 g MJ^{-1} and resulted in aboveground biomass of 20 Mg ha^{-1} and grain yields of 8 Mg ha^{-1} in Tunisia (Latiri-Souki et al., 1998), similar to our results. A 1.7 g MJ^{-1} RUE was reported in an irrigated

experiment in southern Italy (Albrizio and Steduto, 2005), and the remaining RUE were considerably lower than the maximum RUE values we report.

In order to calculate wheat WUE, seasonal ET_c was derived from a soil water balance from neutron probe data. Seasonal I_c ranged from 16 to 38 mm under dryland management, and from 28 to 47 mm under irrigation; whereas seasonal ET_c ranged from 440 to 757 mm in the 2012-13 growing season, and from 304 to 766 mm in the 2013-14 growing season (Table 4.4). The highest ET_c were measured in the irrigated treatments, where management strived to avoid water deficit stress and supplemental irrigation increased the consumption of PAW stored in the profile at time of sowing. Providing 78 mm of irrigation increased seasonal ET_c by 196 mm at Perkins; and providing 168 mm of irrigation increased seasonal ET_c by 219 mm at Stillwater during the 2012-13 growing season. During the 2013-14 growing season, irrigated wheat at Stillwater and Perkins had seasonal ET_c ranging between 758 and 766 mm, which were greater than the ET_c measured in the dryland treatments (304 to 409 mm; Table 4.4). Strong correlations existed between seasonal ET_c and aboveground biomass ($r^2 = 0.96$, $p < 0.0001$) or grain yield ($r^2 = 0.86$, $p < 0.001$).

Water use efficiency (WUE) was calculated as the ratio of grain yield to seasonal ET_c and ranged from 7.8 to 12.6 kg ha^{-1} mm^{-1} during the 2012-13 growing season and from 8.5 to 10.1 kg ha^{-1} mm^{-1} during the 2013-14 growing season (Table 4.4). These WUE values are close to, or above, most of the studies published for wheat grown in the southern Great Plains (Fig. 4.4). Data collected from five studies across TX and KS, as well as data reported in our research, indicates that average WUE increases with increased grain yields and follows a similar trend to the quadratic response reported by Musick et al. (1994). Analysis of the residuals between the data we report and the modeled WUE for the same yield levels based on the model developed by Musick et al. (1994) resulted in average residual of 1.06 kg ha^{-1} mm^{-1}, indicating that the intensive management of winter wheat in central Oklahoma led to WUE values slightly above the

WP reported by Musick et al. (1994) for a similar yield level (Fig. 4.4). Still, the WUE values we report are well below maximum wheat WUE values derived from boundary functions analysis between seasonal water supply and grain yield which generally lies around 16-22 kg ha^{-1} mm^{-1} (Passioura, 2006; Patrignani et al., 2014; Sadras and Angus, 2006). Boundary function analysis originates from only the most efficient observations of yield at given amount of water supply. This indicates that although the intensive management we provided slightly increased wheat WUE when compared to average management (Fig. 4.4), it is still well below the maximum wheat WUE possible for those levels of water supply.

4.4. CONCLUSIONS

While our hypothesis that maximum wheat yields in the southern Plains could reach values similar to those measured in other parts of the world was not supported by the data, our research provides empirical evidence for wheat yields as high as 7.68 Mg ha^{-1} when grown under non-limiting conditions, which is similar to the maximum ever reported wheat yield in Texas and higher than any reported yield in Oklahoma. The differences between maximum yields in the southern Great Plains and those achieved in the United Kingdom or New Zealand are likely due to lower incident R_s and higher temperatures during the anthesis – physiological maturity interval, a shorter and warmer grain filling period resulting in low HI, as well as a greater protein concentration in hard red winter wheat grown in the southern Great Plains relative to feed wheat (New Zealand) or soft wheat (United Kingdom) classes. Additionally, we provide empirical evidence for maximum RUE of 1.9 g MJ^{-1} and seasonal WUE of 12.6 kg ha^{-1} mm^{-1}. Grain yield and RUE values from our study are among the highest reported parameter values for the southern Great Plains, and RUE is close to the highest reported in the world literature. Wheat WUE was still well below values derived from boundary function analysis. We established that total seasonal precipitation, as well as PQ in the 31-d prior to anthesis, act as coarse regulators of wheat yield in the southern Great Plains, inducing yield differences from 3.06 to 7.11 Mg ha^{-1}.

Incident R_s during the reproductive phase induced differences in grain yield from 6.67 to 7.68 Mg ha^{-1} and was denominated a fine regulator of wheat grain yields in the absence of water deficit stress. To our knowledge, this is the first complete assessment of winter wheat grown under non-limiting conditions in the southern Great Plains.

4.5. REFERENCES

Acreche, M.M., G. Briceno-Felix, J.A.M. Sanchez and G.A. Slafer. 2009. Radiation interception and use efficiency as affected by breeding in Mediterranean wheat. Field Crops Res. 110: 91-97.

Acreche, M.M. and G.A. Slafer. 2009. Variation of grain nitrogen content in relation with grain yield in old and modern Spanish wheats grown under a wide range of agronomic conditions in a mediterranean region. J. Agric. Sci. 147: 657-667.

Albrizio, R. and P. Steduto. 2005. Resource use efficiency of field-grown sunflower, sorghum, wheat and chick-pea.I. Radiation use efficiency. Agric. For. Meteorol. 130: 254-268.

Allen, R.G., L.S. Pereira, D. Raes and M. Smith. 1998. Crop evapotranspiration: Guidelines for computing crop water requirements. Irrigation and Drainage Paper No. 56, FAO, Rome, Italy.

Amir, J. and T.R. Sinclair. 1991. A model of water limitation on spring wheat growth and yield. Field Crops Res. 28: 59-69.

Armour, T., P. Jamieson, A. Nichols and R. Zyskowski. 2004. Breaking the 15 t/ha wheat yield barrier: A discussion. In: Proceedings of the 4th Intern. Crop Sci. Congress, Brisbaine, Australia. Sept. 26 - Oct. 1.

Barraclough, P.B., J.R. Howarth, J. Jones, R. Lopez-Bellido, S. Parmar, C.E. Shepherd, et al. 2010. Nitrogen efficiency of wheat: Genotypic and environmental variation and prospects for improvement. Eur. J. Agron. 33: 1-11.

Calderini, D.F., L.G. Abeledo, R. Savin and G.A. Slafer. 1999a. Effect of temperature and carpel size during pre-anthesis on potential grain weight in wheat. J. Agric. Sci. 132: 453-459.

Calderini, D.F., L.G. Abeledo, R. Savin and G.A. Slafer. 1999b. Final grain weight in wheat as affected by short periods of high temperature during pre- and post-anthesis under field conditions. Aust. J. Plant Physiol. 26: 453-458.

Campbell., G.S. and R. Diaz. 1988. Simplified soil-water balance models to predict crop transpiration. ICRISAT: Patancheru, India.

Connor, D.J., R.S. Loomis and K.G. Cassman. 2011. Crop ecology: Productivity and management in agricultural systems. Cambridge Univ. Press, Cambridge, UK.

Curtis, B., S. Rafaram and G. Macpherson. 2002. Wheat in the world. Bread wheat: Improvement and production. FAO Plant Prod. and Protec. Series. Food Agric. Org. Unit. Nations, Rome, Italy.

Danielson, R., P. Sutherland and A. Klute. 1986. Porosity. Methods of soil analysis. Part 1. Physical and mineralogical methods: 443-461.

Decker, J.E., F.M. Epplin, D.L. Morley and T.F. Peeper. 2009. Economics of five wheat production systems with no-till and conventional tillage. Agron. J. 101: 364-372.

Edwards, J.T. 2013. Iba. Okla. St. Univer. Ext. Facts L-416, Okla. St. Univer. Coop. Ext. Serv., Stillwater, OK.

Edwards, J.T., B.F. Carver, G.W. Horn and M.E. Payton. 2011. Impact of dual-purpose management on wheat grain yield. Crop Sci. 51: 2181-2185.

Edwards, J.T., R.D. Kochenower, R.E. Austin, M.K. Inda, B.F. Carver, R.M. Hunger, et al. 2007. Oklahoma small grains variety performance tests 2006-2007. Okla. St. Univ. Depart. Plant soil sci. Prod. Tech. Rep. Pt-2007-6.

Evans, L.T. and R.A. Fischer. 1999. Yield potential: Its definition, measurement, and significance. Crop Sci. 39: 1544-1551.

Evett, S.R., J.A. Tolk and T.A. Howell. 2003. A depth control stand for improved accuracy with the neutron probe. Vadose Zone Journal 2: 642-649.

Fischer, R.A. 2007. Understanding the physiological basis of yield potential in wheat. J. Agric. Sci. 145: 99-113.

Fischer, R.A. and G.O. Edmeades. 2010. Breeding and cereal yield progress. Crop Sci. 50: S85-S98.

Frankenberger, J.R., S. Dun, D.C. Flanagan, J.Q. Wu and W.J. Elliot. 2011. Development of a GIS interface for WEPP model application to Great Lakes forested watersheds. In: D. C. Flanagan, J. C. Ascough II and J. L. Nieber, Eds., Proceedings of the International Symposium on Erosion and Landscape Evolution (ISELE). ISELE paper no. 11139, ASABE, September 18-21, 2011, Anchorage, AK.

Frederick, J.R. and P.J. Bauer. 2000. Physiological and numerical components of wheat yield. In: E. H. Satorre and G. A. Slafer, Eds., Wheat: Ecology and physiology of yield determination. Food Products Press, Binghamton, NY. p. 503.

Hay, R. and J. Porter. 2006. The physiology of crop yield. 2nd ed. Ed. Blackwell Publishing, Oxford, UK.

Karcher, D.E. and M.D. Richardson. 2005. Batch analysis of digital images to evaluate turfgrass characteristics. Crop Sci. 45: 1536-1539.

Latiri-Souki, K., S. Nortcliff and D.W. Lawlor. 1998. Nitrogen fertilizer can increase dry matter, grain production and radiation and water use efficiencies for durum wheat under semi-arid conditions. Eur. J. Agron. 9: 21-34.

Ludlow, M. and R. Muchow. 1990. A critical evaluation of traits for improving crop yields in water-limited environments. Adv. Agron. 43: 107-153.

Muchow, R.C. and T.R. Sinclair. 1994. Nitrogen response of leaf photosynthesis and canopy radiation use efficiency in field-grown maize and sorghum. Crop Sci. 34: 721-727.

Munier-Jolain, N.G. and C. Salon. 2005. Are the carbon costs of seed production related to the quantitative and qualitative performance? An appraisal for legumes and other crops. Plant Cell Environ. 28: 1388-1395.

Musick, J.T., O.R. Jones, B.A. Stewart and D.A. Dusek. 1994. Water-yield relationships for irrigated and dryland wheat in the US Southern Plains. Agron. J. 86: 980-986.

Nix, H. 1976. Climate and crop productivity in Australia. In: S. Yoshida, Ed. Climate and rice. IRRI, Los Baños, Philippines. p. 495-507.

Passioura, J. 2006. Increasing crop productivity when water is scarce - from breeding to field management. Agric. Water Manage. 80: 176-196.

Patrignani, A., C.B. Godsey, T.E. Ochsner and J.T. Edwards. 2012. Soil water dynamics of conventional and no-till wheat in the southern Great Plains. Soil Sci. Soc. Am. J. 76: 1768-1775.

Patrignani, A., R.P. Lollato, T.E. Ochsner, C.B. Godsey and J. Edwards. 2014. Yield gap and production gap of rainfed winter wheat in the southern Great Plains. Agron. J. 106: 1329 - 1339.

Peake, A.S., N.I. Huth, P.S. Carberry, S.R. Raine and R.J. Smith. 2014. Quantifying potential yield and lodging-related yield gaps for irrigated spring wheat in sub-tropical Australia. Field Crops Res. 158: 1-14.

Purcell, L.C. 2000. Soybean canopy coverage and light interception measurements using digital imagery. Crop Sci. 40: 834-837.

Ratliff, L.F., J.T. Ritchie and D.K. Cassel. 1983. Field-measured limits of soil-water availability as related to laboratory-measured properties. Soil Sci. Soc. Am. J. 47: 770-775.

Raun, W.R., J.B. Solie and M.L. Stone. 2011. Independence of yield potential and crop nitrogen response. Prec. Agric. 12: 508-518.

Reynolds, M.P., A. Pellegrineschi and B. Skovmand. 2005. Sink-limitation to yield and biomass: A summary of some investigations in spring wheat. Ann. Appl. Biol. 146: 39-49.

Sadras, V.O. and J.F. Angus. 2006. Benchmarking water-use efficiency of rainfed wheat in dry environments. Aust. J. Agric. Res. 57: 847-856.

Shearman, V.J., R. Sylvester-Bradley, R.K. Scott and M.J. Foulkes. 2005. Physiological processes associated with wheat yield progress in the UK. Crop Sci. 45: 175-185.

Sinclair, T.R. 2006. A reminder of the limitations in using Beer's law to estimate daily radiation interception by vegetation. Crop Sci. 46: 2343-2347.

Sinclair, T.R. 2013. Transpiration: Moving from semi-empirical approaches to first principles. In: D. Fleisher, Ed. Symposium - Improving tools to assess climate change effects on crop

response: Modeling approaches and applications: I. Am. Soc. Agron., Crop Sci. Soc. Am., and Soil Sci. Soc. Am., Tampa, FL. Available at: https://dl.sciencesocieties.org/publications/meetings/2013am/11501 (verified 01 April 2015).

Sinclair, T.R. and R.C. Muchow. 1999. Radiation use efficiency. Adv. Agron. 65: 215-265.

Slafer, G.A., F.H. Andrade and E.H. Satorre. 1990. Genetic-improvement effects on preanthesis physiological attributes related to wheat grain-yield. Field Crops Res. 23: 255-263.

Slafer, G.A., R. Savin and V.O. Sadras. 2014. Coarse and fine regulation of wheat yield components in response to genotype and environment. Field Crops Res. 157: 71-83.

Snape, J., V. Hyne and K. Aitken. 1993. Targeting genes in wheat using marker mediated approaches. Proceedings of the 8th Intern. Wheat Gen. Symp.: 749-759.

Soltani, A. and T.R. Sinclair. 2012. Modeling physiology of crop development, growth and yield. CAB International, Cambridge, MA.

Tanner, C.B. and T.R. Sinclair. 1983. Efficient water use in crop production: Research or re-search? In: H. M. Taylor, W. R. Jordan and T. R. Sinclair, Eds., Limitations to efficient water use in crop production. ASA-CSSA-SSSA, Madison, WI. p. 1-27.

True, R.R., F.M. Epplin, E.G. Krenzer and G.W. Horn. 2001. A survey of wheat production and wheat forage use practices in Oklahoma. B-815. Okla. Coop. Ext. Serv., Stillwater, OK.

USDA-NASS. 2014. United States Department of Agriculture. National Agricultural Statistics Service. Available at: http://www.nass.usda.gov/Statistics_by_State/Oklahoma/Publications/County_Estimates/index.asp (data retrieved July 2014).

Van Roekel, R.J. and L.C. Purcell. 2014. Soybean biomass and nitrogen accumulation rates and radiation use efficiency in a maximum yield environment. Crop Sci. 54: 1189-1196.

Wardlaw, I.F. 1994. The effect of high-temperature on kernel development in wheat - variability related to pre-heading and postanthesis conditions. Aust. J. Plant Physiol. 21: 731-739.

Wiegand, C.L. and J.A. Cuellar. 1981. Duration of grain filling and kernel weight of wheat as affected by temparature. Crop Sci. 21: 95-101.

Yang, H.S., A. Dobermann, J.L. Lindquist, D.T. Walters, T.J. Arkebauer and K.G. Cassman. 2004. Hybrid-maize - a maize simulation model that combines two crop modeling approaches. Field Crops Res. 87: 131-154.

Table 4.1. Description of soil fertility and physical properties for five experimental sites in central Oklahoma. Soil type, pH, extractable phosphorus (P), potassium (K), calcium (Ca), magnesium (Mg), are representative of the 0 – 45 cm layer, and fraction of sand and clay, volumetric water content at saturation (θ_S), at drained upper limit (θ_{DUL}), at and lower limit (θ_{LL}), bulk density (ρ_b), and available water holding capacity (AWHC) are representative of the 0 – 120 cm layer. Physical properties are average of six 20-cm soil layers (0 – 120 cm) and four replications.

Site	Soil type†	pH‡	P	K	Ca	Mg	Sand	Clay	θ_S§	θ_{DUL}¶	θ_{LL}#	ρ_b	AWHC††
			mg kg^{-1}				g kg^{-1}			m^3 m^{-3}		Mg m^{-3}	mm
Chickasha	Haplustoll	7.9	44	164	1931	396	230	171	0.48	0.27	0.07	1.37	234
Lahoma	Argiustoll	5.7	37	241	1365	363	348	243	0.43	0.28	0.14	1.52	179
Perkins Irrigated	Argiustoll	5.8	88	99	940	219	571	164	0.40	0.26	0.10	1.60	197
Perkins Dryland	Argiustoll	5.8	23	101	1085	301	606	164	0.41	0.24	0.09	1.57	173
Stillwater	Paleustoll	6.0	77	161	1786	436	270	319	0.39	0.31	0.18	1.61	153

† - USDA, Soil Conservation Service.

‡ - Soil pH (1:1 soil/water ratio).

§ - volumetric soil water content at saturation (subtraction of the ratio soil bulk density over particle density from a unit).

¶ - volumetric soil water content at the drained upper limit (determined by saturating the soil in the field for several consecutive weeks and waiting for drainage to cease).

- volumetric soil water content at the lower limit (pressure plate methodology).

†† - The sum of soil water content between θ_{DUL} and θ_{LL} for each layer multiplied by the layer's length (20 cm) summed for the entire 120-cm depth represents available water holding capacity of the root zone (AWHC, 0 - 120 cm).

Table 4.2. Dates of planting, emergence, anthesis, physiological maturity, and harvest at the seven dryland and four irrigated site-years in central Oklahoma.

Management	Site	Growing season	Day of Year				
			Planting	Emergence	Anthesis	Maturity	Harvest
Dryland	Chickasha	2012-2013	292	300	117	157	163
		2013-2014	295	307	119	149	164
	Lahoma	2012-2013	279	289	136	167	175
	Perkins	2012-2013	291	300	116	160	176
		2013-2014	284	295	115	144	162
	Stillwater	2012-2013	293	302	120	164	177
		2013-2014	284	293	116	147	166
Irrigated	Perkins	2012-2013	291	300	121	168	176
		2013-2014	284	295	118	154	162
	Stillwater	2012-2013	279	289	122	169	177
		2013-2014	284	293	119	157	166

Table 4.3. Cumulative precipitation and mean values for incident solar radiation (R_s), maximum temperature (T_{max}), minimum temperature (T_{min}), and relative humidity (R.H.) during the 2012-13 and 2013-14 growing seasons at the study locations in central Oklahoma. Departure from the 17-year mean (1997 – 2014) are shown in parenthesis.

Growing Season	Site	Season	Precipitation	R_s	T_{max}	T_{min}	R.H.
			mm	MJ m^{-2} d^{-1}	°C		%
2012-13	Chickasha	Fall†	22 (-16)	13.5 (-0.8)	20.6 (-3.1)	3.1 (-6.4)	63.8 (-6.3)
		Winter‡	133 (+20)	10.8 (+0.4)	12.1 (+0.7)	-2 (+0.2)	71.5 (+0.9)
		Spring§	432 (+191)	20 (+0.9)	21.9 (-0.7)	8.3 (-0.7)	70 (+1.7)
	Lahoma	Fall	13 (-21)	14 (-0.3)	20.6 (-1.8)	3.9 (-5.3)	57.2 (-12.5)
		Winter	107 (+17)	11.1 (+0.8)	10. 3 (+1)	-3.3 (-0.3)	66.6 (-4.7)
		Spring	253 (+33)	20.4 (+1)	21.6 (+0.5)	8.4 (+0.6)	69.8 (-0.2)
	Perkins	Fall	17 (-33)	12.6 (-1.1)	20 (-2.9)	4 (-6.3)	54 (-12.8)
		Winter	144 (+31)	9.9 (0)	11.6 (+1.2)	-1.2 (+0.3)	65.1 (-3.2)
		Spring	425 (+140)	18.9 (+0.2)	21.8 (0)	10 (+0.6)	68.4 (+1.8)
	Stillwater	Fall	11 (-34)	12.6 (-1)	19.9 (-3.2)	2.7 (-6.7)	56.3 (-11.3)
		Winter	115 (+3)	10.1 (+0.5)	11.8 (+1.2)	-2.4 (+0.1)	65 (-3.4)
		Spring	416 (+130)	19.1 (+0.7)	22.1 (+0.1)	9.8 (+0.9)	67.1 (+0.5)
2013-14	Chickasha	Fall	37 (-1)	10.2 (-4.1)	14.1 (-9.5)	1.8 (-7.6)	70.1 (0)
		Winter	45 (-68)	11.1 (+0.7)	9.7 (-1.7)	-5.2 (-3)	66.9 (-3.6)
		Spring	247 (+5)	21.6 (+2.5)	23.6 (+1)	8.5 (-0.5)	62.6 (-5.8)
	Perkins	Fall	36 (-14)	10.1 (-3.7)	15.2 (-7.7)	3.6 (-6.7)	67.8 (+1)
		Winter	35 (-77)	10.2 (+0.3)	8.7 (-1.7)	-4.4 (-2.9)	64.3 (-3.9)
		Spring	246 (-39)	21 (+2.3)	23.1 (-0.6)	8.9 (-0.6)	60.5 (-6.1)
	Stillwater	Fall	49 (+4)	10.2 (-3.4)	15.5 (-7.6)	2.9 (-6.4)	67.8 (+0.1)
		Winter	29 (-83)	10.4 (+0.7)	8.7 (-1.9)	-5.4 (-3)	64.6 (-3.7)
		Spring	195 (-91)	21.1 (+2.6)	23.5 (+1.5)	8.9 (-0.3)	60.2 (-6.5)

† - Fall encompasses the period from planting date until November 30th

‡ - Winter encompasses the months of December, January, and February

§ - Spring encompasses the period between March 1st and harvest date

Table 4.4. Least square means for aboveground dry matter at physiological maturity (Dry biomass), harvest index (HI), grain yield, spikes m^{-2}, kernels m^{-2}, individual kernel weight, grain protein concentration, crop evapotranspiration (ET_c), interception by the canopy (I_c), maximum and seasonal radiation use efficiencies (RUE), and water use-efficiency (WUE) for the 2012-13 and 2013-14 growing seasons. Grain yield and protein concentration are reported in 135 g kg^{-1} water basis. Significances of sources of variation are shown.

Growing season	Location	Dry biomass	HI	Yield	Spikes m^{-2}	Kernels m^{-2}	Kernel Wt.	Protein concentration	ET_c †	I_c‡	Max. RUE§	Seasonal RUE	WUE¶
2012-2013		Mg ha^{-1}		Mg ha^{-1}		x 10 3	mg	g kg^{-1}	mm		g MJ^{-1}		kg ha^{-1} mm^{-1}
	Chickasha	19.6 A#	0.36 AB	7.11 A	807 C	16.7 B	31.6 B	124 B	684 B	37 C	1.6	0.8 BC	10.4 BC
	Lahoma	14.0 C	0.40 A	5.53 C	764 C	15.1 B	29.6 BC	120 B	440 D	32 D	1.4	0.7 C	12.6 A
	Perkins I.††	19.0 A	0.35 AB	6.67 AB	808 C	15.4 B	35.6 A	112 C	721 AB	47 A	1.6	0.8 BC	9.4 CD
	Perkins D.‡‡	15.8 B	0.37 A	5.78 C	740 C	16.4 B	27.6 CD	144 A	525 C	38 B	1.4	0.8 B	11.0 AB
	Stillwater I.§§	19.1 A	0.31 B	5.92 C	1272 A	21.8 A	27.0 CD	120 B	757 A	50 A	1.8	0.9 B	7.8 D
	Stillwater D.	16.5 B	0.40 A	6.50 B	948 B	20.5 A	24.9 D	125 B	538 C	37 C	1.7	1.1 A	11.2 AB
	Source of variation												
	Location	***	*	***	***	***	***	***	***	***	ns	***	***
2013-2014													
	Chickasha	13.2 B	0.30 B	3.45 B	860 C	15.5 B	25.7 C	15.2 A	397 B	16 C	1.1 B	0.8 C	8.7 B
	Perkins I.	20.4 A	0.41 A	7.42 A	1020 AB	21.2 A	37.8 A	117 B	766 A	28 A	1.7 A	1.1 A	9.7 A
	Perkins D.	9.9 C	0.33 B	3.06 B	757 C	12.1 C	29.4 B	145 A	304 C	21 B	0.8 C	0.6 D	10.1 A
	Stillwater I.	20.5 A	0.38 A	7.68 A	1051 A	21.7 A	37.0 A	116 B	758 A	28 A	1.9 A	0.9 B	10.1 A
	Stillwater D.	12.2 B	0.29 B	3.43 B	892 BC	13.4 BC	27.1 C	155 A	409 B	23 B	0.8 C	0.7 D	8.4 B
	Source of variation												
	Location	***	**	***	**	***	***	***	***	***	***	***	**

*, **, and *** - significant at $p < 0.05$, 0.01, and 0.001, respectively.

ns - non-significant.

† - Seasonal crop evapotranspiration, determined from a water balance from neutron probe data.

‡ - Canopy precipitation interception, determined as a product of fractional interception derived from leaf area index (Campbell and Diaz, 1988).

§ - Maximum radiation use efficiency, calculated as the slope of the relationship between aboveground biomass and cumulative intercepted radiation (Muchow and Sinclair, 1994) using data collected during the spring.

¶ -Water use-efficiency, calculated as the ratio grain yield over cumulative evapotranspiration (ET_c).

- Different letters within a column and year denote that means differed ($\alpha = 0.05$) as determined by a Tukey test.

†† - I., irrigated management.

‡‡ - D., dryland management.

§§ - Severe lodging (8 in a 0-10 scale) occurred in Stillwater irrigated during the 2012-13 growing season.

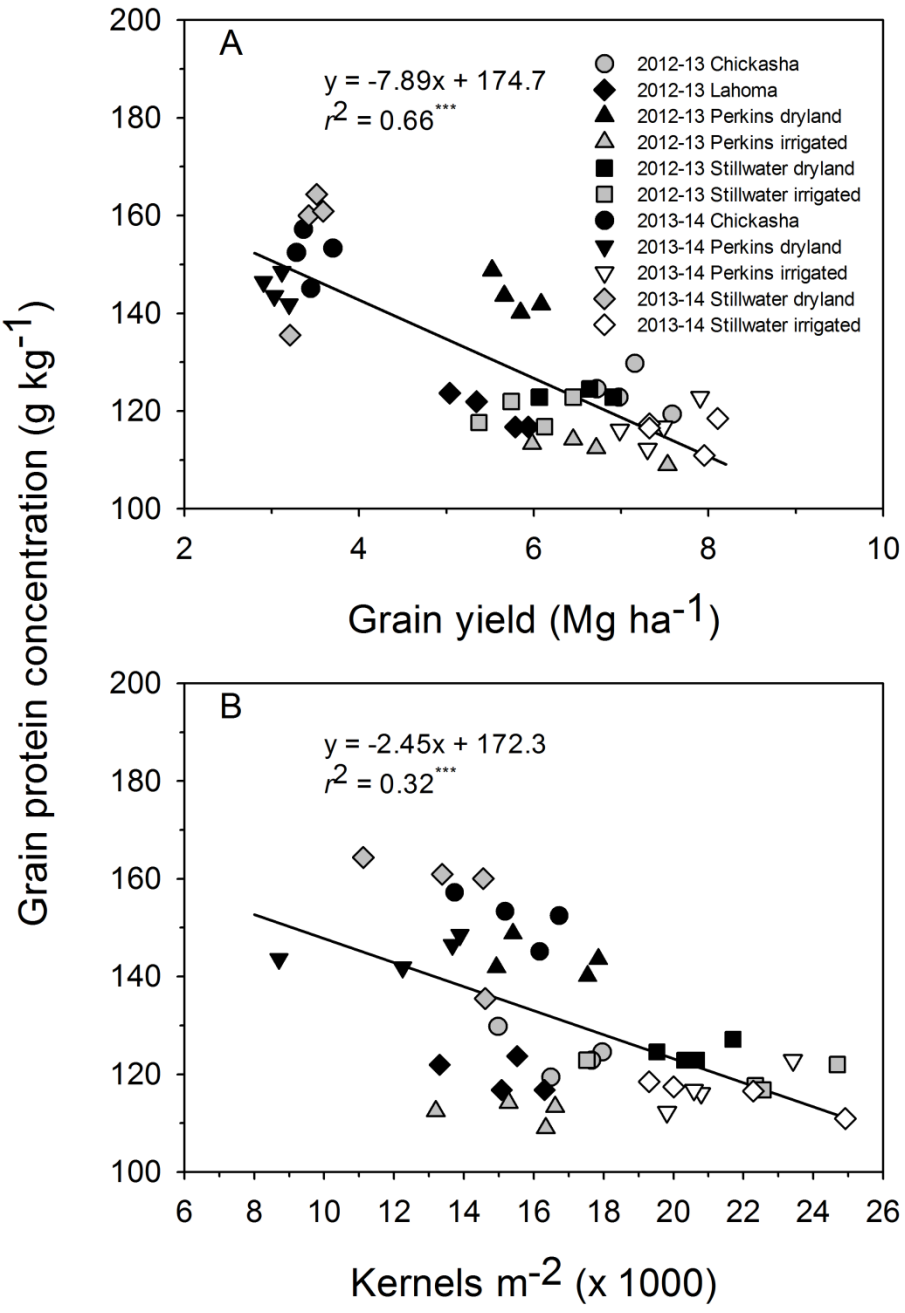

Figure 4.1. Grain protein concentration as function of (A) grain yield and (B) kernels m^{-2} for winter wheat grown under non-limiting conditions on eleven site-years in central Oklahoma during the 2012-13 and 2013-14 growing seasons. Grain protein concentration and grain yield are reported in a 13.5% moisture basis.

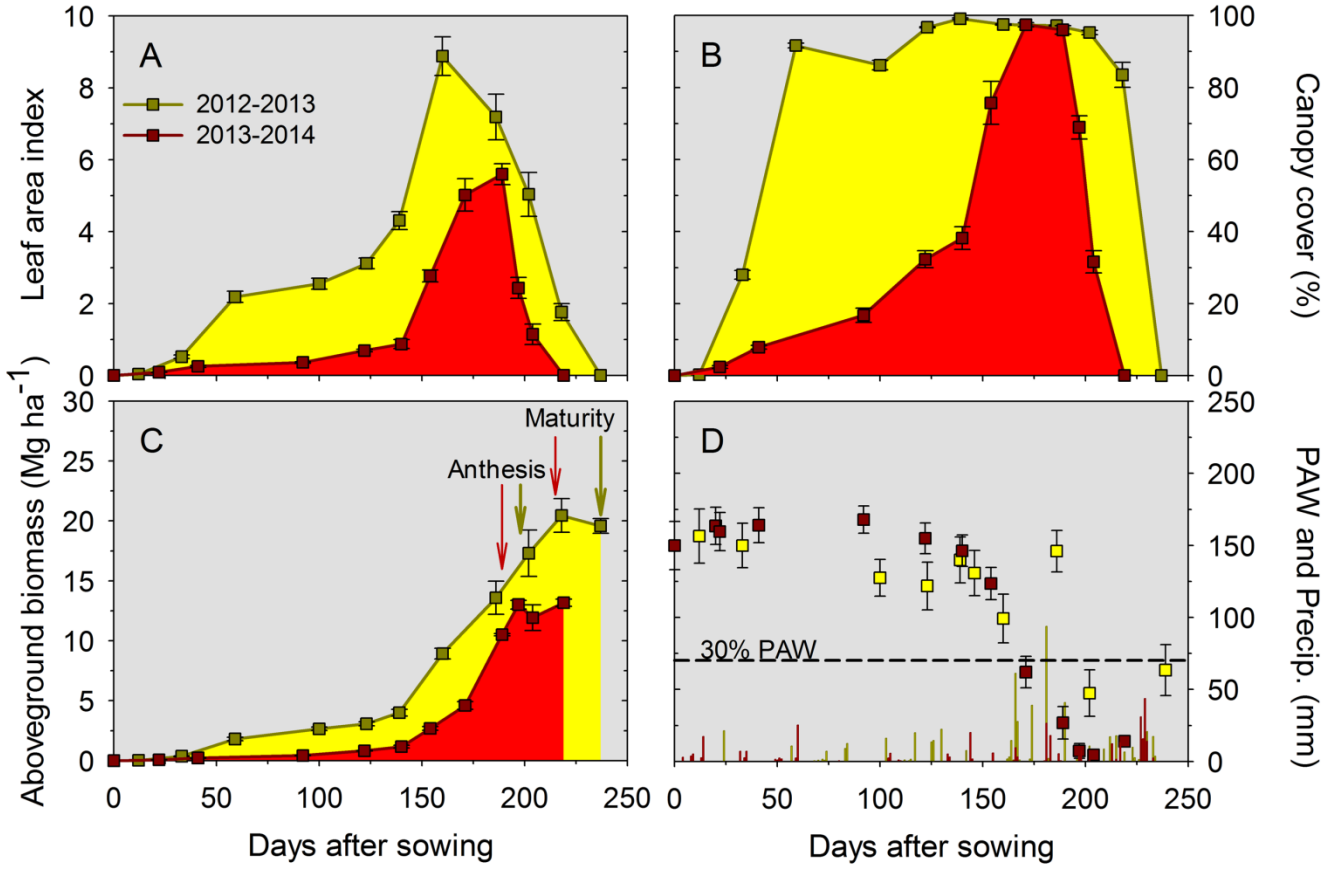

Figure 4.2. Dynamics of (A) leaf area index, (B) percent canopy cover, (C) aboveground biomass and dates for anthesis and physiological maturity, and (D) plant available water (PAW, scatter plots), precipitation (Precip., vertical bars), and drought threshold indicated as 30% PAW (dashed line) during the 2012-13 (yellow) and 2013-14 (red) growing seasons for winter wheat grown under non-limiting conditions at Chickasha, OK. Error bars are standard error of the mean.

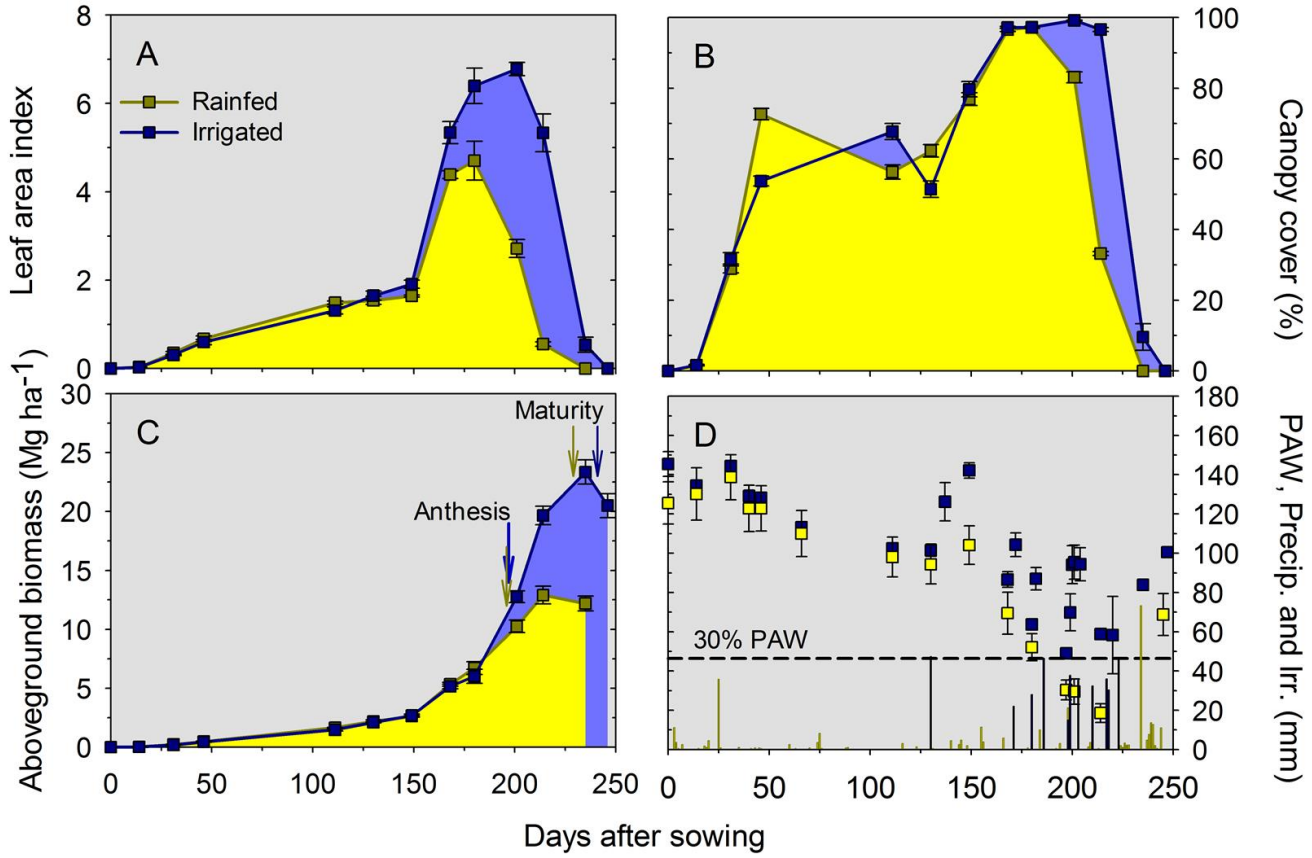

Figure 4.3. Dynamics of (A) leaf area index, (B) canopy cover, (C) aboveground biomass and dates for anthesis and physiological maturity, and (D) plant available water (PAW, scatter plots), precipitation (Precip., vertical yellow bars), irrigation (Irr., vertical blue bars), and drought threshold indicated as 30% PAW, (dashed line) during

the 2013-14 growing season for irrigated (blue) and dryland (yellow) management for winter wheat grown under non-limiting conditions at Stillwater, OK. Error bars are standard error of the mean.

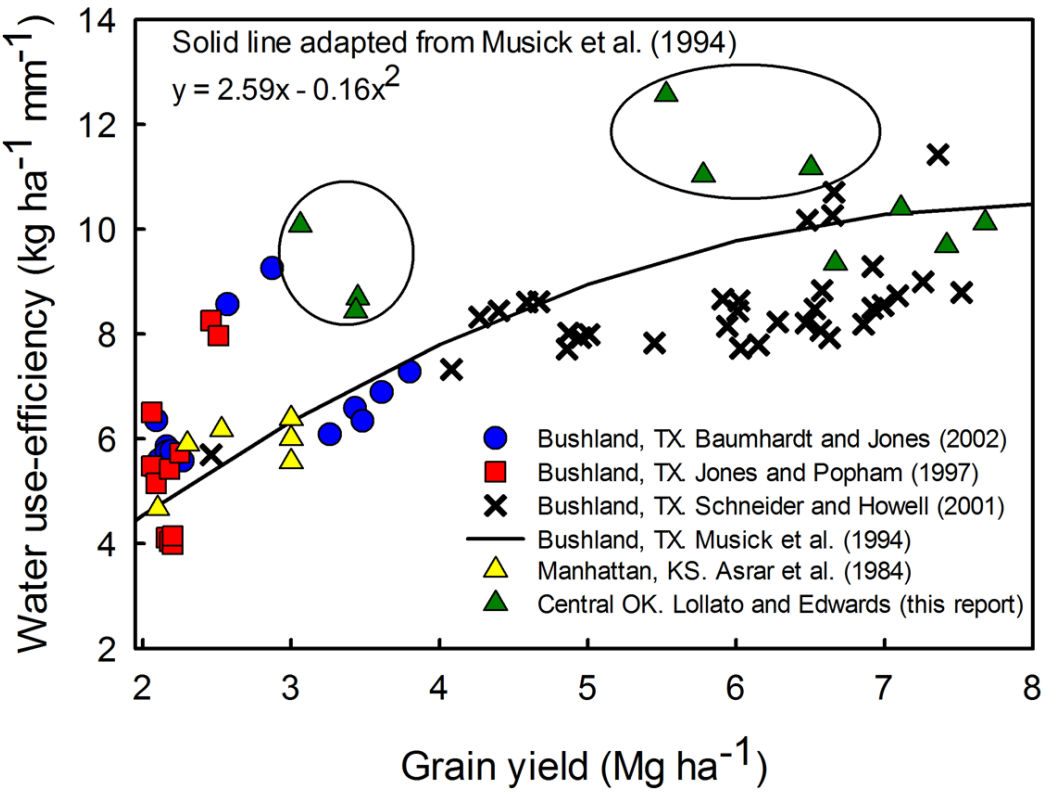

Figure 4.4. Water use-efficiency (WUE) of winter wheat versus grain yield for available literature sources collected in the southern Great Plains (TX, OK, and KS) as well as measurements from the current report during 2012-13 and 2013-14. The solid regression line was reported by Musick et al. (1994) for a comprehensive WUE study in Bushland, TX, and does not represent fit to the datapoints in the figure.

Table S1. Maximum reported values of radiation use efficiency (RUE, g MJ^{-1}) in the literature from a single site-year by source, location, and year of research. Type of RUE is also shown, including intercepted or absorbed, and solar or photosynthetically active radiation (PAR). Reported and converted value of RUE in a cumulative intercepted solar radiation basis is shown.

			Radiation		Maximum RUE	
Source	Year	Location	Intercepted or Absorbed	Solar or PAR†	Reported	Converted‡
Acreche et al. (2009)	2005	Catalonia, Spain	Intercepted	Solar	1.06	1.06
Acreche and Slafer (2009a)	2007	Catalonia, Spain	Intercepted	PAR	1.97	0.99
Albrizio and Steduto (2005)	1998	Valenzano, Italy	Intercepted	Solar	1.7	1.70
Caviglia and Sadras (2001)	1999	Paraná, Argentina	Intercepted	Solar	1.23	1.23
Caviglia et al. (2004)	2000	Balcarce, Argentina	Intercepted	Solar	0.72	0.72
Du et al. (2015)	2013	Jiangsu Province, China	Intercepted	PAR	3.08	1.54
Gallagher and Biscoe (1978)	-	Rothamsted, UK	Absorbed	PAR	3	1.28
Giunta et al. (2009)	2003	Sassari and Oristano, Italy	Intercepted	PAR	2.23	1.12
Heinemann et al. (2006)	2003	Goiás, Brazil	Intercepted	Solar	1.19	1.19
Kiniry et al. (1989) §						
Aase (1978)	1972	Montana, USA	Intercepted	PAR	2.6	1.30
Aase (1978)	1978	Montana, USA	Intercepted	PAR	3.1	1.55
Biscoe and Gallagher (1977)	-	-	Intercepted	PAR	2.7	1.35
Monteith (1977)	-	-	Intercepted	PAR	2.8	1.40
Stapper (1984)	-	Armidale, Australia	Intercepted	PAR	3.1	1.55
Latiri-Souki et al. (1998)	1991	Nabeul, Tunisia	Intercepted	Solar	1.83	1.83
Miralles and Slafer (1997)	1992	Buenos Aires, Argentina	Intercepted	Solar	1.44	1.44
Moreira et al. (2005)	1999	São Paulo, Brazil	Absorbed	PAR	2.66	1.13
Muurinen and Peltonen-Sainio (2006)	2003	Jokioinen, Finland	Intercepted	PAR	2.63	1.32
O'Connell et al. (2004)	1993-1997	Victorian Mallee, Australia	Intercepted	PAR	1.82	0.87
Quanqi et al. (2008)	2005	Shandong, China	Absorbed	PAR	0.75 g mol^{-1}	1.47
Reynolds et al. (2007)	2004	Cd. Obregon, Mexico	Intercepted	PAR	2.09	1.05
Rodriguez and Sadras (2007)	1957-2003	Birchip, Australia	Intercepted	PAR	3	1.50
Rudorff et al. (1996)	1990	Maryland, USA	Absorbed	PAR	3.94	1.61

Source	Year	Location	Radiation		Maximum RUE	
			Intercepted or Absorbed	Solar or PAR†	Reported	Converted‡
Siddique et al. (1989)	1987	Merredin, Australia	Intercepted	PAR	2.97	1.49
Sinclair and Muchow (1999)§						
Calderini et al. (1997)	1991/1992	Buenos Aires, Argentina	Intercepted	Solar	1.25	1.25
Fischer (1993)	1986	Griffith, New South Wales	Absorbed	PAR	3.36	1.51
Garcia et al. (1988)	1982	Texas, USA	Absorbed	PAR	3.82	1.62
Green (1987)	-	Sutton Bonnington, UK	Absorbed	PAR	4.07 mmol hex. mol^{-1}	1.28
Gregory and Eastham (1996)	1992	East Beverley, Australia	Intercepted	PAR	1.68	0.84
Gregory et al. (1992)	1988	East Beverley, Australia	Intercepted	PAR	1.74	0.87
Wilson and Jamieson (1985)	-	Lincoln, New Zealand	Intercepted	PAR	2.38	1.19
Yunusa et al. (1993)	1990	Perth, Australia	Intercepted	PAR	2.93	1.47
van Delden (2001)	1998	Marknesse, The Netherlands	Intercepted	PAR	2.77	1.39
Whitfield and Smith (1989)	1984	Tatura, Australia	Intercepted	Solar	1.45	1.45

† - PAR - Photosynthetically active radiation

‡ - RUE converted to intercepted solar radiation basis as detailed in Sinclair and Muchow (1999)

§ - Review of studies reporting RUE compiled in this manuscript

4.6. SUPPLEMENTAL REFERENCES

Aase, J.K. 1978. Relationship between leaf area and dry-matter in winter wheat. Agron. J. 70: 563-565.

Acreche, M.M., G. Briceno-Felix, J.A.M. Sanchez and G.A. Slafer. 2009. Radiation interception and use efficiency as affected by breeding in Mediterranean wheat. Field Crops Res. 110: 91-97.

Acreche, M.M. and G.A. Slafer. 2009a. Grain weight, radiation interception and use efficiency as affected by sink-strength in mediterranean wheats released from 1940 to 2005. Field Crops Res. 110: 98-105.

Albrizio, R. and P. Steduto. 2005. Resource use efficiency of field-grown sunflower, sorghum, wheat and chick-pea I. Radiation use efficiency. Agric. For. Meteorol. 130: 254-268.

Biscoe, P.V. and J.N. Gallagher. 1977. Weather, dry matter production, and yield. In: J. J. Landsberg and C. V. Cutting, Eds., Environmental effects on crop physiology. Academic London. p. 75-100.

Calderini, D.F., M.F. Dreccer and G.A. Slafer. 1997. Consequences of breeding on biomass, radiation interception and radiation-use efficiency in wheat. Field Crops Res. 52: 271-281.

Caviglia, O.P. and V.O. Sadras. 2001. Effect of nitrogen supply on crop conductance, water- and radiation-use efficiency of wheat. Field Crops Res. 69: 259-266.

Caviglia, O.P., V.O. Sadras and F.H. Andrade. 2004. Intensification of agriculture in the south-eastern Pampas - I. Capture and efficiency in the use of water and radiation in double-cropped wheat-soybean. Field Crops Res. 87: 117-129.

Du, X., B. Chen, T. Shen, Y. Zhang and Z. Zhou. 2015. Effect of cropping system on radiation use efficiency in double-cropped wheat–cotton. Field Crops Res. 170: 21-31.

Fischer, R.A. 1993. Irrigated spring wheat timing and amount of nitrogen fertilizer.2. Physiology of grain yield response. Field Crops Res. 33: 57-80.

Gallagher, J.N. and P.V. Biscoe. 1978. Radiation absorption, growth and yield of cereals. J. Agric. Sci. 91: 47-60.

Garcia, R., E.T. Kanemasu, B.L. Blad, A. Bauer, J.L. Hatfield, D.J. Major, et al. 1988. Interception and use efficiency of light in winter-wheat under different nitrogen regimes. Agric. For. Meteorol. 44: 175-186.

Giunta, F., G. Pruneddu and R. Motzo. 2009. Radiation interception and biomass and nitrogen accumulation in different cereal and grain legume species. Field Crops Res. 110: 76-84.

Green, C.F. 1987. Nitrogen nutrition and wheat growth in relation to absorbed solar-radiation. Agric. For. Meteorol. 41: 207-248.

Gregory, P.J. and J. Eastham. 1996. Growth of shoots and roots, and interception of radiation by wheat and lupin crops on a shallow, duplex soil in response to time of sowing. Aust. J. Agric. Res. 47: 427-447.

Gregory, P.J., D. Tennant and R.K. Belford. 1992. Root and shoot growth, and water and light use efficiency of barley and wheat crops grown on a shallow duplex soil in a Mediterranean-type environment. Aust. J. Agric. Res. 43: 555-573.

Heinemann, A.B., L.F. Stone, A.D. Didonet, M.G. Trindade, B.B. Soares, J.A.A. Moreira, et al. 2006. Eficiência de uso da radiação solar na produtividade do trigo decorrente da adubação nitrogenada. Rev. Bras. Eng. Agric. Amb. 10: 352-356.

Kiniry, J.R., C.A. Jones, J.C. Otoole, R. Blanchet, M. Cabelguenne and D.A. Spanel. 1989. Radiation-use efficiency in biomass accumulation prior to grain-filling for 5 grain-crop species. Field Crops Res. 20: 51-64.

Latiri-Souki, K., S. Nortcliff and D.W. Lawlor. 1998. Nitrogen fertilizer can increase dry matter, grain production and radiation and water use efficiencies for durum wheat under semi-arid conditions. Eur. J. Agron. 9: 21-34.

Miralles, D.J. and G.A. Slafer. 1997. Radiation interception and radiation use efficiency of near-isogenic wheat lines with different height. Euphytica 97: 201-208.

Monteith, J.L. 1977. Climate and efficiency of crop production in Britain. Philos. Trans. Royal Soc. London Ser. B - Biol. Sci. 281: 277-294.

Moreira, M.A., B.F.T. Rudorff, J.C. Felício, J.G. Freitas and M.S. Targa. 2005. Variação espectral e eficiência de uso da radiação fotossinteticamente ativa em ensaio com genótipos de trigo. Bragantia 64: 331-338.

Muurinen, S. and P. Peltonen-Sainio. 2006. Radiation-use efficiency of modern and old spring cereal cultivars and its response to nitrogen in Northern growing conditions. Field Crops Res. 96: 363-373.

O'Connell, M.G., G.J. O'Leary, D.M. Whitfield and D.J. Connor. 2004. Interception of photosynthetically active radiation and radiation-use efficiency of wheat, field pea and mustard in a semi-arid environment. Field Crops Res. 85: 111-124.

Quanqi, L., C. Yuhai, L. Mengyu, Z. Xunbo, Y. Songlie and D. Baodi. 2008. Effects of irrigation and planting patterns on radiation use efficiency and yield of winter wheat in North China. Agric. Water Manage. 95: 469-476.

Reynolds, M.P., A. Pellegrineschi and B. Skovmand. 2005. Sink-limitation to yield and biomass: A summary of some investigations in spring wheat. Ann. Appl. Biol. 146: 39-49.

Rodriguez, D. and V.O. Sadras. 2007. The limit to wheat water-use efficiency in eastern Australia. I. Gradients in the radiation environment and atmospheric demand. Aust. J. Agric. Res. 58: 287-302.

Rudorff, B.F.T., C.L. Mulchi, C.S.T. Daughtry and E.H. Lee. 1996. Growth, radiation use efficiency, and canopy reflectance of wheat and corn grown under elevated ozone and carbon dioxide atmospheres. Remote Sens. Environ. 55: 163-173.

Siddique, K.H.M., R.K. Belford, M.W. Perry and D. Tennant. 1989. Growth, development and light interception of old and modern wheat cultivars in a Mediterranean-type environment. Aust. J. Agric. Res. 40: 473-487.

Sinclair, T.R. and R.C. Muchow. 1999. Radiation use efficiency. Adv. Agron. 65: 215-265.

Stapper, M. 1984. The use of a simulation model for the prediction of wheat cultivar response to agroclimatic factors in semi-arid regions. Ph.D. Dissertation, Univ. New England, Armidale, Australia.

Van Delden, A. 2001. Yield and growth components of potato and wheat under organic nitrogen management. Agron. J. 93: 1370-1385.

Whitfield, D.M. and C.J. Smith. 1989. Effects of irrigation and nitrogen on growth, light interception and efficiency of light conversion in wheat. Field Crops Res. 20: 279-295.

Wilson, D. and P. Jamieson. 1985. Models of growth and water use of wheat in new zealand. Wheat growth and modelling. Springer. p. 211-216.

Yunusa, I.A.M., K.H.M. Siddique, R.K. Belford and M.M. Karimi. 1993. Effect of canopy structure on efficiency of radiation interception and use in spring wheat cultivars during the preanthesis period in a mediterranean-type environment. Field Crops Res. 35: 113-122.

CHAPTER V

METEOROLOGICAL LIMITS TO WINTER WHEAT PRODUCTIVITY AND RESOURCE USE-EFFICIENCY IN THE SOUTHERN GREAT PLAINS

ABSTRACT

Wheat (*Triticum aestivum* L.) yields in the southern Great Plains have been nearly stagnant for the last 30-yr, and some of the yield stagnation may be caused by the meteorological characteristics of the region. Our objectives were to identify geospatial gradients in key weather variables and to assess the meteorological drivers of wheat productivity and resource-use efficiency across Texas, Oklahoma, and Kansas. Water-limited wheat aboveground biomass and grain yield (Y_w) were simulated for 28 consecutive years at 37 locations across the southern Great Plains using Simple Simulation Modeling – Wheat (SSM-Wheat), actual soil and weather data, planting date, and population density. Regional gradients in meteorological variables were determined for (i) the entire crop cycle, (ii) pre- and post- anthesis, or (iii) jointing-anthesis interval, and Y_w were related back to these variables using linear and stepwise multiple regression. Boundary function analysis determined water productivity (WP), and transpiration- and radiation- use-efficiency (TE and RUE). Strong latitudinal gradients occurred for temperatures and longitudinal gradients for precipitation, evapotranspirative demand, and solar radiation. Wheat Y_w averaged 6.0 Mg ha^{-1} and followed the longitudinal precipitation gradient

increasing from west (3.5 Mg ha^{-1}) to east (6.9 Mg ha^{-1}). Interannual Y_w variability was large with coefficient of variation (CV) ranging from 0.11 to 0.5 from east to west. Meteorological variables accounting for major portions of the Y_w variability were water supply (precipitation + PAW_s) in the west (81.7%) and cumulative solar radiation (R_s) during the anthesis – physiological maturity in the east (86.9%). Temperatures during the anthesis-physiological maturity phase negatively affected grain yields across all locations and years (8% of Y_w variability). Wheat WP (19.1 kg ha^{-1} mm^{-1}), TE (24.2 kg ha^{-1} mm^{-1}), and RUE (0.86 g MJ^{-1} based on incident R_s) compared well with published literature and can be used as benchmarks for other studies in the region.

Keywords: yield potential, maximum attainable yields, yield gap; winter wheat; water-use efficiency, radiation-use efficiency, evapotranspiration, meteorology, geospatial gradients, boundary function.

Abbreviations: CV: coefficient of variation; ET_c: crop evapotranspiration; ET_o: reference evapotranspiration; NASA Power: National Aeronautics and Space Administration Prediction Of Worldwide Energy Resource; NOAA: National Aeronautics and Space Administration; PAW: plant available water; PAWC: plant available water capacity; PAW_s: plant available water at sowing; PQ: photothermal quotient; R_s: incident solar radiation; RUE: radiation-use efficiency; SSM-Wheat: Simple Simulation Modeling Wheat; TE: transpiration efficiency; T_{max}: maximum daily temperature; T_{min}: minimum daily temperature; WP: water productivity; YVI: yield variance index; Y_w: water-limited yield; θ_{DUL}: volumetric soil water content at the drained upper limit; θ_{LL}: volumetric soil water content at the lower limit; θ_S: volumetric soil water content at saturation; θ_v: volumetric soil water content.

5.1. INTRODUCTION

Approximately 8 million hectares are planted to winter wheat every year in the southern Great Plains of the United States (32 – 40°N; 96 – 103°W), mostly in the states of Kansas, Oklahoma, and Texas. Total annual production from the three states combined often surpasses 14 million metric tons, accounting for ~30% of the U.S. wheat production (USDA-NASS, 2014). Recent analysis of historical wheat yields in the southern Great Plains indicates that average farm yield have been nearly stagnant for the last 30-yr (Patrignani et al., 2014). Similar yield plateaus are true for several other wheat producing regions of the world such as India and across much of Europe (Grassini et al., 2013). One reason for yield plateaus is average farm yields approaching the environmental potential yield for that region, leaving a small exploitable gap (Lobell et al., 2009). This holds true for high-yielding systems such as wheat grown in Europe (Grassini et al., 2013). However, wheat yields in the southern Great Plains are remarkably low for cereal production in developed countries and are far below the environmental potential (Licker et al., 2010; Patrignani et al., 2014). Efforts to identify the causes of yield stagnation in the southern Great Plains, an important wheat producing region in the global wheat scenario, are warranted.

State level wheat yields in the states of Kansas, Oklahoma, and Texas, have not surpassed 3 Mg ha^{-1} in the last 30-yr period, with county level yields ranging from 0.2 to 3.6 Mg ha^{-1} (Patrignani et al., 2014). These yield levels are well below the highest wheat yields (6.8 to 8.2 Mg ha^{-1}) ever reported for the southern Great Plains (Lollato and Edwards, 2015; Musick et al., 1994), indicating that the observed yield plateau is more likely resultant from either lack of investment in agricultural inputs or limitations imposed by weather or soil, rather than a small gap between farmer and potential yields (Grassini et al., 2013; Mueller et al., 2012; Patrignani et al., 2014). Possible management-related causes of the yield stagnation in the southern Great Plains are lack of crop rotation in continuous wheat systems (Bushong et al., 2012), acidic soils due to ammonium-based nitrogen fertilizer (Schroder et al., 2011), decreased soil fertility and water

holding capacity due to topsoil erosion (Patrignani et al., 2014), and dual-purpose management where wheat is grown for forage (i.e. grazing) and grain (Edwards et al., 2011). While possible management practices leading to yield stagnation were discussed for the region (Patrignani et al., 2014), there is still a need to the extent to which extent meteorological variables impact wheat potential yield in the southern Great Plains as an effort to elucidate the main causes of yield stagnation and variability.

Yield potential is the yield of a cultivar grown in an environment to which it is adapted, with non-limiting nutrient and water conditions, and with effective control of pests, diseases, and weeds (Evans, 1993). A crop's yield potential is ultimately determined by its genetic characteristics, and its interaction with the region's climatic (e.g. incident solar radiation, temperature, and photoperiod) and edaphic (e.g. soil fertility, erodibility, and water holding capacity) factors. Environmental-limited potential yield can be decreased due to inadequate water supply in rainfed agricultural systems; thus, the degree of water limitation needs to be taken into account when determining the water-limited potential yield (Y_w) in these systems (Connor et al., 2011). Thus, Y_w is location-specific. For instance, the Y_w of soft winter wheat grown in the United Kingdom has been suggested to be 10.4 Mg ha^{-1} (Fischer and Edmeades, 2010). At the Yaqui Valley in Mexico, potential yield of irrigated spring wheat was estimated at 9 Mg ha^{-1} (Fischer and Edmeades, 2010); whereas the cool and radiation-intense summer in New Zealand has led to feed wheat Yw as high as 15 Mg ha^{-1} (Armour et al., 2004). Research results suggest that the Y_w of winter wheat in the southern Great Plains is around 5.5 to 7.1 Mg ha^{-1} (Lollato and Edwards, 2015). These results are based on eleven site-years where all biotic and abiotic stresses were properly controlled; thus, they are a good indication of the Y_w of winter wheat in Oklahoma. However, they are most likely not representative of average Y_w over several years for the region as a robust assessment of a region's Y_w via well managed field studies is costly and impracticable (Cassman et al., 2003).

Simulation of Y_w across several sites and years using validated crop models is a reliable alternative to costly field studies for assessment of long-term environmental Y_w for a given region (Van Ittersum et al., 2013). Simulation models account for different weather conditions across years and regions; as well as for interactions among crops, weather, and soils; allowing for detailed analyses of Y_w for a certain cropping system (Van Ittersum et al., 2013). Also, it facilitates analysis of geospatial gradients of weather variables and their influence in crop potential productivity (Grassini et al., 2009). Crop simulation models have been widely used to assess wheat Y_w for wheat systems of the globe, including: the Yaqui Valley in Mexico (Bell and Fischer, 1994; Lobell and Ortiz-Monasterio, 2006); the Pampas region in Argentina (Menendez and Satorre, 2007); India (Aggarwal and Kalra, 1994; Aggarwal et al., 1994); and the wheat producing regions of Australia (Asseng et al., 1998; Hochman et al., 2009; Peake et al., 2014), Russia (Schierhorn et al., 2014), Spain (Abeledo et al., 2008), and China (Liang et al., 2011; Lu and Fan, 2013). Still, analysis of the effects of weather on winter wheat Y_w using validated crop models has not been reported for the southern Great Plains. This analysis could help elucidate whether meteorological variables are partially causing the observed yield stagnation in the region.

Beyond the low average wheat yields historically achieved in the southern Great Plains, the region is characterized by high year-to-year variability in both average wheat grain yields and total regional production (Patrignani et al., 2014). The high yearly variability in wheat productivity was suggested to be associated with variability in weather conditions (Patrignani et al., 2014), which makes biological sense for rainfed cropping systems (van Wart et al., 2013b). High year-to-year variability in grain yield is especially important in regions with erratic precipitation patterns where the majority of the crops are grown under rainfed conditions (Aggarwal and Kalra, 1994; van Wart et al., 2013b). The analysis of Y_w using simulation models across a wide range of locations throughout several years results in probability distributions with mean and range, which can characterize the regional year-to-year variability (Van Ittersum et al.,

2013) and allows for an estimate of annual Y_w variance and its association with observed variability in weather (Aggarwal and Kalra, 1994).

In modern rainfed agriculture, such as most of the wheat grown in the southern Great Plains, water is generally the most limiting resource to crop productivity (Connor et al., 2011). Quantification of the maximum yield per unit water supply provides a benchmark that can be used by farmers to set yield goals based on available water, and to identify limiting factors to on-farm productivity other than water supply (Grassini et al., 2009; Passioura, 2006). Grain yield plotted against seasonal water supply or crop evapotranspiration (ET_c) can provide an estimate of the system's water productivity (WP) and the crop's transpiration efficiency (TE) by fitting a linear function in the most efficient datapoints (French and Schultz, 1984). The linear function represents the maximum production efficiency for a given amount of seasonal water or ET_c. Previous efforts in determining the WP for wheat systems in the southern Great Plains resulted in WPs ranging from 16.7 kg mm^{-1} in Bushland, TX (Sadras and Angus, 2006), to 22 kg mm^{-1} in west-central Oklahoma (Patrignani et al., 2014). In wheat systems in the southern Great Plains, WP appears to be influenced by geographical location as function of the steep longitudinal precipitation gradient (Patrignani et al., 2014). Elucidation of geospatial gradients as efforts to benchmark WP and TE can help identify the physiological frontier for water-limited productivity.

The objectives of this research were (i) to find geospatial patterns in meteorological variables associated with crop productivity (i.e. solar radiation, temperature, precipitation, and evapotranspirative demand) across the southern Great Plains; (ii) to define the long-term yield Y_w of winter wheat in the region based on a simulation analysis; (iii) to identify weather factors across the geospatial climatic gradients that explain spatial and temporal variation in winter wheat Y_w; and (iv) to define WP, TE, and RUE of wheat grown under non-limiting conditions for different regions within the southern Great Plains.

5.2. MATERIAL AND METHODS

5.2.1. Model description and performance evaluation

The SSM-Wheat crop simulation model (Soltani et al., 2013; Soltani and Sinclair, 2012) is a radiation-driven crop simulation model that simulates daily wheat growth and development based on soil characteristics and observed daily weather. Simulations of wheat growth and development in SSM-Wheat are for a crop free of limitations caused by diseases, insects, weeds, and also nutrient deficiencies (user option). Crop response to vernalization and photoperiod are accounted for, and reductions in potential productivity result from water stress, occurrence of limiting temperatures, or inadequate photoperiod. Crop transpiration is simulated as function of crop daily dry matter production, effective daily vapor pressure deficit, and a transpiration efficiency coefficient (Tanner and Sinclair, 1983), which results in realistic water use estimations based on crop biomass production (Soltani and Sinclair, 2012). Every coefficient used in SSM-Wheat can be calculated from field collected data, which allows for parameterization of the model for different conditions based on field measurements. Recent analysis of model robustness and transparency indicates an advantage to the SSM-Wheat model when compared to other wheat simulation models in transparency and robustness (Soltani and Sinclair, 2015).

We derived parameter values for the SSM-Wheat model using field collected data for wheat growth, development, and yield, under non-limiting conditions in seven dryland site-years in Oklahoma where crop management strived to minimize biotic and abiotic stresses, approaching the Yw of winter wheat (Lollato and Edwards, 2015). Parameter values were calibrated using data for phenology (i.e. days to anthesis, physiological maturity, and harvest maturity), growing season dynamics for aboveground biomass, leaf area index, and plant available water (PAW) in the top 1200 mm of the soil profile, and with harvested grain yield and harvest index. Model was then validated for phenology (days to harvest maturity) and grain yield using data from 37 trials

where yield-limiting and yield-reducing factors were apparently successfully controlled across Kansas and Oklahoma (Table 5.1). Simulations were performed using daily weather data retrieved from the nearest ground-based meteorological station from the Kansas Mesonet (http://mesonet.k-state.edu/) and Oklahoma Mesonet (http://www.mesonet.org/). Simulations used the reported soil characteristics and management practices (e.g. sowing date, plant population, etc.), and simulated dates and grain yields were compared to observed values using absolute and normalized root mean square error (RMSE and $RMSE_n$, respectively) with the goal to achieve $RMSE_n < 5\%$ for dates of phenological events, and $RMSE_n < 10\%$ or 20% for grain yield in the calibration and validation datasets, respectively (Jamieson et al., 1991).

5.2.2. Simulated winter wheat Y_w

Simulation of rainfed winter wheat Y_w was performed for 37 locations across the wheat growing region of the southern Great Plains (Fig. 5.1) using 28 consecutive years of weather data (1986 to 2014), for a total of 1036 simulated site-years. Final simulated Y_w for the southern Great Plains was estimated by weighting mean simulated Y_w from each location by the 10-yr average area planted to winter wheat in the respective county where the meteorological station was located (Lu and Fan, 2013). A 28-yr period of consecutive weather data at a given location should be sufficient to account for the year-to-year weather variability in regions such as the southern Great Plains, characterized by highly variable climate (van Wart et al., 2013b).

Simulations were performed using predominant soil type surrounding the weather station and proper sowing date and plant population for each simulation site, following the approach suggested by Grassini et al. (2009) and Van Wart et al. (2013a). Predominant agricultural soil series were determined by selecting an area of approximately 40,000 ha centered on each meteorological station's geographic coordinate using the Web Soil Survey (USDA-NRCS, 2014b), and typical soil physical properties for each soil series used as model input were obtained

from the official soil series descriptions (USDA-NRCS, 2014a). Soil physical properties included soil depth, texture, and plant available water holding capacity (PAWC) for the soil series (Table 5.2). Rooting depth for wheat simulations was set to 1400 mm based on typical water extraction patter of wheat (Canadell et al., 1996; Xue et al., 2003). Planting date represented the most active planting period for winter wheat for each location as reported in USDA-NASS (2010), and fine-tuned with the official variety trial network (Edwards et al., 2013; Lingenfelser et al., 2013; Neely et al., 2013) and crop management guides (Krenzer, 2000; Shroyer et al., 1996) from each state (Table 5.2). Optimal plant population followed recommended practices from the aforementioned sources for each location and ranged from 1.6 to 3.5 million plants ha^{-1}, increasing from west to east following the precipitation gradient (Table 5.2). Plant available water at sowing (PAW_s) was estimated for each site-year using an empirical approach based on total summer fallow precipitation normalized by the soil's PAWC as described in chapter II in this dissertation.

5.2.3. Data quality control and estimation of missing parameters

The SSM-Wheat model operates in daily time steps and therefore requires a complete daily weather dataset to simulate Y_w. To achieve a complete dataset, daily weather records were retrieved from a minimum of two different weather stations for a given location. Ground-based measured weather data were collected from Kansas and Oklahoma Mesonet networks, as well as from the National Oceanic and Atmospheric Administration Climatic Data Center (NOAA, http://www.ncdc.noaa.gov/). Data from the Mesonet networks, including minimum (T_{min}) and maximum (T_{max}) temperatures, solar radiation (R_s), and precipitation, were used as primary weather source for crop simulations in Kansas and Oklahoma, and missing data were identified and replaced with weather data from a nearby NOAA weather station. The NOAA dataset was used as primary source of weather data for Texas for T_{min}, T_{max}, and precipitation, while satellite-derived R_s data were retrieved from the National Aeronautics and Space Administration Prediction of Worldwide Energy Resource (NASA Power, http://power.larc.nasa.gov/). The use

of satellite-derived R_s from NASA Power coupled to temperatures and rainfall information from the nearest ground-based meteorological station resulted in similar simulated Y_w for cereals across the globe when compared to ground-based measured R_s (Van Wart et al., 2013a).

Remaining missing values for T_{max}, T_{min}, precipitation, or R_s, were replaced with satellite derived data from NASA for the same geographical location as the original weather station as specified by latitude and longitude. Substituting missing data with satellite derived daily data is a reasonable approach given the high correlation satellite-derived data had with station-measured values in a subset of our dataset for T_{min} ($r^2 = 0.94^{***}$, n = 118,585), T_{max} ($r^2 = 0.92^{***}$, n = 118,585), R_s ($r^2= 0.93^{***}$, n = 136,882), and 15-day cumulative rainfall ($r^2= 0.53^{***}$, n = 114,973). The NASA POWER dataset had daily values for the entire time-series included in this study except for precipitation, which required eliminating 53 site-years in the final analysis (approximately 5% of the total simulated site-years) due to missing daily precipitation data. The complete weather dataset may be made available upon request from the authors.

5.2.4. Effect of climatic variation on potential yield

Yield stability is an important aspect in regions with erratic precipitation pattern, as highly variable weather can lead to great year-to-year variability in grain yields (van Wart et al., 2013b). Historic weather data allows for frequency distribution analysis of grain yields, providing means to evaluate the probability of obtaining a certain yield as well as to assess the impact of climate on a crop's vulnerability (Aggarwal and Kalra, 1994). The effect of climatic variation on wheat yields was assessed for each location according to Eq. [1]:

$$YVI = \frac{0.75Y - 0.25Y}{0.50Y} \quad [1]$$

where *YVI* is the yield variance index, 0.75*Y*, 0.25*Y*, and 0.50*Y* are the yields at the 75th, 25th, and 50th percentiles, respectively (Aggarwal and Kalra, 1994). In this analysis, the larger the *YVI*,

the larger is the variance in yields associated to climate. Climate variability was also assessed using the interannual coefficient of variation (CV) within a given location.

5.2.5. Geospatial gradients of meteorological variables

The long growing season of winter wheat, encompassing warm weather during fall, cold weather during winter, and warm weather again during spring, can preclude any significant relationships between grain yield and meteorological variables averaged over the entire growing season (Barkley et al., 2014). Therefore, it is helpful to divide the growing season and relate yields to meteorological variables observed during growth phases more sensitive to environmental limitations. In wheat, the weather between joiting and anthesis seems to have a crucial impact in grain yields (Barkley et al., 2014; Nalley et al., 2009). Thus, for each simulated site-year, mean values for meteorological variables were estimated using data (i) from sowing to physiological maturity; (ii) from sowing to anthesis; (iii) from stem elongation until anthesis; and (iv) from anthesis to physiological maturity. Weather variables were cumulative R_s, daily T_{max}, T_{mean}, and T_{min}, cumulative precipitation, and cumulative reference evapotranspiration (ET_o), the latter estimated using the FAO-56 procedure (Allen et al., 1998). Site-years were individually screened for freeze occurrence during the period between simulated stem elongation and termination of seed growth and site-years when $T_{min} < -2°C$ during this period were not included in the final analysis. A total of 11% of the site-years were excluded due to freeze occurrence, for a final dataset of 870 site-years across the southern Great Plains. The long-term, freeze-free mean of each variable at each location, were then plotted against latitude and longitude to identify geospatial weather patterns. Regression analyses were performed to identify linear or quadratic relationships between geographic coordinates and meteorological variables, as well between Y_w and the same meteorological variables.

5.2.6. Effects of geospatial gradients in wheat Y_w

The effects of weather on simulated wheat Y_w were first evaluated for all simulated site-years across the southern Great Plains (Fig. 5.1, n = 870). Data points were then divided and analyzed by sub-region within the southern Great Plains due to the strong longitudinal precipitation and Yw gradients ($p < 0.001$). Sub-regions were west (longitude < 100°W, $n = 144$), west-central (100°W < longitude < 98.5°W, $n = 259$), east-central (98.5°W < longitude < 97°W, $n = 265$), and east (longitude < 97°W, $n = 202$).

The degree of linear dependence between each meteorological variable and winter wheat Y_w was studied using Pearson's correlation coefficient for the entire crop cycle, the pre- and post-anthesis phases, as well as the time period immediately prior to anthesis. Analyses were performed for the whole region and for each individual sub-region. To determine whether using only the weather immediately prior to anthesis or using weather pre- and post-anthesis as independent variables explained significantly more of the variation in Y_w (dependent variables) as compared to using mean values of the entire crop cycle, forward stepwise multiple-regression was performed similarly to the approaches adopted by Grassini et al. (2009) and Van Wart et al. (2013a). The weather variables used as independent variables for each site-year were average daily T_{max}, T_{min}, and T_{mean}, cumulative R_s, cumulative precipitation, and cumulative ET_o. In this approach, cumulative R_s in the period was used rather than daily average values to account for different crop cycles' lengths (Grassini et al., 2009). Additionally, the effects of PAW_s on wheat Y_w, as well as of photothermal quotient (PQ; ratio of mean R_s over T_{mean} during the stem elongation to anthesis period) on grain yield were tested as independent variables in the multiple regression.

Stepwise regression analyses started with weather variables averaged for the entire crop cycle and T_{mean} as independent variables. We then evaluated whether using T_{min} and T_{max}

explained a greater proportion of the variation in Y_w than did T_{mean}. The next step in the stepwise multiple regression was to substitute each individual weather variable averaged for the whole crop cycle by the same variable divided in both pre- and post-anthesis phases, comparing the explanatory power of the regression model to the original model after each substitution. Finally, weather variables observed immediately prior to anthesis (i.e. stem elongation to anthesis period) were evaluated as independent variables in the multiple regression. The degree of collinearity among independent variables was evaluated using the variance inflation factor (VIF) and collinearity was considered to occur when VIF > 10 (Dormann et al., 2013). The final regression model was composed only by non-collinear variables that were significant at *P*-value ≤ 0.05. The partial influence to the regression sums of squares (%SSR) was used to evaluate the influence of each meteorological variable on the variation of Y_w for the whole region and for each sub-region. Linear and quadratic relationships, Pearson's correlation coefficients, and multiple regression analysis were performed using the R program software (R Foundation for Statistical Computing, Vienna, Austria).

5.2.7. Regional patterns of wheat WP, TE, and RUE

Maximum boundary-functions (French and Schultz, 1984) between Y_w and (i) water supply, (ii) crop evapotranspiration (ET_c), or (iii) seasonal incident R_s were generated using quantile regression (Cade and Noon, 2003) for freeze-free site-years for the whole region and for each individual sub-region. Water supply was calculated for each site-year as the sum of PAW_s in the upper 1.4 m soil depth and precipitation accumulated from sowing to physiological maturity. The range in water supply, ET_c, or incident R_s levels in which Y_w was responsive to changes in water or radiation input (i.e. interval between the lowest water supply or ET_c up to 500 mm; or lowest incident R_s and 3200 MJ m^{-2}) was divided in 10 equally spaced intervals used to derive the boundary functions. Boundary functions were created as the regression between 95th percentile Y_w within each class to the mid-point of water supply, ET_c, or incident R_s for that class, following

the approach adopted by Grassini et al. (2009). The relationship between Y_w and seasonal water supply was defined as WP, the relationship between Y_w and seasonal ET_c was defined as TE, and the relationship between aboveground biomass and incident R_s was defined as RUE. Minimum water losses or non-intercepted R_s for each region were estimated as the *x*-intercept of the boundary function (French and Schultz, 1984).

5.3. RESULTS

5.3.1. Evaluation of model robustness

The SSM-Wheat model simulated wheat phenology very well, with $RMSE_n < 5\%$ for both the calibration and validation datasets and a total of 88% of simulated days for a phenological event within ±5% of measured days (Fig. 5.2a). Model performance was considered satisfactory for simulated yield in the calibration ($RMSE_n = 10\%$) and validation ($RMSE_n = 14\%$) datasets (Fig. 5.2b). The SSM-Wheat underestimated grain yields at Stillwater in the calibration dataset and overestimated grain yield in six site-years across Oklahoma and Kansas in the validation dataset. Careful evaluation of the weather during these particular growing seasons revealed a severe water deficit during most of the growing season in Stillwater during 2013-14 despite yields of 3.45 Mg ha^{-1} (Lollato and Edwards, 2015). The long-term severe water deficit resulted in yield underestimation by the SSM-Wheat, which simulates water stress based on relative soil PAW. Nonetheless, severe water deficit stresses occurred in four additional site-years among the calibration and validation datasets, and were well simulated by SSM-Wheat (Fig. 5.2b). Evaluation of the weather during the six site-years where model overestimated grain yield indicated occurrence of freeze events during wheat reproductive stages. Although the SSM-Wheat simulates the effects of low temperatures on decreased green leaf area and rate of biomass production (Soltani and Sinclair, 2012), the detrimental effects caused by freeze on grain yield are not simulated and need to be accounted for. Thus, sites when freeze occurred during the

reproductive stages were excluded from the final analysis. Model performance was satisfactory when simulating growing season dynamics for aboveground biomass, leaf area index, and PAW in the 7 site-years used as calibration dataset (data not shown).

5.3.2. Simulated PAW at wheat sowing

Median simulated PAW_s using the empirical model developed in chapter III of this dissertation for 998 site-years across the southern Great Plains (including site-years when late season freeze occurred) was 0.68 PAWC, with a CV of 0.25 (Fig. 5.3a). One half of the simulated PAW_s values in the southern Great Plains were between 0.56 and 0.8 PAWC, which agrees well with 29 site-years of field collected data for wheat PAW_s in central Oklahoma where 65% of the values fell within 0.4 and 0.8 PAWC (Lollato et al., *unpublished*). When PAW_s was evaluated individually for each sub-region within the southern Great Plains, there was a clear trend of lower and more variable PAW_s in the west (median = 0.57 PAWC, CV = 0.3; Fig. 5.3b) as compared to the west-central (median = 0.64PAWC, CV = 0.25; Fig. 5.3b), east-central (median = 0.74, CV = 0.21; Fig. 5.3c), or east (median = 0.75 PAWC, CV = 0.2; Fig. 5.3c). The empirical model we used simulates PAW_s /PAWC as an exponential rise to the maximum within the PAWC interval using cumulative precipitation during the fallow period normalized by the soil's PAWC as independent variable (Lollato et al., *in preparation*). Thus, the trend of drier profile towards west is function of the steep longitudinal precipitation gradient in the southern Great Plains.

5.3.3. Geospatial gradients in meteorological variables

In the southern Great Plains, different gradients in meteorological variables occur depending on the phase of crop development, the direction considered, and the meteorological variable being evaluated (Fig. 5.4). When considering the sowing – physiological maturity interval, cumulative R_s was relatively constant across the range of latitudes studied (Fig. 5.4a). However, latitudinal gradients in cumulative R_s occurred when considering the individual

intervals within the growing season (Figs. 5.4b-d). Specifically, cumulative R_s increased linearly from south to north during the sowing-anthesis interval (Fig. 5.4d), and followed a quadratic responses with greater cumulative R_s in latitudes between 33° and 37° when considering the the period immediately jointing-anthesis (Fig. 5.4c) or anthesis-physiological maturity (Fig. 5.4d). Stronger geospatial trends occurred when cumulative R_s was plotted against longitude (Figs. 5.4e-h), with cumulative R_s during the sowing-physiological maturity interval decreasing from 4212 MJ m^{-2} in the west to 2654 MJ m^{-2} in the east (Fig. 5.4e).

Latitudinal trends in T_{mean} were more apparent than those trends in cumulative R_s, with T_{mean} during the entire crop cycle decreasing from 12.3°C in southern TX to 7.6°C in northern KS (Fig. 5.4a). Similar latitudinal linear trend in T_{mean} was observed for the sowing – anthesis interval (Fig. 5.4b). Interestingly, T_{mean} followed a positive linear latitudinal trend during the anthesis – physiological maturity interval, increasing from 18.8°C in the south to 22.4°C in the north (Fig. 5.4d). Despite the relatively small difference, warmer T_{mean} during the reproductive stages in KS as compared to TX are mainly a function of delayed reproductive period in KS due to a colder spring delaying wheat development. Consequently, the mean simulated reproductive period in KS started May 18th (mean anthesis date) and ended June 22nd (mean physiological maturity date), while in TX it started on average April 12th and ended May 22nd. Conversely, T_{mean} was relatively constant from west to east (Fig. 5.4e-h).

No trends in cumulative precipitation occur from south to north, regardless of the period considered (Fig. 5.5a-d). Likewise, cumulative ET_o during the intervals sowing – physiological maturity (Fig. 5.5a) and sowing – anthesis (Fig. 5.5b) did not show gradients as function of latitude. The only latitudinal gradients in cumulative ET_o occurred during the stem elongation – anthesis and the anthesis – physiological maturity intervals (Fig. 5.5c-d), when cumulative ET_o tended to decrease from south (207-212 mm) to north (160-178 mm). On the other hand, steep longitudinal gradients occurred for cumulative precipitation and ET_o for the whole crop cycle as

well as all individual studied periods within the cycle (Fig. 5.5e-h). Growing season precipitation increased from 141 mm in the west to 631 mm in the east, whereas atmospheric water demand followed the opposite trend and decreased from 929 mm in the west to 607 mm in the east, creating a strong longitudinal gradient in water deficit from west to east (cumulative ET_o – cumulative precipitation; $r^2 = 0.88$, $p < 0.001$). Similar trends in cumulative precipitation and ET_o occurred for the different phases of crop development studied (Fig. 5.5f-h). Additionally, the variability in spatiotemporal cumulative precipitation was greater than that observed in cumulative ET_o, with precipitation CV ranging from 0.46 to 0.72 and ET_o CV ranging from 0.14 to 0.21 (Fig. 5.5e-h). The variability in precipitation is greater during the period joiting-anthesis (CV = 0.72, Fig. 5.5g) and during the period from anthesis to physiological maturity (CV = 0.67, Fig. 5.5h). Coincidently, these periods combined encompass most of wheat grain yield determination (Slafer et al., 1990).

5.3.4. Long-term simulated wheat aboveground biomass and Y_w

Long-term mean potential wheat aboveground biomass production in the 37 locations and 28 years studied across the southern Great Plains ranged between 10 and 20.4 Mg ha^{-1}, and mean wheat potential aboveground biomass weighted by the area planted to winter wheat in the period 2004-2014 within the county where the meteorological station was geographically located was 16.6 Mg ha^{-1} (Fig. 5.6a). Mean simulated wheat Y_w ranged between 3.0 and 8.5 Mg ha^{-1} (Fig. 5.6a), and mean Y_w weighted by the planted area was 6.0 Mg ha^{-1} with interquartile range (IQR) from 4.9 to 7.1 Mg ha^{-1}. Longitudinal gradients occurred for both mean wheat potential biomass production and Y_w (Fig. 5.6a). In fact, linear plateau models described mean potential biomass and Y_w as function of longitude, with wheat biomass and yield productivity increasing with an increase in longitude from 103°W to ~98.5°W, and plateauing in easternmost longitudes (from ~98.5°W to 95°W). This finding is consistent with Patrignani et al. (2014), who found yields were not water limited in the 400-600 mm range which begins ~98.5°W. There was a weak

quadratic latitudinal gradient in mean aboveground biomass productivity (r^2 = 0.14, p < 0.05), with greater biomass produced in intermediate latitudes (35°N – 37°N); and no latitudinal gradient in grain yield (data not shown). The temporal variation in wheat Y_w, measured using both CV and YVI, followed a longitudinal gradient and decreased linearly from west to east (Fig. 5.6b). The CV ranged from 0.11 to 0.5 and the YVI from 0.14 to 0.7. Due to the strong longitudinal gradient in wheat potential productivity, the remaining analyses were performed by the individual sub-regions within the southern Great Plains (i.e. west, west-central, east-central, and east).

The sub-regions in which mean simulated potential biomass and Y_w increased with an increase in longitude were the west and west-central (Fig 5.6a). Median Y_w for winter wheat grown in the west sub-region of the southern Great Plains (longitude < 100°W, n = 144) was 3.5 Mg ha^{-1} with an IQR from 2.7 to 4.6 Mg ha^{-1}, and a range from 0.6 to 9.3 Mg ha^{-1} (Fig. 5.7). Spatiotemporal variability in grain yield in the west sub-region was the greatest among studied regions, with YVI = 0.54 and CV = 0.42. In the west-central sub-region (100°W < longitude < 98.5°W), Y_w increased as compared to the west sub-region and ranged between 2.1 and 11.5 Mg ha^{-1}, with median of 5.8 Mg ha^{-1} and an IQR from 4.5 to 7.2 Mg ha^{-1} (Fig. 5.7). This region was also characterized by high year-to-year variability in grain yields, with CV = 0.33 and YVI = 0.48. In the sub-regions east of longitude 98.5°W (i.e. east-central and east sub-regions), mean potential simulated aboveground biomass and grain yields were greater and less variable than in the west, plateauing at 17.6 and 6.9 Mg ha^{-1}, respectively, and showing no trend in response to longitude (Fig. 5.6a). Simulated Y_w in the east-central sub-region (98.5°W < longitude < 97°W) were the greatest among all sub-regions and ranged from 1.4 to 11 Mg ha^{-1}, with median of 7.0 Mg ha^{-1} and an IQR from 5.8 to 8.2 Mg ha^{-1} (Fig. 5.7). Variability in grain yields associated with weather decreased to a CV = 0.25 and YVI = 0.33. In the east portion of the wheat producing region in the southern Great Plains (longitude > 97°W), simulated Y_w were similar to those

observed in the east-central region and ranged from 2.7 to 10.3 Mg ha^{-1}, with an IQR from 5.9 to 7.9 Mg ha^{-1}, and median of 6.9 Mg ha^{-1} (Fig. 5.7). This region was characterized by the lowest variability in simulated grain yields, with CV = 0.22 and YVI = 0.29. All the simulated Y_w were below the ~12.9 Mg ha^{-1} theoretical limit to wheat potential (Sinclair, 2013), and 94% of the simulated Y_w were within maximum yields reported for the region.

5.3.5. Geospatial variation in wheat Y_w

Across the southern Great Plains, highest wheat Y_w was achieved in locations with plentiful precipitation and high average T_{min} during the growing season, abundant cumulative R_s and low average T_{max} during the anthesis – physiological maturity interval, great profile PAW_s, and low cumulative ET_o during the sowing – anthesis interval (Table 5.3). Within each individual sub-region, the west and west-central sub-regions were characterized by stronger correlations between wheat Y_w and cumulative precipitation and PAW_s (Table 5.3). Although still significant, these correlations weakened towards east, where the correlation between Y_w and cumulative R_s and T_{max} during the anthesis – physiological maturity interval, as well as PQ, strengthened (Table 5.3). Duration of grain fill was reduced by 0.5 day for each 1°C increase in T_{max} during the anthesis – physiological maturity interval ($r^2 = 0.71$, $p < 0.001$), resulting in lower grain yields in years with higher T_{max} during the grain filling period. Stronger correlations between Y_w with water input (i.e. growing season precipitation and PAW_s) in the west are clearly function of the strong opposite longitudinal gradients in growing season precipitation and ET_o, creating a water deficit gradient that increases towards west. Thus, water becomes a more important determinant of dryland wheat productivity in the west and west-central sub-regions. Conversely, the east sub-region of the southern Great Plains is characterized by greater precipitation totals, and R_s during the anthesis – physiological maturity interval becomes a stronger determinant of grain yield.

The relative influence of each meteorological variable on wheat Y_w was evaluated using the percent sums of squares of each individual variable (excluding residual) in the stepwise multiple regressions performed for freeze-free site years (Table 5.4). Freeze-free site years were used because the SSM-Wheat model does not simulate the effects of freeze during the reproductive cycle on grain yield. Across all site years, stepwise multiple regressions that included all variables partitioned between pre- and post-anthesis, explained 78% of the variation in Y_w (Table 5.4). The greatest proportion of the variation in wheat grain yield across the southern Great Plains were explained by variation in pre- and post-anthesis cumulative precipitation, and post-anthesis cumulative R_s and average T_{max} (%SS = 37.3, 14.6, 29.5, and 7%, respectively, Table 5.4). Analyses of the determining factors for wheat Y_w by sub-region within the southern Great Plains indicate that the relative importance of cumulative precipitation decreases from west to east (%SS = 67.3% to null) accompanied by an increase in the relative importance of cumulative R_s during the anthesis – physiological maturity interval (%SS = 3.3 to 86.9%; Table 5.4). Additionally, the explanatory power of the multiple regression model of wheat Y_w in the west and west-central sub-regions was improved when temperatures were discriminated into T_{min} and T_{max}, while in the east-central and east sub-regions a single parameter T_{mean} sufficed. This was probably a result of the greater amplitude in daily temperature in the west as compared to eastern locations within the studied region (longitudinal gradient T_{max} - T_{min}; $r^2 = 0.77$, $p < 0.001$).

5.3.6. Regional patterns of WP, TE, and RUE

Water productivity, calculated as the slope of the relationship between the 95th percentile grain yield and seasonal water supply (PAW_s + growing season precipitation), was 19.1 ±1.2 kg ha^{-1} mm^{-1} pooled across all the studied sites the southern Great Plains (Fig. 5.8a). This analysis resulted in significant scatter in grain yields at seasonal water supply levels above approximately 500 to 600 mm, indicating greater water losses associated with greater water supply. In fact,

simulated water losses via evaporation, runoff, and deep drainage, were all positive and linearly associated with increased seasonal water supply, as was residual soil water left by the wheat crop in the soil profile at physiological maturity ($p < 0.001$, $r^2 = 0.64$, 0.68, 0.35, and 0.56). Across all simulated site-years, evaporative losses averaged 154 mm and accounted for 67 ± 9% of simulated water losses, runoff averaged 76 mm and accounted for 29 ± 9% of water losses, and deep drainage averaged 13 mm and accounted for 4 ± 5% of simulated water losses. Residual soil water at maturity averaged 90 mm, which is equivalent to ~0.37 PAWC, indicating a high depletion of profile soil water by the wheat crop during the reproductive phase towards physiological maturity. This aligns well with 58 sampled PAW at wheat harvest, which averaged 0.33 PAWC (Chapter III). Seasonal water losses estimated as the *x*-intercept in the boundary function analyses indicate that, under the most efficient water use, water losses average 59 mm (Fig. 5.8a).

The individual sub-regions within the southern Great Plains resulted in varying aboveground biomass and grain yield WP (Table 5.5), with a quadratic trend of low WP in the west (biomass WP = 38.7 ± 4.1 kg ha^{-1} mm^{-1}; and yield WP = 16 ± 1.9 kg ha^{-1} mm^{-1}), higher WP in the west-central sub-region (biomass WP = 41.3 ± 5.7 kg ha^{-1} mm^{-1}; and yield WP = 24.2 ± 3.1 kg ha^{-1} mm^{-1}), and lower WP in the east-central sub-region (biomass WP = 38 ± 3.1 kg ha^{-1} mm^{-1}; and yield WP = 17.8 ± 4.5 kg ha^{-1} mm^{-1}). Water productivities in the east region were extremely low (biomass WP = 23.1 ± 8.9; and yield WP = 10.2 ± 4.8) due to the great seasonal water supply, typical in the region, resulting in a great percentage of the water supply being lost. The boundary function methodology was developed in regions where growing season water supply generally does not exceed 500 mm (Passioura, 2006) and have not been compared to actual data for regions with growing season precipitation > 500 mm (Patrignani et al., 2014); thus, the results from the east sub-region may not actually reflect actual wheat WP.

Transpiration efficiency, calculated with the same procedure as the WP but using seasonal crop evapotranspiration (ET_c) as the independent variable, was 24.2 ±1.6 kg ha^{-1} mm^{-1} for the southern Great Plains (Fig. 5.8b). Relating wheat yields to seasonal ET_c resulted in less scattered points than relating it to water supply as losses associated with evaporation, runoff, and deep percolation are not included in the graph other than as the *x*-intercept, which is greater than in the WP approach. Seasonal ET_c ranged from 155 to 733 mm and seasonal water losses, estimated as the *x*-intercept in the boundary function analyses, were 77 mm, all values within the range reported for the region (Lollato and Edwards, 2015). Despite the reduced scatter when compared to WP, differences between maximum and minimum simulated wheat Y_w for a given range in ET_c ranged from 0.7 Mg ha^{-1} (190-225 mm ET_c) to 9.1 Mg ha^{-1} (435-470 mm ET_c), elucidating the importance of variation in meteorological variables dictating wheat yield variability within a given ET_c range. Our analysis indicate that this yield variability for a given ET_c range is mainly governed by differences in cumulative R_s and average T_{max} during the anthesis – physiological maturity interval, as well as average T_{min} during the pre- and post-anthesis phases of crop development.

Radiation use efficiency on an incident solar radiation basis was 0.86 ± 0.07 g MJ^{-1} for the southern Great Plains (Fig. 5.8c) and followed the opposite pattern of that obtained for WP and TE in the sub-regions, increasing from 0.43 and 0.69 g MJ^{-1} in the west and west-central sub-regions, to 0.8 and 1.15 g MJ^{-1} in the east-central and east sub-regions (Table 5.5). The lesser RUE in the western sub-regions is function of the greater total seasonal R_s (i.e. 3878 MJ m^{-2} in the west) when compared to eastern sub-regions (i.e. 2856 MJ m^{-2} in the east) as well as water deficit stress characteristic in the west, which decreases RUE (Sinclair and Muchow, 1999). This analysis resulted in significant scatter in grain yields at seasonal incident R_s levels above ~3,000 MJ m^{-2}, indicating greater non-intercepted R_s at high R_s supply levels (Fig. 5.8c).

5.4. DISCUSSION

5.4.1. Winter wheat yield potential in the southern Great Plains

Simulated winter wheat Y_w using long-term (28-yr) weather data across 37 locations spanned a geographic range (31.7°N-39.8°N; 94.8°W-102.7°W) that encompassed the majority of wheat producing region in the southern Great Plains. Within this region and time period, mean simulated wheat Y_w weighted by each location's area planted to winter wheat in the last 10-yr was 6.0 Mg ha^{-1}, with one half of the simulated Y_w values between 4.9 and 7.1 Mg ha^{-1}. Our results confirm previous research performed with historical county-level yield data in Oklahoma, which concluded that Y_w of winter wheat in the region was approximately 6.7 Mg ha^{-1} (Patrignani et al., 2014), and are in agreement with field-plot research where yield limiting factors were properly controlled and maximum attained wheat yields ranged from 3.1 to 7.7 Mg ha^{-1} (Lollato and Edwards, 2015).

These Y_w are significantly lower than the suggested wheat Y_w for other regions of the world. For instance, Fischer and Edmeades (2010) suggested that the winter wheat Y_w in the United Kingdom is 10.4 Mg ha^{-1}, whereas an Y_w of 8 Mg ha^{-1} was suggested for China (Lu and Fan, 2013). The values we suggest for the southern Great Plains are also lower than the 9 Mg ha^{-1} irrigated spring wheat in Mexico (Fischer and Edmeades, 2010), the 7-8 Mg ha^{-1} wheat Y_w in northern India (Aggarwal and Kalra, 1994) or the 7.2-8.9 Mg ha^{-1} long term average yield simulated in Germany (Van Wart et al., 2015). Still, our results compare well to research on wheat Y_w in regions characterized by lower precipitation totals, such as 6.1-7.1 Mg ha^{-1} in Spain (Abeledo et al., 2008), and 6-7 Mg ha^{-1} in central India (Aggarwal and Kalra, 1994); and seem to be above the 4.93-5.3 Mg ha^{-1} Y_w obtained in Australia (Hochman et al., 2013), 4.3-5.6 Mg ha^{-1} in Russia (Schierhorn et al., 2014), and 3.5-5 Mg ha^{-1} in southern India (Aggarwal and Kalra, 1994). Highest wheat Y_w generally occur in regions with plentiful precipitation, cool

temperatures which extend crop cycle and grain filling periods, and northernmost latitudes with greater daily R_s during the grain filling period. Additionally, regions with these characteristics have less Y_w variability, which allow farmers to invest in the wheat crop with a more reliable return.

Wheat yield variability, as expressed by the CV in yields across years, has been reported to be as low as 0.05 in Europe (Van Wart et al., 2015). The high yield predictability leads farmers to invest in the wheat crop, with an average fertilizer input of 190 kg N, 31 kg P_2O_5, and 39 kg K_2O per hectare in the United Kingdom for an average country yield above 8 Mg ha^{-1} (Fischer and Edmeades, 2010). The high average farmer yields leads to narrow yield gaps in Western Europe (10-30%), as regional yields are close to the Y_w (Fischer and Edmeades, 2010; Licker et al., 2010). The yield variability in the southern Great Plains in our results was much greater, with CV and YVI ranging from 0.11 and 0.14 in the eastern portion to 0.5 and 0.7 in the west. Despite the relatively low CVs in the east (i.e. 0.11), the majority of the winter wheat growing region is located west of longitude 97°W and was characterized by CV above 0.2 and YVI above 0.3. The unpredictability in Y_w across the majority of the wheat growing region of the southern Plains renders producers reluctant to invest in the crop, which is highlighted by average fertilization rate of 65 kg N ha^{-1} (Patrignani et al., 2014) as compared to 190 kg N ha^{-1} in Europe. Low average input leads to lesser farmer yields and the resultant yield gap relative to Y_w of ~4.7 Mg ha^{-1} or 70% of Y_w (Licker et al., 2010; Patrignani et al., 2014). Therefore, there is evidence that the typical meteorology in the region, which causes great yield variability and low yield predictability, is contributing to the yield gaps and possibly yield stagnation in the region. Producers are reluctant to invest in the crop, shortening average farmer yields and leading to a large yield gap.

5.4.2. Meteorological variables dictating wheat yields in the southern Great Plains

Cumulative precipitation accounted for the largest proportion of the variation in simulated rainfed wheat Y_w across the southern Great Plains. Similarly, Barkley et al. (2014) evaluated the effects of weather on wheat yields across Kansas using historical data from variety performance tests and suggested that rainfall distribution is often the most limiting factor for wheat productivity across the northern region of the southern Great Plains. Holman et al. (2011) also highlighted the importance of growing season precipitation for wheat yields in western Kansas. In Oklahoma, Patrignani et al. (2014) demonstrated that wheat yields are limited by water supply when growing season precipitation is less than approximately 400 mm, a value beyond which wheat yields become limited by other factors. Our analysis expanded the results from the published literature to the whole southern Great Plains, and demonstrated that although cumulative precipitation accounted for a great proportion of the wheat yield variability throughout the region, it was a more important factor in the west and west-central sub-regions.

Our results also indicate a strong positive effect of cumulative R_s (3.3 to 86.9% of SS) and a negative effect of average T_{max} or T_{mean} (0.9 to 8.6% of SS) both during the anthesis – physiological maturity interval, on wheat Y_w. These results agree well with a field study evaluating meteorological factors leading to record-breaking wheat yield in the region, which determined that precipitation is coarse regulator of wheat Y_w, and R_s during anthesis – maturity a fine regulator of wheat Y_w (Lollato and Edwards, 2015).The positive association of increased R_s during the reproductive stages and grain yield results from increased kernel weight (Wardlaw, 1994), as 70 to 90% of wheat the kernel weight comes from photosynthates produced during grain fill (Frederick and Bauer, 2000). Increased temperatures during the reproductive stages of wheat, on the other hand, can hasten wheat senescence, and decrease kernel weight and grain yield (Asseng et al., 2011; Fischer, 2007). The negative association of wheat yield to temperature

during the reproductive stages have been documented for western Kansas (Holman et al., 2011) and other wheat growing regions of the world (Licker et al., 2013).

We established longitudinal gradients in aboveground biomass and grain yields, which allowed for the division of the studied region into four sub-regions with similar meteorology. The individual meteorology of different regions often leads to regional-specific drivers of winter wheat grain yield. In the western and drier sub-regions of the southern Great Plains, Y_w were closely associated to cumulative precipitation and average T_{min} during the pre- and post-anthesis phases and with profile PAW_s; while Y_w were more closely associated with cumulative R_s and T_{mean} during the anthesis – physiological maturity phases in the eastern sub-regions where precipitation is more predictable. These findings agree with previous research demonstrating the importance of PAW_s for winter wheat in the western portion of the southern Great Plains (Norwood, 2000; Stone and Schlegel, 2006), and also agrees with Passioura (2006), who found that radiation rather than rainfall amount is the main limiting factor for wheat yields when cumulative seasonal precipitation >500 mm. The importance of understanding how the meteorology in individual regions dictate crop growth and yield was highlighted by Licker et al. (2013), who compared two contrasting winter wheat growing regions in Europe using multiple regression analysis and concluded that the interannual variability in wheat yields were associated with several meteorological variables observed during the growing cycle in each region, but these variables oftentimes did not overlap between regions. For instance, while a decrease in cumulative precipitation during anthesis and grain filling stages was detrimental to winter wheat yields in a region where growing season precipitation averages 397 mm (i.e. during May in Rostov, Russia); it improved grain yields in a region where growing season precipitation averages 564 mm (i.e. during June in Picardy, France) (Licker et al., 2013).

5.4.3. Wheat WP, TE, and RUE in the southern Great Plains

Wheat yield WP in the southern Great Plains was 20.1 kg ha^{-1} mm^{-1}, ranging from 16 kg ha^{-1} mm^{-1} in the west sub-region, to 24.2 kg ha^{-1} mm^{-1} in the west-central sub-region (Table 5.5). Our results align well with previous research which estimated wheat WP in Bushland, TX, as 16.7 kg ha^{-1} mm^{-1} (Sadras and Angus, 2006), in western Oklahoma as 19 kg ha^{-1} mm^{-1}, and in central-western Oklahoma as 22 kg ha^{-1} mm^{-1} (Patrignani et al., 2014). As expected, wheat yield TE was greater than WP and ranged from 20.2 kg ha^{-1} mm^{-1} in the west sub-region to 25.8 kg ha^{-1} mm^{-1} in the west-central sub-region. The TE derived from boundary functions in our study are lower than the maximum reported wheat TE values (i.e. 27 kg ha^{-1} mm^{-1}) but still are well above the mean wheat TE across the world (i.e. 10.9 kg ha^{-1} mm^{-1}) (Zwart and Bastiaanssen, 2004). Radiation use-efficiency based on incident R_s across the studied region averaged 0.9 g MJ^{-1} and decreased from west to east. Considering the average cumulative R_s across all site years of 3340 MJ m^{-2} and an average non-intercepted R_s of 594 MJ m^{-2} (*x*-intercept), RUE in an intercepted R_s basis was 1.1 g MJ^{-1} in the southern Great Plains. Using this approach for the individual sub-regions, RUE for intercepted R_s ranged from 0.51 g MJ^{-1} in the west to 1.7 g MJ^{-1} in the east. Maximum wheat RUE is 1.4 g MJ^{-1} (Sinclair and Muchow, 1999) but values as high as 1.7 to 1.9 g MJ^{-1} have been reported (Lollato and Edwards, 2015).

5.5. CONCLUSIONS

Simulated rainfed wheat Y_w across the southern Great Plains averaged 6.0 Mg ha^{-1} and increased from west (3.5 Mg ha^{-1}) to east (6.9 Mg ha^{-1}). Simulated wheat Y_w was greater than 9 Mg ha^{-1} and close to the theoretical limit in 6% of the studied site-years, but 75% of the growing seasons the characteristic meteorology of the Great Plains did not allow for Y_w greater than 7.1 Mg ha^{-1}. Strong longitudinal gradients in wheat potential productivity and resource use-efficiency occur in this region, with aboveground biomass and grain yield increasing linearly from 103°W to

98.5°W, and plateauing from 98.5°W to 95°W. Additionally, wheat Y_w variability was larger than other wheat producing regions of the world and interannual CV ranged from 0.11 to 0.5 from east to west. This variability and unpredictability in rainfed Y_w likely renders farmers skeptical when deciding whether to invest in the wheat crop, contributing to the large yield gap (~4.1 Mg ha^{-1}) and yield stagnation in the region. Major meteorological variables affecting wheat yields are water supply (PAW_s and precipitation) which accounts for 81.7% of Y_w variability in the west, and cumulative R_s during the anthesis – physiological maturity which accounts for 86.9% of Y_w variability in the in the east. Temperatures during the anthesis-physiological maturity phase were negatively related to grain yields across all locations and years, and accounted for 13.3% of Y_w variability across the southern Great Plains. Wheat WP and TE were highest in the west-central region of the southern Great Plains, and decreased towards west and east; while RUE increased from west towards east. Wheat WP (19.1 kg ha^{-1} mm^{-1}), TE (24.2 kg ha^{-1} mm^{-1}), and RUE (1.1 g MJ^{-1} based on intercepted R_s) derived as boundary functions in our analyses align well with published literature and can be used as benchmarks for farmers to shoot for to increase yields at a given resource level.

5.6. REFERENCES

Abeledo, L.G., R. Savin and G.A. Slafer. 2008. Wheat productivity in the mediterranean ebro valley: Analyzing the gap between attainable and potential yield with a simulation model. Eur. J. Agron. 28: 541-550.

Aggarwal, P.K. and N. Kalra. 1994. Analyzing the limitations set by climatic factors, genotype, and water and nitrogen availability on productivity of wheat. 2. Climatically potential yields and management strategies. Field Crops Res. 38: 93-103.

Aggarwal, P.K., N. Kalra, A.K. Singh and S.K. Sinha. 1994. Analyzing the limitations set by climatic factors, genotype, water and nitrogen availability on productivity of wheat. 1. The model description, parametrization and validation. Field Crops Res. 38: 73-91.

Allen, R.G., L.S. Pereira, D. Raes and M. Smith. 1998. Crop evapotranspiration: Guidelines for computing crop water requirements. Irrigation and Drainage Paper No. 56, FAO, Rome, Italy.

Armour, T., P. Jamieson, A. Nichols and R. Zyskowski. 2004. Breaking the 15 t/ha wheat yield barrier: A discussion. In: Proceedings of the 4th Intern. Crop Sci. Congress, Brisbaine, Australia. Sept. 26 - Oct. 1.

Asseng, S., I. Foster and N.C. Turner. 2011. The impact of temperature variability on wheat yields. Global Change Biol. 17: 997-1012.

Asseng, S., B.A. Keating, I.R.P. Fillery, P.J. Gregory, J.W. Bowden, N.C. Turner, et al. 1998. Performance of the APSIM-Wheat model in Western Australia. Field Crops Res. 57: 163-179.

Barkley, A., J. Tack, L.L. Nalley, J. Bergtold, R. Bowden and A. Fritz. 2014. Weather, disease, and wheat breeding effects on Kansas wheat varietal yields, 1985 to 2011. Agron. J. 106: 227-235.

Bell, M.A. and R.A. Fischer. 1994. Using yield prediction models to assess yield gains - a case-study for wheat. Field Crops Res. 36: 161-166.

Bushong, J.A., A.P. Griffith, T.F. Peeper and F.M. Epplin. 2012. Continuous winter wheat versus a winter canola-winter wheat rotation. Agron. J. 104: 324-330.

Cade, B.S. and B.R. Noon. 2003. A gentle introduction to quantile regression for ecologists. Front. Ecol. Environ. 1: 412-420.

Canadell, J., R.B. Jackson, J.R. Ehleringer, H.A. Mooney, O.E. Sala and E.D. Schulze. 1996. Maximum rooting depth of vegetation types at the global scale. Oecologia 108: 583-595.

Cassman, K.G., A. Dobermann, D.T. Walters and H. Yang. 2003. Meeting cereal demand while protecting natural resources and improving environmental quality. Annual Review of Environment and Resources 28: 315-358.

Connor, D.J., R.S. Loomis and K.G. Cassman. 2011. Crop ecology: Productivity and management in agricultural systems. Cambridge Univ. Press, Cambridge, UK.

Dormann, C.F., J. Elith, S. Bacher, C. Buchmann, G. Carl, G. Carre, et al. 2013. Collinearity: A review of methods to deal with it and a simulation study evaluating their performance. Ecography 36: 27-46.

Edwards, J.T., B.F. Carver, G.W. Horn and M.E. Payton. 2011. Impact of dual-purpose management on wheat grain yield. Crop Sci. 51: 2181-2185.

Edwards, J.T., R.D. Kochenower, R.E. Austin, M.W. Knori, R.P. Lollato, G. Cruppe, et al. 2013. Oklahoma small grains variety performance tests 2012-2013. CR-2141. Oklah. St. Univ. Coop. Ext. Serv., Stillwater, OK.

Evans, L.T. 1993. Crop evolution, adaptation, and yield. Cambridge University Press, Cambridge, UK.

Fischer, R.A. 2007. Understanding the physiological basis of yield potential in wheat. J. Agric. Sci. 145: 99-113.

Fischer, R.A. and G.O. Edmeades. 2010. Breeding and cereal yield progress. Crop Sci. 50: S85-S98.

Frederick, J.R. and P.J. Bauer. 2000. Physiological and numerical components of wheat yield. In: E. H. Satorre and G. A. Slafer, Eds., Wheat: Ecology and physiology of yield determination. Food Products Press, Binghamton, NY. p. 503.

French, R.J. and J.E. Schultz. 1984. Water-use efficiency of wheat in a mediterranean-type environment.1. The relation between yield, water-use and climate. Aust. J. Agric. Res. 35: 743-764.

Grassini, P., K.M. Eskridge and K.G. Cassman. 2013. Distinguishing between yield advances and yield plateaus in historical crop production trends. Nature Communications 4.

Grassini, P., H.S. Yang and K.G. Cassman. 2009. Limits to maize productivity in Western Corn-Belt: A simulation analysis for fully irrigated and rainfed conditions. Agric. For. Meteorol. 149: 1254-1265.

Hochman, Z., D. Gobbett, D. Holzworth, T. McClelland, H. van Rees, O. Marinoni, et al. 2013. Reprint of "Quantifying yield gaps in rainfed cropping systems: A case study of wheat in Australia". Field Crops Res. 143: 65-75.

Hochman, Z., D. Holzworth and J.R. Hunt. 2009. Potential to improve on-farm wheat yield and WUE in Australia. Crop & Pasture Science 60: 708-716.

Holman, J.D., A.J. Schlegel, C.R. Thompson and J.E. Lingenfelser. 2011. Influence of precipitation, temperature, and 56 years on winter wheat yields in Western Kansas. Crop Management 10: 0-0.

Jamieson, P.D., J.R. Porter and D.R. Wilson. 1991. A test of the computer-simulation model ArchWheat1 on wheat crops grown in New-Zealand. Field Crops Res. 27: 337-350.

Krenzer, E.G. 2000. Production management. In: T. A. Royer and E. G. Krenzer, Eds., Wheat management in Oklahoma. E-831. Oklahoma State Univ. Coop. Ext. Serv., Stillwater, OK. p. 11-18.

Liang, W.L., C. Peter, G.Y. Wang, R.H. Lu, H.Z. Lu and A.P. Xia. 2011. Quantifying the yield gap in wheat-maize cropping systems of the Hebei Plain, China. Field Crops Res. 124: 180-185.

Licker, R., M. Johnston, J.A. Foley, C. Barford, C.J. Kucharik, C. Monfreda, et al. 2010. Mind the gap: How do climate and agricultural management explain the 'yield gap' of croplands around the world? Global Ecol. Biogeogr. 19: 769-782.

Licker, R., C.J. Kucharik, T. Dore, M.J. Lindeman and D. Makowski. 2013. Climatic impacts on winter wheat yields in Picardy, France and Rostov, Russia: 1973-2010. Agric. For. Meteorol. 176: 25-37.

Lingenfelser, J., B. Bockus, E. De Wolf, A. Fritz, M. Knapp, J. Whitworth, et al. 2013. 2013 Kansas performance tests with winter wheat varieties. Rep. of Progress 1090. Kansas St. Res. and Ext., Manhattan, KS.

Lobell, D.B., K.G. Cassman and C.B. Field. 2009. Crop yield gaps: Their importance, magnitudes, and causes. Annual Review of Environment and Resources 34: 179-204.

Lobell, D.B. and J.I. Ortiz-Monasterio. 2006. Evaluating strategies for improved water use in spring wheat with CERES. Agric. Water Manage. 84: 249-258.

Lollato, R.P., and J.T. Edwards. 2015. Maximum attainable winter wheat yield and resource use efficiency in the southern Great Plains. Crop Sci., accepted.

Lollato, R.P., A. Patrignani, T.E. Ochsner, and J.T. Edwards. Prediction of plant available water at sowing for winter wheat in the southern Great Plains. In preparation.

Lu, C.H. and L. Fan. 2013. Winter wheat yield potentials and yield gaps in the North China Plain. Field Crops Res. 143: 98-105.

Menendez, F.J. and E.H. Satorre. 2007. Evaluating wheat yield potential determination in the Argentine Pampas. Agric. Syst. 95: 1-10.

Mueller, N.D., J.S. Gerber, M. Johnston, D.K. Ray, N. Ramankutty and J.A. Foley. 2012. Closing yield gaps through nutrient and water management. Nature 490: 254-257.

Musick, J.T., O.R. Jones, B.A. Stewart and D.A. Dusek. 1994. Water-yield relationships for irrigated and dryland wheat in the US Southern Plains. Agron. J. 86: 980-986.

Nalley, L.L., A.P. Barkley and K. Sayre. 2009. Photothermal quotient specifications to improve wheat cultivar yield component models. Agron. J. 101: 556-563.

Neely, C., A. Ibrahim, J. Rudd, C. Trostle and D. Drake. 2013. 2013 Texas wheat variety trial results. SCSC-2013-06. Texas A&M Agrilife Ext. and Res., College Station, TX.

Norwood, C.A. 2000. Dryland winter wheat as affected by previous crops. Agron. J. 92: 121-127.

Passioura, J. 2006. Increasing crop productivity when water is scarce - from breeding to field management. Agric. Water Manage. 80: 176-196.

Patrignani, A., R.P. Lollato, T.E. Ochsner, C.B. Godsey and J.T. Edwards. 2014. Yield gap and production gap of rainfed winter wheat in the southern Great Plains. Agron. J. 106: 1329 - 1339.

Peake, A.S., N.I. Huth, P.S. Carberry, S.R. Raine and R.J. Smith. 2014. Quantifying potential yield and lodging-related yield gaps for irrigated spring wheat in sub-tropical Australia. Field Crops Res. 158: 1-14.

Sadras, V.O. and J.F. Angus. 2006. Benchmarking water-use efficiency of rainfed wheat in dry environments. Aust. J. Agric. Res. 57: 847-856.

Schierhorn, F., M. Faramarzi, A.V. Prishchepov, F.J. Koch and D. Muller. 2014. Quantifying yield gaps in wheat production in Russia. Environmental Research Letters 9.

Schroder, J.L., H.L. Zhang, K. Girma, W.R. Raun, C.J. Penn and M.E. Payton. 2011. Soil acidification from long-term use of nitrogen fertilizers on winter wheat. Soil Sci. Soc. Am. J. 75: 957-964.

Shroyer, J.P., C. Thompson, R. Brown, P.D. Ohlenbusch, D.L. Fjell, S. Staggenborg, et al. 1996. Kansas crop planting guide. L-818. Kansas St. Univ. Agric. Exp. St. and Coop. Ext. Serv., Manhattan, KS.

Sinclair, T.R. 2013. Transpiration: Moving from semi-empirical approaches to first principles. In: D. Fleisher, Ed. Symposium - Improving tools to assess climate change effects on crop response: Modeling approaches and applications: I. ASA, CSSA, and SSSA, Tampa, FL. Available at: https://dl.sciencesocieties.org/publications/meetings/2013am/11501 (verified 01 April 2015).

Sinclair, T.R. and R.C. Muchow. 1999. Radiation use efficiency. Adv. Agron. 65: 215-265.

Slafer, G.A., F.H. Andrade and E.H. Satorre. 1990. Genetic-improvement effects on preanthesis physiological attributes related to wheat grain-yield. Field Crops Res. 23: 255-263.

Soltani, A., V. Maddah and T.R. Sinclair. 2013. SSM-Wheat: A simulation model for wheat development, growth, and yield. International Journal of Plant Production 7: 711-740.

Soltani, A. and T.R. Sinclair. 2012. Modeling physiology of crop development, growth and yield. CAB International, Cambridge, MA.

Soltani, A. and T.R. Sinclair. 2015. A comparison of four wheat models with respect to robustness and transparency: Simulation in a temperate, sub-humid environment. Field Crops Res. 175: 37-46.

Stone, L.R. and A.J. Schlegel. Yield-water supply relationships of grain sorghum and winter wheat. Agron. J. 98: 1359-1366.

Tanner, C.B. and T.R. Sinclair. 1983. Efficient water use in crop production: Research or re-search? In: H. M. Taylor, W. R. Jordan and T. R. Sinclair, Eds., Limitations to efficient water use in crop production. ASA-CSSA-SSSA, Madison, WI. p. 1-27.

USDA-NASS. 2010. Field crops - usual planting and harvesting dates. United States Department of Agriculture - National Agricultural Statistics Service. Agricultural Handbook N. 628. Washington, DC.

USDA-NASS. 2013. United States Department of Agriculture - National Agricultural Statistics Service cropland data layer. Published crop-specific data layer for the 2013 season [online]. Available at: http://datagateway.nrcs.usda.gov/gdghome_statusmaps.aspx. Accessed 30 July 2014.

USDA-NASS. 2014. United States Department of Agriculture. National Agricultural Statistics Service. Available at: http://www.nass.usda.gov/Statistics_by_State/Oklahoma/Publications/County_Estimates/index.asp (data retrieved July 2014).

USDA-NRCS. 2014a. Official soil series descriptions. Soil Survey Staff. USDA-NRCS, Lincoln, NE. https://soilseries.sc.egov.usda.gov/osdname.asp (accessed 26 June 2014).

USDA-NRCS. 2014b. Web soil survey. Soil survey staff. USDA-NRCS, Lincoln, NE. Available at: http://websoilsurvey.sc.egov.usda.gov/App/HomePage.htm (accessed 26 June 2014).

Van Ittersum, M.K., K.G. Cassman, P. Grassini, J. Wolf, P. Tittonell and Z. Hochman. 2013. Yield gap analysis with local to global relevance-a review. Field Crops Res. 143: 4-17.

Van Wart, J., P. Grassini and K.G. Cassman. 2013a. Impact of derived global weather data on simulated crop yields. Global Change Biol. 19: 3822-3834.

Van Wart, J., P. Grassini, H. Yang, L. Claessens, A. Jarvis and K.G. Cassman. 2015. Creating long-term weather data from thin air for crop simulation modeling. Agric. For. Meteorol. 209: 49-58.

Van Wart, J., K.C. Kersebaum, S.B. Peng, M. Milner and K.G. Cassman. 2013b. Estimating crop yield potential at regional to national scales. Field Crops Res. 143: 34-43.

Wardlaw, I.F. 1994. The effect of high-temperature on kernel development in wheat - variability related to pre-heading and postanthesis conditions. Aust. J. Plant Physiol. 21: 731-739.

Xue, Q., Z. Zhu, J.T. Musick, B.A. Stewart and D.A. Dusek. 2003. Root growth and water uptake in winter wheat under deficit irrigation. Plant Soil 257: 151-161.

Zwart, S.J. and W.G.M. Bastiaanssen. 2004. Review of measured crop water productivity values for irrigated wheat, rice, cotton and maize. Agric. Water Manage. 69: 115-133.

Table 5.1. Dataset of winter wheat yields with no apparent limitation used for validation and testing of model robustness for the SSM - Wheat crop simulation model across the southern Great Plains.

State	Location	Planting year	n	Yield	Source
				Mg ha^{-1}	
OK	Altus	2013	1	1.7	Edwards et al., 2012
	Apache	2012, 2013	2	3.8-4.6	Edwards et al., 2012; 2013
	Balko	2007	1	6.6	Edwards et al., 2008
	Chickasha	2013	1	3.5	Edwards et al., 2013
	Lahoma	2002, 2007, 2011, 2012, 2013	5	4.8-6.1	Edwards et al., 2012 - 2014; Raun et al., 2011
	Marshall	2012, 2013	2	1.8-4.0	Edwards et al., 2013; 2014
	McLoud	2011, 2012, 2013	3	2.5 - 5.2	Edwards et al., 2012 - 2014
KS	Belleville	2011, 2012, 2013	3	5.8-7.1	Lingenfelser et al., 2012 - 2014
	Garden City	2012	1	1.8	Lingenfelser et al., 2012
	Hays	2011, 2012, 2013	3	3.1-5.0	Lingenfelser et al., 2012 - 2014
	Hutchinson	2011, 2012, 2013	3	3.3 - 4.3	Lingenfelser et al., 2012 - 2014
	Manhattan	2011, 2012, 2013	3	3.4 - 4.9	Lingenfelser et al., 2012 - 2014
	Ottawa	2011, 2012, 2013	3	4.7 - 6.5	Lingenfelser et al., 2012 - 2014
	Parsons	2011, 2012, 2013	3	3.3 - 6.3	Lingenfelser et al., 2012 - 2014
	Tribune	2011, 2012, 2013	3	3.0-4.1	Lingenfelser et al., 2012 - 2014

Table 5.2. Dataset for analysis of winter wheat yield potential using 1986 – 2014 weather data across 37 locations in the southern Great Plains. Soil dataset comprises dominant soil series and soil texture, percent of agricultural land represented by the dominant soil series, plant available water capacity (PAWC), and volumetric water content at the lower limit (θ_{LL}) of the dominant soil series. Management dataset comprises typical planting date and plant population for each location. Altitude (Alt.) is also shown.

State†	Location	Alt.	Dominant soil series	Dominant soil texture	Agricultural land‡	θ_{LL}§	PAWC¶	Planting date	Plant population
		m			%	$m^3\ m^{-3}$		DOY	million plants ha^{-1}
TX	Haskell	488	Abilene	Clay Loam	25	0.22	0.18	293	1.91
	Quanah	488	Tillman	Clay Loam	32	0.23	0.15	293	1.91
	Muleshoe	1167	Olton	Clay Loam	56	0.20	0.18	293	1.65
	Brownwood	427	Frio	Silty Clay Loam	16	0.23	0.17	303	1.91
	Crosbyton	917	Olton	Loam	69	0.19	0.18	293	1.91
	Paris	165	Houston Black	Clay	46	0.32	0.17	287	3.52
OK	Alva	439	Pond Creek	Silt Loam	15	0.16	0.19	284	2.82
	Beaver	758	Darrouzett	Clay Loam	21	0.20	0.16	274	1.91
	Bessie	511	St. Paul	Silt Loam	25	0.18	0.20	281	2.93
	Blackwell	304	Kirkland	Silt Loam	32	0.21	0.17	284	2.82
	Boise City	1267	Sherm	Clay Loam	70	0.25	0.16	274	1.91
	El Reno	419	Bethany	Silt Loam	20	0.20	0.19	285	3.19
	Fort Cobb	422	Pond Creek	Fine Sandy Loam	23	0.15	0.16	285	3.19
	Grandfield	341	Westview-Hinkle	Silt Loam	12	0.17	0.20	287	2.97
	Haskell	183	Dennis	Silt Loam	26	0.15	0.20	287	3.52
	Hobart	478	Hollister	Silty Clay Loam	36	0.23	0.17	281	2.93
	Kingfisher	323	Milan	Fine Sandy Loam	24	0.13	0.17	285	3.19
	Lahoma	396	Pond Creek	Silt Loam	39	0.16	0.19	284	2.82
	Marshall	311	Kirkland-Renfrow	Silt Loam	18	0.21	0.17	284	2.82
	Medford	332	Kirkland	Silt Loam	56	0.22	0.16	284	2.82
	Miami	247	Taloka	Silt Loam	31	0.17	0.20	287	3.52
	Putnam	589	St. Paul	Silt Loam	32	0.18	0.20	281	2.93
	Seiling	545	Carey	Silt Loam	44	0.15	0.18	284	2.82
	Stillwater	272	Stephenville-Darnell	Fine Sandy Loam	25	0.12	0.16	285	3.19
	Watonga	517	Lovedale	Fine Sandy Loam	23	0.11	0.14	281	2.93
	Woodward	625	Mansic	Loam	27	0.15	0.17	274	1.91
KS	Garden City	882	Richfield	Silt Loam	31	0.17	0.19	275	1.83
	Hays	619	Harney	Silt Loam	35	0.17	0.21	275	1.83
	Hutchinson	479	Shellabarger	Sandy Loam	24	0.10	0.16	281	2.48
	Manhattan	332	Tully	Silty Clay Loam	6	0.24	0.19	281	2.48
	Ottawa	299	Kenoma	Silt Loam	26	0.22	0.18	281	2.48
	Parsons	288	Kenoma	Silt Loam	21	0.22	0.18	288	2.48
	Rossville	276	Pawnee	Clay Loam	15	0.22	0.16	281	2.48
	Scandia	457	Crete	Silt Loam	36	0.15	0.19	275	2.02
	Silver Lake	271	Pawnee	Clay Loam	18	0.22	0.16	281	2.48
	St. John	587	Saltcreek and Naron	Fine Sandy Loam	15	0.13	0.17	281	2.02
	Tribune	1123	Richfield	Silt Loam	57	0.18	0.19	263	1.83

† USA state (TX: Texas; OK: Oklahoma; KS: Kansas).
‡ Percentage of total agricultural land in the study area (~400 km^2) represented by the dominant soil series. Data derived from Web Soil Survey database (Soil Survey Staff, 2014).
§ Volumetric water content at the lower limit (-1500 kPa) for the 0-120 cm soil layer. Data derived from Web Soil Survey database (Soil Survey Staff, 2014).
¶ Available water holding capacity in the 120-cm depth soil profile. Data derived from Web Soil Survey database (Soil Survey Staff, 2014).

Table 5.3. Pearson's correlation coefficient between winter wheat grain yield and meteorological variables observed during the intervals: sowing to physiological maturity (S-PM); sowing to anthesis (S-A); anthesis-physiological maturity (A-PM); and stem elongation to anthesis (SE-A). Analyses were performed for all site-years (Southern Great Plains) and for individual sub-regions. Number of site-years included in the analysis (*n*) is also shown.

	Southern Great	Sub-region			
Environmental factor	Plains	West	West-central	East-central	East
Precipitation (mm)					
S-PM	0.63***	0.72***	0.71***	0.44***	0.25***
S-A	0.54***	0.50***	0.55***	0.36***	0.21**
A-PM	0.50***	0.57***	0.62***	0.33***	0.16*
SE-A	0.51***	0.51***	0.58***	0.45***	0.14*
Cumulative radiation (MJ m^{-2})					
S-PM	-0.18***	-0.18*	-0.05	0.36***	0.25***
S-A	-0.32***	-0.25**	-0.2**	0.17**	0.01
A-PM	0.5***	0.3***	0.63***	0.78***	0.81***
SE-A	0.08*	0.11	0.17**	0.44***	0.59***
Mean temperature (°C)					
S-PM	0.39***	0.29***	0.2***	0.42***	0.62***
S-A	0.32***	0.27***	0.17**	0.42***	0.63***
A-PM	-0.29***	-0.24**	-0.33***	-0.54***	-0.67***
SE-A	-0.18***	-0.08	-0.26***	-0.32***	-0.41***
Maximum temperature (°C)					
S-PM	-0.09**	-0.03	-0.11	0.2**	0.54***
S-A	-0.09**	-0.01	-009	0.23***	0.55***
A-PM	-0.56***	-0.48***	-0.55***	-0.57***	-0.63***
SE-A	-0.39***	-0.22**	-0.41***	-0.38***	-0.38***
Minimum temperature (°C)					
S-PM	0.65***	0.57***	0.48***	0.46***	0.59***
S-A	0.6***	0.51***	0.41***	0.45***	0.61***
A-PM	0.04	0.14	-0.04	-0.44***	-0.66***
SE-A	0.06	0.08	-0.06	-0.23***	-0.43***
Reference ET (mm)					
S-PM	-0.49***	-0.31***	-0.31***	-0.06	-0.16*
S-A	-0.57***	-0.33***	-0.39***	-0.25***	-0.35***
A-PM	0.01	-0.16	0.17**	0.45***	0.4***
SE-A	-0.17***	-0.01	0.01	0.24***	0.36***
PQ (MJ m^{-2} d^{-1} °C^{-1})†	0.02	-0.1	0.09	0.37***	0.57***
PAW_s (mm) ‡	0.22***	0.42***	0.02	0.1	0.33***
n	870	144	259	265	202

*, **, and *** - Correlation significant at $p < 0.05$, 0.01, and 0.001, respectively.

† - PQ, photothermal quotient.

‡ - PAW_s, plant available water at sowing.

Table 5.4. Multiple regression analysis for water-limited grain yield as affected by meteorological variables during different intervals within the growing season for all simulated site-years (Southern Great Plains, n = 870) and for each individual sub-region. Independent variables are precipitation (Precip.), cumulative solar radiation (R_s), maximum (T_{max}), mean (T_{mean}), and minimum temperatures (T_{min}), cumulative reference evapotranspiration (ET_o), and plant available water at sowing (PAW_s).

					Sub-region							
	Southern Great Plains				West				West-central			
Meteorological variable	d.f.	SS type I	% of SS	F-test	d.f.	SS type I	% of SS	F-test	d.f.	SS type I	% of SS	F-test
Precip. (S-A) †	1	1082	37.3	1163.2***	1	87	29.9	217.0***	1	297	36.6	461.6***
Precip. (A-PM)‡	1	422	14.6	454.1***	1	109	37.4	271.1***	1	240	29.6	372.3***
R_s (S-A)	1	49	1.7	53.0***	-§	-	-	-	1	40	4.9	61.9***
R_s (A-PM)	1	856	29.5	920.6***	1	9	3.3	23.6***	1	124	15.3	193.1***
T_{max} (A-PM)	1	204	7.0	219.6***	1	3	0.9	6.8**	1	70	8.6	108.2***
T_{min} (S-A)	1	77	2.6	82.6***	1	36	12.3	89.1***	-	-	-	-
T_{min} (A-PM)	1	183	6.3	196.3***	1	5	1.8	12.8***	1	19	2.4	30.0***
PAW_s	1	28	1.0	30.3***	1	42	14.4	104.6***	1	21	2.6	32.5***
Residuals	861	801			136	55			251	161		
Total	869	3702			143	346			258	972		
					East-central				East			
					d.f.	SS type I	% of SS	F-test	d.f.	SS type I	% of SS	F-test
Precip. (S-A)					1	103	17.1	135.8***	-	-	-	-
Precip. (A-PM)					1	54	8.9	70.9***	-	-	-	-
R_s (S-A)					-	-	-	-	1	0	<0.1	0
R_s (A-PM)					1	397	66.3	525.9***	1	313	86.9	669.5***
T_{mean} (S-A)					-	-	-	-	1	24	6.5	50.3***
T_{mean} (A-PM)					1	45	7.6	60.1***	1	23	6.5	50.2***
Residuals					260				197			
Total					264	598			201	360		

, * - Significant at $p < 0.01$ and 0.001, respectively.

† S-A: period that encompasses sowing to anthesis.

‡ A-PM: period that encompasses anthesis to physiological maturity.

§ -: meteorological variable was not significant in the final regression model.

Table 5.5. Wheat water productivity (WP) and transpiration efficiency (TE) calculated based on aboveground biomass or grain yield pooled across 37 locations in the southern Great Plains, or divided in four sub-regions following the longitudinal yield gradient: west, west-central, east-central, and east. Average water losses in the growing season are also shown.

	Aboveground biomass			Grain yield		Water losses†	
Region	WP‡	TE§	RUE¶	WP	TE	WP	TE
	kg ha^{-1} mm^{-1}		g MJ^{-1}	kg ha^{-1} mm^{-1}		mm	
Southern Great Plains	33.4 ± 3.5	44.8 ± 3.9	0.86 ± 0.07	19.1 ± 1.3	24.2 ± 1.6	76	77
West	38.7 ± 4.1	45.5 ± 3.1	0.43 ± 0.45	16.0 ± 1.9	20.2 ± 1.8	98	103
West-central	41.3 ± 5.7	46.4 ± 4.2	0.69 ± 0.11	24.2 ± 3.1	25.8 ± 1.9	160	110
East-central	38.0 ± 3.1	50.2 ± 7.7	0.80 ± 0.07	17.8 ± 4.5	24.4 ± 2.9	48	91
East#	23.1 ± 8.9	42.5 ± 6.1	1.15 ± 0.10	10.2 ± 4.8	22.5 ± 2.9	-	32

† Water losses during the growing season, estimated as the x-intercept of the relationship between grain yield and growing season water supply or simulated crop evapotranspiration.

‡ Water productivity, estimated as the slope of the relationship between grain yield and growing season water supply (plant available water at sowing plus precipitation).

§ Transpiration efficiency, estimated as the slope of the relationship between grain yield and simulated crop evapotranspiration in the growing season.

¶ Radiation use efficiency, estimated as the slope of the relationship between aboveground biomass and cumulative incident solar radiation during the growing season.

WP, TE, and water losses calculated for the east sub-region should be used with care, as the methodology we use was developed for wheat grown in regions where growing season rainfall < 500 mm and may not be accurate for regions with consistently greater total water supply such as the east sub-region of the southern Great Plains.

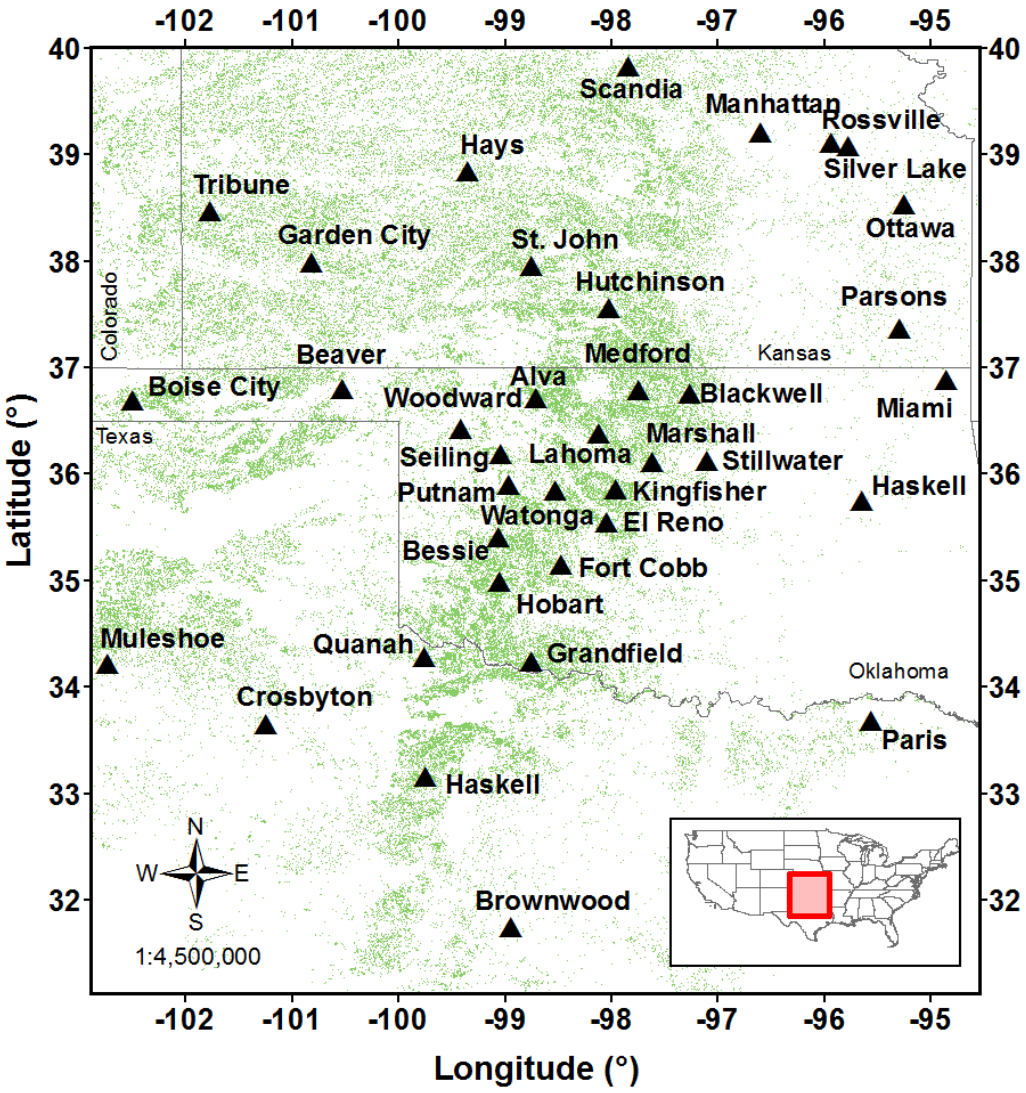

Figure 5.1. Map of the southern Great Plains showing wheat area in green (source: USDA-NASS (2013)). Locations where the long term simulations were performed are represented by black triangles. State name and boundaries are also shown. Inset shows location of study area within the continental U.S.A.

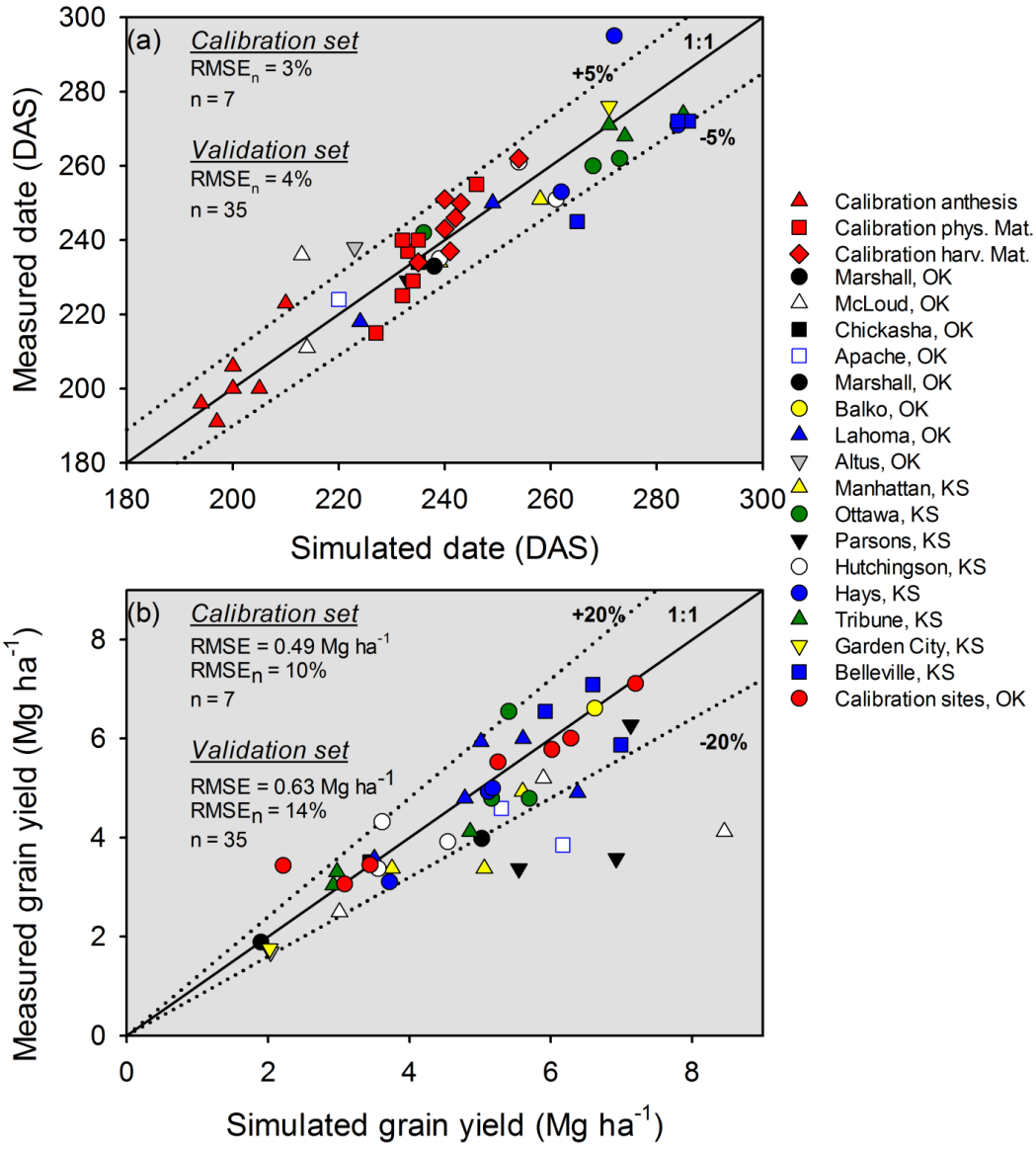

Figure 5.2. Calibration and validation of the SSM-Wheat model for (a) phenology (i.e. dates for anthesis, physiological maturity, and harvest maturity) and (b) grain yield for wheat grown under non-limiting conditions in the southern Great Plains (see Table 5.1 for more details). Solid diagonal line shows 1:1 relationship; dotted lines show ±5% and ±20% deviation from 1:1 line for panels (a) and (b), respectively. Average and normalized root mean square errors (RMSE and $RMSE_n$) for model calibration and validation are also shown.

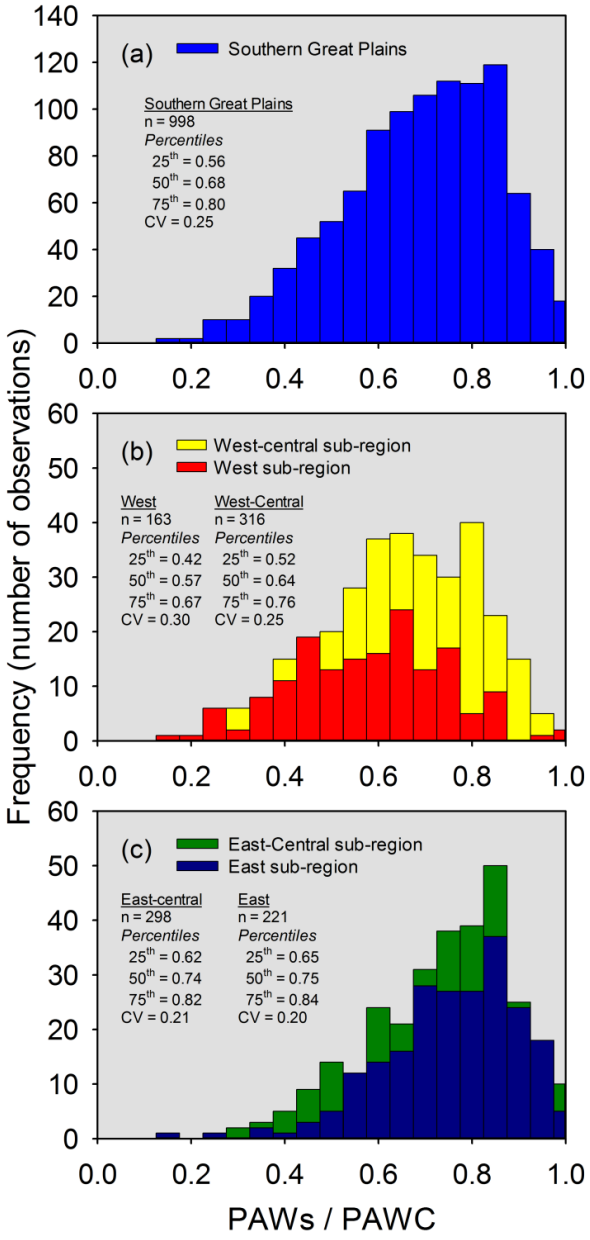

Figure 5.3. Frequency distribution of simulated plant available water at sowing (PAW_s) normalized by the soil's plant available water capacity (PAWC) for (a) all simulated site-years across the southern Great Plains; (b) west and west-central sub-regions; and (c) east-central and east sub-regions. Number of site-years (*n*); 25th, 50th, and 75th percentiles, as well as coefficient of variation (CV) of simulated PAW_s /PAWC are also shown. Simulation of PAW_s was performed based on summer fallow cumulative precipitation (Lollato, *in preparation*).

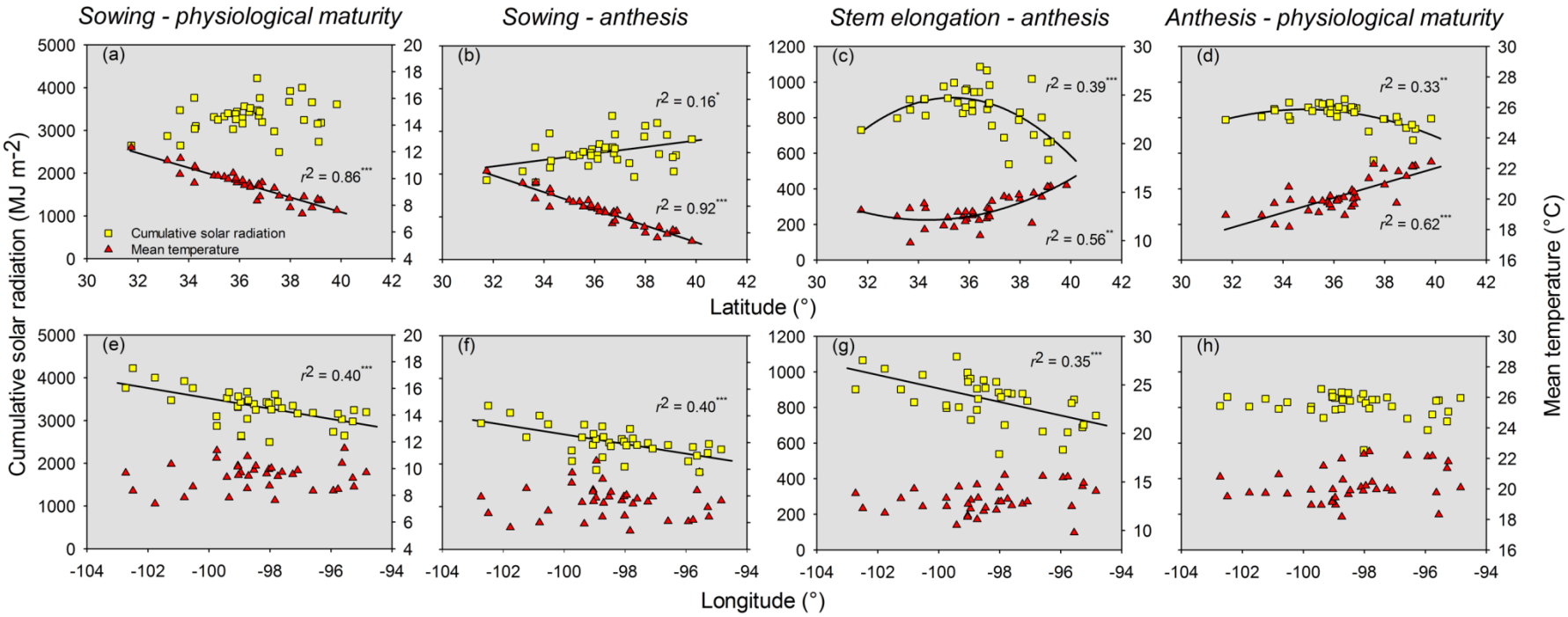

Figure 5.4. Gradients of cumulative solar radiation and mean temperature as affected by latitude (a - d) and longitude (e - h) for the intervals: sowing to physiological maturity (a/e), sowing to anthesis (b/f), stem elongation to anthesis (c/g), and anthesis to physiological maturity (d/h). Points are 28-yr means for a given location excluding years when freeze occurred during the period between simulated stem elongation and termination of seed growth. Symbols *, **, and *** indicate significance at $p < 0.05$, 0.01, and 0.001, respectively.

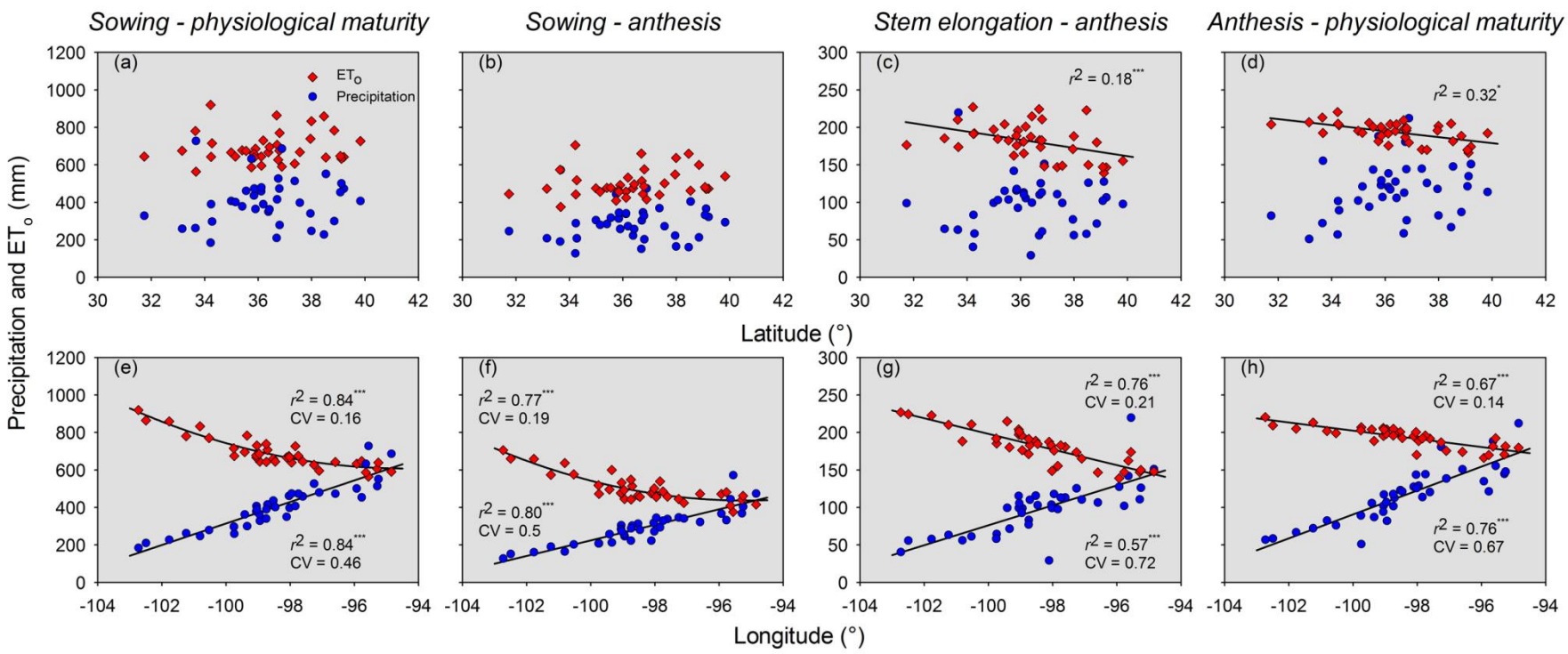

Figure 5.5. Gradients of cumulative precipitation and cumulative reference evapotranspiration (ETo) as affected by latitude (a - d) and longitude (e - h) for the intervals: sowing to physiological maturity (a/e), sowing to anthesis (b/f), stem elongation to anthesis (c/g), and anthesis to physiological maturity (d/h). Points are 28-yr means for a given location excluding years when freeze occurred during the period between simulated stem elongation and termination of seed growth. Symbols *, **, and *** indicate significance at $p < 0.05$, 0.01, and 0.001, respectively.

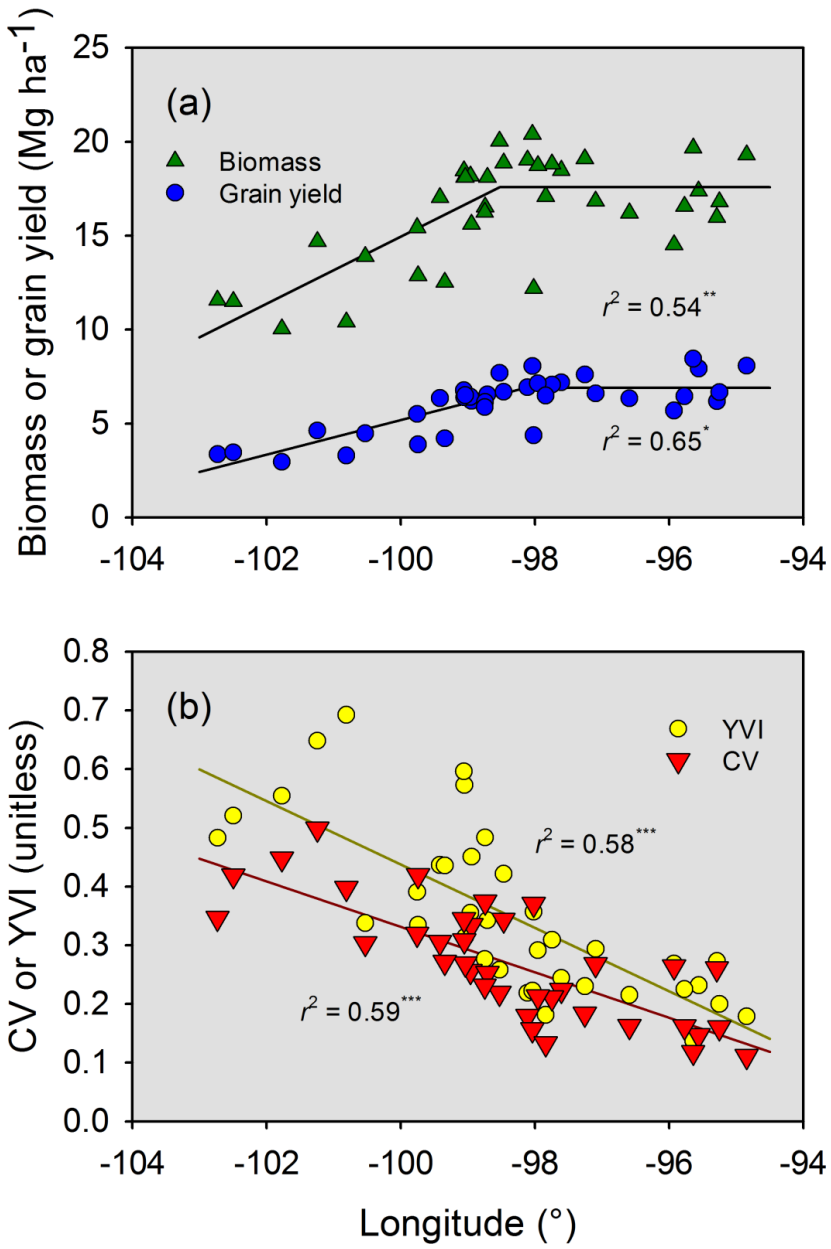

Figure 5.6. Longitudinal gradients of (a) wheat aboveground biomass and grain yield, and (b) coefficient of variation of simulated yield (CV) and yield variance index (YVI). Points are 28-yr means for a given location excluding years when freeze occurred during the period between simulated stem elongation and termination of seed growth. Symbols *, **, and *** indicate significance at $p < 0.05$, 0.01, and 0.001, respectively.

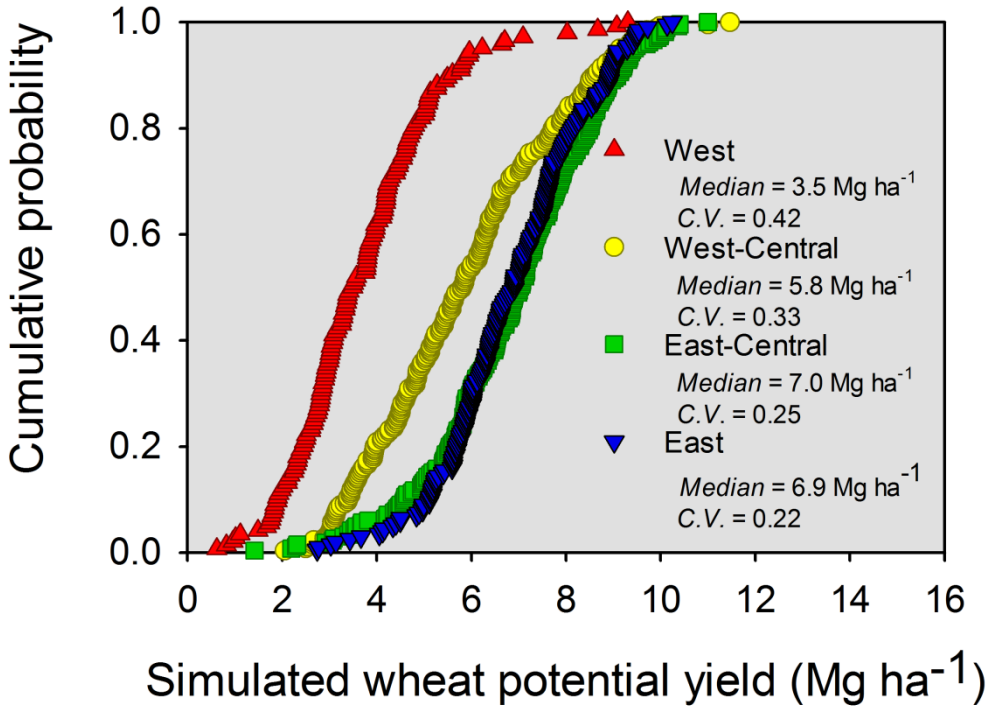

Figure 5.7. Cumulative probability for simulated wheat yield potential in the west (n = 144), west-central (n = 259), east-central (n = 265), and east (n = 202) regions of the southern Great Plains during 28 consecutive growing seasons (1986 – 2014) excluding site-years when freeze occurred during the period between simulated stem elongation and termination of seed growth. Median and coefficient of variation (C.V.) of yields simulated within each region are shown.

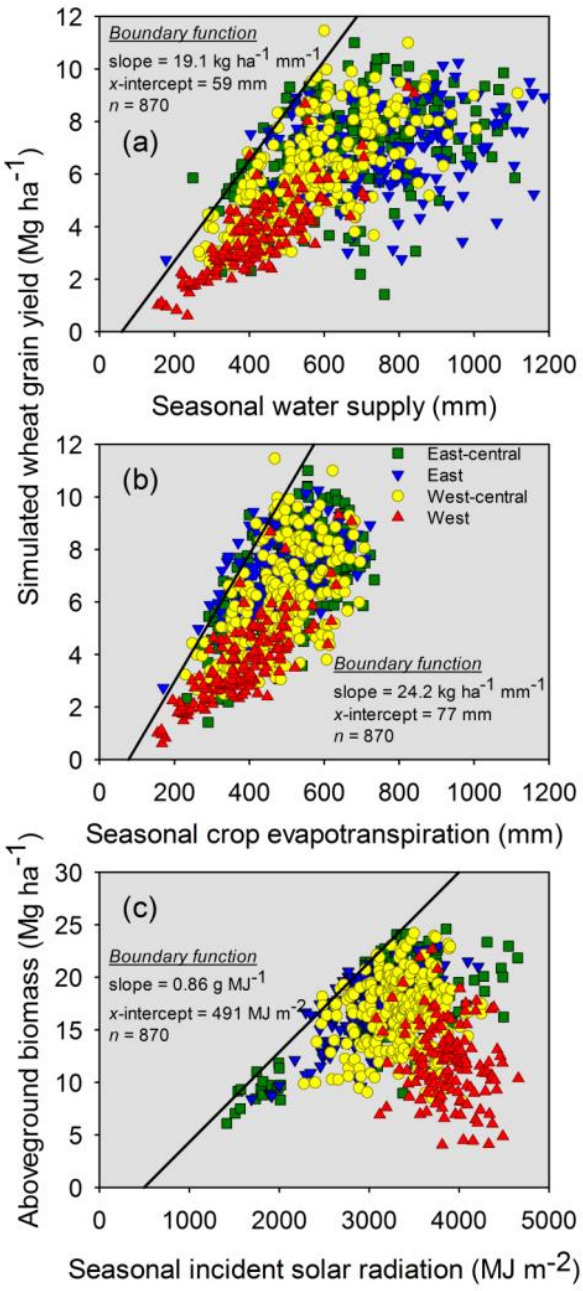

Figure 5.8. Relationships between simulated wheat Y_w and (a) seasonal water supply (PAW_s + precipitation) or (b) simulated seasonal ET_c in the southern Great Plains, and (c) simulated aboveground biomass and seasonal incident R_s. Solid lines are boundary functions for (a) WP, (b) TE, and (c) RUE pooled across the four sub-regions: west (*n* = 144), west-central (*n* = 259), east-central (*n* = 265), and east (*n* = 202). Slopes and *x*-intercepts of the boundary functions are shown. Site-years when freeze occurred

during the period between simulated stem elongation and termination of seed growth were excluded from these analyses.

CHAPTER VI

CONCLUSIONS

6.1. RESEARCH FINDINGS AND CONCLUSIONS

Previous research demonstrated that wheat yield in the southern Great Plains are at a near stagnant state (Patrignani et al., 2014). Yield stagnation in many regions of the world often occurs due to a small difference between regional yield potential and average farmer yield (Grassini et al., 2013). However, this dissertation showed that in the southern Great Plains, yield stagnation is more likely due to a combination of edaphic and meteorological constraints, in addition to typical management practices adopted for hard red winter wheat grown in the region.

Edaphic constraints to winter wheat grown in the southern Great Plains have been suggested as highly erodible soils, adoption of conventional tillage techniques, and the consequent loss of topsoil quality due to soil losses (Patrignani et al., 2014). Additionally, a summary of 61,500 soil samples analyzed by the Soil, Water, and Forage Analytical Laboratory at Oklahoma State University between 2009 and 2013 indicates that 23.8% of the samples resulted in soil pH < 5.5 (Zhang and McCray, 2014), which is considered critical to wheat growth and development. Thus, there is indication that acidic soils may also be contributing to the wheat yield stagnation in the region (Chapter II). This dissertation explored the extent to which acidic soils are contributing to decreased wheat yields in the region under both grain only and dual purpose managements, and evaluated varietal sensitivity to low soil pH and soil Al toxicity to

assess the viability of variety selection as a cost-effective method to overcome low soil pH.

In Chapter II, wheat forage and grain yields were significantly reduced by acidic soils. Threshold pH below which wheat forage and grain yields were reduced were variety-specific, indicating a good potential for variety selection to be used as a method to overcome the negative impacts of acidic soils to a certain extent. Wheat grain yield was shown to be less sensitive to low soil pH than wheat forage yield, with minimum threshold pH for maximum relative grain yields ranging from 4.8 to 5.8 while this range shifted to 5.5 to 6.0 for maximum forage yield. As a consequence, the dual-purpose wheat systems, which are characteristic of approximately half of Oklahoma's wheat cropland (True et al., 2001), is more affected by acidic soils than grain-only due to the cumulative effects of less forage yield at low pH soils and decreased grain yield due to grazing (Edwards et al., 2011).

We demonstrated that forage and grain yields are reduced in acidic soils by lower percent emergence and greater stand variability under low pH / high Al concentration, as well as by a delayed canopy development and decreased maximum percent canopy coverage. Plant population homogeneity is an important factor to be considered when taking mid-season N fertilization decisions for wheat (Arnall et al., 2006). This research showed that acidic soils decrease plant population homogeneity as a minimum pH of 4.5 was needed for wheat to obtain NDVI CV = 17%, and a pH of 4.9 was needed for better stand establishment. Additionally, this research demonstrated that soil acidity not only decreases maximum percent canopy cover, but also delays the increase in the rate of canopy development, which had not been previously reported in the literature. Overall, the findings from Chapter II of this dissertation indicate that while soil pH may be contributing to the observed yield stagnation in the southern Great Plains, wheat variety selection can be an effective method to improve wheat productivity on acid soils with pH > 5.5 when under dual purpose management, and pH > 4.8 when under grain only management. At pH levels below that threshold, other acidity amelioration practices are recommended.

Beyond the edaphic constraints to wheat yield in the region, this dissertation also explored management practices and meteorological factors that might be culminating in the observed yield stagnation. Results from research evaluating wheat grown under intensive management (i.e. non-limiting conditions) at eleven site-years indicate that maximum attainable wheat yields in Oklahoma range from 3.1 to 7.1 Mg ha^{-1} under rainfed conditions, and can reach 7.7 Mg ha^{-1} under irrigated conditions (Chapter IV). These results simultaneously indicate that farmers may not seek the maximum attainable yield in the region, as the yield range 7.1 to 7.7 Mg ha^{-1} is substantially above farmers yield (~2 Mg ha^{-1}); and that the reason for farmers not seeking this yield potential may be the extreme weather conditions leading to great year-to-year variability, evidenced by yields of 7.1 Mg ha^{-1} in 2012-13 followed by 3.1 Mg ha^{-1} under the same management practices in 2013-14.

Evaluation of meteorological dictators of maximum wheat yields with measured yield data in this region indicate that cumulative precipitation and photothermal quotient in the 31-d immediately prior to anthesis are coarse regulators of wheat yields, whereas incident solar radiation during the anthesis to physiological maturity phase is a fine regulator of wheat yield in the absence of water deficit. Comparison of these results with wheat grown in other regions of the world suggest that maximum attainable yields in the southern Great Plains are below those achieved in the United Kingdom (i.e. 10.4 Mg ha^{-1}; Fischer and Edmeades, 2010) or New Zealand (i.e. 15.5 Mg ha^{-1}; Armour et al., 2004) likely due to lower incident solar radiation and higher temperatures during the anthesis – physiological maturity interval, shorter and warmer grain filling period resulting in low HI, and a greater protein concentration in hard red winter wheat grown in the southern Great Plains relative to feed wheat (New Zealand) or soft wheat (United Kingdom) classes. Field research of maximum attainable wheat yield in this dissertation also provides empirical evidence for maximum RUE of 1.9 g MJ^{-1}, which is comparable to the highest RUE reported in the world literature for wheat (i.e. 1.8 g MJ^{-1}; Latiri-Souki et al., 1998), and

WUE of 12.6 kg ha^{-1} mm^{-1}, which is still well below values derived from boundary function analysis (Passioura, 2006; Patrignani et al., 2014; Sadras and Angus, 2006).

This dissertation also provided a long-term (28-yr) assessment of meteorological factors dictating wheat yields across 37 locations in the southern Great Plains using a simulation analysis. Overall, Chapter V of the dissertation established the limits to winter wheat productivity in the southern Great Plains. Simulated yield potential for the entire region spanning the time period 1986 to 2014 was 6 Mg ha^{-1}, and increased linearly with a decrease in longitude from 3.5 Mg ha^{-1} at 104°W to 7.0 Mg ha^{-1} at 98.5°W, plateauing at 7.0 Mg ha^{-1} east until 95°W. Conversely, interannual variability in grain yields was much greater in the west as compared to the east, with year-to-year CV as great as 0.5. These yield variabilities are much greater those measured in other regions of the world where wheat yields are greater, such as the interannual CV of 0.05 for wheat in Germany (Van Wart et al., 2015). The high uncertainty in yield potential, indicated by the great CV across most of the wheat producing region of the southern Plains, most likely render producers reluctant when investing in the wheat crop directly reducing wheat yield potential due to sub-optimal management, which may be contributing to the observed yield stagnation.

Meteorological constraints to maximum wheat yields based on simulation analysis (Chapter V) were remarkably similar to those analyzed using field collected data (Chapter IV). Across the whole studied region, precipitation accounted for 51.9% of the variability in grain yields whereas solar radiation during the anthesis – physiological maturity interval accounted for 29.5%. In the field study shown in Chapter IV, precipitation was considered a coarse regulator of wheat yield whereas solar radiation during the reproductive stages, a fine regulator in the absence of water deficit stress. The relative importance of water supply (precipitation and plant available water at sowing) on wheat yield potential decreased from 81.7% in the west to null in the east, opposite of the trend for importance of solar radiation during the anthesis – physiological

maturity interval (3.3 to 86.9%). These findings agree with Passioura (2006) who suggested wheat yields become radiation-limited when growing season precipitation exceeds ~500mm, typical in the eastern portion of the southern Great Plains. Temperatures during the anthesis – physiological maturity interval had a negative impact on wheat grain yields regardless of the studied sub-region, which is supported by a wealth of literature studying the effects of temperatures during the reproductive stages on wheat yields (Calderini et al., 1999a; Calderini et al., 1999b; Fischer, 2007; Wiegand and Cuellar, 1981).

Chapter V also established benchmarks for water productivity and transpiration efficiency that can be used by farmers and crop consultants who seek to maximize yields at a certain amount of water supply. Water productivity of 870 simulated site-years in the southern Great Plains was 19.1 kg ha^{-1} mm^{-1} and transpiration efficiency, 24.2 kg ha^{-1} mm^{-1}. Both parameters followed a quadratic shape, with greatest values on the west-central region and decreasing towards east and west, agreeing well with previously published literature for the region (Patrignani et al., 2014; Sadras and Angus, 2006). These benchmarks of water productivity can be translated into useful tools for farmers and crop consultants as data needed for comparison are easily collectable (grain yield and seasonal water supply), and farmer's field water productivity can be compared to be benchmark to identify limiting factors and evaluate management strategies to produce more harvestable grain yield with the same amount of resource.

Appropriate evaluation of the system's water productivity was only possible with reliable estimates of plant available water at sowing, as initiating crop simulation models with differing initial PAW_s can lead to different estimates of water productivity (Grassini et al., 2009). In Chapter III of this dissertation, we demonstrated that initializing mechanistic soil water balance models at the start of the preceding summer fallow using a lognormally distribution of PAW following wheat harvest with mean in the dry range of PAWC allows for acceptable predictions

of PAW_s and uncertainty estimation for wheat in the southern Great Plains, which eliminates the need for subjective PAW_s values that can lead to errors in estimations of yield and water productivity. Also, we developed non-linear models to predict PAW_s based on non-growing season precipitation total and the soil's plant available water capacity, which had slightly inferior but acceptable performances in predicting PAW_s when compared to the mechanistic model dual K_c.

Overall, these research findings suggest that the yield stagnation in the southern Great Plains can be partially explained by the high year-to-year variability in grain yield potentials, which renders farmers skeptical when adopting improved management practices (Connor et al., 2011) and restricts maximum attainable yields. Instead, farmers may seek to maximize profitability and may not manage the crop for maximum yields as in other regions of the world such as the United Kingdom where yield potential is greater and less variable (Fischer and Edmeades, 2010). In this reduced-input farming system, variety selection can be the used as a cost-effective method to overcome acidic soil problems for soils with pH > 4.8 (grain only) or 5.5 (dual purpose) and avoid expenses and uncertain returns associated with liming.

6.2. REFERENCES

Armour, T., P. Jamieson, A. Nichols and R. Zyskowski. 2004. Breaking the 15 t/ha wheat yield barrier: A discussion. In: Proceedings of the 4th Intern. Crop Sci. Congress, Brisbaine, Australia. Sept. 26 - Oct. 1.

Arnall, D.B., W.R. Raun, J.B. Solie, M.L. Stone, G.V. Johnson, K. Girma, et al. 2006. Relationship between coefficient of variation measured by spectral reflectance and plant density at early growth stages in winter wheat. J. Plant Nutr. 29: 1983-1997.

Calderini, D.F., L.G. Abeledo, R. Savin and G.A. Slafer. 1999a. Effect of temperature and carpel size during pre-anthesis on potential grain weight in wheat. J. Agric. Sci. 132: 453-459.

Calderini, D.F., L.G. Abeledo, R. Savin and G.A. Slafer. 1999b. Final grain weight in wheat as affected by short periods of high temperature during pre- and post-anthesis under field conditions. Aust. J. Plant Physiol. 26: 453-458.

Connor, D.J., R.S. Loomis and K.G. Cassman. 2011. Crop ecology: Productivity and management in agricultural systems. Cambridge Univ. Press, Cambridge, UK.

Edwards, J.T., B.F. Carver, G.W. Horn, and M.E. Payton. 2011. Impact of dual-purpose management on wheat grain yield. Crop Sci. 51: 2181-2185.

Fischer, R.A. and G.O. Edmeades. 2010. Breeding and cereal yield progress. Crop Sci. 50: S85-S98.

Fischer, R.A. 2007. Understanding the physiological basis of yield potential in wheat. J. Agric. Sci. 145: 99-113.

Grassini, P., K.M. Eskridge and K.G. Cassman. 2013. Distinguishing between yield advances and yield plateaus in historical crop production trends. Nature Communications 4.

Grassini, P., H.S. Yang and K.G. Cassman. 2009. Limits to maize productivity in western corn-belt: A simulation analysis for fully irrigated and rainfed conditions. Agric. For. Meteorol. 149: 1254-1265.

Latiri-Souki, K., S. Nortcliff and D.W. Lawlor. 1998. Nitrogen fertilizer can increase dry matter, grain production and radiation and water use efficiencies for durum wheat under semi-arid conditions. Eur. J. Agron. 9: 21-34.

Passioura, J. 2006. Increasing crop productivity when water is scarce - from breeding to field management. Agric. Water Manage. 80: 176-196.

Patrignani, A., R.P. Lollato, T.E. Ochsner, C.B. Godsey and J. Edwards. 2014. Yield gap and production gap of rainfed winter wheat in the southern Great Plains. Agron. J. 106: 1329 - 1339.

Sadras, V.O. and J.F. Angus. 2006. Benchmarking water-use efficiency of rainfed wheat in dry environments. Aust. J. Agric. Res. 57: 847-856.

True, R.R., F.M. Epplin, E.G. Krenzer, and G.W. Horn. 2001. A survey of wheat production and wheat forage use practices in Oklahoma. B-815. Okla. Coop. Ext. Serv., Stillwater, OK.

Van Wart, J., P. Grassini, H. Yang, L. Claessens, A. Jarvis and K.G. Cassman. 2015. Creating long-term weather data from thin air for crop simulation modeling. Agric. For. Meteorol. 209: 49-58.

Wiegand, C.L. and J.A. Cuellar. 1981. Duration of grain filling and kernel weight of wheat as affected by temperature. Crop Sci. 21: 95-101.

Zhang, H., and B. McCray. 2014. Oklahoma agricultural soil test summary 2009-2013. Oklahoma State Univ. Coop. Ext. Serv. Current Report CR-2274, Stillwater, OK.

APPENDICES

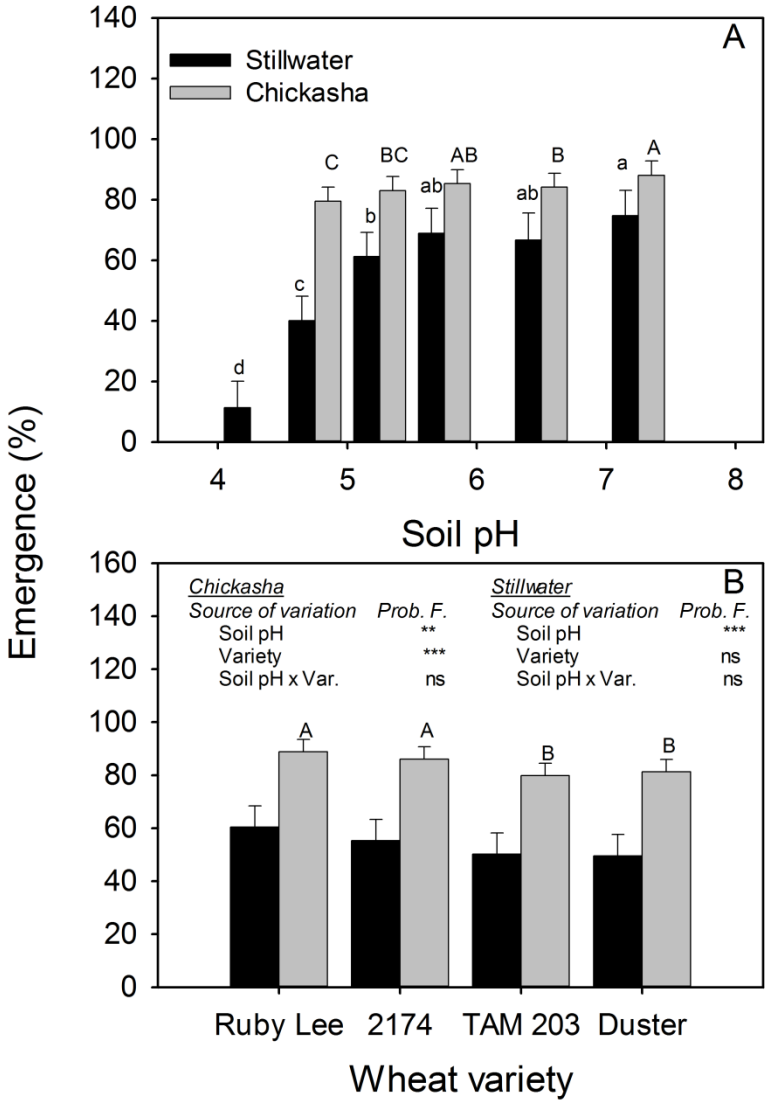

A-1. Analysis of variance of wheat percent emergence as affected by (A) soil pH and (B) wheat variety pooled across the growing seasons of 2012-13, 2013-14, and 2014-15 at Stillwater and Chickasha, OK. Interaction term was not significant.

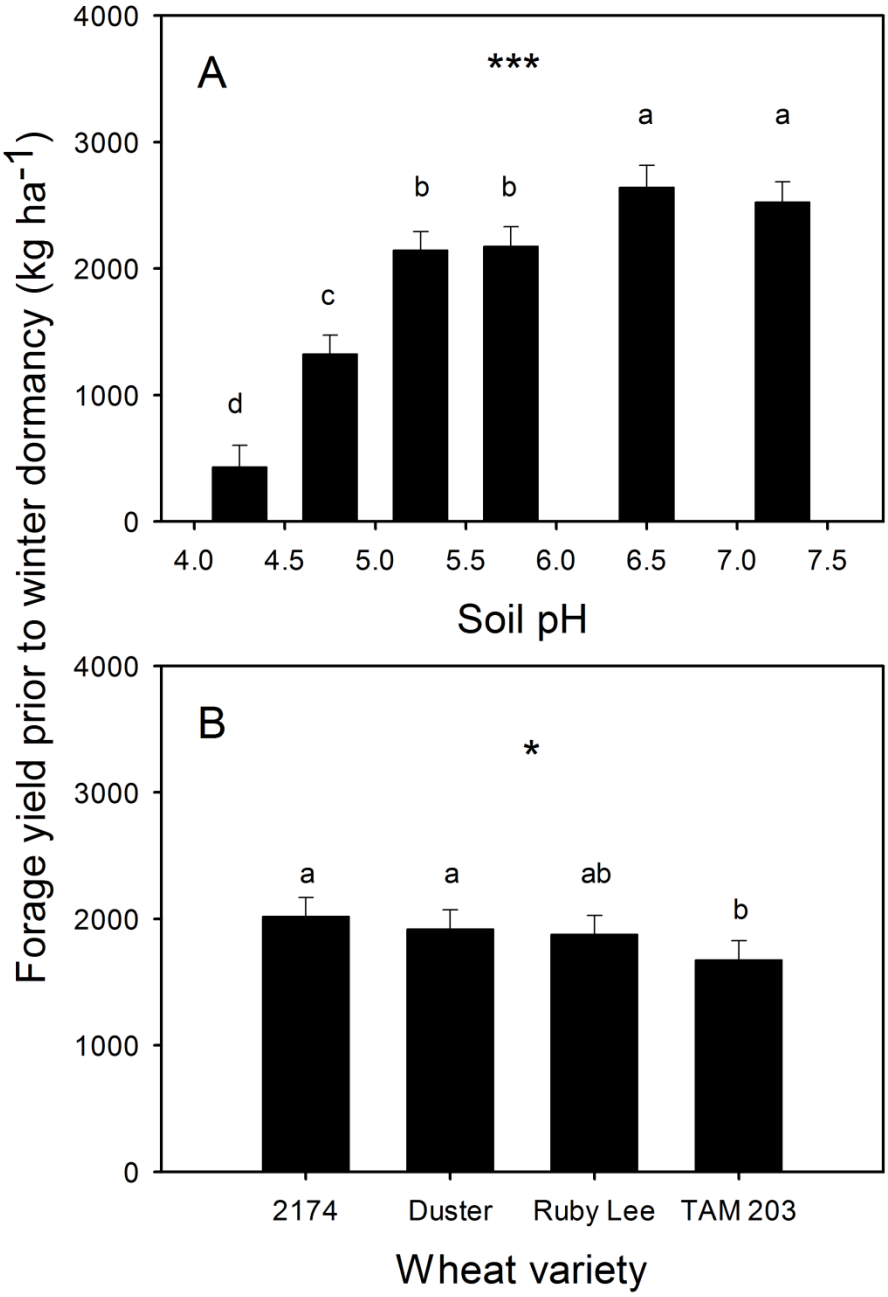

A-2. Analysis of variance of wheat forage yield prior to winter dormancy as affected by (A) soil pH and (B) wheat variety pooled across the growing seasons of 2012-13, 2013-14, and 2014-15 at Stillwater and Chickasha, OK. Interaction term was not significant.

A-3. Analysis of variance of wheat grain yield as affected by soil pH and wheat variety for the growing seasons of 2012-13, 2013-14, and 2014-15 at Stillwater and Chickasha, OK. Interaction term was not significant.

		Location and growing season					
		Stillwater			Chickasha		
Main effect		2012-13	2013-14	2014-15	2012-13	2013-14	2014-15
Soil pH range		kg ha^{-1}					
	4 - 4.5	2633 c†	-‡	965 c	-	-	-
	4.5 - 5	3776 b	1927	2893 b	-	1354 c	2469 b
	5 - 5.5	4451 a	1898	3713 a	-	1625 b	3596 a
	5.5 - 6	4612 a	2180	3737 a	4145	-	3680 a
	6 - 6.9	4765 a	1986	3766 a	4341	1678 ab	3661 a
	> 7	4323 a	2023	3610 a	-	1948 a	3635 a
Variety							
	2174	4162 a	1717 c	2858 b	4172 b	1923 a	3099 c
	Duster	4067 ab	2240 a	2908 b	2514 a	1795 a	3650 a
	Ruby Lee	4297 a	2140 ab	3765 a	4527 a	1402 b	3271 bc
	TAM 203	3850 b	1914 bc	2908 b	3758 c	1486 b	3613 ab
Source of variation							
	Soil pH	***	ns	***	ns	**	***
	Variety	*	*	***	***	**	**
	Soil pH x Var.	ns	ns	ns	ns	ns	ns

*, **, and *** - significant at $p < 0.05$, 0.01, and 0.001, respectively.

ns, non-significant.

† - Least square mean within column and main effect s followed by the same letter are not statistically different ($p > 0.05$)

‡ - Soil pH range not achieved with amendment application and therefore inexistent at that site-year.

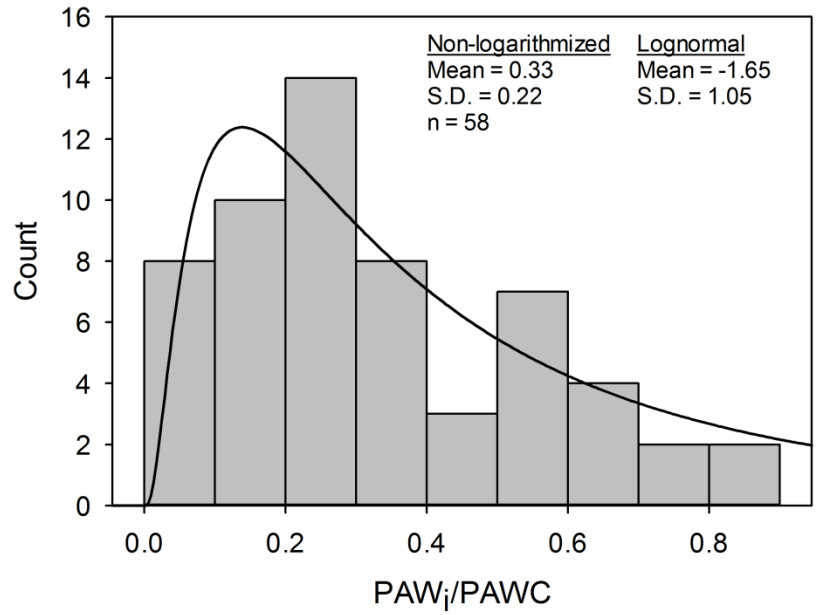

A-4. Distribution of residual plant available water plant following wheat harvest (PAW_i) normalized by plant available water capacity (PAWC) in the 0 – 120 cm layer for 58 site-years measured across Oklahoma. Chapter III.

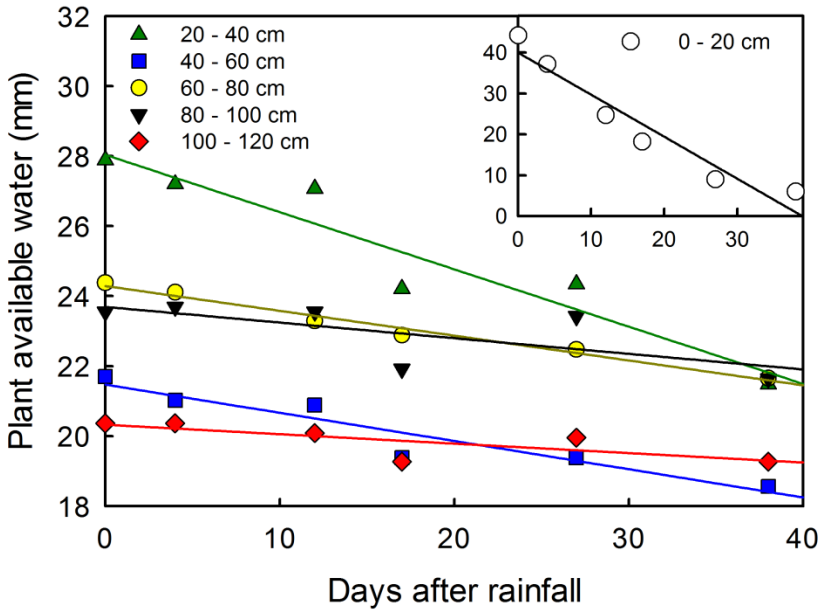

A-5. Change in the soil water storage of different layers of the soil profile during a 38-day period without measurable precipitation (August 17th to September 24th, 2013) in a Norge Loam at Stillwater, OK. Chapter III.

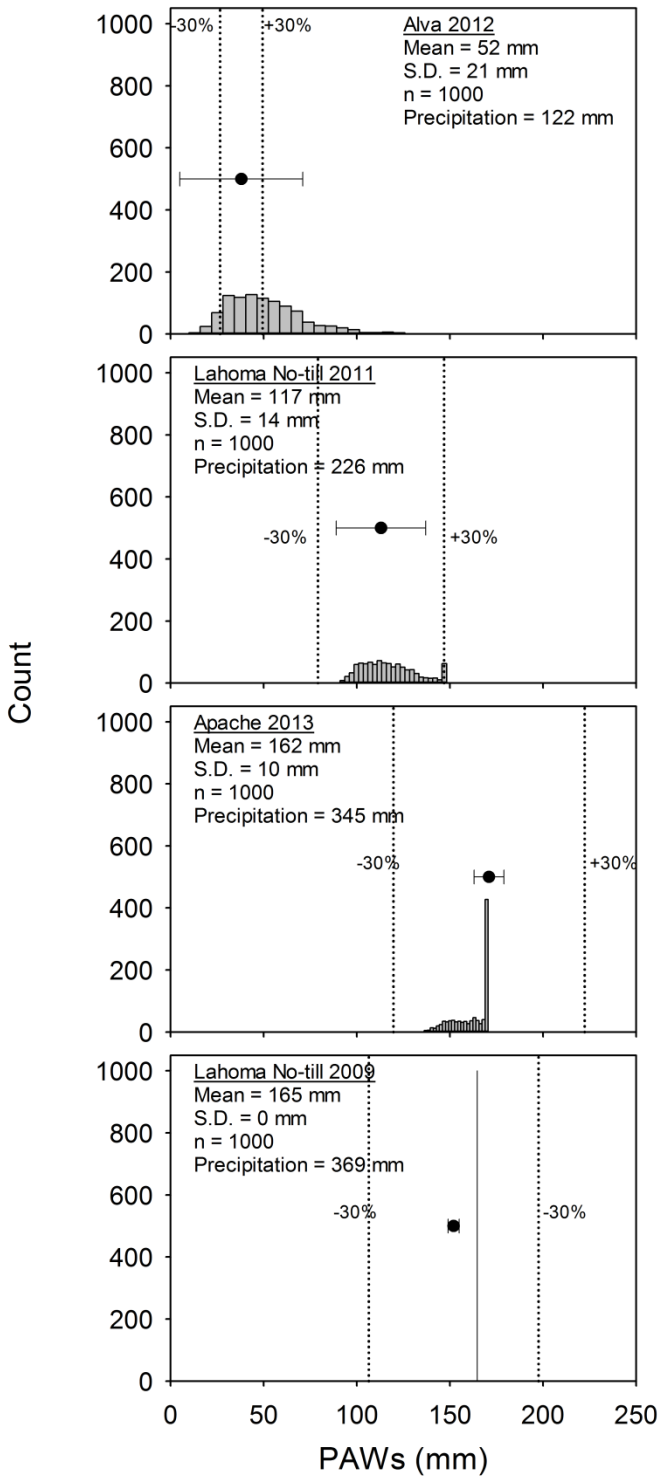

A-6. Distribution of simulated plant available water at sowing (PAW_s) in the 0 – 120 mm soil layer as affected by fallow precipitation total increasing from top panel to bottom panels. Increase in fallow precipitation total led to convergence of simulated PAW_s as evidenced by narrower distribution of PAW_s. Chapter III.

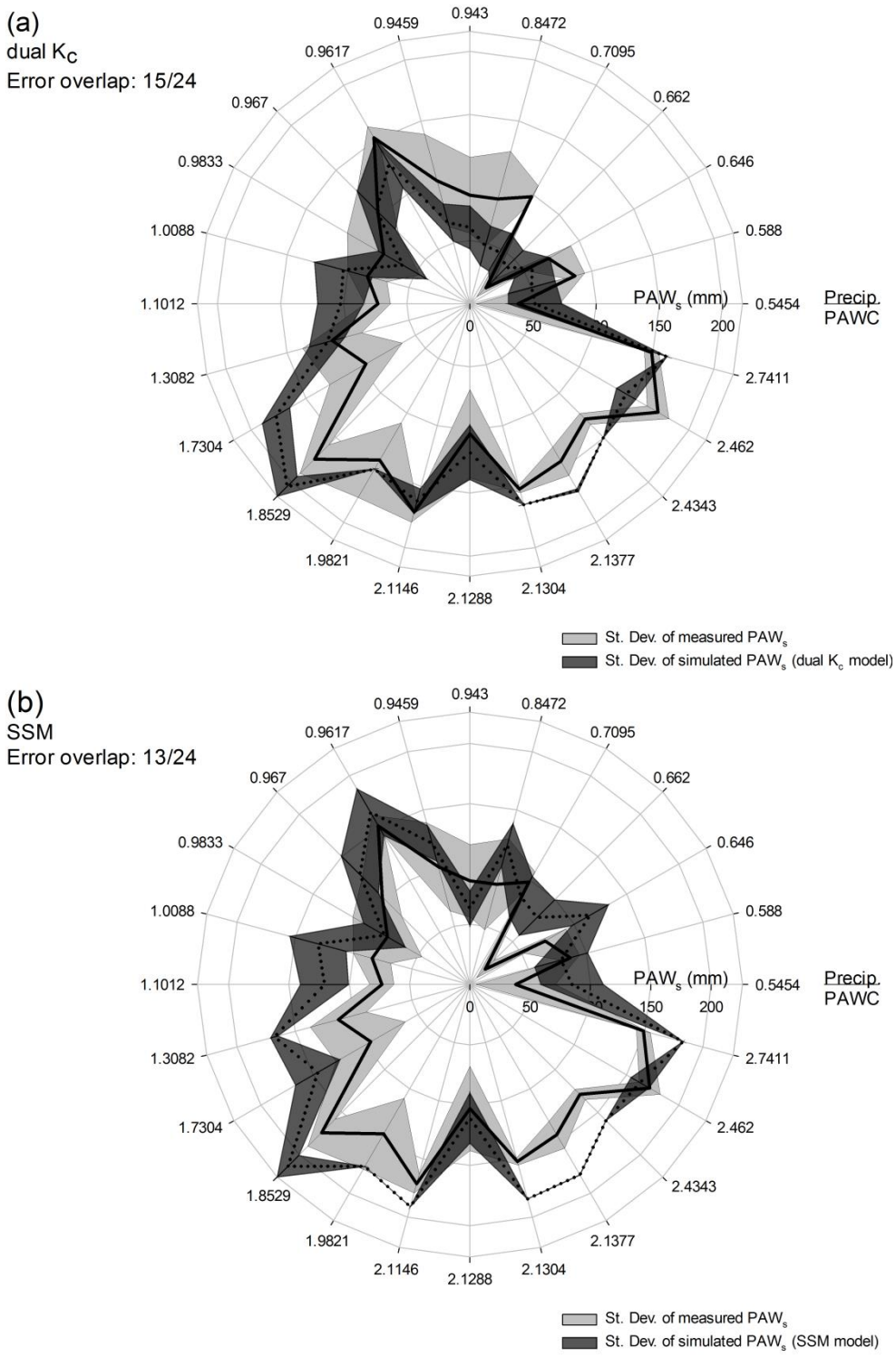

A-7. Mean and standard deviation of plant available water at sowing (PAW_s) measured (solid line, light grey area at both panels) and simulated by the (a) dual crop coefficient model (dual K_c, dotted line and dark grey area in upper panel) or by the (b) simple simulation modeling (SSM, dotted line and dark grey area in lower panel) as affected by total precipitation during the fallow period normalized by each location's plant available water capacity of the soil. Chapter III.

A-8. Soil profiles included in Chapters III, IV, and V of this dissertation with soil physical parameters shown by soil layer. Values are volumetric water content at saturation (S), field capacity (FC), and wilting point (WP), and total water in mm at the permanent wilting point (WPw), each layers plant available water capacity (PAWC), and measured plant available water at wheat sowing (PAW_s) measured October 2012 and 2013.

Soil layer	S	FC	WP	WPw	PAWC	PAW_s 2012	PAW_s 2013
cm		$cm^3\ cm^{-3}$				mm	
				Stillwater			
0-10	0.40	0.28	0.11	11	17	8	27
10-20	0.40	0.28	0.11	11	17	12	-
20-40	0.43	0.31	0.16	32	31	13	32
40-60	0.41	0.34	0.22	45	23	2	22
60-80	0.39	0.31	0.20	40	23	11	17
80-100	0.37	0.30	0.19	38	22	16	18
100-120	0.36	0.31	0.20	41	21	16	18
				Lahoma			
0-10	0.43	0.30	0.08	8	23	4	34
10-20	0.43	0.30	0.08	8	23	8	-
20-40	0.44	0.30	0.13	26	34	22	31
40-60	0.44	0.30	0.16	32	28	19	28
60-80	0.40	0.29	0.17	35	23	16	26
80-100	0.41	0.27	0.15	31	23	14	27
100-120	0.43	0.25	0.12	23	27	15	26
				Chickasha			
0-10	0.45	0.31	0.07	7	24	7	25
10-20	0.45	0.31	0.07	7	24	14	-
20-40	0.45	0.29	0.08	16	41	26	27
40-60	0.51	0.27	0.09	18	37	24	24
60-80	0.51	0.25	0.07	14	35	29	27
80-100	0.50	0.24	0.06	12	36	30	21
100-120	0.49	0.24	0.06	12	36	23	11
				Perkins Irrigated			
0-10	0.45	0.25	0.03	3	22	8	30
10-20	0.45	0.25	0.03	3	22	14	-
20-40	0.41	0.26	0.07	14	38	23	39
40-60	0.40	0.28	0.12	24	33	18	28
60-80	0.37	0.28	0.14	28	29	13	20
80-100	0.37	0.26	0.12	25	28	15	15
100-120	0.37	0.24	0.11	21	26	13	12
				Perkins Dryland			
0-10	0.44	0.25	0.07	7	18	8	22
10-20	0.44	0.25	0.07	7	18	14	-
20-40	0.43	0.27	0.13	25	29	20	28
40-60	0.40	0.27	0.14	28	26	11	25
60-80	0.39	0.23	0.10	20	26	8	19
80-100	0.39	0.21	0.07	14	27	5	18
100-120	0.39	0.21	0.06	13	28	8	18

- Value of PAW_s referent to the 10-20 cm layer is shown together with 0-10 cm layer.

A-9. Soil profiles included in Chapters III and V of this dissertation with soil physical parameters shown by soil layer. Values are volumetric water content at saturation (S), field capacity (FC), and wilting point (WP), and total water in mm at the permanent wilting point (WPw), each layers plant available water capacity (PAWC), and measured plant available water at wheat sowing (PAW_s) measured October 2012 and 2013. na – data not collected.

Soil layer	S	FC	WP	WPw	PAWC	PAW_s 2012	PAW_s 2013
cm		$cm^3\ cm^{-3}$				mm	
				Cherokee			
0-10	0.43	0.29	0.10	10	19	11	35
10-20	0.43	0.29	0.10	10	19	11	-
20-40	0.45	0.29	0.10	21	38	15	33
40-60	0.46	0.30	0.11	22	38	9	27
60-80	0.45	0.30	0.15	31	29	6	18
80-100	0.39	0.25	0.17	33	16	8	13
100-120	0.39	0.25	0.18	36	13	12	15
				Altus			
0-10	0.46	0.35	0.18	18	18	8	7
10-20	0.46	0.37	0.18	18	19	13	-
20-40	0.48	0.39	0.20	39	39	26	0
40-60	0.45	0.39	0.21	43	36	21	0
60-80	0.43	0.40	0.22	44	35	10	0
80-100	0.38	0.38	0.25	50	53	14	0
100-120	0.41	0.38	0.25	50	53	na	6
				McLoud			
0-10	0.43	0.20	0.08	8	13	14	na
10-20	0.43	0.21	0.08	8	13	17	na
20-40	0.43	0.22	0.08	16	29	28	na
40-60	0.49	0.24	0.05	10	37	14	na
60-80	0.47	0.21	0.05	9	34	3	na
80-100	0.48	0.26	0.06	12	40	3	na
100-120	0.52	0.33	0.10	19	46	1	na
				Apache 2012			
0-10	0.44	0.34	0.18	18	15	10	na
10-20	0.44	0.34	0.18	18	16	15	na
20-40	0.43	0.36	0.24	48	25	23	na
40-60	0.42	0.40	0.26	53	27	19	na
60-80	0.40	0.39	0.26	51	26	14	na
80-100	0.41	0.38	0.26	52	25	8	na
100-120	0.36	0.37	0.23	45	29	10	na
				Apache 2013			
0-20	0.47	0.28	0.08	17	38	na	38
20-40	0.47	0.31	0.12	25	38	na	33
40-60	0.47	0.32	0.13	25	38	na	33
60-80	0.44	0.33	0.18	35	32	na	24
80-100	0.41	0.35	0.21	43	28	na	21
100-120	0.41	0.36	0.23	45	27	na	20

- Value of PAW_s referent to the 10-20 cm layer is shown together with 0-10 cm layer.

A-10. Soil profiles included in Chapters III and V of this dissertation with soil physical parameters shown by soil layer. Values are volumetric water content at saturation (S), field capacity (FC), and wilting point (WP), and total water in mm at the permanent wilting point (WPw), each layers plant available water capacity (PAWC), and measured plant available water at wheat sowing (PAW_s) measured October 2012 and 2013.

Soil layer	S	FC	WP	WPw	PAWC	PAW_s 2012	PAW_s 2013
cm		$cm^3\ cm^{-3}$				mm	
				Marshall			
0-10	0.39	0.29	0.15	15	14	2	22
10-20	0.39	0.36	0.15	15	21	9	-
20-40	0.43	0.40	0.22	44	35	15	18
40-60	0.42	0.40	0.23	46	34	13	18
60-80	0.39	0.39	0.24	47	32	11	17
80-100	0.38	0.40	0.24	48	31	10	13
100-120	0.36	0.39	0.22	44	34	18	15
				Alva			
0-10	0.43	0.28	0.10	10	18	7	22
10-20	0.43	0.29	0.10	10	19	9	-
20-40	0.46	0.33	0.14	28	37	8	21
40-60	0.47	0.36	0.15	30	42	2	15
60-80	0.44	0.34	0.14	28	40	0	16
80-100	0.42	0.33	0.14	27	39	17	12
100-120	0.37	0.28	0.14	27	29	5	9
				Chickasha Variety Trial			
0-10	0.44	0.31	0.07	7	24	9	29
10-20	0.44	0.31	0.07	7	24	15	-
20-40	0.45	0.29	0.08	16	41	31	34
40-60	0.49	0.27	0.09	18	37	28	32
60-80	0.47	0.25	0.07	14	35	27	26
80-100	0.46	0.24	0.06	12	36	36	26
100-120	0.44	0.24	0.06	12	36	23	27

- Value of PAW_s referent to the 10-20 cm layer is shown together with 0-10 cm layer.

A-11. Percent sand, clay, and silt, soil textural class, and dry bulk density (DBD) by soil layer for the soil profiles used in Chap. III, IV, and V of this dissertation. Mean and standard deviation are shown. Samples collected during October 2012.

	% Sand		% Clay		%Silt		Textural class	DBD (g cm^{-3})	
Depth	Mean	S.D.	Mean	S.D.	Mean	S.D.		Mean	S.D.
					Stillwater				
0 - 10	25.00	4.15	22.79	4.91	52.26	1.74	Silt Loam	1.63	0.15
10-20	25.86	4.64	23.46	5.31	50.68	5.13	Silt Loam	1.66	0.06
20 - 40	22.14	3.87	34.02	3.14	43.84	6.69	Clay Loam	1.51	0.14
40 - 60	22.78	3.93	39.25	1.97	37.97	3.93	Clay Loam	1.56	0.05
60 - 80	27.69	2.01	36.64	4.39	35.67	4.28	Clay Loam	1.66	0.03
80 - 100	31.04	2.54	33.60	3.89	35.36	3.01	Clay Loam	1.68	0.08
100 - 120	34.69	3.08	33.37	1.23	31.94	2.96	Clay Loam	1.73	0.04
					Lahoma				
0 - 10	35.04	2.48	13.88	4.02	51.08	4.15	Silt Loam	1.56	0.26
10-20	34.41	3.91	15.77	3.67	49.82	2.63	Loam	1.48	0.12
20 - 40	30.06	4.62	26.09	7.13	43.85	2.31	Loam	1.54	0.06
40 - 60	30.13	3.36	31.28	5.76	38.59	3.99	Clay Loam	1.53	0.08
60 - 80	34.55	2.71	30.97	1.67	34.48	11.71	Clay Loam	1.60	0.06
80 - 100	38.55	1.88	27.70	1.23	33.75	11.69	Clay Loam	1.56	0.06
100 - 120	40.80	3.15	24.12	1.07	35.07	2.82	Loam	1.53	0.04
					Chickasha				
0 - 10	32.62	2.14	14.83	2.81	52.55	0.75	Silt Loam	1.48	0.12
10-20	33.11	3.67	14.51	2.18	52.38	3.60	Silt Loam	1.58	0.09
20 - 40	33.86	2.92	15.15	2.73	50.99	2.64	Silt Loam	1.53	0.06
40 - 60	25.49	2.60	19.30	1.23	55.21	2.49	Silt Loam	1.35	0.10
60 - 80	12.30	1.09	19.00	3.12	68.70	3.83	Silt Loam	1.35	0.05
80 - 100	10.18	5.87	20.92	4.01	68.91	4.17	Silt Loam	1.41	0.06
100 - 120	13.36	4.83	16.10	0.61	70.55	5.18	Silt Loam	1.42	0.04

A-12. Percent sand, clay, and silt, soil textural class, and dry bulk density (DBD) by soil layer for the soil profiles used in Chap. III, IV, and V of this dissertation. Mean and standard deviation are shown. Samples collected during October 2012.

	% Sand		% Clay		%Silt		Textural class	DBD (g cm^{-3})	
Depth	Mean	S.D.	Mean	S.D.	Mean	S.D.		Mean	S.D.
					Perkins Irrigated				
0 - 10	59.63	3.97	9.11	1.21	31.26	3.81	Sandy Loam	1.40	0.05
10-20	58.38	5.84	10.05	2.07	31.57	3.85	Sandy Loam	1.58	0.12
20 - 40	49.49	4.43	16.73	2.82	33.78	1.73	Loam	1.62	0.06
40 - 60	45.64	2.03	21.87	1.59	32.49	2.12	Loam	1.59	0.04
60 - 80	54.33	3.24	23.15	0.64	22.52	2.67	Sandy Clay Loam	1.66	0.04
80 - 100	63.27	3.17	19.00	1.47	17.73	1.87	Sandy Loam	1.74	0.02
100 - 120	68.89	2.81	14.53	2.19	16.58	0.80	Sandy Loam	1.70	0.04
					Perkins Dryland				
0 - 10	63.80	1.98	10.07	1.04	26.13	1.10	Sandy Loam	1.35	0.12
10-20	59.04	1.55	13.86	1.03	27.10	1.37	Sandy Loam	1.69	0.03
20 - 40	47.84	2.49	22.83	1.07	29.33	2.48	Loam	1.56	0.06
40 - 60	52.68	3.53	23.50	1.64	23.82	2.34	Sandy Clay Loam	1.60	0.02
60 - 80	61.02	3.62	18.98	2.55	20.00	1.16	Sandy Loam	1.67	0.03
80 - 100	70.04	2.79	11.98	1.63	17.98	2.68	Sandy Loam	1.64	0.06
100 - 120	69.89	5.94	13.56	4.32	16.55	1.69	Sandy Loam	1.64	0.10
					Cherokee				
0 - 10	18.75	1.40	17.07	0.88	64.17	2.28	Silt Loam	1.54	0.07
10-20	18.69	0.53	18.35	0.88	62.96	1.40	Silt Loam	1.54	0.08
20 - 40	26.07	3.65	20.22	0.02	53.71	3.63	Silt Loam	1.46	0.07
40 - 60	33.77	12.93	25.36	5.40	40.87	18.33	Loam	1.40	0.16
60 - 80	41.32	4.17	28.55	8.14	30.13	3.97	Clay Loam	1.45	0.10
80 - 100	55.25	10.61	25.38	3.75	19.37	6.85	Sandy Clay Loam	1.66	0.10
100 - 120	54.80	5.48	12.73	0.02	32.47	5.46	Sandy Loam	1.66	0.02

A-13. Percent sand, clay, and silt, soil textural class, and dry bulk density (DBD) by soil layer for the soil profiles used in Chap. III, IV, and V of this dissertation. Mean and standard deviation are shown. Samples collected during October 2012.

	% Sand		% Clay		%Silt		Textural class	DBD (g cm^{-3})	
Depth	Mean	S.D.	Mean	S.D.	Mean	S.D.		Mean	S.D.
					Altus				
0 - 10	22.38	10.61	34.50	3.71	43.13	6.90	Clay Loam	1.47	0.11
10-20	22.14	8.87	39.09	4.66	38.77	4.21	Clay Loam	1.49	0.08
20 - 40	18.49	8.39	45.56	1.03	35.94	7.36	Clay	1.53	0.06
40 - 60	17.46	9.60	46.89	0.88	35.65	10.47	Clay	1.60	0.04
60 - 80	10.80	1.88	47.49	1.85	41.71	0.03	Silty Clay	1.61	0.14
80 - 100	11.56	4.68	47.42	1.89	41.02	2.79	Silty Clay	1.76	0.11
100 - 120	-	-	-	-	-	-		1.60	-
					McLoud				
0 - 10	48.15	3.52	11.76	1.94	40.09	1.62	Loam	1.46	0.05
10-20	45.75	6.63	13.46	2.93	40.79	3.70	Loam	1.59	0.03
20 - 40	42.10	2.86	13.47	1.47	44.42	3.81	Loam	1.51	0.06
40 - 60	39.42	10.24	12.62	0.02	47.96	10.22	Loam	1.36	0.02
60 - 80	45.39	6.30	11.34	1.28	43.27	5.16	Loam	1.41	0.04
80 - 100	32.70	14.41	13.88	4.59	53.41	10.60	Silt Loam	1.38	0.07
100 - 120	16.91	4.12	20.69	8.56	62.39	4.45	Silt Loam	1.27	0.03
					Apache				
0 - 10	16.11	3.42	25.91	1.52	57.98	2.33	Silt Loam	1.40	0.07
10-20	16.47	5.93	31.22	8.09	52.31	5.08	Silty Clay Loam	1.58	0.05
20 - 40	10.51	4.17	34.06	12.17	55.43	8.00	Silty Clay Loam	1.51	0.04
40 - 60	6.15	0.00	45.95	2.75	47.90	2.74	Silty Clay	1.55	0.05
60 - 80	9.47	0.04	43.97	1.85	46.56	1.81	Silty Clay	1.59	0.09
80 - 100	10.52	1.11	42.64	0.12	46.84	1.24	Silty Clay	1.57	0.01
100 - 120	11.04	2.06	41.90	2.85	47.06	0.78	Silty Clay	1.70	0.05

A-14. Percent sand, clay, and silt, soil textural class, and dry bulk density (DBD) by soil layer for the soil profiles used in Chap. III, IV, and V of this dissertation. Mean and standard deviation are shown. Samples collected during October 2012.

	% Sand		% Clay		%Silt		Textural class	DBD (g cm^{-3})	
Depth	Mean	S.D.	Mean	S.D.	Mean	S.D.		Mean	S.D.
					Marshall				
0 - 10	22.57	4.95	25.28	0.01	52.15	4.94	Silt Loam	1.75	0.28
10-20	14.39	5.28	37.57	10.05	48.04	4.76	Silty Clay Loam	1.60	0.08
20 - 40	8.55	1.04	46.05	3.68	45.40	2.65	Silty Clay	1.55	0.07
40 - 60	8.49	0.03	47.35	1.79	44.15	1.83	Silty Clay	1.57	0.08
60 - 80	9.69	1.19	47.23	1.89	43.08	3.08	Silty Clay	1.63	0.10
80 - 100	5.55	2.89	48.50	0.09	45.95	2.80	Silty Clay	1.68	0.02
100 - 120	3.92	3.53	47.88	2.89	48.20	0.64	Silty Clay	1.74	0.06
					Alva				
0 - 10	25.69	0.55	19.60	0.87	54.71	1.42	Silt Loam	1.58	0.17
10-20	22.97	0.51	20.92	0.91	56.11	0.41	Silt Loam	1.55	0.06
20 - 40	24.20	0.04	28.66	0.92	47.14	0.88	Clay Loam	1.46	0.05
40 - 60	23.91	1.59	35.32	4.65	40.77	3.05	Clay Loam	1.39	0.13
60 - 80	23.03	0.66	31.95	5.51	45.03	4.85	Clay Loam	1.49	0.07
80 - 100	25.33	7.36	30.63	3.67	44.03	3.69	Clay Loam	1.51	0.10
100 - 120	31.64	5.89	26.71	3.58	41.66	9.47	Loam	1.79	0.69
					Chickasha Variety Trial				
0 - 10	30.57	1.77	14.52	0.89	54.92	0.88	Silt Loam	1.42	0.13
10-20	29.65	2.20	16.40	0.01	53.94	2.21	Silt Loam	1.62	0.01
20 - 40	24.15	2.76	18.33	0.91	57.52	1.85	Silt Loam	1.46	0.03
40 - 60	13.15	6.72	18.32	2.68	68.53	4.04	Silt Loam	1.40	0.05
60 - 80	18.57	1.64	14.52	2.70	66.91	4.35	Silt Loam	1.44	0.02
80 - 100	21.20	8.07	14.50	0.90	64.30	7.17	Silt Loam	1.47	0.10
100 - 120	24.78	1.32	12.59	0.00	62.63	1.32	Silt Loam	1.54	0.06

A-15. Percent sand, clay, and silt, soil textural class, and dry bulk density (DBD) by soil layer for the soil profiles used in Chap. III, IV, and V of this dissertation. Mean and standard deviation are shown. Samples collected during October 2013.

	% Sand		% Clay		%Silt		Textural class	DBD (g cm^{-3})	
Depth	Mean	S.D.	Mean	S.D.	Mean	S.D.		Mean	S.D.
					Apache 2013				
0-20	20.26	0.89	16.14	2.19	63.60	1.52	Silt loam	1.41	0.08
20-40	15.68	2.94	24.29	3.73	60.04	1.33	Silt loam	1.40	0.04
40-60	15.70	0.72	25.23	3.26	59.07	3.91	Silt loam	1.41	0.11
60-80	14.01	2.80	29.20	3.26	56.79	4.56	Silty clay loam	1.49	0.08
80-100	15.07	2.45	34.93	2.81	50.00	2.59	Silty clay loam	1.58	0.05
100-120	14.48	2.37	36.10	3.51	49.42	2.65	Silty clay loam	1.55	0.05

A-16. Neutron probe calibration against dry and wet measurements used to measure soil water content to 120 cm depth at five locations across Oklahoma. Data used for Chapters III, IV, and V.

Site	Lat. (°)	Long. (°)	Soil series	Layer	y-intercept	slope	r^2
Stillwater	36.121	-97.094	Norge loam	0-20	-0.1139	0.313	0.98
				20-120	-0.1889	0.2729	0.95
Chickasha	35.045	-97.907	Dale silt Loam	0-20	0.0147	0.1976	0.99
				20-120	-0.1058	0.2615	0.91
Perkins Dryland	35.997	-97.0474	Teller loam	0-20	-0.0258	0.219	0.99
				20-120	-0.075	0.1919	0.97
Lahoma	36.897	-98.1074	Grant silt loam	0-20	-0.0274	0.2535	0.99
				20-120	-0.1469	0.2565	0.95
Perkins Irrigated	35.99	-97.0448	Teller fine sandy loam	0-20	-0.1068	0.3387	0.98
				20-120	-0.1735	0.256	0.91

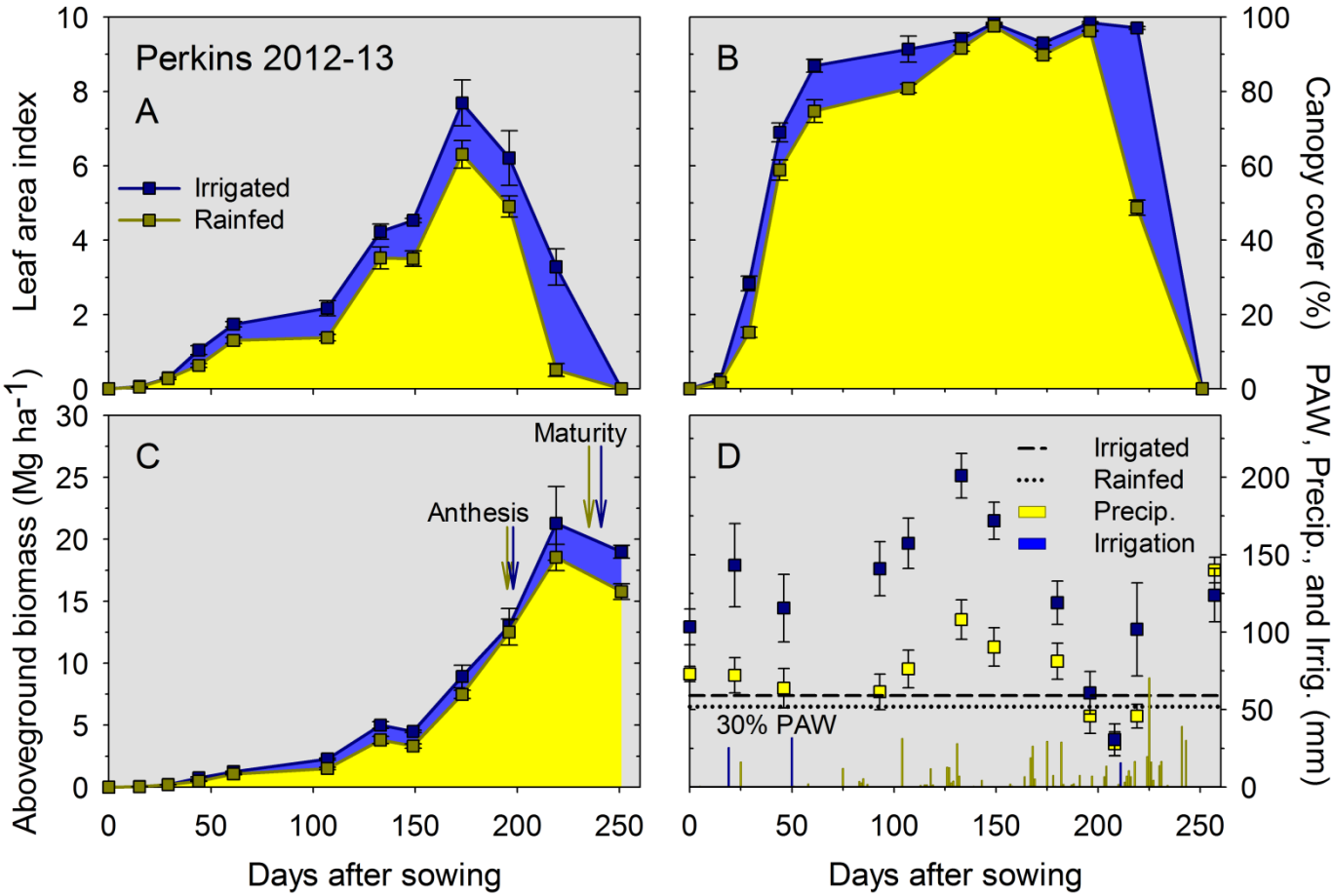

A-17. Dynamics of (A) leaf area index, (B) canopy cover, (C) aboveground biomass and dates for anthesis and physiological maturity, and (D) plant available water (PAW, scatter plots), precipitation (Precip., vertical yellow bars), irrigation (Irr., vertical blue bars), and drought threshold indicated as 30% PAW, (dashed line) during the 2012-13 growing season for irrigated (blue) and dryland (yellow) management for winter wheat grown under non-limiting conditions at Perkins, OK. Error bars are standard error of the mean.

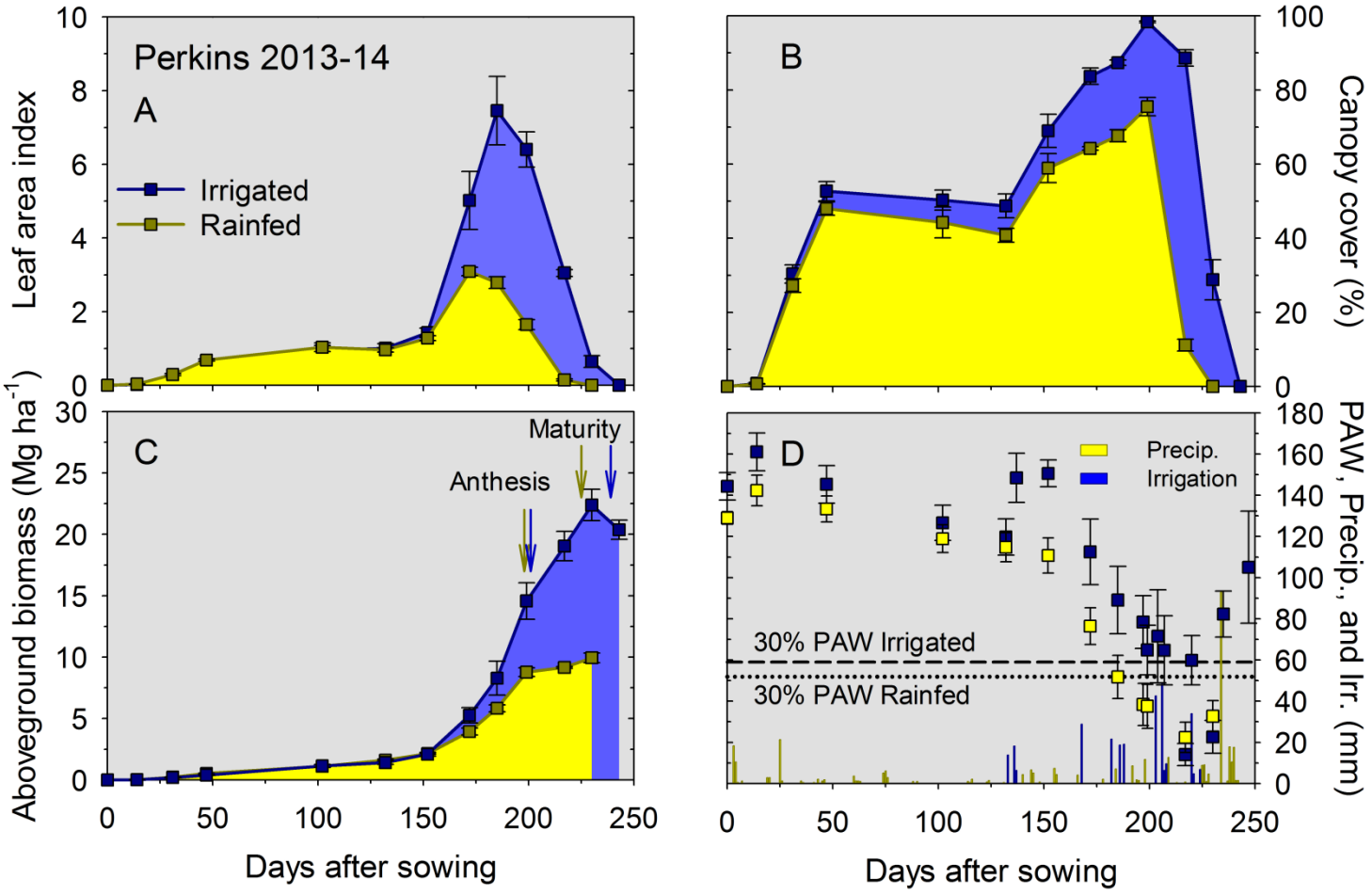

A-18. Dynamics of (A) leaf area index, (B) canopy cover, (C) aboveground biomass and dates for anthesis and physiological maturity, and (D) plant available water (PAW, scatter plots), precipitation (Precip., vertical yellow bars), irrigation (Irr., vertical blue bars), and drought threshold indicated as 30% PAW, (dashed line) during the 2013-14 growing season for irrigated (blue) and dryland (yellow) management for winter wheat grown under non-limiting conditions at Perkins, OK. Error bars are standard error of the mean.

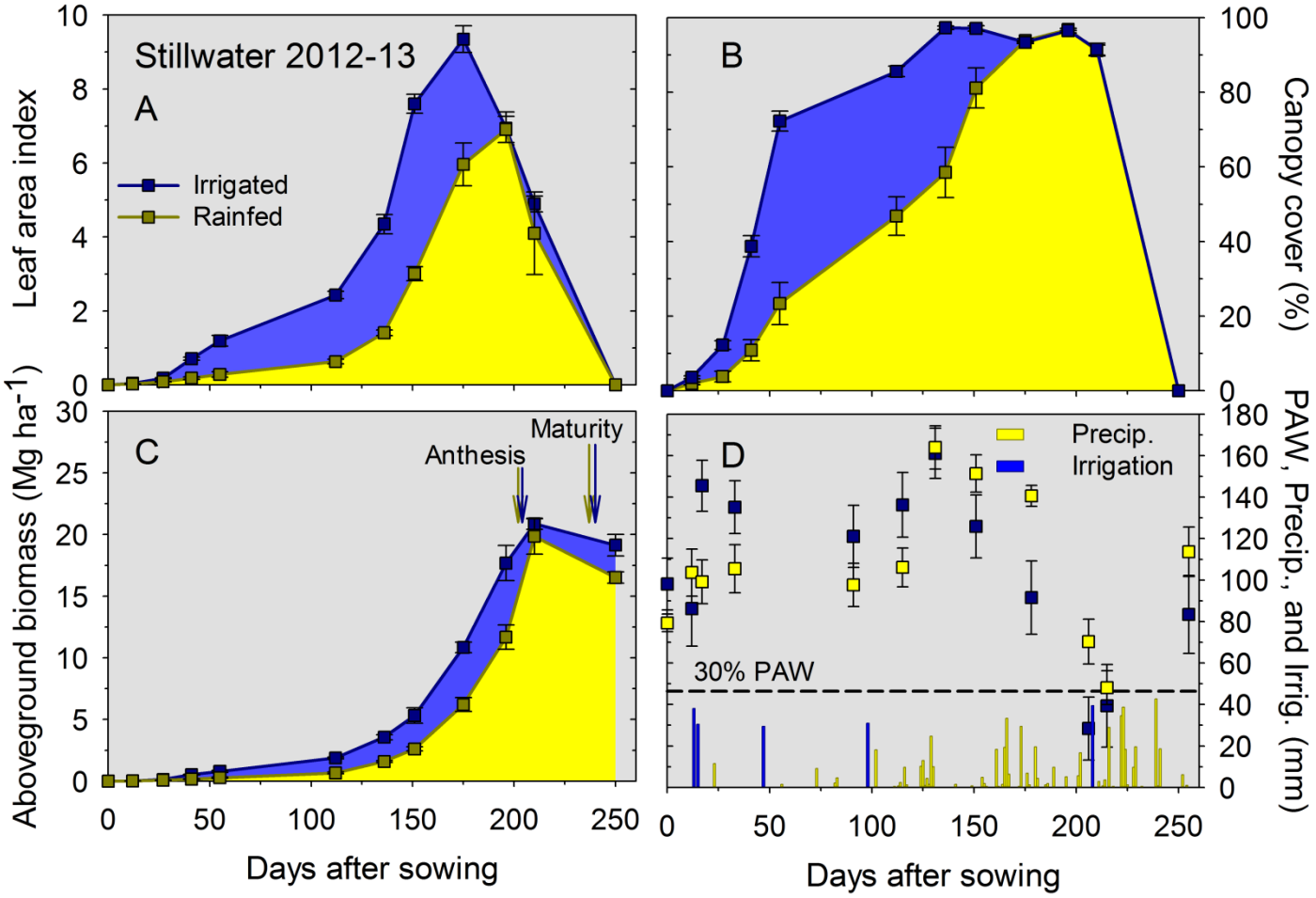

A-19. Dynamics of (A) leaf area index, (B) canopy cover, (C) aboveground biomass and dates for anthesis and physiological maturity, and (D) plant available water (PAW, scatter plots), precipitation (Precip., vertical yellow bars), irrigation (Irr., vertical blue bars), and drought threshold indicated as 30% PAW, (dashed line) during the 2012-13 growing season for irrigated (blue) and dryland (yellow) management for winter wheat grown under non-limiting conditions at Stillwater, OK. Error bars are standard error of the mean.

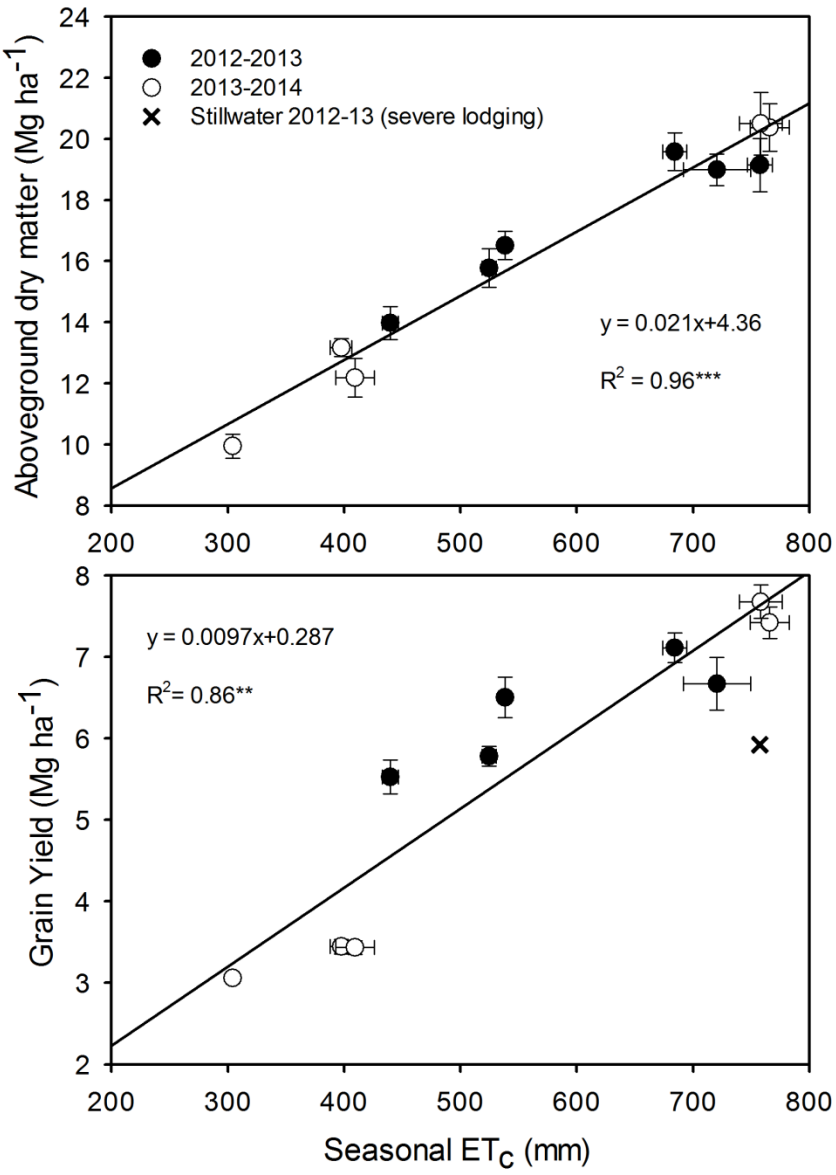

A-20. Linear relationship between measured aboveground dry matter and grain yield for winter wheat grown under non-limiting conditions for 11 site-years in Oklahoma. Data from Chapter IV.

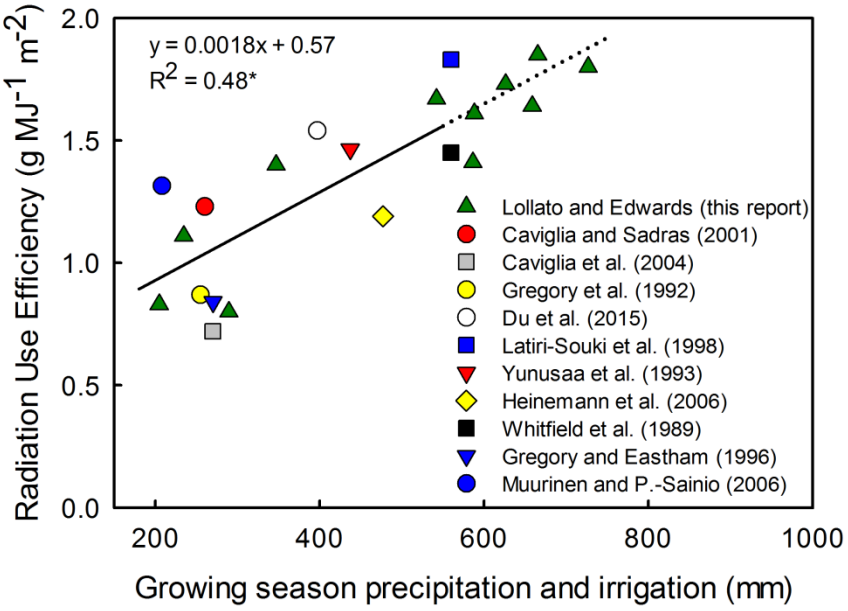

A-21. Literature review of radiation use efficiency as affected by growing season precipitation and irrigation total. Data from Chapter IV.

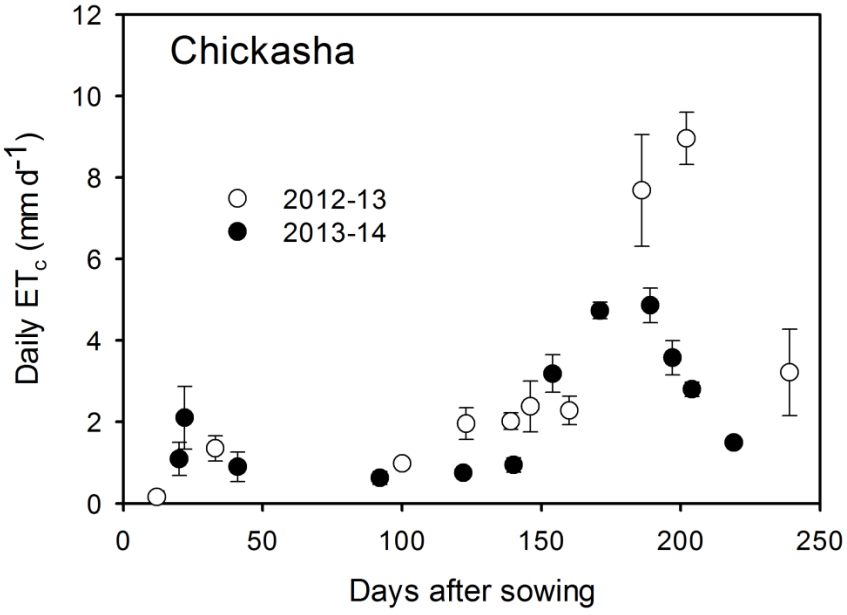

A-22. Daily crop evapotranspiration (ETc) versus days after sowing for winter wheat grown under non-limiting conditions during the 2012-13 and 2013-14 growing seasons at Chickasha, OK.

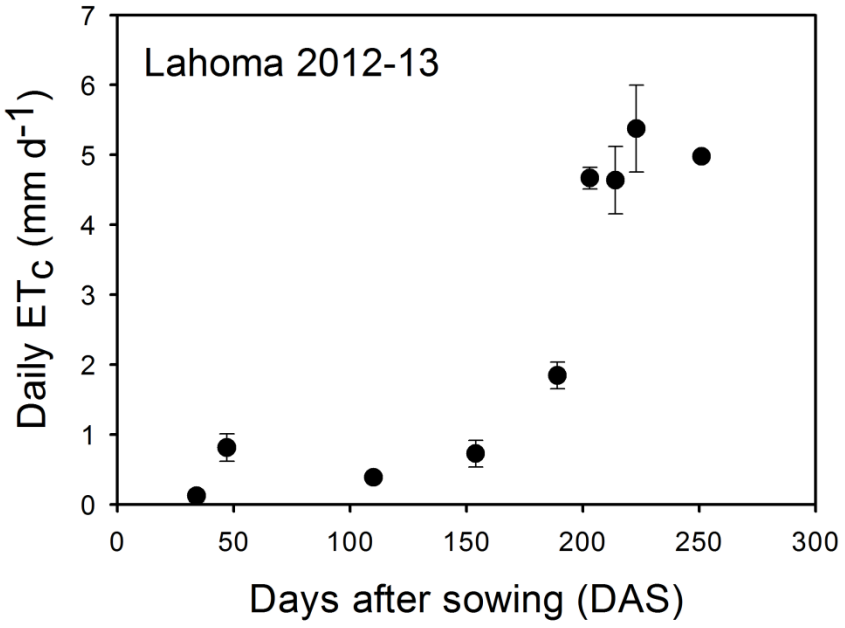

A-23. Daily crop evapotranspiration (ETc) versus days after sowing for winter wheat grown under non-limiting conditions during the 2012-13 growing season at Lahoma, OK.

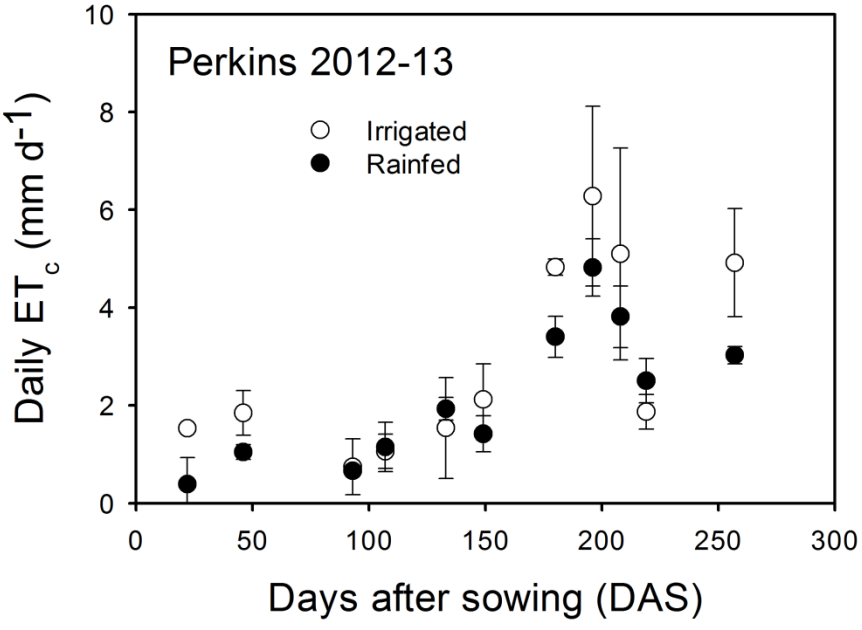

A-24. Daily crop evapotranspiration (ETc) versus days after sowing for winter wheat grown under non-limiting conditions and irrigated or rainfed management practice during the 2012-13 growing season at Perkins, OK.

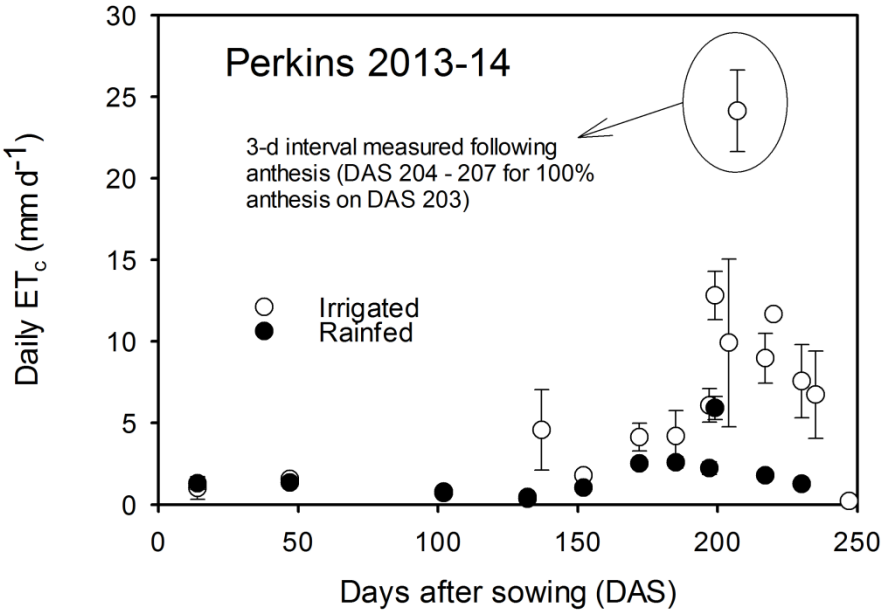

A-25. Daily crop evapotranspiration (ETc) versus days after sowing for winter wheat grown under non-limiting conditions and irrigated or rainfed management practice during the 2013-14 growing season at Perkins, OK.

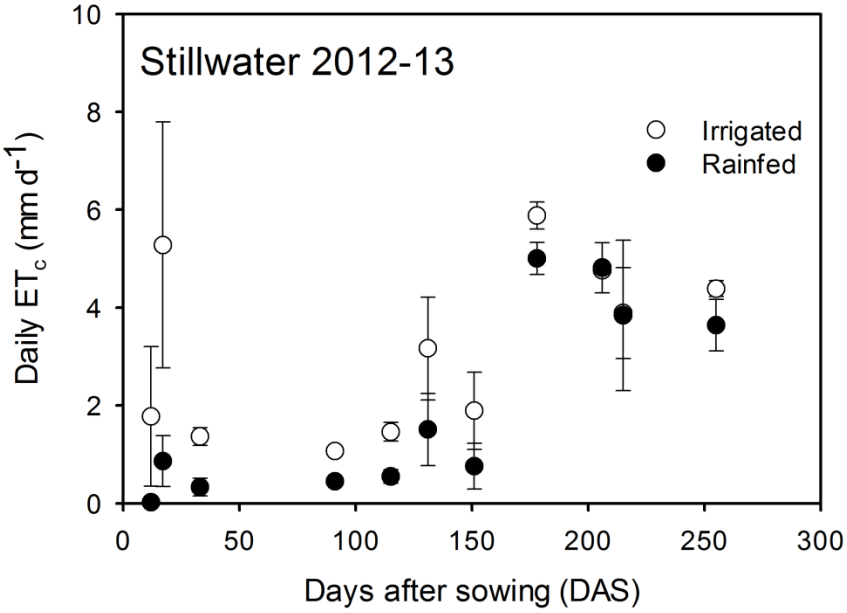

A-26. Daily crop evapotranspiration (ETc) versus days after sowing for winter wheat grown under non-limiting conditions and irrigated or rainfed management practice during the 2012-13 growing season at Stillwater, OK.

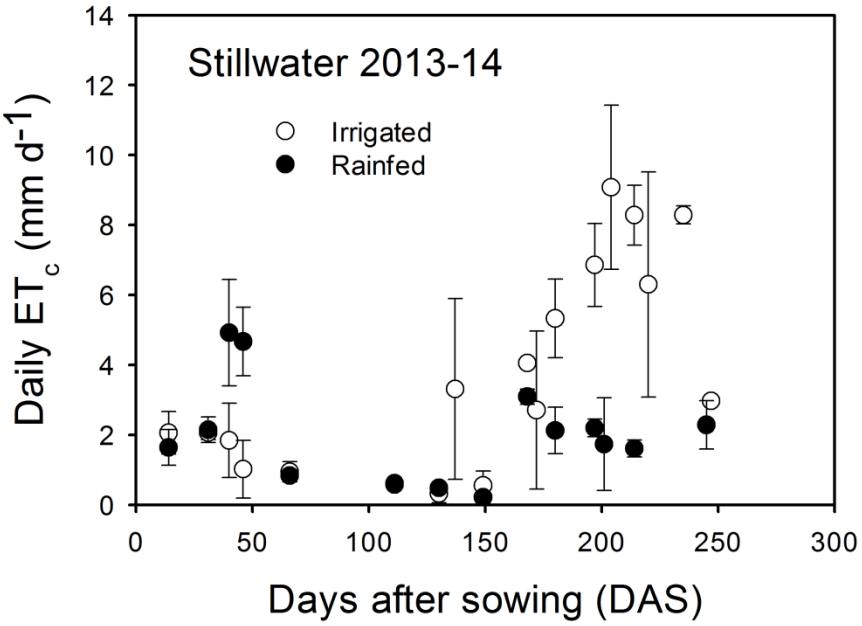

A-27. Daily crop evapotranspiration (ETc) versus days after sowing for winter wheat grown under non-limiting conditions and irrigated or rainfed management practice during the 2013-14 growing season at Stillwater, OK.

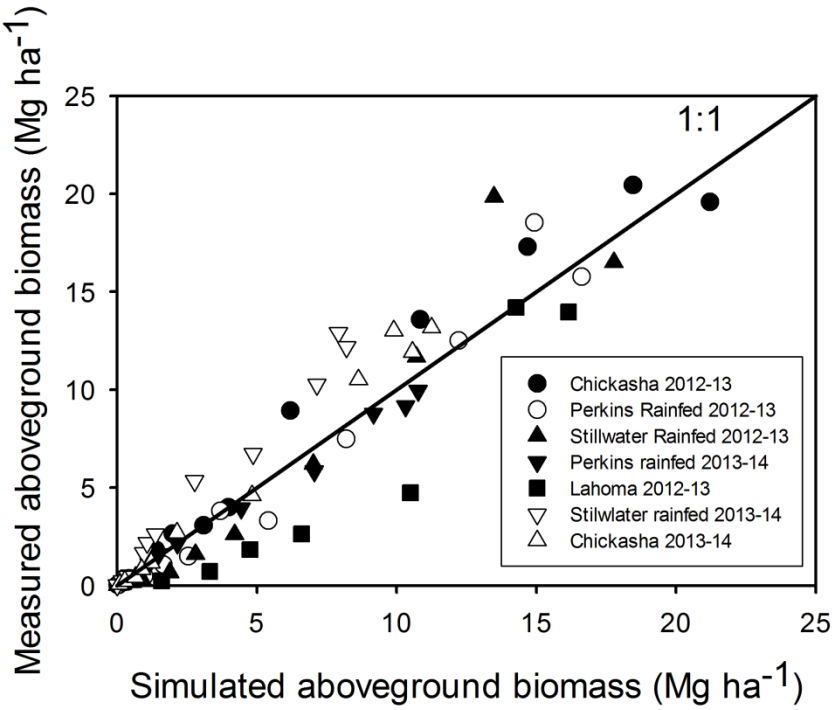

A-28. Performance of the SSM-Wheat model in simulating aboveground biomass on the calibration dataset encompassing seven site-years across Oklahoma during the 2012-13 and 2013-14 growing seasons.

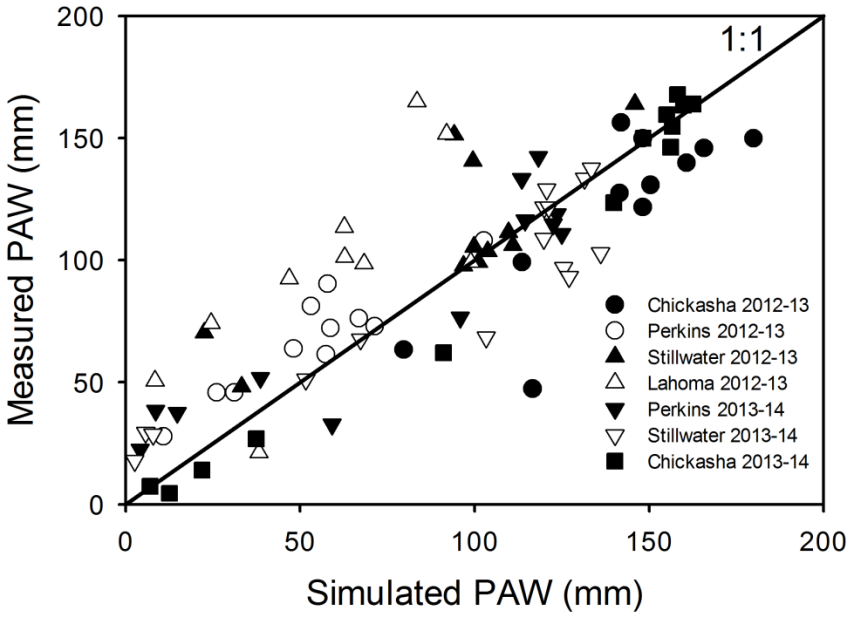

A-29. Performance of the SSM-Wheat model in simulating plant available water (PAW) in the 120-cm soil profile depth on the calibration dataset encompassing seven site-years across Oklahoma during the 2012-13 and 2013-14 growing seasons.

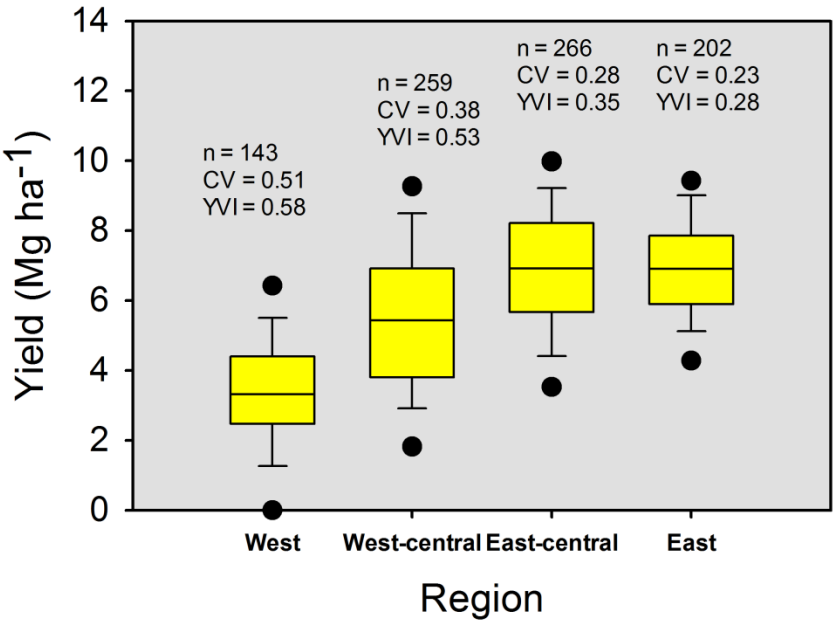

A-30. Box plot of 28-yr simulated yield potential for four sub-regions including a total of 37 locations for 870 simulations. Data from Chapter V.

VITA

Romulo Pisa Lollato

Candidate for the Degree of

Doctor of Philosophy

Thesis: LIMITS TO WINTER WHEAT (*Triticum aestivum* L.) PRODUCTIVITY AND RESOURCE-USE EFFICIENCY IN THE SOUTHERN GREAT PLAINS

Major Field: Crop Science

Biographical:

Education:

Completed the requirements for Doctor of Philosophy in Crop Science at Oklahoma State University, Stillwater, Oklahoma, in July, 2015.

Completed the requirements for Master of Science in Plant and Soil Sciences at Oklahoma State University, Stillwater, Oklahoma in December 2012.

Completed the requirements for Bachelor of Science in Agronomy at Universidade Estadual de Londrina, Londrina, Paraná, Brazil in December 2009.

Experience:

Graduate research assistant in the Department of Plant and Soil Sciences at Oklahoma State University, Stillwater, OK. August 2010 – July 2015.
Junior agricultural analyst for the Agribusiness Intelligence Team at Cargill S/A, São Paulo, São Paulo, Brazil. August 2009 – July 2010.
Intern in the Department of Plant Breeding and Genetics at the Agronomic Institute of Paraná (IAPAR), Londrina, Paraná, Brazil. March 2006 – July 2009.
Intern in the Department of Plant Breeding and Genetics at Instituto Nacional de Tecnología Agropecuaria, Cerrillos, Salta, Argentina. January and February 2008.

Professional Memberships:

American Society of Agronomy (ASA): 2010 – Present
Crop Science Society of America (CSSA): 2010 – Present
Soil Science Society of America (SSSA): 2010 – Present